Catenary Vaults: A solution to low-cost housing in South Africa

Ivanka Bulovic

A research report submitted to the Faculty of Engineering and the Built Environment, University of the Witwatersrand, Johannesburg, in partial fulfilment of the requirements for the degree of Master of Science in Engineering.

Johannesburg 2014

The financial assistance of the National Research Foundation (N R F) towards this research is hereby acknowledged. Opinions expressed and conclusions arrived at, are those of the author and are not necessarily to be attributed to the NRF.

Table of Contents

Declaration

I declare that this research report is my own unaided work. It is being submitted to the Degree of Master of Science to the University of the Witwatersrand, Johannesburg. It has not been submitted before for any degree or examination to any other University.

Signature …………………………………………

Ivanka Bulovic

……… day of ……… year 2014.

Abstract

This report discusses the design approach of catenary vaults in the application of low-cost housing. It investigates the most efficient design, materials and construction methods to provide a sustainable and durable solution to low-cost housing.

Investigation into various materials was carried out and two specific blocks are used in the construction process: the dry-stack interlocking block and the splitter-brick block.

An innovative method of designing catenary curves was developed: The Segmental Equilibrium Method. This design approach focuses on equilibrium equations to define the geometric shape of a catenary under various loading. The method incorporates dead, live and wind loads. The solution obtained is exact and thus proves to be the most superior method in designing catenary curves. The method was compared to the Finite Element Analysis and errors ranged from 0% to 8.9%. Finite Element collaborated with the Segmental Equilibrium Method and verified that the proposed method of analysis can be used in the design of catenary curves.

Finite Element Method was used to analyse temperature loading on the catenary curve. A tensile stress of 0.95N/mm^2 and compressive stress of 1.02N/mm^2 were obtained. These values are within the materials capacity of the brick (1.1N/mm^2 Tension and 7-10 N/mm^2 Compression).

The final structure was built using a sliding steel form work. The construction process was closely documented and is discussed in the report. The problems during construction and solutions are presented. A cost analysis was carried out and compared to other leading projects in South Africa. It was found that the structure is economically competitive, with an average cost of R95 000 ($9 500).

The report concludes that thin shelled structures, in particular catenary vaults, are a viable option for low-cost housing in South Africa.

Acknowledgements

First and foremost, I would like to thank my supervisor Prof Gohnert for his invaluable support and guidance throughout my masters career. Thank you for offering me this amazing opportunity and opening so many doors for me. Your support has been incredible and I am eternally grateful for your commitment in showing me the dream that is civil engineering.

I would also like to thank Ryan Bradley and the entire Lab Staff at Wits for all their support and help. To Eric, Wayne, Henrique, Dumisani, Sam and Sish: this project would not have been possible without your huge contribution during the construction process. Thank you.

To all our sponsors: Hydraform, Spancon, Macsteel, Robor, Wispeco, Afrisam and Lintel Suppliers. Thank you for all your invaluable contribution. Each donation made a huge difference in ensuring the success of this project. We look forward to continuing working with you in the future as this project grows. Hydraform, thank you for dedicating your time, money and irreplaceable labour to this project; you made this project possible.

To National Research Foundation for investing in my research and supporting me financially: thank you.

I would like to thank my sister, Nena; boyfriend, James and my friend, Robyn, who helped motivate me over the past two years.

Lastly and most importantly, my parents: thank you for supporting me financially and emotionally over my entire schooling career and for giving me the opportunity to follow my dreams. I would not be where I am today were it not for you and I am eternally grateful for everything you have done for me.

List of Figures

Chapter 6

Chapter 7

List of Tables

List of Symbols

Description	Symbol
Cartesian x – coordinate	x
Cartesian y – coordinate	y
Section Modulus	Z
Applied Load	P
Thickness	t
Eccentricity	e
Stress	σ
Initial angle, theta	θ
Sum of Moments	$\sum M$
Sum of forces in the y direction	$\sum F_y$
Sum of forces in the x direction	$\sum F_x$
Dead Load	DL
Wind Speed	v
Altitude Constant	k_p
Wind Speed Multipliers	k_z
Wind pressure	q_z
External Pressure Coefficient	C_{pe}
Internal Pressure Coefficient	C_{pi}
Point Load	PL
Ultimate Limit State	ULS
Service Limit State	SLS
Live Load	LL
Wind Load	WL
Horizontal	H

Vertical	V
Capacity Reduction Factor	β
Characteristic Compressive Strength	*fk*
Material Safety Factor	γ_m
Length	L
Height	h
Characteristic Stength	P_u
Yield Strength	f_y
Radius of bar	r
Pie	π
Throat thickness	*a*
Total Service Load	P_s
Compression	C
Tension	T

1. Introduction

1.1. Problem Statement

Many South Africans live a life of extreme poverty with limited access to basic infrastructure, including housing. It is difficult to provide housing for everyone, and this is further exacerbated by the common use of large quantities of concrete as a construction material. Because of the expense, current concrete construction is not a sustainable solution to South Africa’s housing problem. Either a new material or a new design must be established in order to achieve a more economical solution. A clear example of this is RDP housing and its ineffectiveness in alleviating poverty. The cost is high and the quality of construction is poor. In addition, on a daily basis, we are faced with extensive environmental issues caused by the use of concrete, e.g. pollution, flooding, exploitation of resources, heat islands, etc. (Birkinshaw, 2008). A new solution needs to be investigated where the form of housing is cheap, materials are locally obtained. The design and construction is robust and most importantly, the structure is environmentally friendly.

In 2007, it was found that 11 percent of the South African population live in shacks (FinScope, 2007). This number has increased considerably since 2007 and is still on the rise (Birkinshaw, 2008). Birkinshaw (2008) found that the number of South African households residing in shacks is increasing at more than double the rate at which the population is growing, with more than 2 million people currently residing in shacks. The living conditions of these people are extremely low and thousands of related deaths occur every year (Birkinshaw, 2008). Thus, it is important that the basic needs of people are met and their living conditions improved.

To improve living conditions, several factors must be investigated. Firstly, it is important that low energy and locally sourced materials are utilised in the construction process. This will reduce costs to a minimum and provide a more sustainable solution. Secondly, the structures need to be thermally efficient as a major cause of death in informal settlements is as a result of heating during winter. Uncontrolled shack fires are created whilst trying to warm households during the winter months. Lastly and most important, a more structurally robust design needs to be determined to ensure that the inhabitants have a long term home, regardless of the prevailing weather conditions.

We need to respond, and therefore it is important to investigate creative solutions to the housing problems, experienced both in South Africa and around the world. In addition, we are faced with climate change and therefore we cannot construct in the usual manner. Other issues include excessive energy consumption in the production phase, pollution, temperature changes and lack of good thermal properties. The current solution is not sustainable.

Thin shells have been found to be a very effective solution (Joffroy, 1994). They are versatile and easy to construct, requiring minimal amounts of materials. Shell forms can eliminate expensive forces, such as shears and moments, and increase their durability considerably. Thin shells have the ability to resist extreme loading conditions; this is highlighted by a *Youtube* clip in The Weather Channel (2009), documenting a shell home which survived Hurricane Ivan. Thin shells, in conjunction with environmentally agreeable materials, are a superior solution in terms of strength, economy of materials and cost to the consumer.

1.2. Objectives

The objectives of this research report:

- Investigate properties of materials which have low energy consumption, are cheap and locally obtainable
- Investigate various housing forms and determine the most suitable form for low-cost housing, incorporating thin shells
- Establish an effective method of designing and analysing catenary vaults
- Design an effective low-cost housing prototype and identify the important design criteria that needs to be considered
- Construct a durable and structurally efficient low cost housing prototype

1.3. Scope

This research report comprises of ten chapters. The contents of each of the chapters are outlined below:

Chapter 2 highlights previous literature and research done on low-cost housing projects. It highlights the benefits of thin shells as a solution to low-cost housing as well as shortfalls in knowledge on designing catenary vaults. It also discusses various building materials and construction methods required in the use of thin shelled structures.

Chapter 3 investigates various forms and layouts suitable for low-cost housing. This chapter highlights the need for housing; which minimises on thermal energy and natural flow of the energy within the structure. A final prototype design is also presented.

Chapter 4 presents information regarding the various building materials which are used in the construction of the prototype. The advantages and shortfalls are highlighted and guidance as to how the user can produce his own building materials on site.

In Chapter 5, various methods of designing catenary curves are discussed and a new method of design is presented, based on equilibrium principles.

Chapter 6 utilises the method described in Chapter 5, and covers an in-depth step-by-step analysis and design of the catenary roof of the housing prototype. A case study of an existing site is also explored and analysed to highlight various design principles. Finite Element is used to compare the results of the proposed Equilibrium Method, as well as assess temperature loading on the structure.

Chapter 7 covers the design of the remainder of the structure including the slab, the walls, the thrust components and the foundations.

Chapter 8 discusses and illustrates the construction process of the low-cost housing prototype.

A short summary of the costing of the structure is provided in Chapter 9.

Conclusions and recommendations are made in Chapter 10.

2. Literature Review

2.1. Introduction

Throughout the ages, structures and their forms have revolutionised and changed civilization dramatically. This change has been due to technological advances as well as social demands. Thin shelled structures have been in existance from as early as the late 1800’s. Architects and engineers, such as Eduardo Torroja, Heinz Isler, Dante Bini, and the like, were very active in the design and construction of these forms (Wilson, 2005). Architects are interested in and passionate for these structural types because of their diversity and ability to adapt to various climatic conditions (Joffroy, 1994). Their ability to cover larger spaces made them popular in the construction of religious buildings, schools, hospitals and simple low-cost housing (Joffroy, 1994).

Arches, vaults and the like have been around for thousands of years and many can still be found in the Middle East, North Africa and many European countries, where they were widely used (Joffroy, 1994). Even with a decrease in popularity, many of these countries still build these structures to continue the rich heritage and living traditions associated with these building forms.

Timbrel vaults form part of the thin-shell family of structures; however, their specific characteristics warrant a specific definition. It has been found that the most apt description is that “*timbrel vaults are masonry vaults made with brick and mortar, with a good strength in compression, and can be constructed with remarkable thinness and without the use of formwork. Their uniqueness derives from their construction: the bricks are placed flatly, forming one or more layers and they are constructed without centring or other support. The bricks are placed in arches or successive rings to complete the vault*.” (Huerta, The Mechanics of Timbrel vaults: A Historical Outline, 2003, p. 89). Timbrel vaults are an ancient form of construction initially introduced in the fourteenth century, but not until the sixteenth century did it become common practice (Huerta, The Mechanics of Timbrel vaults: A Historical

Outline, 2003). Currently, shells are not commonly used, even though its popularity has increased.

However, it was Rafael Guastavino who put his foot in the door regarding vaulting and he was particularly active in tile vaulting. It was Guastavino's theory of 'cohesive construction' that allowed the methods of construction of timbrel vaults to make the transition into the 20th century and therefore make a monumental imprint in the history of thin shells (Huerta, The Mechanics of Timbrel vaults: A Historical Outline, 2003). He refined the thousand year old building system of 'Catalan Vaulting', which involves a technique involving the erection of thin terra-cotta tiles. Catalan vaulting is the same practice as Timbrel vaulting, varying only by the name given in the various regions in which it is being constructed. Guastavino's tile vaulting technique contributed considerably to many prestigious buildings of his time, but little of his legacy. However, the structural behaviour of the Catalan vault has received considerable attention in literature (Atamturktur, 2006).

Guastavino made a number of material and construction technique breakthroughs. His main construction technique -- "Cohesive Construction Technique"-- is defined as the bond between the terracotta tiles and the Portland cement, due to cohesive forces. His greatest contribution to the technique was altering the traditional gypsum mortar (Plaster of Paris) with rapidly hardening Portland cement, thus enabling him to build vaults that spanned three to five times the typical span of traditional Catalan vaulting (Tarragó, 2002). The technical advancements made by Guastavino, in terms of material breakthroughs, allowed him to enhance his career to world renowned standings, starting with the design and construction of the Boston Public Library. The Guastavino era marks the highest point of the tile vaulting industry and thin shelled structures (Atamturktur, 2006).

Thin shells have become less popular over the years. This has been due to a number of factors, including high labour costs and the high cost of formwork (Wilson, 2005). Many of these factors are also relevant to the decrease in the use of domes, arches and vaulted structures. A major factor in the modern world of construction is the social aspect of acceptance. Thin shells are rejected by people for a number of reasons, ranging from cultural expectations to lack of modernism. Shell structures have been considered an expensive and difficult form of construction, but if designed for local conditions, they can eliminate many of the considered and current problems (Wilson, 2005).

These structures have many advantages. Domes and vaults have been found to be economical, safe and aesthetically pleasing. They require the minimum use of materials, which may be produced locally and at a low cost (Wilson, 2005). Joffroy (1994) outlines a number of advantages and opportunities in using vaults, which include job creation, foreign currency savings, great aesthetic potential, wide variety of uses and economic benefits. Huerta (2003) found that thin shells are an excellent alternative to floor and roof systems, as they provide exceptional fire resistance.

In most parts of the world, there is a significant need for earthquake-safe housing, and these forms have proved to be extremely effective in resisting these natural disasters (Joffroy, 1994). Through the use of innovative techniques, many of the above stated problems can be eliminated. The use of vaults and shells in construction are relatively foreign in this age; however, there is constant research and development programmes being carried out to improve the design and construction of shells. Recent interest and improved technology have allowed for the design and construction of these unique structures to be mastered once again and a considerable amount of increased knowledge to be added to this research field. (Joffroy, 1994).

A significant cost in the construction of low-cost housing is the roof structure, and the deficiency of good quality and readily available materials. An alternative structural form is necessary to minimise these costs, preserve tradition and make use of local and easily accessible materials. This form needs to satisfy local conditions which include cultural, economic and climatic aspects. In the form of vaults, Joffroy (1994) provides a valuable alternative.

"*Dome structures not only provide great strength, but do it by using less material than other structures."* (Wilson, 2005, p. 9)

2.2. Materials

Shell structures have been built for centuries using various building materials, ranging from straw and grass to reinforced concrete. The construction of thin shells in modern-day sees the use of reinforced concrete to be most effective due to its strength and durable characteristics. For this reason, most of the available literature refers to ‘*thin shell concrete structures’* and ‘*advancements in reinforced concrete shells*’ (Cowan, 1977).

There are a number of material options that require investigation when designing and constructing a thin shelled structure. Wilson (2005) constructs his structures out of reinforced concrete as this allows for versatility in design and thus allows for the construction of any desired shape. It also allows for thicker, larger structures to be built, without the need for complex thin shell theory to be applied. Concrete is readily available in many locations and requires minimal maintenance if used correctly. However, it is an expensive method of construction due to the need for cement and steel reinforcing. Guastavino rejected the use of reinforced concrete due to the excessive cost incurred in their construction and “*problems with irregular setting of the concrete*” (Huerta, The Mechanics of Timbrel vaults: A Historical Outline, 2003, p. 104). Cement requires a large amount of energy in the production phase, and is responsible for emitting greenhouse gases into the atmosphere. Thin shells require a much smaller volume of material when compared to standard methods of construction, and this makes them more economical and therefore results in a large reduction in energy consumption and pollution (Wilson, 2005). A new building material needs to be established to further reduce the cost of construction. It is important to note that due to the thin nature of shells, bricks and tiles may be used in their construction.

2.2.1. Tiles

There is a considerable amount of information covering the structural mechanics of reinforced concrete thin shells. However, there is far less literature on the structural behaviour of tile vaulting. Although this type of construction has been around for over seven hundred years, interest in building these types of structures declined during the twentieth century (Ochsendorf, 2010). It is only recently that a renewed interest in tile vaulting has been established, as the properties of this material allows for more advantageous construction projects to be carried out with respect to available skills, flexibility within the structure and construction costs (Ochsendorf, 2010). Not to mention the much lower environmental impact in comparison with reinforced concrete shells.

Guastavino established that due to the lighter weight of the tiles, they create a lower horizontal thrust than conventional masonry structures. Tiles are brittle, and therefore they are strong in compression, but very weak in tension. This is important for the modelling and designing process as no unwanted forces are to be created in the construction phase otherwise the material may fail (Ochsendorf, 2010). The lack of space between and around the tile does not allow for safety reinforcing to be positioned in a structurally viable way.

Huerta (2003) identified that the main reason behind the use of "*fast-setting mortar*" and "*thin-brick*" (Ramage, 2004) or tiles is that not only do these materials allow for large areas to be covered "*gracefully and economically*", but have also found that low levels of tensile forces, shear forces and moments have been detected in these structures during various load tests.

Figure 2-1, by Guastavino, is a good example that demonstrates the construction process and hence the method of using tiles and fast setting mortar for construction purposes (Ochsendorf, 2010). Figure 2-1 explains how the first layer utilises fast setting mortar to obtain the correct geometry. Each succeeding layer is laid by applying a layer of mortar, the first layer which now acts as formwork.

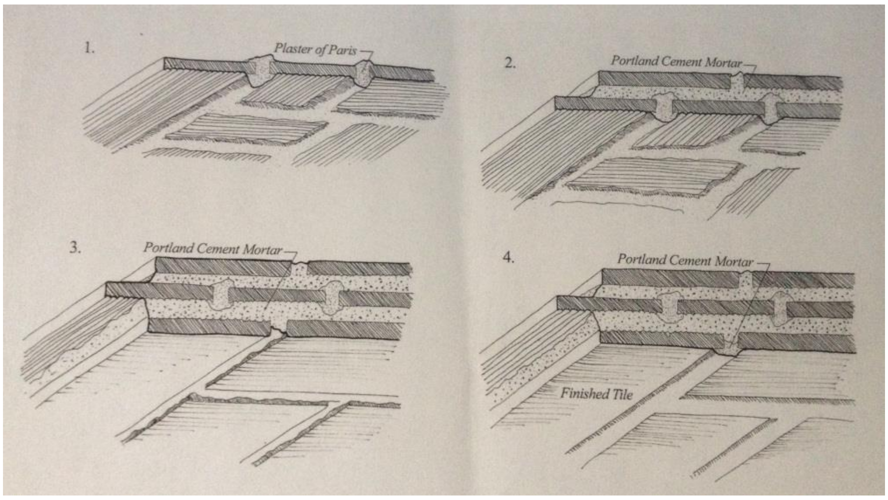

Figure 2-1: ***Four stages of mature Guastavino tile construction procedure*** **- Ochsendorf (2010, p 127)**

Investigations into the viability of the use of masonry methods for present times are currently underway, with the initiation of various projects around the construction of tile vaults. One such project is the construction of vaults from stabilized earth tiles in Mapungubwe in Limpopo, South Africa (Figure 2-2). A paper presented on this project states that "*Currently, research is being undertaken both to increase the strength of the tiles in compression, tension and shear, and to simplify the method of construction to facilitate less-skilled workers with relatively low levels of supervision*" (Fitchett, 2009b).This is an indication of attempts to re-employ the use of tiles in vault construction as it is proven to be a successful method. The Mapungubwe project was highly successful and won various architectural awards due to its aesthetic appeal.

1994).

Figure 2-2: Mapungubwe Interpretation Centre

2.2.2. Bricks and Blocks

2.2.2.1. Solid Components

Joffroy (1994) identifies various building materials and addresses their pros and cons in terms of construction. The adobe block is one which is prepared by moulding soil and allowing it to dry. This is done in wooden moulds and dried in the open air (Bahar *et al*., 2004). It is the least expensive material, easily adaptable to shape, size and method of construction. However, the strength of this block is low and exhibits poor mechanical properties (Joffroy, 1994). It also exhibits unsatisfactory results in terms of surface cracking, durability and water resistance. However, metallic moulds and mechanical compaction are used to improve the blocks performance (Bahar *et al*., 2004). This material is predominantly used in self-building housing projects in rural areas (Bahar *et al*., 2004).

Gothic cathedrals, and other old architecture, were constructed with the use of stones (Fitchen, 1961). Stones offer various possibilities, but they are heavy, time consuming to shape and possess highly variable mechanical properties (Joffroy, 1994).

The oldest form of earth construction is that of rammed earth. It involves pouring the material into pre-prepared formwork. The material consists of earth stabilised by natural fibres or binders, and is poured in sections and compacted manually to construct an entire wall. The properties of the soils used should include large grain sizes. There are a number of projects that can be found in Algiers, Algeria where prototypes and housing projects have made use of rammed earth methods (CNERIB, 1991). This method has also been used to construct low cost grain silos where earth material was stabilised with wheat straw (Bartali, 1991).

The fired solid brick is an expensive form of construction but generally performs well for all dimensioned buildings and is versatile in its shape and size. The fired hollow brick is lighter than the standard solid brick but requires special application techniques (Joffroy, 1994).

The compressed cement bonded earth block (CCBEB) is a viable alternative to more costly forms of construction, i.e. the fired brick. This block has good mechanical strength, but may deteriorate when exposed to water (Joffroy, 1994). Cement Stabilised Earth Blocks (CSEB) are blocks made from raw or mixed soils, stabilised with cement or fly ash, poured into a press and compressed with either a manual or mechanical press, forming the required building block (Auroville Earth Institute, 2012).

There has been considerable research done in CSEB, particularly in Algeria, as a solution to low-cost housing (Bahar *et al*., 2004). Earth construction is relatively abundant and makes use of cheap labour. Soil-based construction methods have been used throughout North Africa for centuries, particularly in the form of blocks, and in Algeria, the earth block is the most commonly used building material. However, it was found that the problems associated with earth blocks are that of shrinkage cracking, low strength and lack of durability. Therefore, continuous maintenance is required and technological improvements are needed to resist the effects of water. Furthermore, soils vary from one region to another and this needs to be incorporated in the experimentation and specification process. These historic structures are an inspiration to modern architecture, but there is a need to improve the properties of these materials. Through considerable experimentation, it was found that the best option is that of cement stabilisation in conjunction with mechanical compaction (Bahar *et al*., 2004).

A major obstacle in masonry development is that of social status. Earth construction is considered a material for the poor, due to its low quality and durability, as well as affordability and abundance. However, materials such as cement, aggregate, steel and fired bricks are lacking. Sometimes these materials need to be imported, and are expensive. Concrete, besides the high cost, is found to have a low thermal performance. Therefore, it is important for future construction to lean more towards environmentally friendly and cheaper materials. Earth construction is a strong and viable solution, which has considerable traditional meaning within the local communities, as well as excellent thermal properties (Bahar *et al*., 2004).

2.2.2.2. Binder Components

Mortar is a component that is overlooked when discussing optimisation of material costs. The four major alternatives in the use of low-cost housing are: earth mortar, stabilized earth mortar, lime-sand mortar, gypsum mortar and cement-sand mortar (Joffroy, 1994). All of the above alternatives vary depending on whether bricks or tiles are used in conjunction with the binder for construction and their components.

Cement-sand mortar is the most readily used binder, but also has a high cost. It is important to limit the amount of cement used in the mortar so as to minimise the costs without jeopardising the overall strength. The mortar is very effective in bonding good quality fired earth bricks as well as sand-cement blocks. They have been effective in the construction of medium-span vaults (Joffroy, 1994).

Earth mortar is historically used to bond adobe blocks, fired bricks and stone. The mortar has excellent sticking abilities and allows for easy construction of vaults, without the need for shuttering. However, it is extremely susceptible to shrinkage so it is important that straw or sand is added to a mix which contains an excessive amount of clay content (Joffroy, 1994).

Stabilised earth mortar is earth mortar with the addition of a stabiliser in the form of cement, lime, plaster or bitumen. This mix is also effective in conjunction with fired bricks or compressed earth blocks (Joffroy, 1994).

Lime-sand mortar is useful in that it is very malleable and sets extremely slowly, thus increasing the workability of the mortar. However, this mortar does portray average characteristics and relatively low strength. There are methods to improve it through the addition of crushed brick or pozzolanas. It is generally used in conjunction with fired blocks or stone (Joffroy, 1994).

Lastly, gypsum mortar sets extremely quickly allowing the application of adhesive techniques to be used. This mortar can be stabilised through the addition of lime. Therefore, smaller scale vaults or models can be made quickly and efficiently using this mortar (Joffroy, 1994). It has been found that a fast setting mortar, such as gypsum mortar, has needs that must be met to ensure that the construction is done correctly and the bricks adhere effectively. Ramage (2004) found that by soaking the bricks in water, before applying the plaster, allowed the mortar to adhere better to the brick. The mortar also needs to be mixed in small batches and applied to one brick at a time.

2.2.3. Surface Protection

Depending on the type of materials the engineer decides to use, various maintenance problems can occur, i.e. durability problems, infiltration, cracking, etc. In particular, it is important to protect vaults and domes from infiltration of rainwater and preserve its durability. This can be done in a number of ways with the main aim consisting of channelling the water away from the building using downpipes or waterspouts. Depending on the budget at hand, various methods of surface protection can be applied (Joffroy, 1994).

Various forms of materials, as discussed previously, differ in terms of maintenance and effects caused by weathering. Almost all shells made of earth bricks, concrete or clay bricks are extremely susceptible to cracking when constructed with tension-weak materials. This leads to infiltration and water damage. While adobe blocks and other earth based blocks and bricks require more maintenance as water damage will cause durability issues (Joffroy, 1994).

An earth plaster is the cheapest solution but requires regular maintenance depending on the quantity and nature of rainfall, the area in which it is situated and the various forms of weathering it is exposed to. A sand-cement mortar would crack as it is too rigid; therefore, a corresponding membrane should be used in conjunction. The better render solution is one of lime-sand and gypsum-lime-sand, as they have greater malleability but some maintenance would still be required (Joffroy, 1994).

A further option for surface protection is a form of roof covering. Adding another layer of material on top of the vault will protect the primary layer. Previous and current solutions include thatch, tiles, stones, etc. These can also provide another means of directing the water away from the roof without much notable infiltration. If done correctly, these solutions can still be cheap and extremely effective, requiring minimal maintenance (Joffroy, 1994).

A common method which has been applied to a number of projects is the use of membranes as a layer on the outer surface of the vault or dome. This can be done in a single or multiple layers of bitumen-based membrane, metal leaves or acrylic-fabric membranes. Another popular membrane is that of waterproof paint. This solution, although effective, is relatively expensive (Joffroy, 1994). An example of this form of waterproofing can be found at The Sparrow Aids Village in Johannesburg (Figure 2-3). This village has experienced considerable cracking and a membrane has been applied on the outer surface of the domes to minimise water damage. The membrane used is a fabric over which an acrylic waterproof paint is applied. This material is extremely effective, as it is flexible and capable of withstanding thermal movements. It has improved the domes quality considerably, and now there is minimal, if any, water infiltration within the domes.

Figure 2-3: ***Left:*** **A cracked dome at the Sparrow Aids Village;** ***Right:*** **A membrane layer is applied to the cracked dome**

The choice of the shape is crucial in terms of construction and economic efficiency. The ideal option in minimising infiltration problems is to construct a sloping roof. This allows for the water to drain naturally off the structure and not gather in a section of the roof, resulting in infiltration. Infiltration is generally not an issue for rounded structures, as these forms are quite steep and only a small gradient is required to allow for natural drainage.

2.3. Forms, Modelling and Spacing

Form finding is an extremely complex process which entails finding a shape which is structurally sound. This step is generally done well through the observation and identification of problems in other structures of similar form. Mimicking natural shapes is extremely important in order to achieve a strong solution; with one of the best examples being that of an egg. Although an egg is made of somewhat weak and soft materials, its oblong shape is extremely strong. There are many forms of vaults ranging from the barrel vault, being the simplest, to more complex vaults like the domical vault and so forth (Joffroy, 1994).

Safety is essential when designing structures, and many countries worldwide need to design for seismic action. Thin shells have been found to be extremely effective in terms of withstanding earthquakes, hurricanes and the like (Wilson, 2005). Building a domed house is a safer, more economic, longer lasting and easier option than building a standard similar sized house (Wilson, 2005). A good example of this is the construction of a home on Pensacola Beach, Florida, designed by Arnold Wilson. The house withstood Hurricane Ivan with minimal damage, while surrounding properties, following standard designs, collapsed (The Weather Channel, 2009). Furthermore, the structure withstood a further two hurricanes, Denis and Katrina. Wilson (2005, p. 13) states that "*The storm surge forced water through the ground floor garage and tore away the breakaway staircase. The living quarters were undamaged*."

Fire is another safety feature that needs to be incorporated in all designs. The South African Standards Code of Practice stipulates that there must be a specified amount of time that the structure needs to be standing so that all personnel in the building can evacuate safely (SABS 0100-1: South African Standard Code of Practice; The structural use of concrete, 2000). In 1988, a large domed grain storage facility in Alabama caught alight and burned for 20 days without collapse (Wilson, 2005). Eventually, a dust explosion occurred within the structure and the top of the dome burst off, allowing for a relief valve to be created, and in turn saved many lives as well as the surrounding property (Wilson, 2005).

The process of form finding, with regards to thin shells and vaults, is not well covered. One exception is the engineer Heinz Isler – who is considered the pioneer of the fabric form-finding method. "*A method of form-finding used by Heinz Isler is to suspend a membrane between supports disposed in the same relative positions as in the real structure and leave it to deform under its own uniform weight. Under this load the membrane takes up a shape such that, within it, only tensile forces are present, as a cloth affords no resistance to bending or compression*" (Chilton, 2000, p. 35). Once the cloth is suspended from all four points, it can be soaked in water and frozen or covered in self-setting polyester resin, until a solid form is achieved. The form is inverted so that the cloth will be in pure compression as opposed to its natural, hanging tensile state, thus achieving the desired shape (Chilton, 2000).

Atamturktur (2006) investigates the effects of vibration and dynamic testing of spherical structures in order to test the structural form. He also utilises his research to investigate various design methods.

Atamturktur bases his design procedure of domes on the Finite Element Method of modelling. He describes finite element analysis (FEA) as an "*approximate numerical method that solves for the distribution of forces, displacements, or strains in a system*" (Atamturktur, 2006, p. 90). His approach in completing an FEA is to "*build an analytical model, which idealizes the variables of the structure under study: geometry, material properties, and boundary conditions, as well as existing or possible loadings…fine tuning the FE model by comparisons of analytical and experimental frequencies and mode shapes*" and finalizing the procedure "*with the determination of the static state of stress, strain and displacements*" (Atamturktur, 2006, pp. 90-91). As with any project, it is important to make valid assumptions in order to design the structure efficiently. The most important assumptions that are noted by Atamturktur include: a uniform thickness of the shell, all materials can be assumed to be isotropic and homogeneous, the structure is subject to linear elastic behaviour of materials and minimal deflections occur.

Various research has been completed in the construction of medieval vault erection, in particular gothic cathedrals. Gothic cathedrals date back to as far as the 12th century and many of them are still around today. Their structural knowledge was far advanced in comparison to their technology and various observations have been made that are of significant importance (Fitchen, 1961).

Fitchen (1961) identifies that the simplest and truest type of vault is that of a semi-cylindrical barrel vault. They are structurally sound and extremely simple to construct. The semi-cylindrical barrel vault was extremely common and extensively used within the gothic cathedrals, but a problem with this form was that it did not span very effectively, prohibiting the maximum height that was to be achieved, as well as minimising the amount of light made available within the structure. The semi-cylindrical vault was found to be a poor form structurally for cathedrals. A new shape and solution needed to be found.

As the Gothic era progressed, it was found that many of these vaults tended to be strongly pointed at the tip and this caused many structural troubles in the form of cracking and even collapse. Thus, after considerable experimentation, it was found that a structure which carried no surcharge and therefore, only supports itself would prove to be the ideal form. This, in short, is the catenary form (Fitchen, 1961).

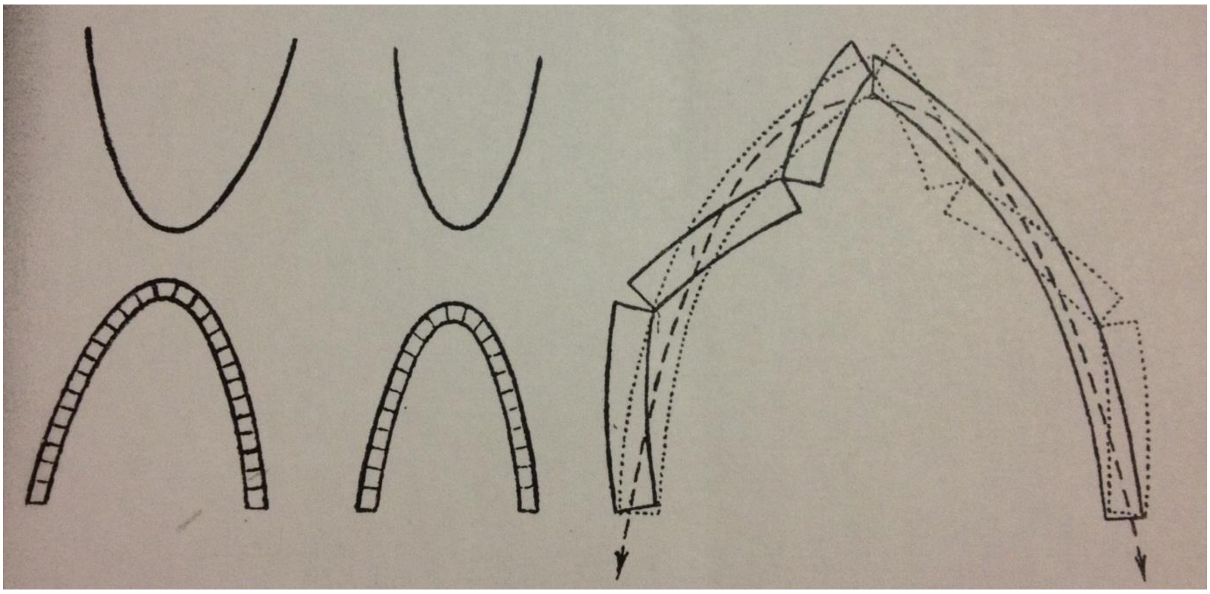

Figure 2-4: ***The catenary Curve and the Gothic Pointed Arch*** **- Fitchen (1961, pp. 81)**

A catenary is a curve which is created when a chain or cable is allowed to hang loosely from two edge points, and creates a natural curve that is in complete tension (Figure 2-4). If this chain was rigid so that it does not deform when flipped, it would be found to be completely in compression. This compressive form is a catenary. This method is particularly effective as it ensures that the line of thrust is on the centre line of the shell, which therefore eliminates the creation of the pointed arch. However, due to other forms of loading, including wind, thermal loads, etc., it is important to ensure the thrust line is kept within the middle third of the thickness of the structures to prevent the development of tensile forces and possibly cracking. (Fitchen, 1961).

Conant (1944, p. 127) states:

"*the pointed arch is an approximate catenary, and it is a fact that unless an arched structure has the catenary form, extra strength is needed in the arch to keep itself intact, quite aside from the thrusting action generated in an arch of any kind."*

Fitchen (1961) discusses that because no gothic cathedral or arches had an actual catenary curve, the builders had to make adjustments to prevent them from deforming or cracking. This was done by placing a layer of light-weight rubble, tiles, copper coverings or any other such material, on top of the curved structures.

Research has found that the catenary is the most effective shape, predominantly due to the natural shape of the curve under self-weight. Joffroy (1994, p. 9) states that *“The catenary vault is very common as its form gives maximum stability for a minimum use of material”.*

There are various aspects that need to be considered when selecting your form and design. Joffroy (1994) suggests the following as the most important architectural and engineering design considerations:

- Building
- Spatial considerations
- Building complexity
- Architectural appearance
- Acoustics
- Stability of vaults/arches and supports
- Details and finishing

The method of building is an area which plays a significant role in determining the overall cost of the structure. The size and shape will depend on the building method, as well as amount of scaffolding necessary to complete the project. These aspects will determine the preferred dimensions for the structure (Joffroy, 1994).

Spatial considerations in designing are of extreme importance. An advantage of using vaults and arches is that of both increased variable space and height. However, the challenges of creating dead space needs to be considered when designing a dome. Architecturally, this is important in terms of usability. The building should not contain dead space; particularly within low cost housing. The maximum space needs to be available to the home owner for usability and flexibility to move between these spaces (Joffroy, 1994) (Figure 2-5).

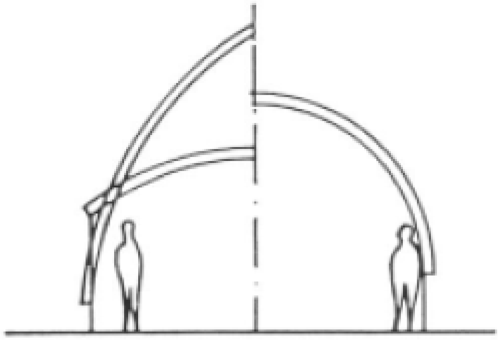

Figure 2-5: Maximising on space and usability in various forms and designs - Joffroy (1994, p 16)

The method of constructing these structures can range from basic construction methods to extremely complex. A sophisticated system is the most efficient and optimal route and makes use of its materials effectively and keeps costs at a low. However, a sophisticated system can be challenging as construction is more complex, increasing the chances of mistakes during construction. A simple construction process is generally preferred to eliminate the possibility of any mistakes, and to ensure that the structure is as optimal as possible (Joffroy, 1994).

The architect plays an important role in the design phase of the project. They can offer many design variations of the structure whilst adding considerable aesthetic appeal. The architect can effectively optimise the space availability of the structure. They are essential in ensuring social acceptability and cultural preservation (Joffroy, 1994).

Acoustics is an aspect generally over looked but very common in curved shapes. Depending on the intended use of the space, a high degree of reverberation can be created, and this can serve as a disadvantage or an asset. There are various simple methods that can be implemented to minimise the acoustical effects; such as suspending cloths (Joffroy, 1994).

Vaults and arches, due to their high thrust forces, need to be designed and supported effectively in order to prevent the structure from collapse. A thrust force is that force which pushes out the supporting bases. The size of it will vary depending on its degree of flatness, the span and weight of the structure. Therefore, the structure needs to be as close as possible to the line of thrust to ensure that the form is stable. There are a number of ways to contain the thrust force; these include cancelling it out by juxtaposition, widening the walls, adding buttresses and ties or ring-beams (Joffroy, 1994). The use of buttresses is very common in the design of shells. The function of the buttress is to channel the outward thrust from the vault to the vertical walls and in turn, to the ground, safely (Ochsendorf, 2010).

The catenary form allows for more flexibility and leeway to the desires and needs of the designer, such as high levels of light. One of the distinctive features of gothic cathedrals is the numerous glass windows and the amount of light. This was identified and applied to many of the cathedrals that can still be seen today.

Joffroy (1994, p. 17) emphasises the importance of using catenaries: "*In the case of vaults, for evenly distributed loads, the best form resembles that of an inverted suspended chain (catenary). This applies both to flatter and slender forms.*"

Some examples of projects that have successfully made use of catenaries include:

- Keleti Railway Station, Budapest, Hungary
- Casa Mila, Barcelona, Spain (Figure 2-6)
- Sheffield Winter Gardens, Sheffield, England (Figure 2-6)
- Gateway Arch, St Louis, United States (Figure 2-7)
- The Pantheon, Rome, Italy (Figure 2-7)

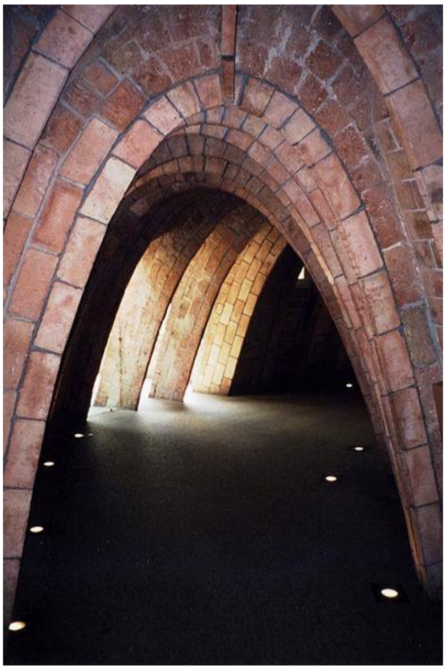


Figure 2-6: Casa Mila, Barcelona (left - (Sennott, 2004)) and the Sheffield Winter Gardens, England (right - (Hymers, 2005))


Figure 2-7: Gateway Arch, US (left (Grigonis, 2011) -) and the Pantheon, Rome (right)

2.4. Construction Methods

"*In all cases, the professional training which is given during project implementation is an asset which can benefit the whole community. Involving local tradesmen,* *entrepreneurs, architects, engineers and draftsmen, ensures the possibility of spontaneous and correct replication of the building models proposed and their dissemination."* (Joffroy, 1994, p. 12)

Shell structures have a unique shape which requires skilled labour for successful construction. Professional training needs to be provided to construction workers to ensure that the desired form, which is of critical importance, is achieved to prevent structural damage or failure. This technique can be mastered relatively quickly with the use of correct tools and effective training. In addition, the engineer also requires specialised knowledge and understanding in the theory of thin shells before attempting to design such a structure (Joffroy, 1994). The architect needs to have a broad knowledge of the form to enable the efficient use of technology in terms of creativity and evolution (Joffroy, 1994).

There are various forms of construction that have been identified and used in the medieval times. The foremost construction methods used include earth mounded form (both in full and in section), continuous wooden boarding formwork, and a sectioned boarded formwork using much less wood. As can be noted, wood was the predominant material used in formwork, due to its inexpensiveness and availability (Fitchen, 1961).

We have advanced considerably in both technology and knowledge on construction since medieval times. Various more modern construction methods have been explored all over the world using an assortment of materials. The majority of the information that is available is on reinforced concrete shells are found in publications such as Wilson (2005), Allen and Zalewski (2010) and Cowan (1977). There is very little information on tile or brick construction, but there are a few recurring methods which appear in majority of the reviewed journals e.g. inflatable formworks, visual guides, Cupola Tracer, etc. (Gohnert, 2011).

2.4.1. With Formwork

Arches, vaults, domes and cupolas require different methods of construction. The focus will be predominantly on arches and vaults, which are built in a very similar manner.

The first suggestion is one of constructing a formwork of the same shape as the arch or vault. The formwork material is usually, but not exclusively, wood or metal. The formwork needs to be collapsible and therefore easily removable once the structure is complete. This not only eases the construction process, but also allows for the reuse of materials. Therefore, the formwork should be robust and precise to ensure maximum quality. This method is effective in low-cost housing schemes where structures have the same shape; therefore, the formwork can be reused, minimising construction costs. Other types of formwork include that of earth formwork and balloons. Earth formwork is used as a base when building with blocks and bricks, which are covered by a layer of mortar forming the desired shape. However, this is not a reusable type of formwork and is also more time consuming (Joffroy, 1994).

A sliding formwork is limited to only barrel vaults, but proves to be a very effective option. The sliding formwork method is extremely economical as the formwork is simply repositioned through sliding, as stages of the vault are completed (Joffroy, 1994). The method of sliding was used in the construction of several abandoned buildings in the township of Bapong, South Africa (Figure 2-8 and 2-9). These structures have been standing for decades, but are in excellent condition due to their high quality construction. It is important to note that even if the design is excellent, the method of construction is just as important and sliding formwork allows these precise shapes to be constructed effectively.

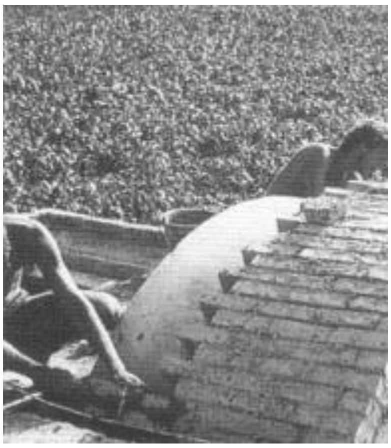

Figure 2-8: A sliding formwork used to construct a vault (Joffroy, 1994, p 20)

Figure 2-9: The vaulted roof in Bapong Township was constructed with a sliding formwork

Another method of construction, which has not been used as much as standard formwork, is one of an inflatable balloon. It is an effective way of building as it is extremely economic since it can be easily reused (Wilson, 2005). This method was suggested by Wilson (2005) and the use is demonstrated in Talocchino's (2005) masters' dissertation. Wilson (2005) used the balloon method to create a shell out of reinforced concrete. Talocchino's (2005) shell was constructed in Johannesburg (Central Johannesburg College). The shell was constructed by inflating a large balloon, with a shape identical to the shape of the shell. Contrary to Wilson, Talocchino was able to reuse his formwork, since it was deflated and removed after construction.

Other projects done in Southern Africa have used other innovative methods of construction. In Buane, Mozambique, a Cupola tracer was used to form a shell which rotated around a centre pole as formwork. This formwork was built using the exact dimensioning of the domed shape, thus guiding the workers during construction. They only had to turn the rotating arm to place the bricks in the correct positions. The major drawback with this method was the difficulty in constructing the apex, as the bricks were slipping with the use of conventional mortar. Thus, an earth mound formwork was used for the final stages of construction. This caused major inconsistencies in the construction as the precise shape could not be achieved at the apex (Gohnert, 2011).

Using formwork eases and speeds up the process of construction, however, certain structures have curves and forms that are too complicated or expensive to replicate and manufacture; therefore, construction without formwork needs to be explored.

2.4.2. Without Formwork

Arches can be built in a simple manner without the use of formwork. This is done by constructing each succeeding course slightly higher than the preceding one and so the previous layer is used as formwork.

The ‘Splice’ method is the most economic and efficient method. By using small and fairly thin members, each successive layer makes use of the previous layers mortar, improving its cohesion. It is therefore laid in layers, face on, at a steep angle to the vertical so that it doesn’t collapse. This principle can be used with varying shapes and sizes to build barrel, groined, dominical, etc. vaults (Joffroy, 1994).

Joffroy (1994) also determines that one can build a structure ‘by eye’ with the assistance of light tools and guides, such as masonry to ensure the accurate shape is obtained.

The final method of construction is that of *increasingly inclined rings*. This is a method which consists of constructing rings of tiles or bricks in layers, from the bottom up to the apex. Each successive layer decreases in diameter as construction moves up towards the centre. The technique is similar to that of the ‘slice’ method, where a simple rotating guide is implemented to delineate the general shape in the air before the correct form is built (Joffroy, 1994).

An example of the ‘no formwork’ construction method is that of Ramage (2004). Ramage constructed his own Catalan vault in hope of investigating various construction methods and highlighting their various strengths and weaknesses.

Ramage (2004) refers to Catalan vaulting as a “*monumental construction method*”, which relies on fast-setting mortar for construction and the structural form for strength. This method, also referred to as the Cohesive Construction technique, requires no formwork, even when spanning large open spaces. This is important as the most valuable aspect of the vault is the final form once completed. This technique allows for effective spanning of large areas, gracefully and economically.

The groin sections (of parabolic shape) in Ramage's vault were not constructed using this technique and thus formwork had to be built for these sections, allowing for easy construction. The central vault is therefore defined by the curves of the groin. Wooden battens were cut to length and used as a guide to direct the builder during construction. After the formwork had been designed and finalised, construction began and the first layer was laid using Plaster-of-Paris, setting in approximately 10 seconds. "*This is the key to the system: a fast setting mortar on two edges of a tile allows it to hold itself after being tapped into place. No formwork is needed*" (Ramage, 2004).

This structure was made using thin bricks (not tiles) and proved to be extremely effective. He started construction at the corners, working his way to the centre of the vault. The second layer is applied directly on the first layer, which now serves as formwork. The second layer was laid in conjunction with weatherproof Portland Cement Mortar instead of quick-drying plaster, as instant setting is no longer a concern. Ramage built his structure by standing on the outside to allow for easier access, but it is important to note that typically such a structure is built whereby the builder stands at the centre of the form and builds in a circular fashion around him and eventually from below. The application of these techniques, and essentially the shape and form of the vault, ensure that the structure is of the highest strength and within a day, the tiles have set and are able to hold their entire weight.

The Mapungubwe project utilized a very simple but effective method of construction: '*Without formwork or centring, the masons construct much of the vault by sighting between completed portions and curved plywood guides'* (Fitchett, 2009b, pg. 4). The construction process does need to be monitored by an experienced contractor to ensure that every tile gets placed in the correct position. It is also important to construct large reinforced concrete buttresses as the span of the vault needed several layers of tiles to achieve the required strength, hence creating a greater horizontal thrust (Fitchett, 2009b).

Atamturktur (2006) makes a very important note on horizontal thrust. He discusses how Guastavino and other scholars believed that a unified dome exerts minimal horizontal thrust, but since these structures are clearly not perfectly rigid, a larger horizontal thrust needs to be considered in the designing process. Despite Guastavino's arguments, his calculations have always taken horizontal thrust into account. Thus, it is important that a base is set during construction to resist horizontal thrust, i.e. steel ties or buttresses.

The construction market is a relatively conservative market and a new idea is generally relatively difficult to implement. Thus, prototypes and pilot projects are necessary to promote such activities and convince the market of the success of this form. This can also be done through the construction of buildings of interest, which the general public is more likely to appreciate and support. The public has a social responsibility in determining what an acceptable structure is. By providing them with an understanding of the possibilities that these structures can offer, we will more likely be successful in convincing the public that these forms are the future. This can be utilised to implement a more economic housing project. However, in developing countries, where funds are not as readily available for construction, rash and successful pilot projects of housing can be sufficient, but are more risky in not being socially accepted (Joffroy, 1994).

High quality design and construction are important factors in gaining public confidence around new types of structures. For example, excessive cracking and sloppy construction can create uneasiness within the public about the structural robustness of such a form. Efficiency is a good indication; a structure which takes months to build with constant delays does not offer a sustainable and effective solution to the public. Thus, good organization and effective planning on site will provide the public with the confidence they require to accept the newer structural forms, such as thin-shelled structures (Joffroy, 1994).

2.5. Conclusion

Thin-shelled structures are a possible solution to the low-income housing problems experiences in South Africa and other developing countries across the world. The aim of this thesis is to establish a proficient low-cost housing solution through the process of form-finding, design and construction of a prototype home that will be monitored in the future. This research attempts to design the cheapest, most efficient, and strongest shape for the specific purpose that these structures become an answer the South Africa’s housing problem.

3. Layout and shape establishment

3.1. Design Considerations

”House design can be defined as the organization of space in such a manner as to provide for the domestic needs of present day society in the most economical and efficient way” (Calderwood, 1953, p. 33)

There are a number of aspects that need to be considered when selecting the internal layout of a house. The circulation of the house is defined by the overall flow and practicality of each room in relation to the remaining rooms to create a normal living environment. A good circulation throughout the house indicates a good layout where each room needs to be strategically positioned (Calderwood, 1953). Low-cost housing has less flexibility in changes in design due to the lack of space. Because of this it is even more essential to establish a good layout to maximise on the space that is available.

There are a number of key elements that have been highlighted by Calderwood (1953). Window arrangements, kitchen to bathroom distances and bedroom placement are essential. It is essential that bedrooms have some sense of seclusion, even in a low-cost house. Various examples of bad circulation were examined. The main areas of bad practice include: minimal seclusion of bedrooms, all rooms opening off the kitchen, common bathrooms placed between bedrooms, etc. Highly complex arrangements are also ineffective and expensive. They generally tend to create a lack in comfort and ease of living i.e. external bathrooms, major storage areas, etc. Figures 3.1 and 3.2 are examples of poorly designed houses. A simple design is usually the most effective solution, as demonstrated in Figure 3.3.

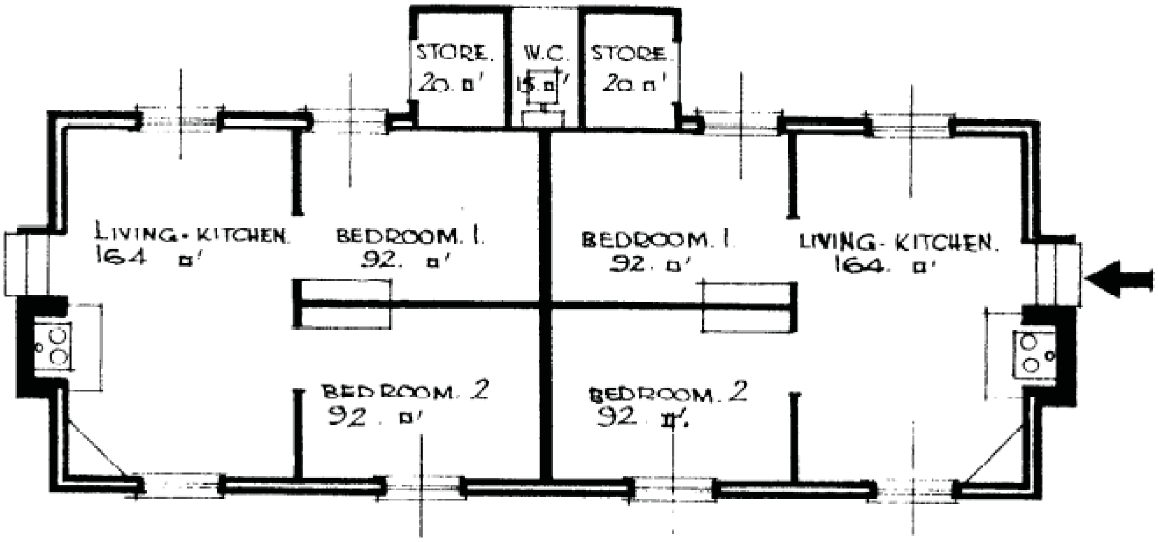

Figure 3-1: Type Plan Built in MacNamee Village, Port Elizabeth (Calderwood, 1953, p19-21)

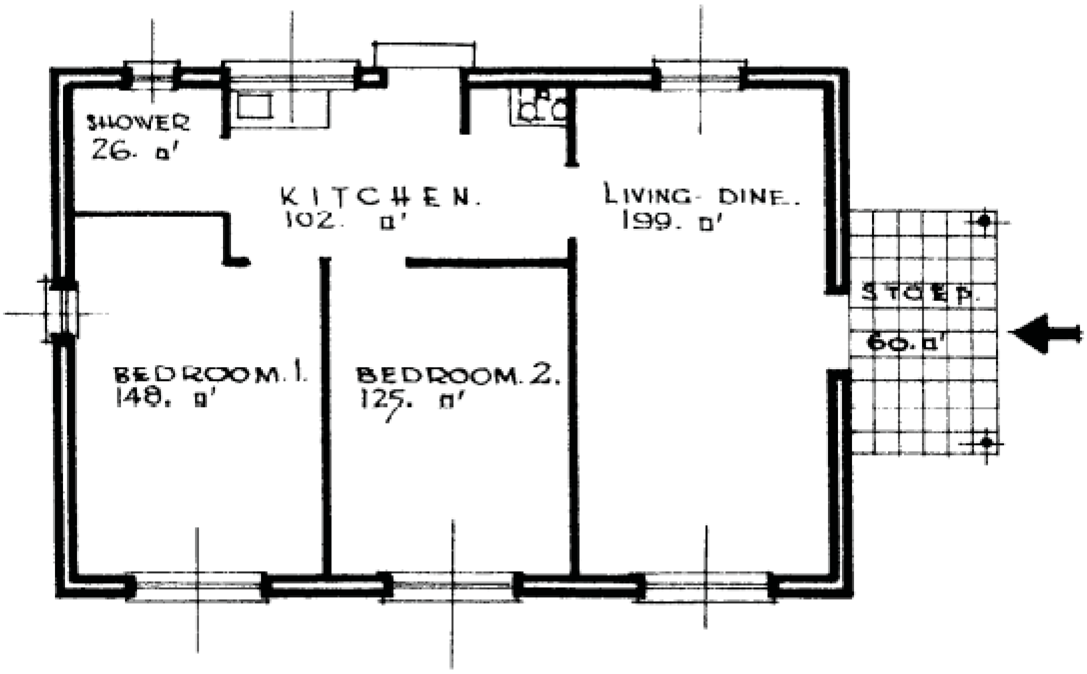

Figure 3-2: Type Plan Built in Orlando, Johannesburg (Calderwood, 1953, p19-21)

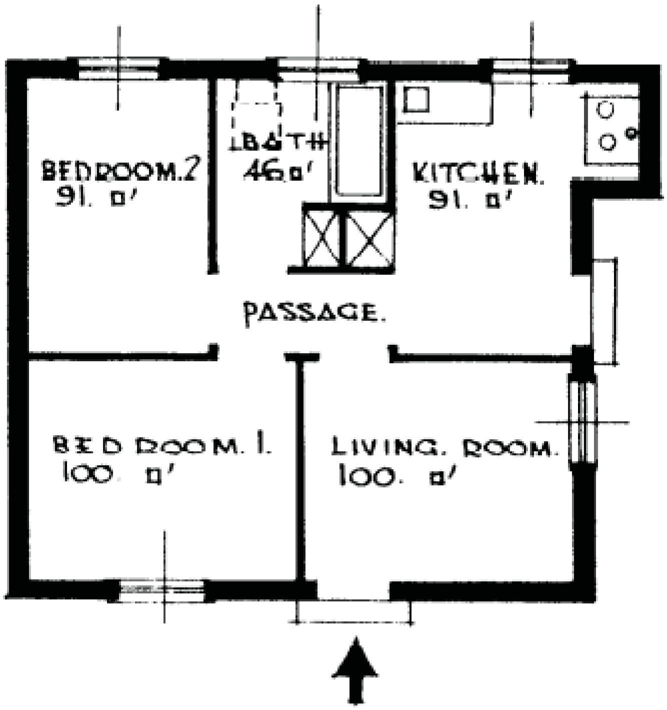

Figure 3-3: Type Plan Built in Sharpe Township, Vereeniging (Calderwood, 1953 p19-21)

When selecting a layout for low-cost housing, it is essential to ensure that all basic needs of people are met in such a small space. This incorporates protection to people against weather conditions, crime and other such elements. However, the main challenge is providing a flexible plan which can satisfy people's needs at present as well as for future generations (Calderwood, 1953). Social design is important as demands of people are constantly changing and acceptance by society is important to ensure that the project/prototype is effectively implemented. The design needs to be simple to ensure that all costs are minimised, but also to allow for adaptiveness. This may be in the form of design, construction materials or methods.

Another field that is extremely important in the housing construction industry is that of site selection. Site selection has direct bearing on the success of a project. The type of environment established and developmental costs vary considerably, with different sites. When selecting a site, the following aspects need to be taken into consideration: zoning, health, transport, job opportunities, services, topography, soil conditions, social survey, area and shape of the site and the cost of the land

(Calderwood, 1953). For many low-cost housing programmes, choice in site is limited, but these areas can still be explored in improving the existing site.

3.2. Design Selection

The currently implemented low-cost housing scheme in South Africa is RDP (Reconstruction and Development Programme) housing. This housing project has proven to be unsuccessful and has created considerable outcry amongst communities. The sizes of the houses range from approximately 36-45 square metres (City of Johannesburg, 2008) and cost between R50000 and R70000 to construct (SAPA, 2011). The aim of this research is to provide a house for people which is more spacious and environmentally friendly, while still being competitive in the cost market.

When selecting a layout and shape, the major aim is to optimise costs and space. The most efficient shape for housing is a square one. Even though this shape appears to be smaller than a rectangular one, it is in fact the optimal solution to provide maximum space.

It is difficult to cut down on construction costs, particularly in the low-cost sector, so it is important to perform a general cost breakdown to establish which area uses up majority of the funds. Two sources, Taylor (2011) and Braxton (2013), discuss the cost breakdown when constructing a typical house. They found that approximately 25 percent of the funds are spent on the roofing system. In some instances, as much as a third of the costs were used for roof construction (Minke, 2000). Thus, this indicates that the roof is the most economically sensitive area in a house. Walls are found to be the least sensitive, as they can be constructed using almost any material. Services and finishes are the areas which utilise the most funds and are variable depending on the extent of finishing required.

The typical roofing system is trusses and tiles, or in the case of low-cost housing, sheet metal. Both of these solutions are impractical as the cost is either too high or the quality too low. However, even though there are many options in the roofing sector, none of these provide a cheap and structurally effective solution. Within the low-cost housing sector, it is extremely common that people make use of corrugated steel as a roofing material. This solution is not sustainable, however cheap. Some of the major problems highlighted with this form of roofing include poor thermal properties, high maintenance costs due to poor resilience to weather and noise created during rain or hail. Rhyner *et al*. (1998) found that there are major energy savings when constructing with curved forms. There is an approximate energy saving of 22% when using curved instead of flat roofs.

Thus, a new option needs to be considered in the low-cost housing sector, which will keep costs at a minimum, improve structural performance, resilience and thermal efficiency. Thin shells have proven to be an extremely economical and structurally exceptional solution. Therefore, the concept of designing a square household with a vaulted roof was created. These structures have the ability to span very large areas and have been found to be the most economical means of construction. A vaulted roof would create more space, while simultaneously keeping the costs at a minimum, as only a single layer of bricks are required. However, the shape of the vault is an essential aspect in the structural success of the solution.

Talocchino (2005) did considerable research in form finding and identifying the ideal shape. During his investigation, he stated that the catenary was in fact the best structural shape as it eliminated all forces except for compressive forces, but it had a high level of wasted space (Talocchino, 2005). This is essential when considering low-cost housing solutions, as space is minimal and needs to be optimised to its best ability. However, the difference between the two investigations is that Talocchino's made use of thin shells for the entire structure while the proposed design uses them as the roof structure.

Both housing ideas are extremely innovative. However, a vaulted roof and standard lower floor is a combination of both current and novel design methods, and thus more likely to be socially accepted. The lower level is designed as an ordinary house, while a vaulted roof allows for more space within the structure. Therefore, a catenary vault is selected to act as the roof structure. If the roof is constructed at a very steep angle, there is minimal space wastage as the upper floor can be utilised and minimal dead space is created. It is also important to consider furniture within a house, i.e. fridge, cupboards, beds, etc. By creating a square lower level, this allows for no loss of space whilst still minimising construction costs with the construction of a vaulted roof.

A number of other areas were also considered in the selection of the design, but most importantly, the ability for this prototype to act as a home. Even though this is a low-cost housing solution, it is still important that it exhibits homely characteristics to ensure social acceptability and an overall approval from society.

Low-cost houses are extremely cramped. Unfortunately this is inevitable and thus it is important to create a sense of space, even if there isn't much. The idea of maximising on space with a high roof was also justified when it was decided to create a double volume area. The high roof would allow for more air and light to penetrate the house and in turn create this desired sense of space. A general design was selected (Figure 3-4) and an analysis was performed to ensure that the design is a structurally viable solution.

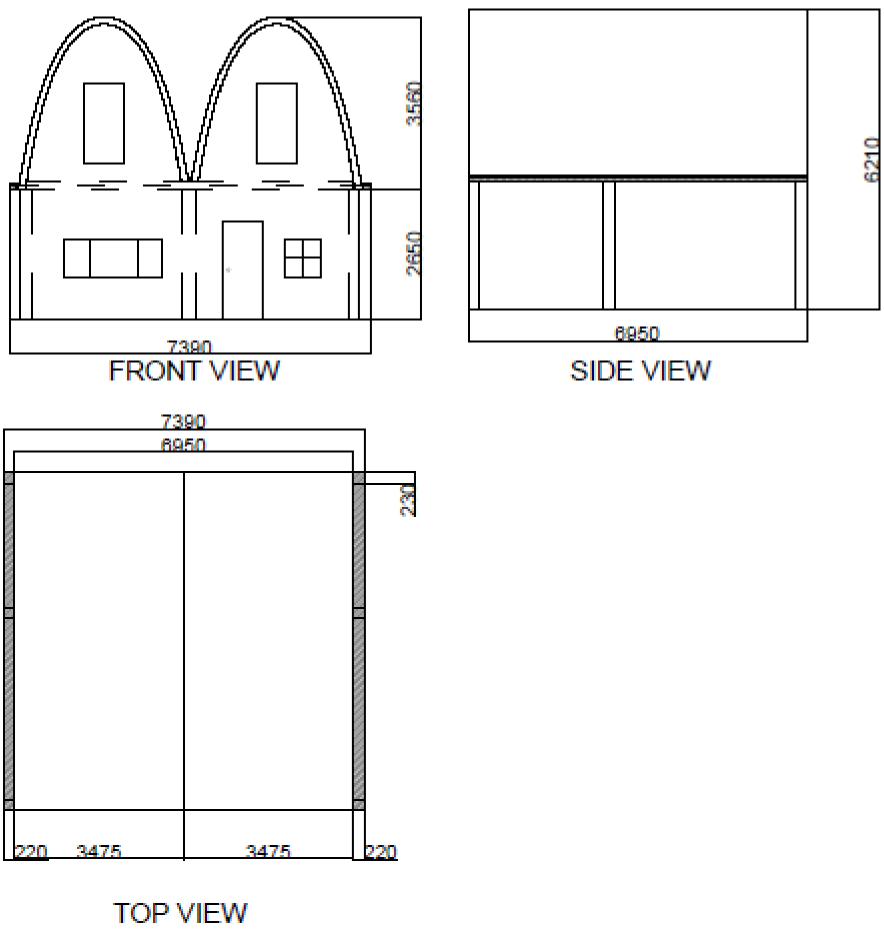

Figure 3-4: Layout of housing prototype

The general layout of the housing prototype is illustrated in Figure 3-4, while the selected internal layout is shown in Figure 3-5 below. The internal layout is orientated so that the lounge and bedroom face eastwards, thus maximising on morning sun. The upper floor space is utilised as a bedroom that is not generally found in typical housing designs. This space was selected to maximise on the number of residents per house without creating a sense of overcrowding.

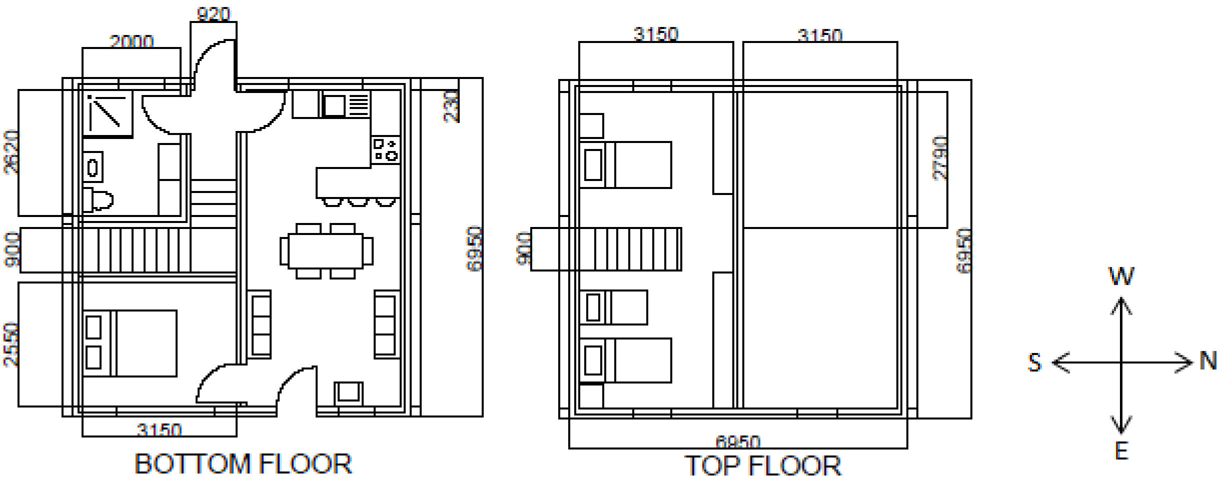

Figure 3-5: Interior Layout of housing prototype

4. Materials Investigation

Majority of houses in South Africa are built using ordinary clay or cement bricks. Even though these materials are very cheap, they are not a sustainable solution as they are environmentally harmful, particularly in the production phase. Transport is also a major concern when it comes to rural construction. Transporting the materials to site is expensive and difficult, creating major unnecessary cost increases. Thus, it is necessary to consider other more sustainable options. In this section, we will discuss the material properties that are required when constructing a low-cost house. In particular, Hydraform produced cement stabilised earth bricks will be analysed. A thorough investigation into Hydraforms material selection, testing and brick production will be discussed.

4.1. Introduction

Cement Stabilised Earth Bricks (CSEB) are a relatively new material in the construction industry, showing its face for the first time in the 19th century in Europe (Auroville Earth Institute, 2012). Since then, the concept has rapidly grown in popularity and its various uses can be seen throughout the world. The use of soil as a building material has been investigated extensively before it was able to compete with the current cement bricks. A major problem with soil is that it lacks strength and durability. However, after continuous research and testing in stabilisers, compression machines and material studies, CSEB has improved drastically. Today, the CSEB is able to compete with conventional bricks in terms of performance and cost, where savings are approximately 18% (Uzoegbo & Hobona, 1999). Rhyner *et al.* (1998), found that the insulation properties of these bricks are excellent and a 33% saving in electrical energy is possible.

Although CSEB have many favourable properties, there have been many debates regarding their appropriateness. They are generally perceived as inferior, due to the lack of standards in the construction industry, as well as social unacceptability, primarily with people with low income. CSEB also has a poor reputation, and assumed to be weak in compressive strength.

However, Houben & Boubekeur (1998) found that these bricks have sufficient strength to construct a two to three storey buildings. Since 1998, there has been considerable ground breaking work in the production and use of CSEB. Hydraform, a leading brick and block making Machine Company, are achieving compressive strengths of as high as 10MPa. These strengths are considerably higher than what is needed for the construction of a simple house.

Hydraform have put a foot in the door with their innovative and affordable brick machines worldwide. They have proved that the CSEB, if made properly, is just as effective and durable as the current cement bricks. The dry-stack interlocking block has also reduced construction speeds by approximately half, with its quick and efficient stacking system. The other block that is used in the construction of this prototype house is the Hydraform splitter-brick block.

4.2. Production process

The materials, mix ratios and other specifications in the production of these bricks can be found in the Hydraform training manual (2012). A two week research programme at the Algerian research facilities, CNERIB, was completed during the duration of the project. Research, tests and investigation into various materials were performed. Bricks were produced and various tests were carried out to investigate their strength and durability. This section covers the general method of producing CSEB. The information provided is a combination of Hydraform methods, as well as the research and work experience obtained in Algeria.

4.2.1. Soil Selection

In order to achieve the best blocks, it is important to ensure that the correct soil is used in the production process. The type of soil is particularly important in ensuring that the correct strength is achieved. Hydraform use a sandy-loam soil, found at least 1m below the ground, which contains more sand than clay and fines, and no organic material (Hydraform, 2012). Auroville Earth Institute (2012) stipulates that no top soil may be used due to having a high content of organic matter. Correct amounts of both clays and sands are important, as the clay improves the bricks workability while the sand is the binder which essentially provides the strength. This is not always possible as soils vary considerably at different sites. When one considers that the aim of this project is to establish a housing solution, which can be implemented anywhere, a soil selecting guide is of utmost importance in ensuring that the most suited soil in the area is found and used. Hydraform (2012) provides a guide that helps the user to locate the most suitable soil at a perspective site. The three most important considerations when selecting a soil include: finding a well-graded soil (clay content ranging between 15% and 35%) and a soil that is free of roots, leaves or any other organic material (Hydraform, 2012).

There are a number of field tests which can be done to check the adequacy of the soil, i.e. the visual test, the wash test, the jar test and the shrinkage test. Each of these tests have different indicators which determine the quantity of clay and sand present in the mix. (Hydraform, 2012)

4.2.2. Mix ratios

Mix ratios for block production vary depending on the required strength. The blocks used in this project are 10MPa in strength. For this strength a general mix ratio for cement to soil is 1:8. This strength is sufficient to support a double storey building. The colour of the blocks will vary according to the type of soil that is used and can be modified with the use of cement dyes (Hydraform, 2012) or oxides.

Hydraform (2012) provides a valuable site guide in measuring the correct mix ratios. By using a wheelbarrow, an accurate material mix is established with minimal effort, e.g. one bag of cement (50kg) mixed with four wheelbarrows (65L each) produces a 10MPa block. This is extremely effective, since simplicity is crucial in low cost projects.

There are many advantages associated with CSEB. However, there is one area in which these materials suffer from durability issues. Durability is an aspect in which CSEB are lacking. Since the blocks are predominantly made up of soil, they are affected by water. There has been considerable research in water proofing the blocks with various additives. In the blocks made by Hydraform, a chemical called Pareflo is used. Pareflo is added into the mix, prior to production. This chemical acts as a water repellent without affecting the mechanical strength of the block (Chryso, 2008). Pareflo has improved the material durability, but it has also been found to be environmentally sustainable (Chryso SA, 2012).

4.2.3. Production

The production process of the bricks and blocks is very simple. First, the material is sieved to ensure any unwanted particles are removed. A 8-10mm sieve can easily be made on site by using local materials to create a frame and some mesh. Secondly, the desired mix ratio is determined and the materials are mixed together while slowly adding water. It is important that the correct clay content is achieved otherwise the soil will be difficult to handle. The soil should have a clay content between 15 and 35 percent. The clay content can be determined using a number of tests; i.e. visual test, jar test, wash test, etc., but the most accurate is the shrinkage test. By measuring the shrinkage of the soil in a mould, the clay content can be determined. The soil-cement mix is mixed either by hand or by using a pan mixer. The mix is determined by the material volume (Hydraform, 2012).

The mix is then checked to ensure it has the correct moisture content. A drop test is used to establish whether more water or soil/cement mix needs to be added (Figure 4-1). The water content can also be checked by producing a block and observing any cracking or changes in block length that may occur. A short, wet block with cracks indicates too much moisture. While a very dry mix will produce a long, brittle, unworkable block. The water content required depends on the moisture content of the soil but is usually approximately one litre per block. However, sometimes the water content is correct but the blocks still vary in length. This can be due to insufficient material being poured into the chamber, or the operator is not allowing the machines to complete the full compressive action before removing the bricks from the chamber. Thus, it is necessary that the machine operators have sufficient training so that the blocks produced are of good quality.

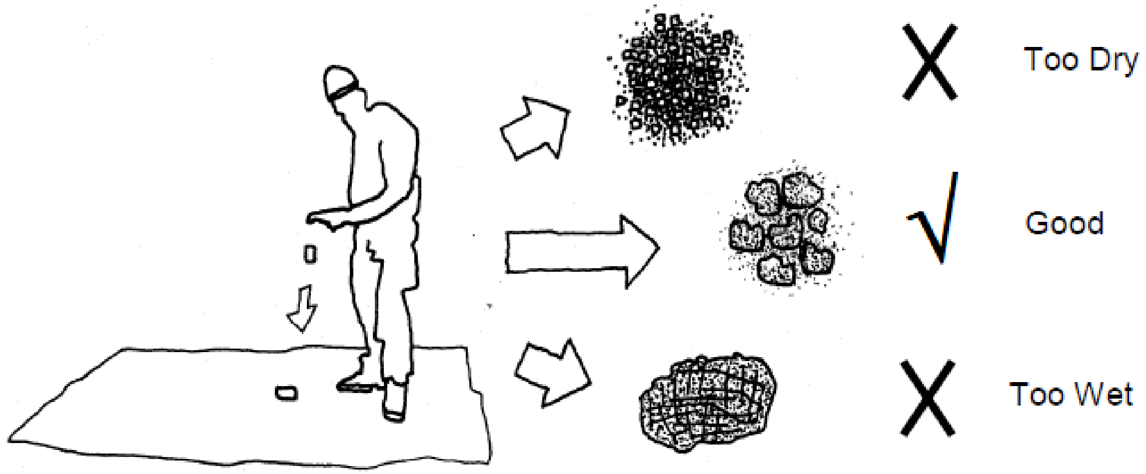

Figure 4-1: The Drop Test (Hydraform, 2012, p 32)

Once the blocks have been produced, they need to be stacked and allowed to cure. As these blocks are predominantly soil based, they cannot be stacked too high so as not to damage the bottom blocks. It is advised that the blocks are stacked more than five bricks before they are covered with a plastic sheet and left to cure for seven to fourteen days. Undoubtedly, if the blocks are cured for longer then they gain further strength. It is important to note that the blocks are cured and not burnt, as is common with normal fired bricks. This further decreases the environmental impacts that are associated with brick production. Figure 4-2 describes the strength development for a 7MPa CSEB.

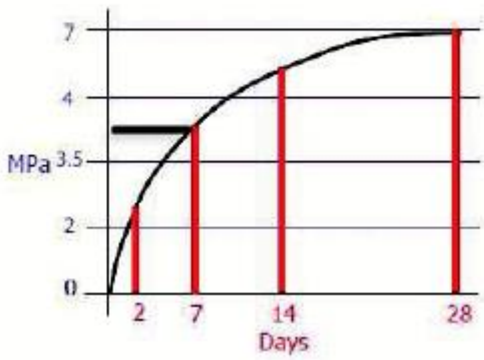

Figure 4-2: Curing curve for a 1:12 block (Hydraform, 2012, p 37)

When building, in a barren rural area, it is important to consider the water requirements of the blocks. There needs to be access to water, or sufficient water on site, to ensure that the blocks can be constructed and that enough water is available for curing. Generally the latter of the two is overlooked. And, if the blocks are not cured properly, then they may not gain their required strength.

4.2.4. Problems in production

There are many challenges in the production phase of the building materials. A major one is a lack of training in the use of the machines, resulting in the production of poor quality blocks. This also includes the lack of expertise in maintaining the machinery, which is demonstrated when blocks with rounded edges or reduced interlocking are produced.

Inadequate mix ratios are an even more common challenge in block production and are likely to occur. This includes having too much or too little water, and having cement or soil in the mixing step. Inadequate mix ratios result in problems such as rough surfaces, cracks in the block and varying block dimensions.

4.3. Material properties

Hydraform are the current leaders in the production and testing of CSEB blocks in South Africa. Hydraform (2012) performs a number of tests to ensure that the necessary compressive strength is achieved. Thus, a simple compression test is performed throughout the production phase to provide a rough estimate of the strength of the bricks and blocks. This test is not as accurate as laboratory tests, but it is designed to give a rough estimate to ensure that the mix is sufficient. The block tester consists of a simple device that utilises a jack and gauge to obtain the failure compressive strength of the produced bricks. Such a test is vital when working and producing blocks on site, if there is no access to sophisticated laboratory tests.

Material properties of CSEB blocks obtained from various literature and for different experiments are summarised in Table 4-1.

Table 4-1: Material properties of CSEB

Property	**Hydraform**	**Auroville**	**Wits University**
Density (kg/m³)	1950	1900-2200	1900-1950
Poisson's ratio	-	0.15-0.35	0.2
28 Day Compressive Strength (MPa)	7-10	5-7	5-5.4
28 Day Tensile Strength (MPa)	~1.1	1-2	1.18-1.4
Youngs modulus (MPa)	-	700-1000	3500
Thermal conductivity/coefficient of thermal expansion (mm/m°C)	-	0.01-0.015	-

The reported values were obtained from Auroville Earth Institute (2012), Magaia (2003) and Fernandez (2003) from Wits University, and publications and testing from Hydraform.

The two blocks that are utilised in this project are the Hydraform dry-stack interlocking block and the Hydraform Splitter-brick Block. The dry stack block is used to speed up the construction process and minimise costs. The splitter brick block is used in the vault due to its relevant size and to ensure that a strong joint is created between the bricks. This is attributed to the grove in the brick, allowing it to act as a key between each layer.

4.3.1. Dry-stack interlocking Blocks

Dry-stack interlocking blocks have proven to be one of the most ingenious inventions since the introduction of CSEB. Hydraform makes these blocks so they are almost identical to standard clay bricks in terms of strength, while also possessing many more added benefits. They can be produced from either soils or recycled material and still achieve a very high compressive strength.

Many benefits have been noted when changing from standard brick-mortar construction to dry-stack interlocking construction. It is common for a house to be constructed with double brick, connected with mortar. However, Hydraform have managed to eliminate the need for any mortar by merely interlocking the blocks. This results in considerable cost and time savings, as construction is quick and efficient. These bricks also provide a lovely face brick finish, eliminating the need for plaster.

These blocks are particularly effective in walls and other vertically loaded structural members. Since they are dry-stack, they can only support nominal horizontal forces. The blocks, however, can be used like conventional mortared bricks if they are required to carry horizontal forces. In this case, the user would still have cost savings as the mortar required would be approximately three quarters of that required for double brick, because there are a smaller number of joints and no centre joint.

All the interlocking bricks used in this project are 10MPa in compressive strength, after 14 days of curing. A 1:8 mix ratio is used to achieve this strength. Hydraform provide a number of machines and moulds to satisfy the various sizes of required blocks. The block dimensions used in the production of the low-cost house are presented in Figure 4-3 and an image of the final product in Figure 4-4.

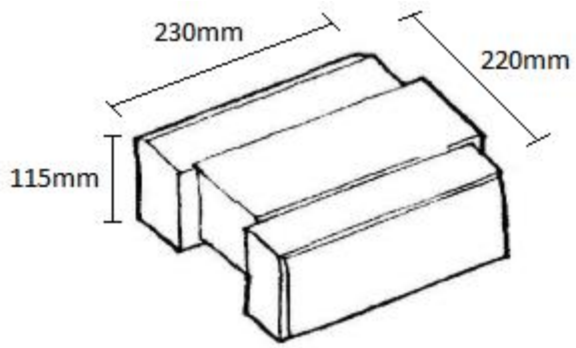

Figure 4-3: Dimensions of the dry-stack interlocking block

Figure 4-4: The Dry-stack Interlocking Blocks used in the construction of the prototype

4.3.2. Splitter-Brick Block

The current splitter-brick block is a single block which splits up into three separate normal sized bricks as shown in Figure 4-5.

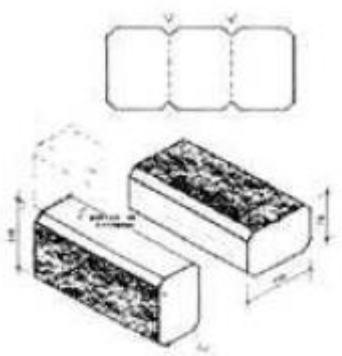

Figure 4-5: Image of the split-brick block that separates into 3 individual bricks (Hydraform, 2012, p 53)

A problem with this type of block is that the central piece has two rough sides as opposed to the outer ones which have one each. This is generally undesirable as most users are looking for a smooth finish rather than a rough one. The middle brick is usual disposed of due to its undesired look. This results in considerable wastage of material. Therefore, in this project, Hydraform is testing a new mould that has been developed which splits a single block into two separate bricks instead of three. The rough sides can now be hidden or mortared in and there is minimal wastage of material.

An image of the brick used in construction, and its dimensions, are shown in Figures 4-6 and 4-7.

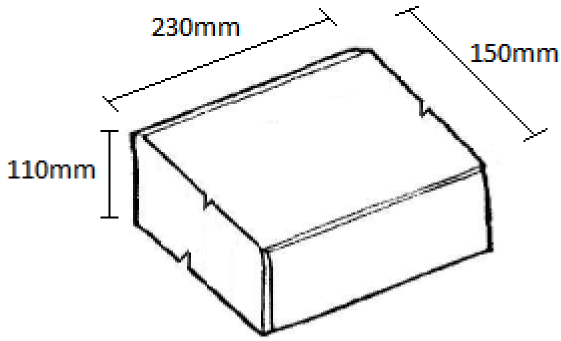

Figure 4-6: Dimensions of the "half" split-brick block used in the prototype

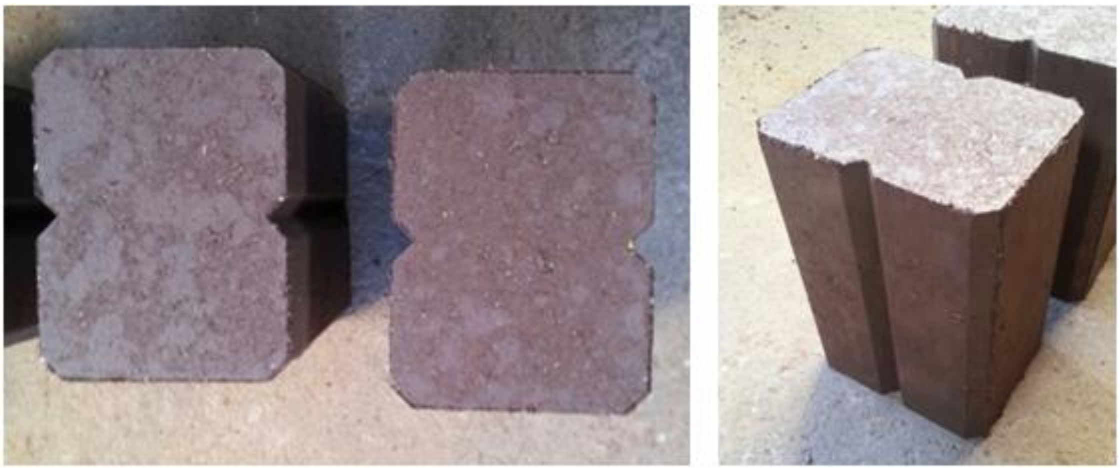

Figure 4-7: Image of the split-brick block used in the construction of the vault roof in the prototype as supplied by Hydraform

5. Method of Analysis for a Catenary Curve

5.1. Introduction

"*The ideal shape for resisting loads distributed uniformly along a surface is a* catenary, *the curve taken under its own weight by a hanging chain or cable"* (Allen & Zalewski, 2010, p. 65)

The process of designing and analysing a catenary curve is a field which has not been extensively explored or discussed. Allen & Zalewski (2010) briefly discuss the method of design using Hooke's Law and then elaborate on the Graphical Method of design. Catenary curves are the most natural and efficient form, yet they are not utilised or explored as much as they should be. If a simple and effective method of designing a catenary curve can be established, the curve can be utilised at a greater scale, encouraging more efficient and structurally sound design.

5.2. Mathematical definition

The catenary curve equation was established in the 17th century by Huygens, Bernoulli and Leibniz (Carlson, 2013).

Mathematically, it is defined by the following equation:

$$y = a \cosh\left(\frac{x}{a}\right) \tag{5-1}$$

Where *'x'* represents the vertex when x=0, and '*a'* is a parameter that can be any number except zero, and controls how rapidly the curve "opens up". The parameter '*a'* can also be described as the scaling factor for the curve. (Weisstein, n.d.)

This mathematical representation of the curve is ineffective in design as it fails to take variable loading into account. The equation merely describes the shape of the curve and the relationship between its '*x*' and '*y*' variables.

5.3. The Graphical method

The Graphical method is a method of approximation which is carried out by assuming a curve and then working backward to establish the actual, true curve. The final result is achieved using an iterative approach. The method was established to suit the geometrical properties of a parabola (Allen & Zalewski, 2010).

Allen & Zalewski (2010, p. 65) provide an in-depth example of designing a cylindrical shell roof using the graphical method. It can be summarised as follows (Figure 5-1):

1. Select three main points that the curve should pass through. These usually include the two end points and the midpoint. The aim is to develop a “pole” that will allow the curve to pass between these three unique points. A pole is a reference point that is used to generate the required polygon e.g. the centre pole for a circle.
2. Select a general curve. This is usually achieved initially assuming a parabolic curve. If the parabolic curve is flat, the parabolic curve approximates the catenary curve.
3. Separate the curve into the desired number of increments and estimate the loads exerted on those sections. These are calculated as surface loads, not horizontal projections. Note that the loads are not uniform in each segment and a total load is merely required.
4. Once the total value is calculated, it can be applied as a horizontal line load. The aim is to create a “trial” polygon which will then be used to establish the true curve.
5. A convenient trial pole is selected and used to construct the trial force polygon. The base of the polygon is drawn using the same increments established in step 3 and connected to the pole. The trial force polygon is then used to establish the angles of the segments along the curve, i.e. o’a, o’b, etc. Refer to Figure 5-1.
6. Connect points x’ and z’ to y’ to draw lines x’y’ and z’y’.
7. Through the trial pole draw two lines with the same gradients as x’y’ and z’y’ which cut on the base at m and n.

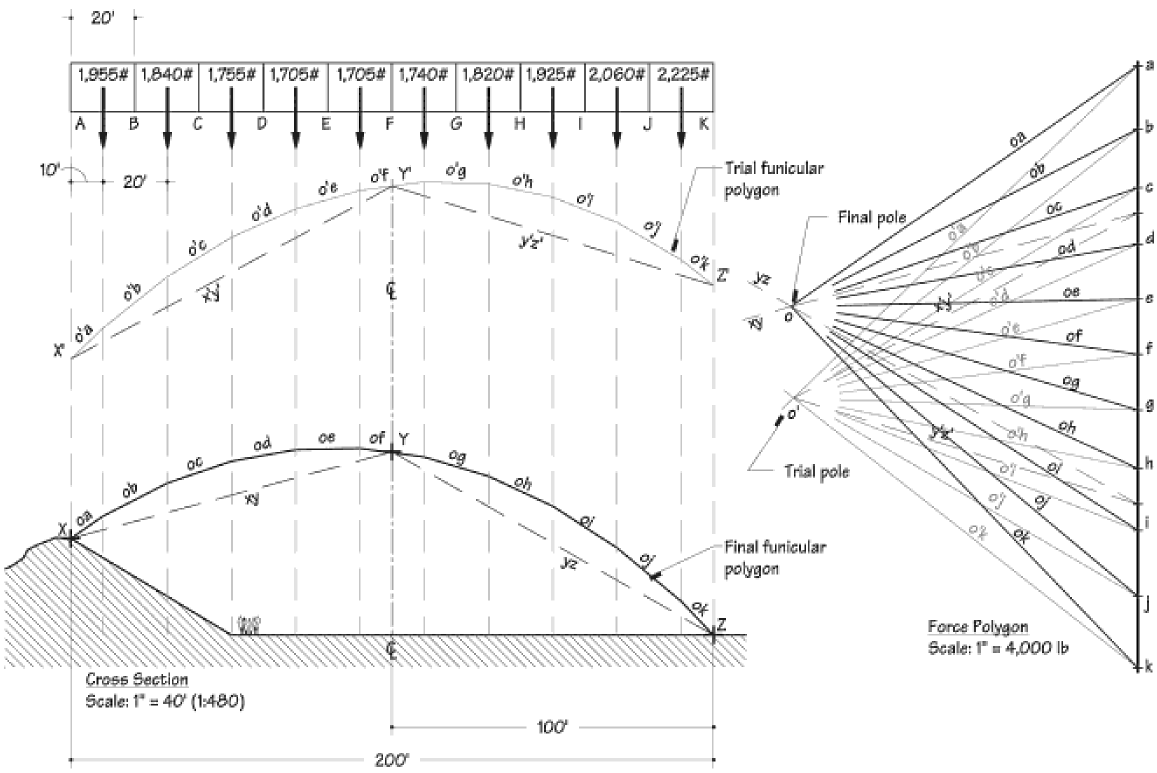

Figure 5-1: The graphical method (Allen & Zalewski, 2010, p 76)

8. At the true curve, connect the end points to the midpoint creating lines xy and yz. These are the true closing strings. Through point's m and n, draw lines of the same gradients as xy and yz. Their intersection creates the real, final pole.
9. New rays are drawn from final point o to the respective base points *a* to *k*. The rays are used to determine the angle of each segment *oa* to *ok* and the true curve is determined.

This method has been found to be accurate in determining the internal forces of any structure and it works well for vertical loads. The method is, however, labour intensive and complex when dealing with a form other than the parabolic form (Allen & Zalewski, 2010). There is considerable difficulty in modelling and analysing horizontal forces when using the graphical method. There is little guidance in designing and modelling complex lateral forces such as wind or snow. Allen & Zalewski (2010) suggest that this method not be used when modelling such complex shapes, particularly under lateral loading, but to rather design an approximate shape and then stiffen the curve to provide resistance to these forces. Otherwise, a new method needs to be explored.

5.4. Segmental Equilibrium Method

5.4.1. Introduction

In the 1670's, a Scientist by the name of Robert Hooke expressed considerable interest in catenary curves and how they work. His aim was to determine the ideal shape of an arch. With this in mind, Hooke established that the inverted catenary was the ideal shape for an arch. He also stated that if an arch of another shape is effective, it is merely because somewhere in the thickness of the membrane, a catenary can be found (Huerta, 2006).

Hooke performed most of his experiments using hanging chain models. When analysing the models more closely, Hooke found that in order for the hanging chain to be in pure tension, and therefore the inverted arch to be in pure compression, both have to be in equilibrium. Thus, Hooke's principle was born (Allen & Zalewski, 2010).

The graphical method struggles to incorporate any lateral forces, due to the complexity of the method. It is important to establish a mathematical method which incorporates both horizontal and vertical forces i.e. the segmental equilibrium method.

5.4.2. Theoretical basis

The equilibrium method is a mathematical method which utilises the loading on the structure to establish the thrust line of the curve. The line of thrust is a representation of equilibrium within the structure. It can be described as "*a theoretical line that represents the path of the resultants of the compressive forces through the structure"* (Allen & Zalewski, 2010, p. 219).

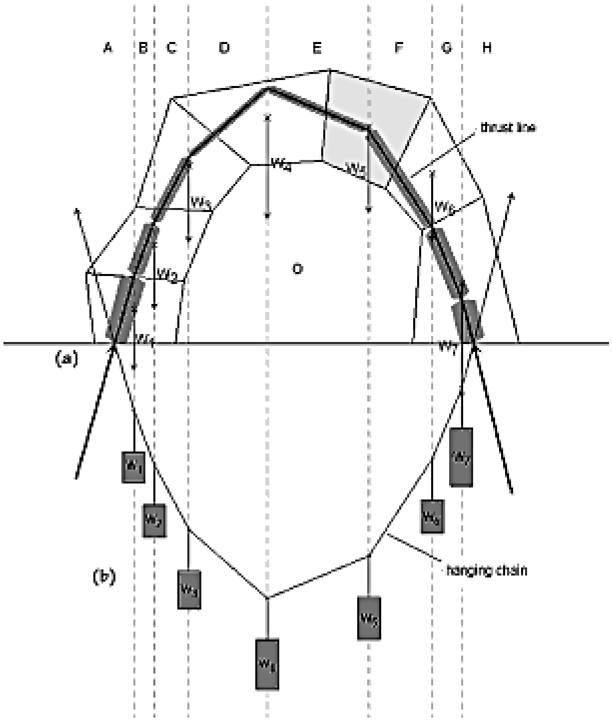

Figure 5-2: Hanging chain with its inverted form and corresponding thrust line through the thickness of the curve (Allen & Zalewski, 2010, p 220)

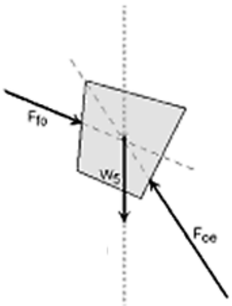

Figure 5-3: All internal and external forces applied to each segment, in equilibrium (Allen & Zilewski, 2010, p 220)

Figures 5-2 and 5-3 demonstrate how equilibrium is used in each section to determine the overall thrust line of the structure. Each individual segment is analysed, incorporating all the forces and loads exerted on it. The arch is held in place by the compressive forces, applied from one block to the other. Since we know that each block carries the compression force exerted by blocks on either side of it, they can be combined with the external loads, as well as its' self-weight to determine the line of thrust of the structure (Allen & Zalewski, 2010).

If the equilibrium line, i.e. the thrust line, extends to the edge or outside of the thickness of the material, tensile forces are created which result in cracking, and possibly failure. If the thrust line reaches the edge cracking will occur, or in some instances hinges will form, as high stresses are created at those particular points (Figure 5-4).

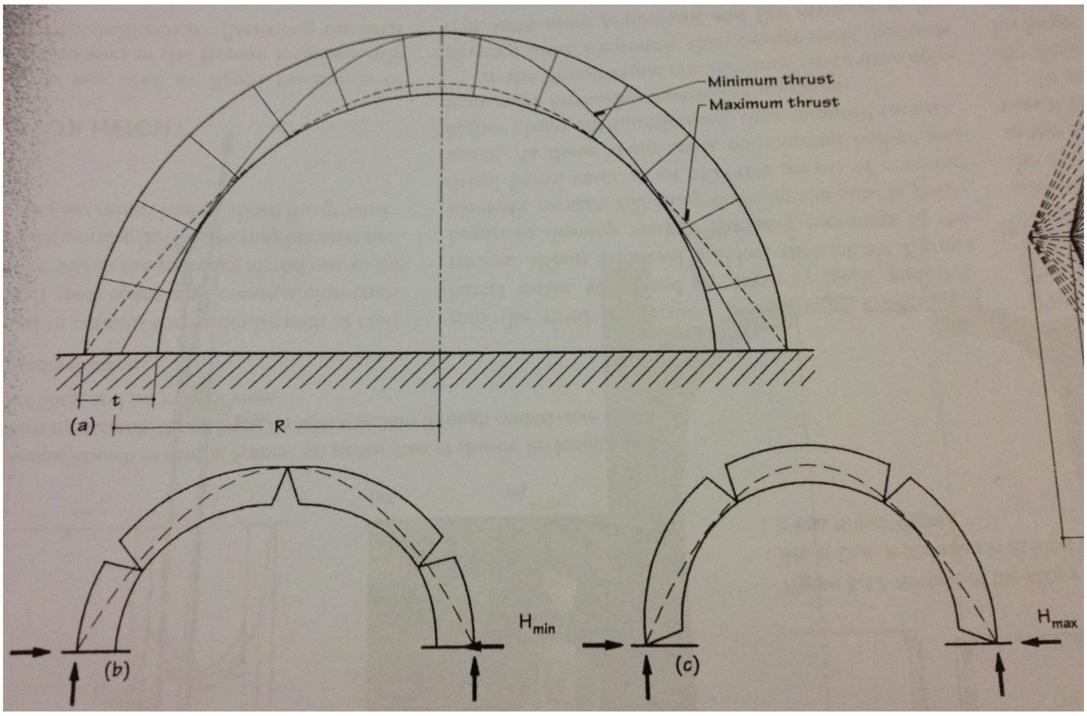

Figure 5-4: (a) Maximum and minimum thrusts lines within the vault, (b) Minimum thrust lines and (c) maximum thrust lines can cause cracking in the vault (Allen & Zalewski, 2010, p 221)

5.4.3. The Middle-Third concept

There are a number of ways to analyse the design results of a catenary. The more effective method is that of the middle third. This consists of choosing a constant thickness for the vault and checking that all the thrust lines, for the various load cases fall within the middle third of the section. This method was chosen as the thickness of the CSEB remains constant throughout. Majority of the vaults that have been built are made from either concrete or bricks. Both of these materials have minimal tensile strength. If the thrust line falls within the middle third of the section, the material will be in compression. However, if the thrust lines move out of the middle third, those areas will be subjected to tensile forces and cracking may occur (Allen & Zalewski, 2010). The aim is to avoid any tensile forces, since most masonry materials are not designed to carry these forces effectively. The middle-third theory is substantiated as follows:

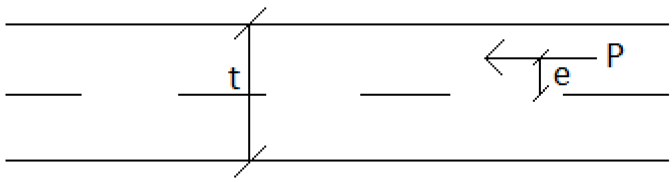

$$\sigma = \frac{P}{A} \pm \frac{Pe}{Z} \tag{5-2}$$

$Z = \frac{bt^2}{6}$ and the section width=1

$$\sigma = \frac{P}{t \times 1} \pm \frac{Pe6}{t^2 \times 1}$$

Solve for σ=0

$$\cancel{t \times 0} = \frac{P\cancel{t}}{\cancel{t}} - \frac{6Pe\cancel{t}}{t^{\cancel{2}}}$$

$$\frac{\cancel{P}e6}{\cancel{P}t} = \frac{\cancel{P}}{\cancel{P}}$$

$$\frac{e6}{t} = 1$$

$$e = \frac{t}{6}$$

e is only half of the middle third

$$\boldsymbol{2e = \frac{t}{3}} \tag{5-3}$$

5.4.4. Method of Design

The segmental equilibrium method of design is a new method of determining the shape of a catenary shell. Not only is the method computerized but incorporates complex loading arrangements, such as wind and non-symmetrical gravity loads. It must also be noted that the finite element methods are used to analyse a pre-determined shape. The segmental equilibrium method determines the shape, as well as the membrane forces (i.e. thrust line). This method is easily set up in Excel and allows for analysis and design of catenary curves. A step-by-step explanation of the method is provided.

1. Begin by inputting all the necessary material properties. These include density and Youngs modulus.
2. Pick a set of general dimensions for the structure, including the height and width of the curve. It is important to have some idea of the size of the curve that is desired. The solution is iterative and therefore these dimensions will change slightly throughout the analysis. If the desired curve is flat, the user may estimate the shape of the curve using a parabolic equation.
3. Input the length of barrel vault you wish to design. It is simplest to pick a 1m length, a segment which represents the length of the shell.
4. Select an initial segment size. The segment height is not necessarily a true reflection of the actual segment height, but rather a segment height so that the coordinates of the curve can be calculated. The shorter the segment height, the more segments, but the more accurate the curve will be. The height can be an arbitrary value or it can represent the size of the brick and mortar joint.
5. Select an initial angle at the reaction. This angle is the starting angle at the left hand base of the shell. This angle is depicted in Figure 5-5. The angle of the reaction is also the angle at the base of the shell.

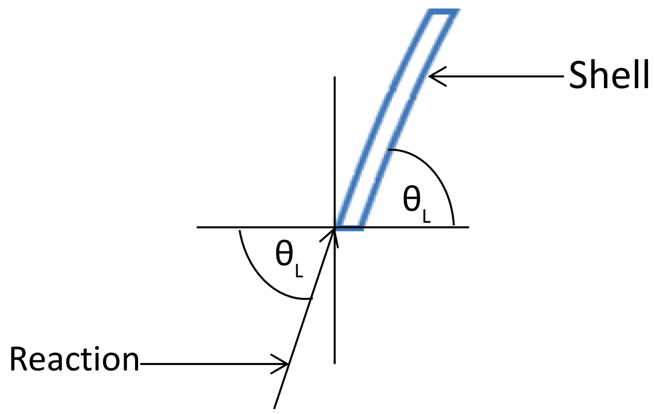

Figure 5-5: The Initial angle at which the reaction force is orientated

Note that the higher the value of θ, the steeper the curve. The angle will vary depending on the nature of the load.

6. Choose the number of segments that are needed in the analysis. This can be adjusted accordingly. The flatter the segments, the more you will need to complete the length of the curve and vice versa.

   Note: Steps 4 to 6 are incremental. The thrust force and thrust line will change with each loading pattern. However, it is easier to select a finite number of segments, which remains constant for each loading pattern.

   All the required material properties and geometric parameters have now been inputted. These are inputted in the corresponding columns in Table 5-1. Next step is to set up the loading.

7. The following loads can be incorporated into the spread sheet: Dead Loads, Live Loads, Wind Loads, and Snow Loads. Snow loads will be ignored in this analysis, as they are not relevant to Southern Africa. Once the loads have been calculated, they are transformed into point loads and applied at the centroid of each segment.

   Note: Before the loads are transformed into point loads they are calculated as follows: the dead load as a surface load, live loads as horizontal projections and wind load as a surface pressure.

8. The following ultimate load cases are investigated, according to the loading code SABS 0160-2 (2009):
    - 1.5*Dead Load
    - 1.2*Dead Load + 1.6*Live Load
    - 1.2*Dead Load + 0.5*Live Load + 1.3*Wind Load
    - 0.9*Dead Load + 1.3*Wind Load
9. Now set up your spread sheet (Table 5-1). The following headings are recommended, but can differ depending on the user and what is required in the calculations.

Table 5-1: The spread sheet layout for the equilibrium method (Figure 5-6)

Segment No.	Height of Segment	Weight	Left Angle	Left Thrust x	Left Thrust y	**Left Thrust Resultant**	Right Thrust x	Right Thrust y	**Right Thrust Resultant**	Right angle	Co-ordinates	
											X	Y

10. The first step is to calculate the actual shape of the curve. Therefore, only gravitational forces are taken into account.
    <u>*Assumption*</u>: The thrust line established from the self-weight is the centre line of the curve.
    When applying live and wind loads at a later stage, the same analysis process applies.

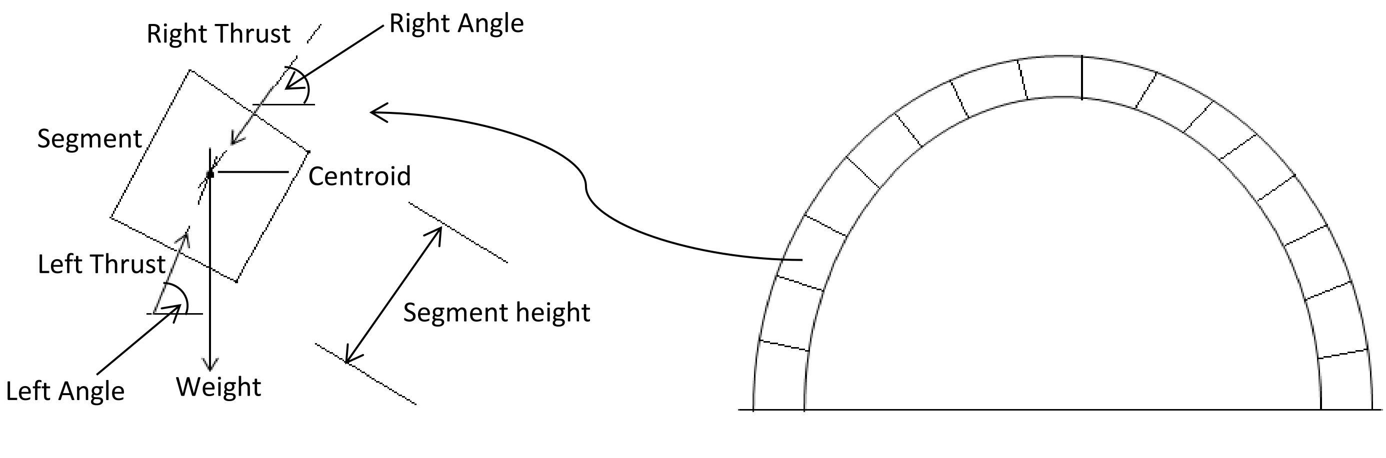

Figure 5-6: A diagram illustrating the meaning of each heading in table 5-1

11. The gravitational loading is applied as a point load at the centroid of each segment. At this moment, all the loading is constant and vertical, inputted in the column labelled *weight*. This value will vary with the various loading combinations and patterns. Each segment is loaded individually.
12. Columns marked *Segment no., Height of Segment* and *Left Angle* consist of the values chosen in steps 4 to 6.
13. The first force, *Left Thrust y,* is now calculated. The first and last vertical reactions are merely the total weight divided by two as the curve is symmetrically loaded. This can also be calculated through equilibrium equations such as ∑M=0.
14. Now *Left Thrust x* and ***Left Thrust Resultant*** can be calculated. This is done through the use of trigonometry as depicted in Figure 5-7.

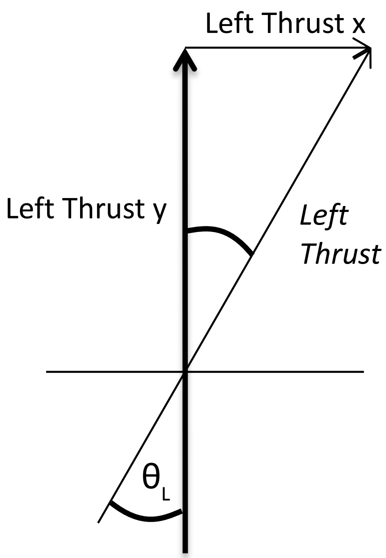

Figure 5-7: Trig is used to obtain the remaining components of the *Left Thrust y* Force

15. From here the *Right Thrust x, Right Thrust y and* ***Right Thrust Resultant*** are calculated. These forces are calculated at the centroid of the segment and therefore the loading on the segment is incorporated into these calculations. The following equilibrium equations are used in this step: ∑Fy=0 and ∑Fx=0. This is applied as follows:

$$\sum Left\ Thrust\ x + Right\ Thurst\ x = 0 \tag{5-4}$$

And

$$\sum Left\ Thrust\ y + Selfweight\ of\ the\ segment + \ Right\ Thrust\ y = 0 \qquad (5\text{-}5)$$

When other loads are analysed, they are also applied at the centroid of the segment and the different loading components need to be added correctly into the above equations (Figure 5-8).

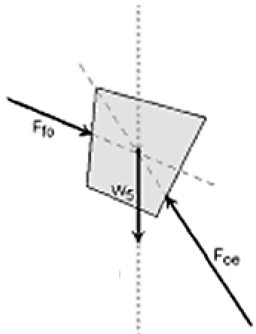

Figure 5-8: Equilibrium at the centre of the segment, combining internal & external forces (Allen & Zilewski, 2010, p 220)

16. The ***Right Thrust*** is now calculated using Pythagoras theorem.
17. The new angle for the next section of the thrust line is calculated using trigonometry as demonstrated in Figure 5-7.
18. Lastly, the co-ordinates are calculated. Each co-ordinate represents the centroid of each segment EXCEPT for the first and last co-ordinates. Co-ordinate (0,0) is NOT the first co-ordinate established. This point is a selected point of axes from where the curve is chosen to begin and is manually inputted by the user. The first calculated co-ordinate is at the centroid as seen in Figure 5-9. Since the calculated co-ordinates are representing the centroids of the segments, the very first and last co-ordinates are inputted to ensure that the extra *length* of structural segment is also depicted in the curve.

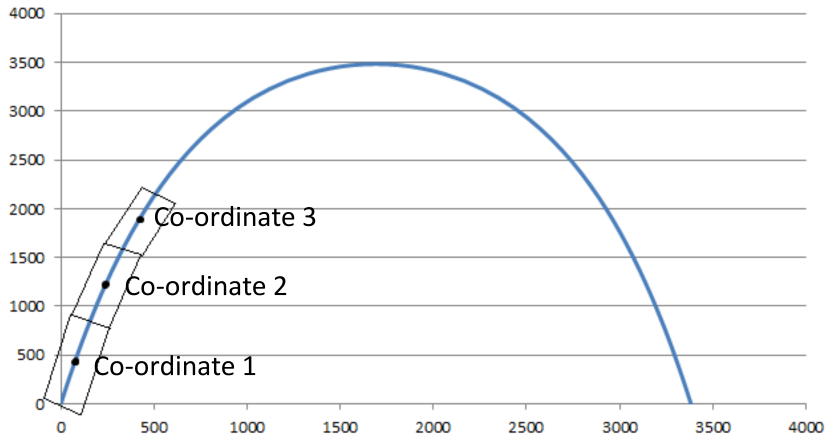

Figure 5-9: Each co-ordinate represents the centroid of the segment. The first and last are inputted manually to account for the geometry (length) of the segment

The co-ordinates are calculated through trigonometry; where the variables used are that of the length of the segment with the corresponding angle, continuously added to the preceding co-ordinate.

19. The remainder of the rows of calculation (i.e. rows two to the final row) in the spread sheet are calculated in an almost identical fashion. The first row of calculation is unique. For rows 2 to the final row, there are two changes in the formulae:
    - The new *Left Angle* is equal to the previous rows *Right Angle*. This is because of vertically opposite angles at a point (refer to Figure 5-7)
    - The new ***Left Thrust Resultant*** force is equal to the previous rows ***Right Thrust Resultant*** force. You are now looking at the succeeding segment, thus the left thrust in the new segment is the right thrust in the old segment.
20. Steps 1 through to 19 can be applied to various curves with different loading cases. The self-weight case determines the centre line for the curve and all other load cases will be adjusted accordingly to best fit the geometry of the curve.
21. Once analysis is finished for all the load cases, it is vital to check that all the curves fall within the required boundary. This boundary is the middle third of

the thickness of the material (refer to section 5.5.3). The check is best done by plotting the curves on the same set of axis as the middle third boundaries. The middle third is drawn in the same way as the centreline however the geometry is set and properties are adjusted to suit.

22. The final step in the design is to ensure that the material is capable of supporting the curve. The maximum stresses from all analysed load cases are obtained and compared to the materials strength capacity. If all the curves fall within the middle third, then only the compressive strength need be compared. If the curves fall outside of the middle third, then the tensile strengths also need to be checked or the thickness of the shell increased. The maximum deflections are also obtained for further design requirements.

5.5. Finite Element Method

Finite element method (FEM) is the most commonly used method in structural design and is extremely effective, when used correctly. However, if the user is not aware of its limitations, the results could be detrimental. In addition, designs which require an in-depth mathematical understanding should generally avoid using FEM, and the designer should rather consider a different approach in solving the problem.

Bathe & Chapelle (2011) provide an in-depth guide on how to analyse thin shelled structures using finite element analysis. The thin nature and complexity of the curve makes these structures difficult to model. Even though FEM is widely used, it was initially designed to solve thin shells, as first principle methods were too complex (Argyris, 1954).

When modelling complex structures, such as thin shells, there are a number of ‘rules’ that need to be followed. Subjects such as element size, element type, type of analysis, constraints, etc. need to be carefully selected. The curves and geometry of thin shells are the main aspects that make them very difficult to model.

There are a few points to take into consideration when modelling thin shells to ensure that the results achieved are accurate. These include:

- Sharp changes in geometry cause major discrepancies in the results. The elements need to be smooth and continuous (Talocchino, 2005).
- The shape should never be modelled using linear elements, but rather quadrilateral or triangular. If quadrilateral elements are to be used, they need to be either eight or nine node to improve accuracy.
- All elements need to be orientated in the correct direction i.e. all elements are created in a clockwise direction so that all the same faces face outwards.
- Use as many elements as possible when meshing the model. This improves the accuracy, as the elements are smaller. It also minimises the number of linear, rigid sections as there are more points allowing for smoother changes in geometry.
- When modelling symmetrical objects, only small segments need be modelled and not the entire object as long as the correct constraints are applied.

The assumptions made and process followed in designing this vault will be discussed at a later stage.

6. Structural Analysis and Design of Catenary Vaults

6.1. Introduction

In this chapter, the segmental equilibrium method will be applied to design the catenary vaults of the prototype structure. All analysis will be performed as well as an investigation into a case study situated in South Africa. This section will focus on the roof structure and the adequacy of this method in structural design. The shape of the structure, as discussed in Chapter 3, is a square structure with two vaulted sections acting simultaneously as the roof and upper storey.

The loading is designed in accordance with SABS 0160 (2009). All finite element analysis done for both the case study and actual design are carried out in LISA version 7.7.1, a finite element programme. The results of the FEA analysis and equilibrium method are compared to check the accuracy of the results.

6.2. Case study: Bapong

6.2.1. Introduction

Bapong is a township situated just off the R556 en route to Sun City in North-West province, South Africa. The case study consists of a series of vaulted structures that have been abandoned, located on the end of a school property. They are unique in shape and have made use of the catenary vault in its design (Figures 6-1 to 6-3).

Figure 6-1: Bapong case study location: image obtained off Google Earth

Figure 6-2: Bapong township, a set of abandoned structures

Figure 6-3: The abandoned structures are in impeccable condition even with no maintenance

A site visit was arranged to inspect these structures and assess their condition as well as to highlight any major problems with their design and construction. These structures have proved to be extremely durable and structurally efficient. They are estimated to be approximately 20 years old with no apparent maintenance over the years.

The structures showed minimal deterioration and minor cracking. However, along the apex, or high point of the vaults, a crack had occurred, as seen in Figure 6-4. This was recurring in all the roof structures and no certain cause for the cracking was identified. Thus, a detailed finite element analysis was carried out to establish what has caused the recurring cracking.

Figure 6-4: A crack occurs at the centre, or high point, of all the roof structures

In the structures, both buttresses and steel ties were present. It is not clear whether the buttresses had a structural or aesthetic purpose. However, the steel ties are structural elements used to restrain the horizontal thrust force exerted by the vault (Figure 6-5).

Figure 6-5: Steel ties are present in the structure to restrain the thrust force

The shape of the roof is a catenary, and because of its shape the shell is in excellent condition. This is a valuable case study which highlights the high level of sustainability and durability of vault structures.

6.2.2. Finite Element Results

A finite element analysis was carried out to investigate the cause of the cracking in the vaults. Various loading conditions were investigated. The shape was modelled in LISA, a finite element programme. The elements used are nine noded shell quadrilaterals. The end conditions are applied at the relevant nodes. It is essential that these end conditions are accurate, as they will create major discrepancies in the results if modelled incorrectly. The edges of the roof are connected to the end walls and therefore pinned along the edges. It was also noted, at the site visit, that the edges of the vault were tied in to the wall. This meant that all edges of the vault were restrained, and thus all edges must be modelled as pinned connections (Figure 6-6).

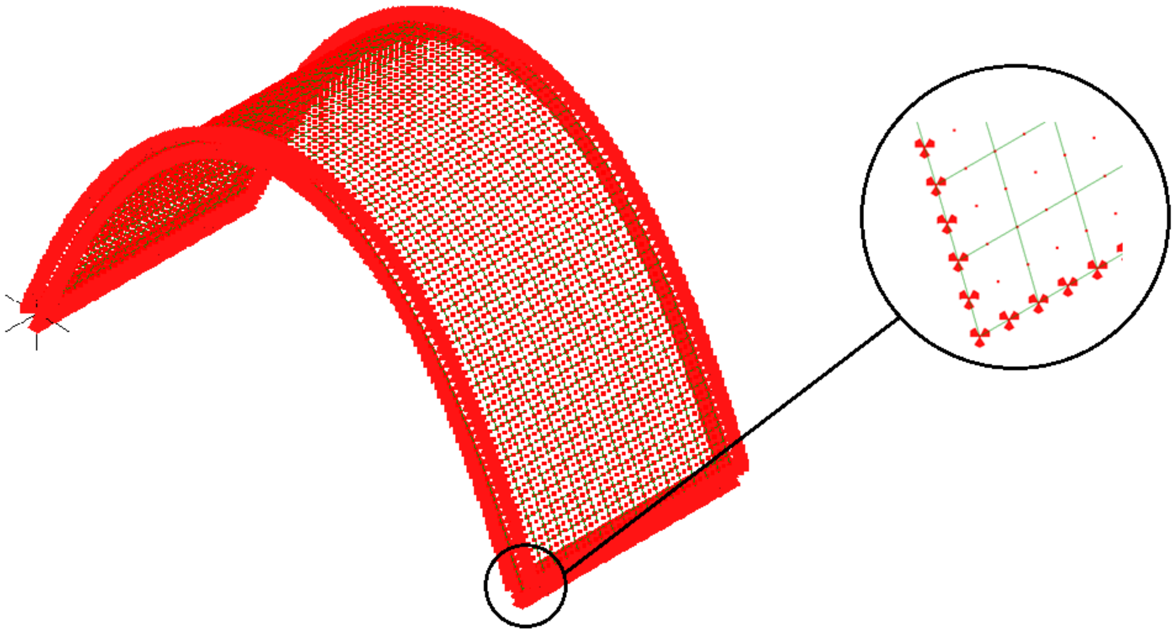

Figure 6-6: All the edges of the vault must be restrained in all directions (i.e. pinned connection) due to its direct connection to the surrounding wall

The vault is subjected to live loads, wind loads and temperature loads.

The analysis was performed and it was found that temperature loading caused considerable changes in stresses along the apex of the structure. This is due to the vault being unable to expand or contract, as no expansion joint is present between the vault and wall. This causes the structure to crack when it expands or shrinks as it is unable to move freely, thus resulting in extremely high stresses at the edges. Figures 6-7 and 6-8 are results of the analysis of two different loading combinations, both including temperature changes, which show the distribution of stresses along the vault. At the centre it is clear that there is a sudden change in stresses from compressive to tensile, causing cracking in the vaults.

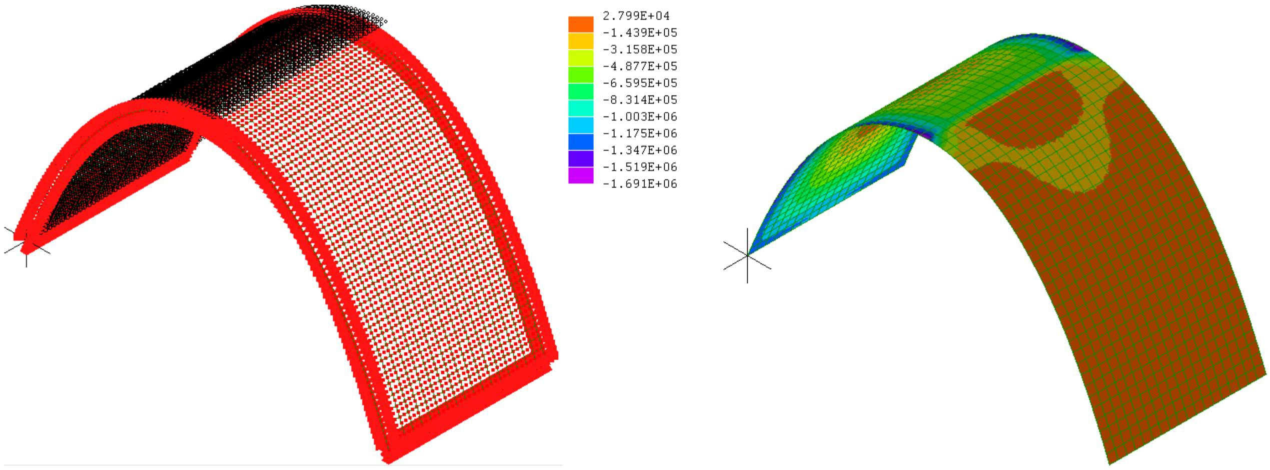

Figure 6-7: Results of the load case whereby the structure has a temperature loading along the left side of the vault

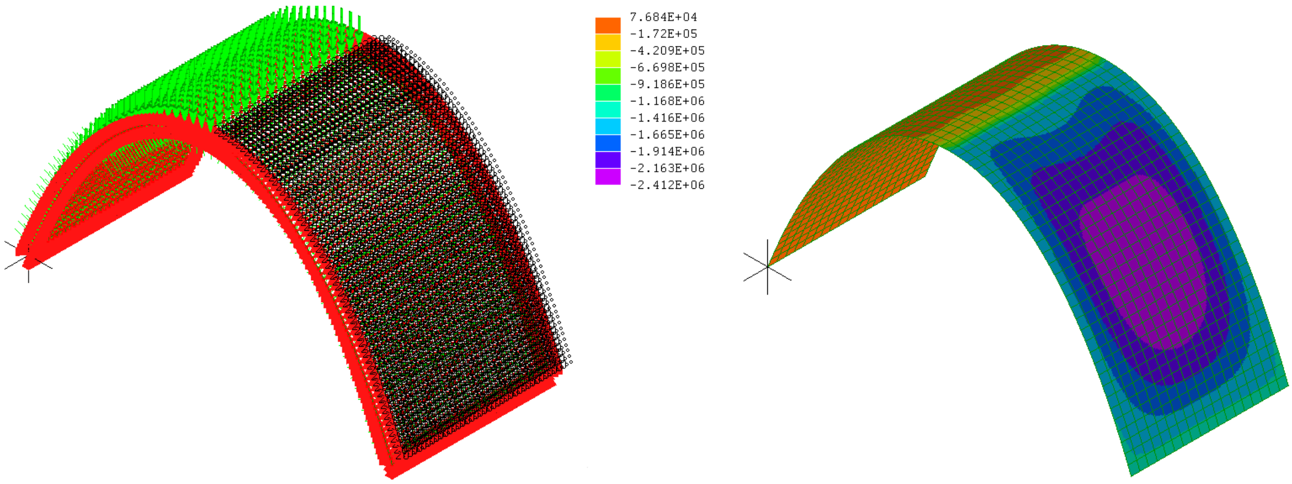

Figure 6-8: Results of a load case whereby the structure has a full wind load, temperature loading along the right side of the vault and a live loading along the left side of the vault

Note that positive values are tensile and negative values are compressive. Due to the restraining of the edges of the vault, considerable tensile forces formed at the apex, which caused cracking. Figure 6-7 shows that a tensile patch forms at the top of the structure when it is under dead and temperature loads. Figure 6-8 shows a clear change from compressive to tensile stresses along the apex of the vault. The cracking of the vault can also be explained in conjunction with Figure 6-9. Figure 6-9 shows how a vault under dead loading will experience certain compressive forces, never exceeding the materials capacity and the minimum compressive force at the apex. However, when a thermal load is applied to a restrained structure, the vault cannot move freely, thus creating additional tensile forces within the material. When the forces reach the apex, as seen in Figure 6-9, the amount of tension exceeds the maximum allowable tensile stress within the material, resulting in cracking.

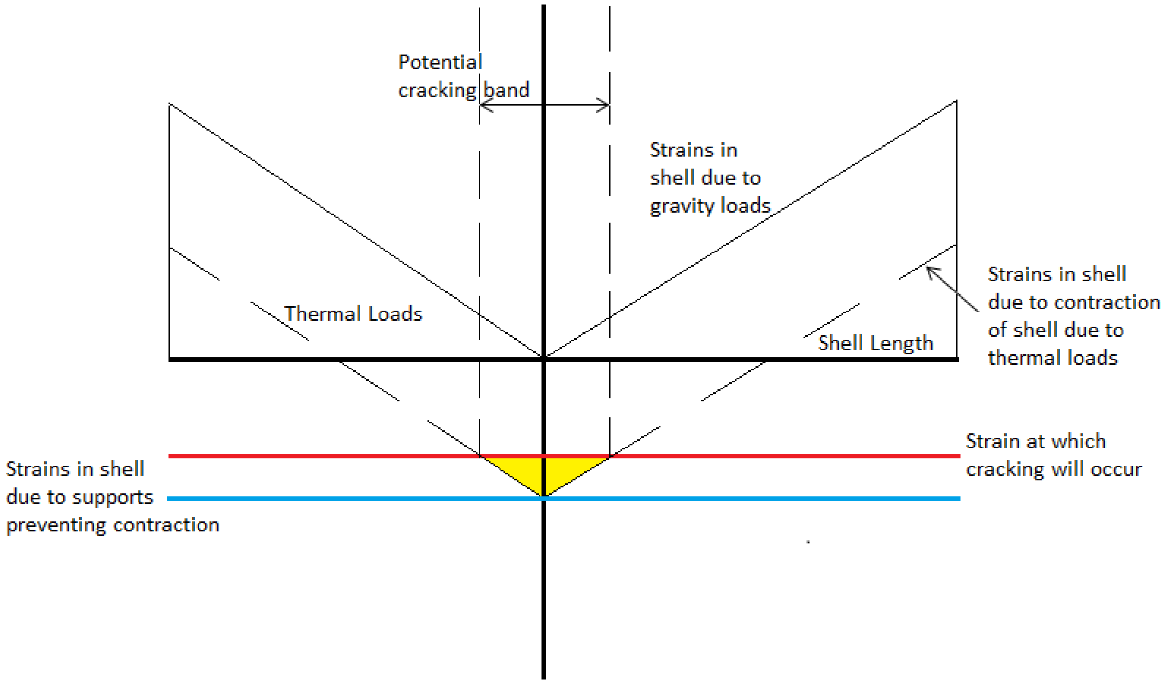

Figure 6-9: A graphical explanation of cracking in a restrained vault after thermal loads are applied

Thus, we can conclude that it is evident that an expansion joint must be incorporated where the vault meets the wall, to allow the roof to expand and contract without being restrained. This will reduce, if not eliminate, these drastic changes in stresses along the centre of the vault and in turn, eliminate cracking. The form is clearly unique, extremely efficient and durable. The design of the vault is instrumental in ensuring a sustainable structure is constructed.

6.3. Loading

The loading for a catenary vault is complex and requires investigation into a number of various pattern loadings. The segmental equilibrium method incorporates dead, live and wind loading. Temperature loading is usually analysed in finite elements, as it is too complex to incorporate into the computerised equilibrium method.

- *Dead Load/Self-weight*

  The self-weight of the structure is the force exerted by the weight of the vault materials, i.e. the loading that the structure is permanently supporting.

  The dead load in this design consists of the materials within the structure. Therefore, the material properties of the blocks, mortar, plaster, etc. are included as dead loads. The load is calculated as a uniformly distributed load (UDL) over the surface of the structure. The calculation of the dead load for the vaulted roof is as follows:

$$Dead\ Load = \ Block\ self\ weight + plaster\ self\ weight$$

  The self-weight of both the block and plaster is calculated as follows:

$$Self\ weight = Density\ \times Gravitational\ constant\ \times thickness$$

  Thus the dead load exerted on the structure is:

$$DL = (1950 \times 0.115 \times 9.81) + (2300 \times 0.03 \times 9.81) = 2.88kN/m^2$$

- *Live loading*

  The live load is obtained from the loading code SABS 0160-2 (2009), and applied in a number of pattern loading combinations on the structure.

  The live loading selected in the design of the roof structure is for maintenance and repair, i.e. an inaccessible roof load. The loading provided is a horizontal UDL of *$0.25kN/m^2$,* or a concentrated point load of *0.9kN* applied over an area of *$1m^2$.*

- *Wind loading*

  The wind loading was done in accordance with SABS 0160-3 (2009). It is calculated as a surface pressure over the different sections of the structure and applied accordingly.

  Considerable research has demonstrated that curved structures resist wind loads extremely well. There is no official wind loading guide for catenary curves; however, SABS 0160-3 (2009) addresses vaulted roofs and domes and this method was applied to this project. In some instances, when the vaults are extremely high, it is recommended to apply the same theory as you would for a pitch roof (Blackmore & Tsokri, 2006). Thus, by combining both theories, wind loading values are calculated and applied to the vaulted roof.

The construction of this structure is to occur in Johannesburg. The aim is to apply this project as a low-cost housing solution, thus the structure will be located in townships or other densely inhabited areas. The following wind loading values are selected:

$$v = 40m/s \ \ (wind\ speed\ for\ Johanneeburg\ area)$$
$$Class\ B$$
$$Category\ 3$$
$$k_p = 0.5\ (a\ constant\ for\ specified\ altitudes)$$
$$Height\ of\ structure = 2.65m + \ {\sim}3.4m \ \cong \ 6m$$

Note: *Class B* is to determine forces on structural members as well as resultant forces and overturning moments for structures which do not exceed 50m in any dimension. *Category 3* is selected for closely spaced obstructions, generally the size of domestic housing (i.e. fully or substantially developed suburbs, industrial areas and towns).

Once these initial values are set, the steps as outlined in SABS 0160-3 (2009) are followed so that all wind pressures applied over the structure are calculated. In order to calculate an accurate wind pressure over the structure, the wind speed multiplier, k_z, will need to be adjusted to suit a 6m height. This is done simply by interpolating the existing values in the 5-10m range.
A k_z value of 0.654 is obtained and the wind pressure is calculated as follows:

$$q_z = k_p[v(k_z)]^2 \tag{6-1}$$

$$q_z = 0.5[40(0.654)]^2$$
$$= 342\ N/m^2$$

The external pressure coefficients, C_{pe}, are obtained from Figure 14 in SABS 0160-3 (2009, p37). The pressure distribution over a vaulted roof is summarised as follows:

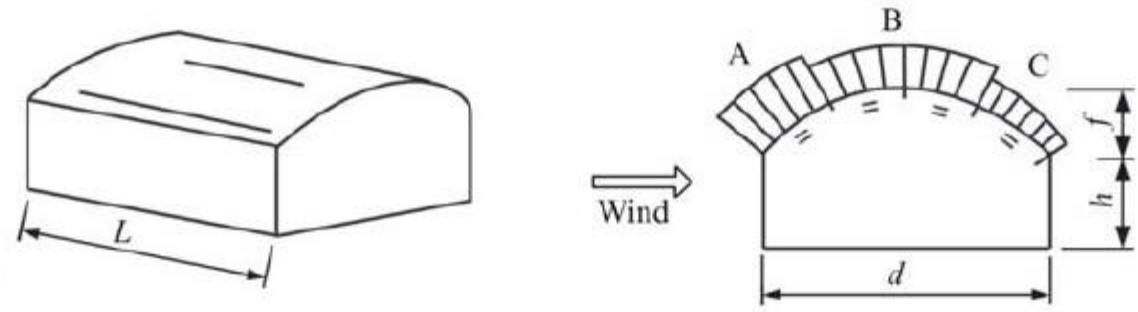

Figure 6-10: Wind distribution over a vaulted roof with a rectangular base (SABS 0160-3, 2009, p37)

The pressure over the surface of the vault is separated into quarters where the first quarter has a pressure *A*, the second and third a pressure *B* and the fourth a pressure *C*. It is important to note that Figure 6-10 represents positive pressure values acting downward. Thus, all negative values are applied in the opposite direction, i.e. acting upwards. The first vault's C_{pe} values are calculated as explained above. However, for the second vault, the values and distribution changes slightly as stated by the multi-span roof wind theory in Figure 13c, SABS 0160-3 (2009, p36).

The external pressure coefficients for the structure, for wind angles of 0° and 180°, are summarised in Figure 6-11.

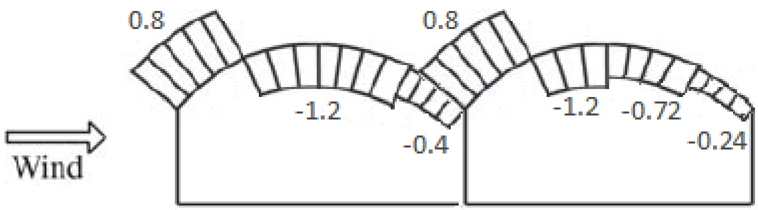

Figure 6-11: External pressure coefficients for a multi-span vaulted roof

If the direction of the wind changes to 90°, two different pressure space configurations are assessed.

If the vaults are assumed to behave in a similar manner as a duo-pitched roof, a pressure distribution as described in SABS 0160-3 (2009) is applied as follows (Figure 6-12):

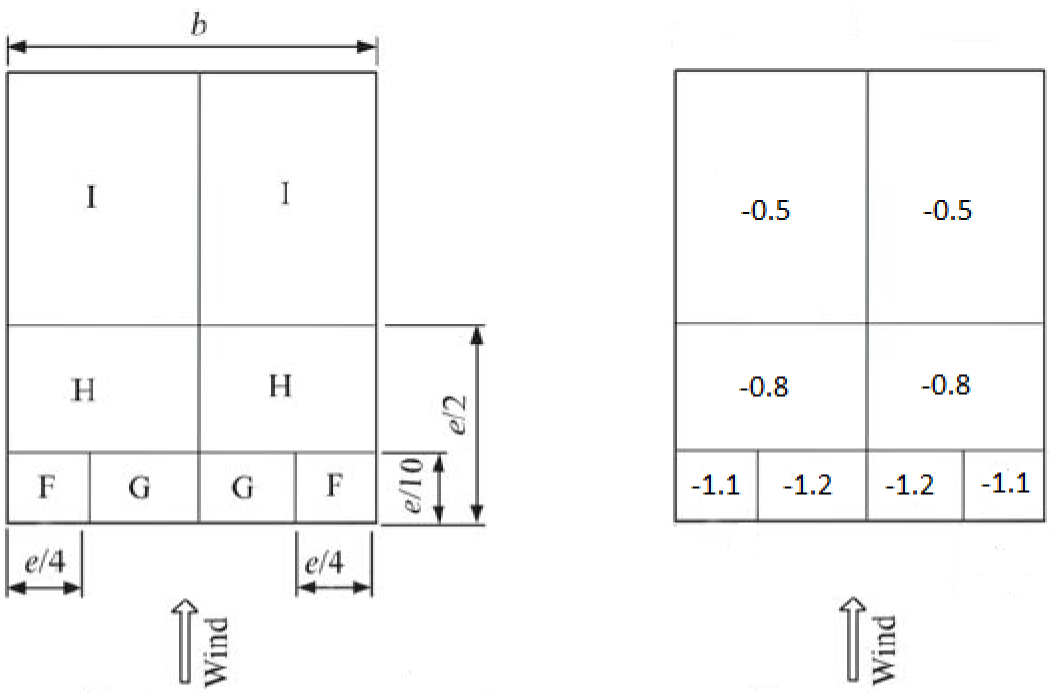

Figure 6-12: ***Left*** **- Wind pressure distribution as seen in SABS 0160-3 (2009, p 31);** ***Right*****-The final external pressure values applied in the prototype as per code**

The external pressure coefficients distribution for a curved roof, according to Blackmore & Tsokri (2006), is presented in Figure 6-13. These curves do not consider catenary vaults, but can be applied as a possible loading pattern.

There are no published codes or literature describing the exact wind distribution on the surface of a catenary vault and therefore these various scenarios are analysed to ensure the worst loading pattern is accounted for.

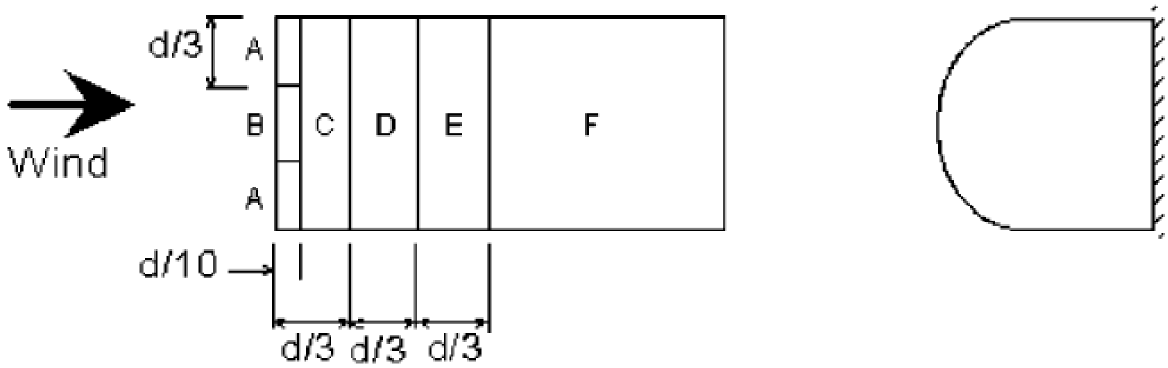

Figure 6-13: External pressure coefficient distribution over a curved roof (Blackmore & Tsokri, 2006, p 837)

When values of A to F are calculated, they are found to have the same values found in Figure 6-12, following an almost identical distribution.

In order to calculate the final wind pressure values applied onto the vaulted roof, a simple calculation must be applied to each of the sections for both wind directions of θ=0°/180° and 90°.

$$Wind\ Pressure = (C_{pe} - C_{pi}) \times q_z \qquad (6\text{-}2)$$

C_{pi} values of 0 and -0.2 are investigated and all wind pressures are calculated and applied to the vaults. Table 6-1 summarises the wind pressure configurations applied to the vaults during analysis.

Table 6-1: Wind pressure distribution (N/m^2) values on the catenary roof

<table>
<tr><th rowspan="3">Wind Angle</th><th rowspan="3">Section</th><th colspan="2">Wind Pressure (N/m²)</th><th colspan="2">Wind Pressure (N/m²)</th></tr>
<tr><td colspan="2">$C_{pi}=0$</td><td colspan="2">$C_{pi}=-0.2$</td></tr>
<tr><td>1st Vault</td><td>2nd Vault</td><td>1st Vault</td><td>2nd Vault</td></tr>
<tr><td rowspan="4">Θ=0° and 180°</td><td>A</td><td>273.6</td><td>273.6</td><td>342</td><td>342</td></tr>
<tr><td>B (1st half)</td><td>-410.4</td><td>-410.4</td><td>-342</td><td>-342</td></tr>
<tr><td>B (2nd half)</td><td>-410.4</td><td>-246.2</td><td>-342</td><td>-177.8</td></tr>
<tr><td>C</td><td>-136.8</td><td>-82.1</td><td>-68.4</td><td>-13.7</td></tr>
<tr><td rowspan="4">Θ=90°</td><td>F</td><td colspan="2">-376.2</td><td colspan="2">-307.8</td></tr>
<tr><td>G</td><td colspan="2">-410.4</td><td colspan="2">-342</td></tr>
<tr><td>H</td><td colspan="2">-273.6</td><td colspan="2">-205.2</td></tr>
<tr><td>I</td><td colspan="2">-171</td><td colspan="2">-102.6</td></tr>
</table>

- *Temperature loading*

  Temperature loads have been found to cause significant cracking, and yet they are very often overlooked. This load varies according to the environment in which the structure is situated (i.e. some places experience temperature changes of 5°C throughout the day while others can range by as much as 30°C). In Johannesburg, a temperature difference of 20°C is normally assumed.

6.4. Loading Combinations and Patterns

A number of loading combinations and patterns were investigated in both the Excel and the finite element analysis of design, as per SABS 0160 (2009). The following loading ultimate limit state combinations were assessed:

- 1.5 x Dead Load
- 1.2 x Dead Load + 1.6 x Live Load
- 1.2 x Dead Load + 0.5 x Live Load + 1.3 x Wind Load
- 0.9 x Dead Load + 1.3 x Wind Load

The following service limit state combinations were investigated as well:

- 1.0 x Dead Load
- 1.1 x Dead Load + 1.0 x Live Load
- 1.1 x Dead Load + 0.3 x Live Load + 0.6 x Wind Load
- 1.0 x Dead Load + 0.6 x Wind Load

Once the safety factors are established and the loading combinations applied, it is important to explore various pattern loadings. This is done to ensure that all possible loading patterns have been taken into account when the structures final design is established, and is therefore designed for the 'worst case' scenario. In the current analysis, the only loads that are applied in various patterns are that of live loads and temperature loads. The wind loading, although different for various designs, is a set pressure over the surface, as identified in Table 6-1. The dead load is constant.

A finite element analysis was performed to identify the most severe live loading patterns. The final loading patterns that are investigated are shown in Figure 6-14. Each of these loading patterns were applied individually, resulting in six live loading combinations. They include: a horizontal projectile load over the full length (Figure 6-14a) and the two separate halves (Figures 6-14b and c), a point load at the centre (Figure 6-14d), at a quarter length (Figure 6-14e) and at three quarters length (Figure 6-14e).

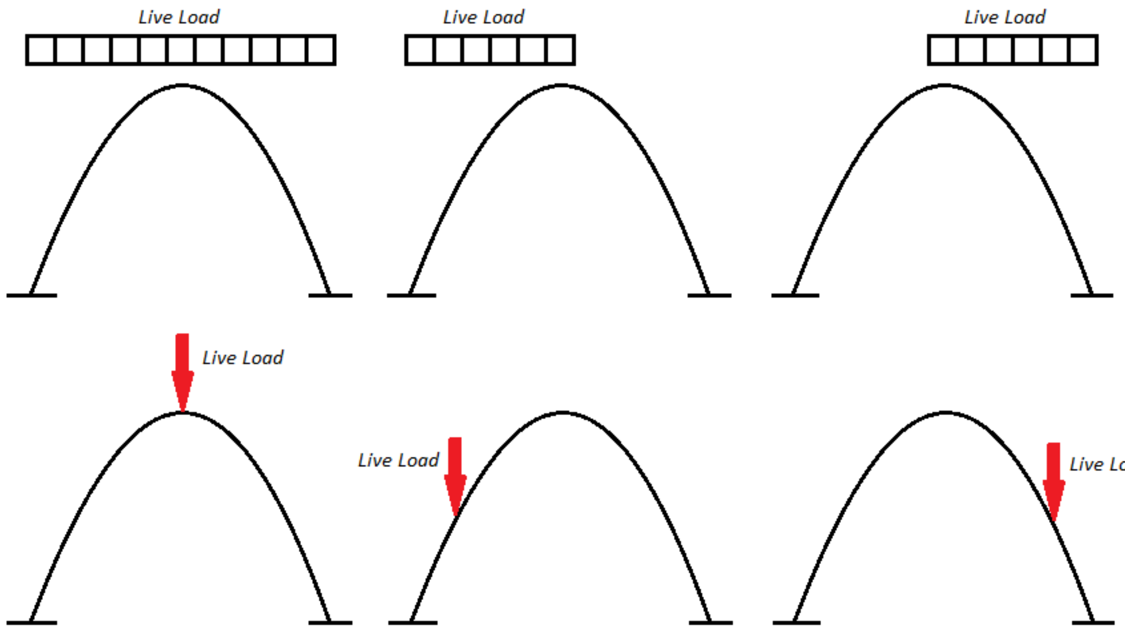

Figure 6-14: Loading patterns for the applied live loads: (a) Full horizontal projection, (b) half load over the left half, (c) half load over the right half, (d) point load at the centre, (e) point load at a quarter length, (f) point load at three quarters.

The temperature loading was assessed and selected in a similar manner to the live loading. The key loading patterns are summarised in Figure 6-15. Positive and negative temperature changes, resulting in shrinkage and expansion, were investigated.

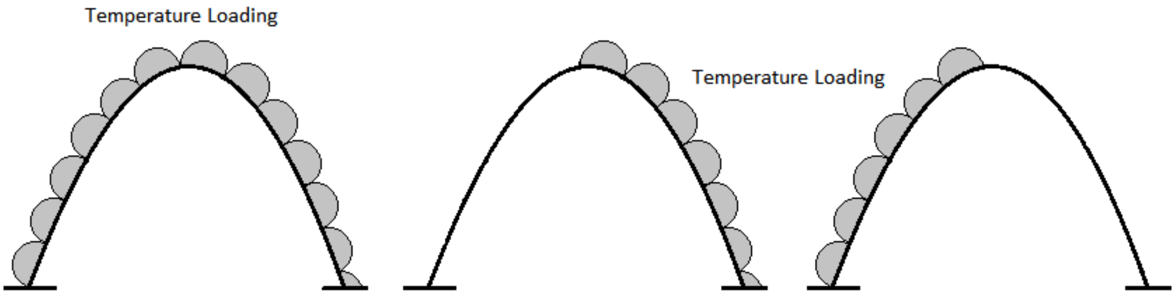

Figure 6-15: Investigated loading patterns for temperature loads: (a) temperature loading over the entire structure, (b) temperature loading over the right half of the structure, (c) temperature loading over the left half of the structure

6.5. Design Process using the Segmental Equilibrium Method

Chapter 5 discussed the process by which a catenary curve is designed using the segmental equilibrium method. In this section, the process of designing the roof structure of the prototype will be discussed in detail.

6.5.1. Dead Load Design

The first step is to establish the geometry of the curve. The user has a general idea of the dimensions of the curve, i.e. its length and height. All the designs are done to a metre length vault section. Gravity loading determines the dimensions of the vault; however, the lateral forces determine the required thickness of the shell. All final calculations were done in Excel spread sheets (Appendix A). The steps presented below can be followed in the spread sheet on page 99. The process is as follows:

1. Input all the material properties:
   - Density = 1950kg/m^3
   - Young's Modulus = 3500MPa
2. Add the initial vault dimensions. These are important when you are iterating to ensure that the curve spans the required vault size. These values are the initially assumed dimensions as discussed in Chapter 3.
   - Height = 3.5m
   - Length = 3.4m
3. Select an initial segment size. The segment height chosen was 130mm. This height was selected to allow for higher accuracy in shorter heights but with more number of segments spanning the length of the curve. The length of the segment will vary with each load case. It was roughly estimated that 63 segments were to be used. This number is a random estimate; however, the more segments you have the higher the accuracy.
4. An initial angle of 80° is selected as the vault is predominantly vertical. This value will also change with each load case in the iterative approach.
5. The various loads are now incorporated into the spread sheet and all factors are applied. In this example, only the gravity loads will be discussed. These loads are transformed into point loads that are applied at the centre of each segment (Table 6-2 and 6-3). These point loads are calculated according to

the length of the segment, thus with a differing segment height, the value of the point load will also vary.

Table 6-2: Dead Loads applied to the vault

Loads		
Dead Load		Units
Bricks/Masonry weight per block	2.88	kN/m^2
Weight of each segment as a point load	0.37	kN

Table 6-3: Loading combinations applied in analysis of vault

Load combinations		
	ULS	DL (kN)
LC1	1.5DL	0.56
	SLS	DL (kN)
LC1	1.0DL	0.37

6. The spread sheet is now set up as demonstrated in point 9 of section 5.5.4. The thrust line under gravitational forces can now be calculated. In this section, we are only discussing the dead load applied to the structure which will be constant at each segment; thus, the value in the *weight* column is identical for each segment. All the previously chosen values are inputted into the spread sheet. These include initial segment height, angle and number of segments. The first row of calculation is the most unique and complex as values may need to be manually inputted or calculated in a separate spreadsheet. The remaining rows of calculation follow a continuous pattern generated from the previous rows of results. All steps can be followed in the spread sheet presented on page 99 (Figure 6-16).
7. The first calculation includes establishing the exact value of the left thrust force, which is also the reaction force at the left end of the curve. Since the loading is symmetrical over the structure, a simple equilibrium calculation can be done to establish the vertical component of this force, i.e. $\sum Fy=0$. The left

and right reaction forces are identical and thus the total dead load is calculated and halved.

$$Left\ Thrust\ Force\ (y) = \frac{0.559 \times 63}{2} = 17.63kN$$

8. *Left Thrust x* and ***Left Thrust Resultant*** are calculated using trigonometry as follows:

$$Left\ Thrust = \frac{Left\ Thrust\ (y)}{sin\theta} = \frac{17.63}{\sin(80)} = 17.90kN$$

$$Left\ Thrust\ (x) = Left\ Thrust\ \times cos\theta = 17.90\ \times \cos(80) = 3.11kN$$

Note: The chosen sign notation indicates that any forces to the right and up are positive.

9. The remaining steps will follow a continuous pattern throughout the spread sheet. *Right thrust x* and *right thrust y* are calculated through equilibrium equations, i.e. ∑Fy=0 and ∑Fx=0. This is done at the centre of the segment, where equilibrium is calculated around that point incorporating all the various loading. In this case, there are no horizontal loads applied to the structure, only a vertical dead load. Thus, the *right thrust x* is identical in magnitude but opposite in direction to *left thrust x*.

$$Left\ Thrust\ x + Right\ Thrust\ x = 0$$

$$Right\ Thrust\ x = -Left\ Thrust\ x = -3.11kN$$

The *right thrust y* has to account for the reaction force from the left as well as any external vertical forces.

$$Left\ Thrust\ y + Right\ thrust\ y + Dead\ Load = 0$$

$$Right\ Thrusy\ y = -Left\ Thrust\ y - Dead\ Load = -17.63 - (-0.559)$$
$$= -17.07kN$$

The ***Right Thrust Resultant*** force can now be calculated using Pythagoras theorems:

$$Right\ Thrust = \sqrt{17.07^2 + 3.11^2} = 17.35kN$$

10. The new angle is calculated. This is done using the newly calculated right side forces and trigonometry.

$$\theta = \tan^{-1}\left(\frac{Right\ Thrust\ y}{Right\ Thrust\ x}\right) = \tan^{-1}\left(\frac{17.07}{3.11}\right) = 79.68°$$

11. Finally, the co-ordinates of the centre of the first segment are calculated. This is the start of the thrust line. The co-ordinates are calculated using trigonometry as follows.

$$x = Length\ of\ block\ \times \cos(\theta) = 130\ \times \cos(80) = 22.57mm$$

$$y = Length\ of\ block\ \times \sin(\theta) = 130\ \times \sin(80) = 128.03mm$$

Note that the angle used is the old angle and not the new one calculated in point 10. These points represent the centre of the segment and therefore do not start at (0,0). Thus, each succeeding co-ordinate will be calculated as before, using trig, but simultaneously added to the preceding co-ordinate. This is covered in point 14.

12. The first row of calculation is now complete. The second row needs to be set up accordingly and all the succeeding rows of calculation follow the same formulae as row 2. The Excel spread (see page 99) sheet highlights in green the values that are carried over from the previous row, i.e. the ***Right Thrust Resultant*** Force becomes the ***Left Thrust Resultant*** Force in the succeeding row and the newly calculated right angle becomes the left angle on the succeeding row. Now that the ***left thrust*** force is calculated, the *left thrust x* and *left thrust y* are calculated using trig in conjunction with the new angle.

$$Left\ Thrust\ y = 17.347\ \times \sin(79.69) = 17.07kN$$

13. The right thrust values and new angle are calculated in the same manner as in step 9 and 10.
14. The new co-ordinate is calculated in the same way as point 11; however, it is added to the preceding co-ordinate.

$$x_2 = x_1 + Height\ of\ segment \times \cos(\theta) = 22.57 + 130 \times \cos(79.68) = 45.86mm$$

$$y_2 = y_1 + Height\ of\ segment \times \cos(\theta) = 128.03 + 130 \times \cos(79.68) = 255.92mm$$

15. Steps 12 to 14 are repeated for all of the remaining segments, resulting in a final thrust line.
16. As mentioned previously, each co-ordinate represents the centre of the segment. Thus, the first half and last half of the segment (i.e. height) are not incorporated into the calculation. In order to complete the curve, (0,0) is inputted as the first co-ordinate to ease calculations, and the final co-ordinate is calculated very simply. The values to be added in the x and y co-ordinates are given as the difference between the first and second co-ordinate. Since the first co-ordinate is (0,0) the value of the second is the difference, and need only be added to the final point.

$$x_{final} = 3518.11 + 22.57 = 3540.69mm$$

$$y_{final} = 128.03 - 128.03 = 0mm$$

The final dimensions of the curve, with the assumed initial inputs, were too high and exceeded the intended height of the shell. Thus, the above process was repeated, in an iterative approach, by varying the initial angle and the segment height until a more satisfactory set of dimensions was achieved.

The final initial angle is 80.5° and a segment height of 128.2mm. This provided us with a final curve with a vault height of 3482.85mm and a width of 3383.37mm. The final spread sheet for the calculation of the thrust line under dead load, and essential the final geometry, can be found in Appendix A.

Segment no.	Height of Segment	Weight	Left Angle	Left Thrust x	Left Thrust y	**Left Thrust Resultant**	Right Thrust x	Right Thrust y	**Right Thrust Resultant**	Right angle	Co-ordinates X	Co-ordinates Y
1	130	0.56	80.00	3.11	17.63	17.90	-3.11	-17.07	17.35	79.68	0.00	0.00
2	130	0.56	79.68	3.11	17.07	17.35	-3.11	-16.51	16.80	79.34	22.57	128.03
3	130	0.56	79.34	3.11	16.51	16.80	-3.11	-15.95	16.25	78.97	45.87	255.92
[illegible]	[illegible]	[illegible]	78.97	3.11	[illegible]	[illegible]	-3.11	-15.39	[illegible]	[illegible]	69.92	383.68
[illegible]	[illegible]	[illegible]	78.58	3.11	[illegible]	[illegible]	-3.11	-14.83	[illegible]	[illegible]	94.79	511.28
[illegible]	[illegible]	[illegible]	78.16	3.11	14.83	15.15	-3.11	-14.27	14.60	77.71	120.52	638.70
7	130	0.56	77.71	3.11	14.27	14.60	-3.11	-13.71	[illegible]	[illegible]	[illegible]	765.94
8	130	[illegible]	[illegible]	[illegible]	13.71	14.06	-3.11	-13.15	[illegible]	[illegible]	[illegible]	892.96
9	130	[illegible]	[illegible]	[illegible]	13.15	13.51	-3.11	-12.59	12.97	76.13	203.60	1019.74
10	130	0.56	76.13	3.11	12.59	[illegible]	[illegible]	[illegible]	12.43	75.51	233.50	1146.26
11	130	0.56	75.51	3.11	12.03	[illegible]	[illegible]	[illegible]	11.88	74.84	264.66	1272.47
12	130	0.56	74.84	3.11	11.47	11.88	-3.11	-10.91	11.34	74.10	297.18	1398.34
13	130	0.56	74.10	3.11	10.91	11.34	-3.11	-10.35	10.81	73.29	331.17	1523.81
14	130	0.56	73.29	3.11	10.35	10.81	-3.11	-9.79	10.27	72.39	366.79	1648.84
[illegible]	[illegible]	[illegible]	72.39	3.11	9.79	10.27	-3.11	-9.23	9.74	71.40	404.17	1773.35
[illegible]	[illegible]	[illegible]	71.40	3.11	9.23	9.74	-3.11	-8.67	9.21	[illegible]	[illegible]	1897.26
[illegible]	[illegible]	[illegible]	70.29	3.11	8.67	9.21	-3.11	-8.11	8.69	[illegible]	[illegible]	2020.46
57	130	0.56	-77.23	3.11	-13.71	14.06	-3.11	14.27	14.60	-77.71	3337.08	1019.74
58	130	[illegible]	[illegible]	3.11	-14.27	14.60	-3.11	14.83	15.15	-78.16	3365.83	892.96
59	130	[illegible]	[illegible]	3.11	-14.83	15.15	-3.11	15.39	[illegible]	[illegible]	3393.49	765.94
60	130	0.56	-78.58	3.11	-15.39	15.70	-3.11	15.95	[illegible]	[illegible]	3420.16	638.70
61	130	0.56	-78.97	3.11	-15.95	16.25	-3.11	16.51	[illegible]	[illegible]	3445.90	511.28
62	130	0.56	-79.34	3.11	-16.51	16.80	-3.11	17.07	[illegible]	[illegible]	3470.77	383.68
63	130	0.56	-79.68	3.11	-17.07	17.35	-3.11	17.63	17.90	-80.00	3494.82	255.92
											3518.11	128.03
											3540.69	0.00

An initial assumed brick length of 130mm is applied

The initially assumed angle is inputted

Left Reaction Force of the curve

Left Thrust (line 2) = Right Thrust (Line 1)

Left angle (line 2) = Right angle (Line 1)

Insert co-ordinate (0,0) as a starting point

A constant dead load is applied to all the bricks

Each co-ordinate represent the centre point for the brick

63 bricks are used, as chosen in step 3

Calculate the final co-ordinate, thus taking into account the remainder of the brick

Figure 6-16: An Excel spread sheet showing the design process of a catenary curve subject to dead loading

Once the thrust line under dead load is calculated, the geometry of the curve is set. From here, the thickness of the segment and the middle third parameters can be drawn in (Figure 6-17). This is important so as to ensure that the thrust lines fall within the middle third of the shell thickness and to identify areas of weakness or areas susceptible to tensile stresses.

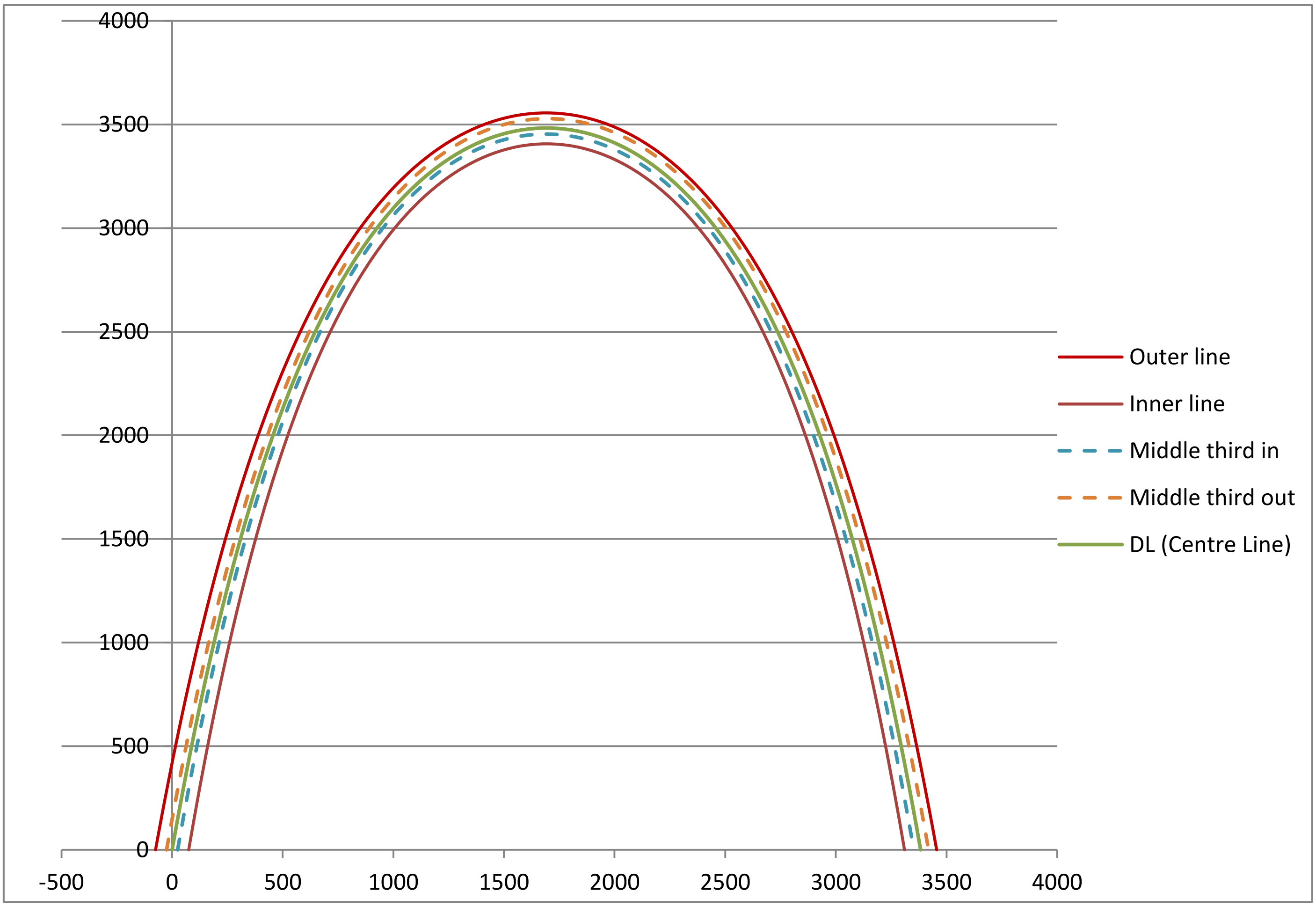

Figure 6-17: A graph representing the final geometry of the vaulted roof

6.5.2. Dead Load, Live Load and Wind Load Analysis

The geometry of the curve is now set, providing a platform from which the remaining loading analysis can commence. The segment height and initial angle will vary with each load case, but only marginally, and therefore less iteration's are necessary to solve for the required geometry. Each thrust line is unique for each load case and the aim is to get it as close as possible to the original (dead load) thrust line, therefore keeping it in the middle third of the segment thickness.

Thrust Line Analysis with only dead loads is relatively simple. The process becomes considerably more complex when a lateral force is applied; such as wind loading. In this section, a detailed step by step design process will be discussed which will cover a number of varying loads. The curve will be subject to a wind load, live load and dead load. The live load is a horizontal projection over all or a portion of the curve, as described in figure 6-5, and the wind load has a C_{pi} value of -0.2. No different to the dead load calculation, the analysis phase begins with an assumed initial angle and segment height. These values are varied to achieve the required geometry for the specific thrust line. In this step, the final values achieved in the dead load calculation are used as the initial guess and then follow an iterative process to calculate the actual angle and segment height. Unlike section 6.6.1, the *final* calculations steps will be covered with the correct angle and segment height value for that specific thrust line.

1. The material properties are as before (refer to step 1 in section 6.6.1) and the thrust line should fit within the middle third, as seen in figure 6-15.
2. The segment height and angle, for the final thrust line, are 133mm and 83.3° respectively. This has been obtained through an iterative process.
3. The load cases are now incorporated into the spread sheet (Table 6-4, 6-5 and 6-6). These loads include live loads, wind loads and dead loads. As before, these loads are transformed from loads and surface loads into point loads, and applied at the centre of each segment.

   The dead load is calculated as a vertical force:

Table 6-4: Dead loads applied to vaulted roof

Loads		
Dead Load		Units
Bricks/Masonry weight per block	2.88	kN/m^2
Weight of each segment as a point load	0.37	kN

The live load is not a UDL over the surface of the structure, as is the dead load, but rather a horizontal projection over the structure and therefore the value of the live load applied is different for each segment. This value depends on the angle at which the segment is situated, i.e. for a steeper section the live load will be less as it covers less of a horizontal distance and vice versa for more horizontal sections (Figure 6-18).

Table 6-5: The value of the live load applied on the vault, obtained from SABS 0160 (2009)

Live Load	0.25	kN/m2

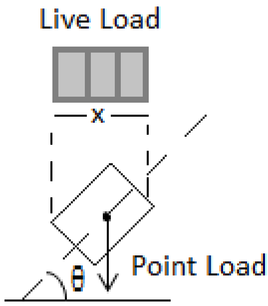

Figure 6-18: A horizontal projection of the live load over a segment

$$Point\ Load\ of\ LL\ per\ segment = Load\ Factor\ \times 0.25\ kN/m^2 \times\ x \qquad (6\text{-}3)$$

Where x is the length of the live load exerted on that segment and is calculated as follows:

$$x = Height\ of\ segment\ \times \cos\ (angle\ of\ segment) \qquad (6\text{-}4)$$

The live load at the apex of the curve is calculated as follows:

$$PL = 0.5 \times 0.25 \times (128.2 \times \cos(5.42)) = 0.016kN$$

This point load is then added to the dead load value at the segment centroid. This value will vary at each segment, depending on the angle of the segment.

The calculation of the wind load is slightly more complex as it has a horizontal and vertical component. The wind load is a pressure over the surface of the vault. As with the other loads, the wind pressure is transformed into a point load and then separated into its relevant components and applied to the segments. It is assumed that the wind load is perpendicular to the segment and thus the components will vary according to the angle of the segment. In this load case, a wind pressure with a C_{pi} value of -0.2 is used.

Table 6-6: Wind Pressures values distributed over the vaulted roof (Refer to Figure 6-10)

Wind Load (kN/m2)	*Cpi=-0.2*	*Point Load (kN)*
1st section (A)	0.342	0.044
2nd and 3rd section (B)	-0.342	-0.044
4th section (C)	-0.068	-0.0089

To calculate the horizontal and vertical components at any given segment, the following steps are followed:

$$Wind\ Load\ H = Factor\ of\ Safety\ \times Wind\ Load \times \sin(Angle\ of\ the\ segment) \quad (6\text{-}5)$$

$$Wind\ Load\ V = Factor\ of\ Safety\ \times Wind\ Load \times \cos(Angle\ of\ the\ segment) \quad (6\text{-}6)$$

If a random segment is selected for analysis, in this case segment no 12, the wind load is calculated as follows:

- This segment falls within the 1st section, therefore Wind Load is 0.044kN.
- The load factor of the current load combination is 1.6
- The angle of the segment is obtained from the DL spread sheet so that the true angle of the segment is used. The angle is 75.58°

$$Wind\ Load\ H = 1.6 \times 0.044 \times \sin(75.58) = 0.055kN$$

$$Wind\ Load\ V = 1.6 \times 0.044 \times \cos(75.58) = 0.014kN$$

These values are reasonable as the segment is at a steep angle, therefore the load will predominantly have a horizontal component.

The loads are inputted into the relevant cells by the user. As noted in the spread sheet, the live loads are only applied from segment 32 onwards as the loading pattern comprises of a live load over the second half of the vault (Figure 6-14c). The wind load is adjusted at every quarter point, as indicated by SABS0160-3 (2009).

A summary of the loading combinations is presented in Table 6-7.

Table 6-7: Loading combinations for the analysis of a catenary vault

	Load combinations					
	ULS	**DL (kN)**	**LL (kN/m²)**	**WL1 (kN)**	**WL2+3 (kN)**	**WL4 (kN)**
LC1	1.5DL	0.552	0	0	0	0
LC2	1.2DL+1.6LL	0.441	0.400	0	0	0
LC3	1.2DL +0.5LL +1.3WL	0.441	0.125	0.057	-0.057	-0.011
LC4	0.9DL+1.3WL	0.331	0	0.057	-0.057	-0.011
	SLS	**DL (kN)**	**LL (kN/m²)**	**WL1 (kN)**	**WL2+3 (kN)**	**WL4 (kN)**
LC1	1.0DL	0.368	0	0	0	0
LC2	1.1DL+1.0LL	0.405	0.250	0	0	0
LC3	1.1DL+0.3LL+0.6WL	0.405	0.075	0.026	-0.026	-0.005
LC4	1.0DL+0.6WL	0.368	0	0.026	-0.026	-0.005

4. Now that the loading columns are complete, the first row of calculations can be set up. The first step is to calculate the *left thrust y*. As discussed previously, this force is the reaction force of the vault on the left hand side. Unlike the previous example, the loading is not symmetrical and the reaction cannot be calculated by simply adding and halving the external loads. The

force can still be calculated through the use of equilibrium, but by utilising a slightly more complex method, i.e. ∑M=0. Each of the external loads are totalled and transformed into a single point load with a corresponding distance to the edge. The dead and live loads are simply multiplied by the length of the load and applied as point loads. The wind loads are transformed in their corresponding sections and applied as point loads in the centroid of each section. It is important to obtain the correct distance to the edge of the vault, as well as angle at which the load is orientated. The loads are separated as presented in figure 6-19.

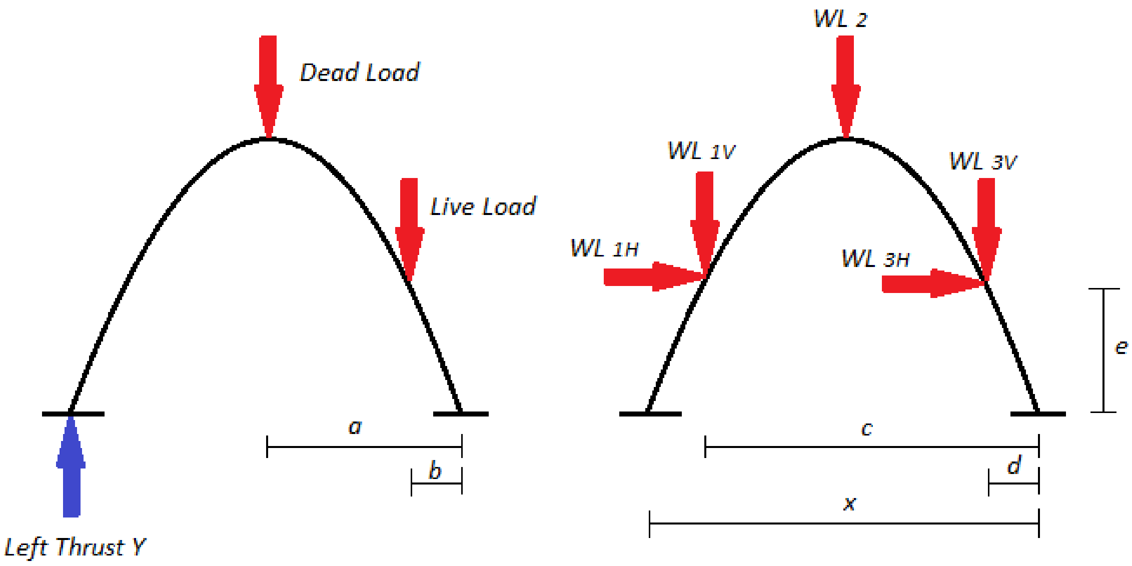

Figure 6-19: A summary of all of the collapsed loads and their distances to edge - *Left:* Dead and Live Loads; *Right:* Wind Loads

The left thrust force is calculated as follows:

$$LT\ Y = \big((DL + WL_2) \times a + LL \times b + WL_{1V} \times c + WL_{3V} \times d - (WL_{1H} + WL_{3H}) \times e\big)/x \tag{6-7}$$

Thus, the value of the *Left Thrust Y* for this load case has a value of 13.24kN.

5. The *Left thrust x* and ***Left Thrust*** are calculated as before:

$$Left\ Thrust = \frac{Left\ Thrust\ (y)}{sin\theta} = \frac{13.24}{\sin(83.3)} = 13.33kN$$

$$Left\,Thrust\ (x) = Left\,Thrust\ \times cos\theta = 13.33\ \times \cos(83.3) = 1.56kN$$

6. The remainder of the steps follow a similar procedure as in section 6.6.1. Previously, when calculating the *Right Thrust x,* it was merely equal to the *Left Thrust x*. However, in this load case, there is an external horizontal force exerted by the wind load that needs to be considered in the calculation. Thus, the *Right Thrust x,* is calculated as follows:

$$Left\,Thrust\ x + Right\,Thrust\ x + Wind\ Load\ (H) = 0 \qquad (6\text{-}8)$$

$$Right\,Thrust\ x = -Left\,Thrust\ x - Wind\ Load\ (H) = -1.56 - 0.056 = -1.61kN$$

The *Right Thrust Y* is calculated, as before, by taking into account all the vertical forces exerted on that particular segment.

$$Left\,Thrust\ y + Right\ thrust\ y + Dead\ Load + Live\ Load + Wind\ Load\ (V) = 0 \qquad (6\text{-}9)$$

$$Right\ Thrusy\ y = -Left\,Thrust\ y - Dead\ Load - Live\ Load - Wind\ Load\ (V)$$
$$= -13.24 - (-0.441) - 0 - (-0.009) = -12.79kN$$

In this load case, the live load is equal to zero for the first calculation and the following 30 as the load only falls over the second half of the vault.

The ***Right Thrust*** is calculated as follows:

$$Right\,Thrust = \sqrt{12.79^2 + 1.61^2} = 12.89kN$$

7. The new angle is calculated:

$$\theta = \tan^{-1}\left(\frac{Right\,Thrust\ y}{Right\,Thrust\ x}\right) = \tan^{-1}\left(\frac{12.79}{1.61}\right) = 82.82°$$

8. Lastly, the co-ordinates of the centre of the first segment are calculated as in section 6.6.1.

$$x = Length\ of\ block\ \times \cos(\theta) = 133\ \times \cos(83.3) = 15.52mm$$
$$y = Length\ of\ block\ \times \sin(\theta) = 133\ \times \sin(83.3) = 132.09mm$$

9. The remaining rows of calculation follow a constant formula. The ***right thrust*** and its components, as well as the new angle are calculated as discussed previously. It is important to note that:
    - ***Right Thrust*** *(Row 1)* = ***Left Thrust*** *(Row 2)*
    - *New Angle (Row 1) = Old Angle (Row 2)*
10. The left thrust components are calculated using trigonometry. Steps 6 to 9 are repeated for each succeeding row.
11. The co-ordinates are calculated in the same manner as step 8; however, they are also added to the preceding co-ordinate.

$$x_2 = x_1 + \ Length\ of\ block\ \times \cos(\theta) = 15.52 + 133 \times \cos(82.82) = 32.14mm$$

$$y_2 = y_1 + Length\ of\ block \times \cos(\theta) = 132.09 + 133 \times \cos(82.82) = 264.05mm$$

All calculations can be followed on page 108.

Segment no.	Height of Segment	DL + LL per block	Wind Load	WL H	WL V	Left Angle	Left Thrust x	Left Thrust y	**Left Thrust Resultant**	Right Thrust x	Right Thrust y	**Right Thrust Resultant**	Right angle	Co-ordinates X	Co-ordinates Y
1	133	0.4414	0.0570	0.0562	0.0094	83.30	1.556	13.242	13.333	-1.612	-12.791	12.892	82.82	0	0
2	133	0.4414	0.0570	0.0562	0.0097	82.82	1.612	12.791	12.892	-1.668	-12.340	12.452	82.30	15.52	132.09
3	[illegible]	0.4414	0.0570	0.0561	0.0100	[illegible]	[illegible]	[illegible]	12.452	-1.724	[illegible]	[illegible]	[illegible]	32.14	264.05
4	[illegible]	0.4414	0.0570	0.0560	0.0104	[illegible]	[illegible]	[illegible]	12.013	-1.780	[illegible]	[illegible]	[illegible]	49.96	395.85
5	133	0.4414	0.0570	0.0560	0.0107	81.15	1.780	[illegible]	[illegible]	[illegible]	-10.985	11.137	80.51	69.05	527.47
6	133	0.4414	0.0570	0.0559	0.0111	80.51	1.836	[illegible]	[illegible]	[illegible]	-10.532	10.701	[illegible]	[illegible]	[illegible]
7	133	[illegible]	[illegible]	0.0558	0.0115	79.82	1.892	10.532	10.701	-1.948	-10.079	10.266	[illegible]	[illegible]	[illegible]
								…							
15	133	0.4414	0.0570	0.0546	0.0164	71.29	2.335	6.894	7.278	-2.390	[illegible]	[illegible]	69.63	357.42	1824.36
16	133	0.4414	0.0570	0.0543	0.0173	69.63	2.390	6.436	6.865	-2.444	[illegible]	[illegible]	67.76	400.09	1950.33
17	133	0.4414	-0.0570	-0.0540	-0.0184	67.76	2.444	5.977	6.457	-2.390	-5.554	6.046	66.72	446.38	2075.01
18	133	0.4414	-0.0570	-0.0536	-0.0195	66.72	2.390	5.554	6.046	-2.336	-5.132	5.639	65.52	496.72	2198.12
19	133	0.4414	-0.0570	-0.0531	-0.0207	65.52	2.336	5.132	5.639	-2.283	-4.711	5.235	64.14	549.29	2320.29
								…							
30	133	0.4414	-0.0570	-0.0244	-0.0515	18.87	1.829	0.625	1.933	-1.805	-0.235	1.820	7.42	1423.54	3457.15
31	133	0.4414	-0.0570	-0.0156	-0.0548	7.42	1.805	0.235	1.820	-1.789	0.151	1.796	-4.84	1549.39	3500.16
32	133	0.4574	-0.0570	-0.0054	-0.0567	-4.84	1.789	-0.151	1.796	-1.784	0.552	1.867	-17.20	1681.28	3517.34
33	133	0.4574	-0.0570	0.0054	-0.0567	-17.20	1.784	-0.552	1.867	-1.789	0.953	2.027	-28.04	1813.80	3506.12
34	133	0.4568	-0.0570	0.0156	-0.0548	-28.04	1.789	-0.953	2.027	-1.805	1.355	2.257	-36.89	1940.86	3466.79
								…							
[illegible]	[illegible]	0.4473	-0.0570	0.0531	-0.0207	-68.97	2.283	-5.938	6.361	-2.336	6.364	6.779	-69.84	2843.61	2194.26
[illegible]	[illegible]	[illegible]	-0.0570	0.0536	-0.0195	-69.84	2.336	-6.364	6.779	-2.390	6.791	7.200	-70.61	2891.35	2070.12
[illegible]	[illegible]	[illegible]	-0.0114	0.0108	-0.0037	-70.61	2.390	-6.791	7.200	-2.401	7.234	7.622	-71.64	2937.19	1945.27
49	133	0.4463	-0.0114	0.0109	-0.0035	-71.64	2.401	-7.234	7.622	-2.412	7.677	8.047	-72.56	2981.34	1819.81
50	133	0.4460	-0.0114	0.0109	-0.0033	-72.56	2.412	-7.677	8.047	-2.423	8.120	8.474	-73.39	3023.23	1693.58
								…							
61	133	0.4443	-0.0114	0.0112	-0.0021	-78.58	2.533	-12.545	12.798	-2.545	12.987	13.234	-78.91	3327.82	536.45
62	133	0.4442	-0.0114	0.0112	-0.0020	-78.91	2.545	-12.987	13.234	-2.556	13.429	13.670	-79.22	3355.82	406.43
63	133	0.4442	-0.0114	0.0112	-0.0019	-79.22	2.556	-13.429	13.670	-2.567	13.871	14.107	-79.52	3382.96	276.23
														3409.29	145.86
														3434.86	0.00

Dead Load only

WL H = WL*sin(orig angle)
WL V = WL*cos(orig angle)

Calculated by using static equilibirum: ∑M=0

Right Thrust (Line 1) = Left Thrust (Line 2)

Right angle (Line 1) = Left Angle (Line 2)

Change in wind pressure at this brick

Insert co-ord as starting point

DL+LL: Live Load is over 2nd half of curve

Figure 6-20: An Excel spread sheet showing the design process of a catenary curve subject to vertical and lateral loading

The final thrust line obtained for this load case is shown in figure 6-21.

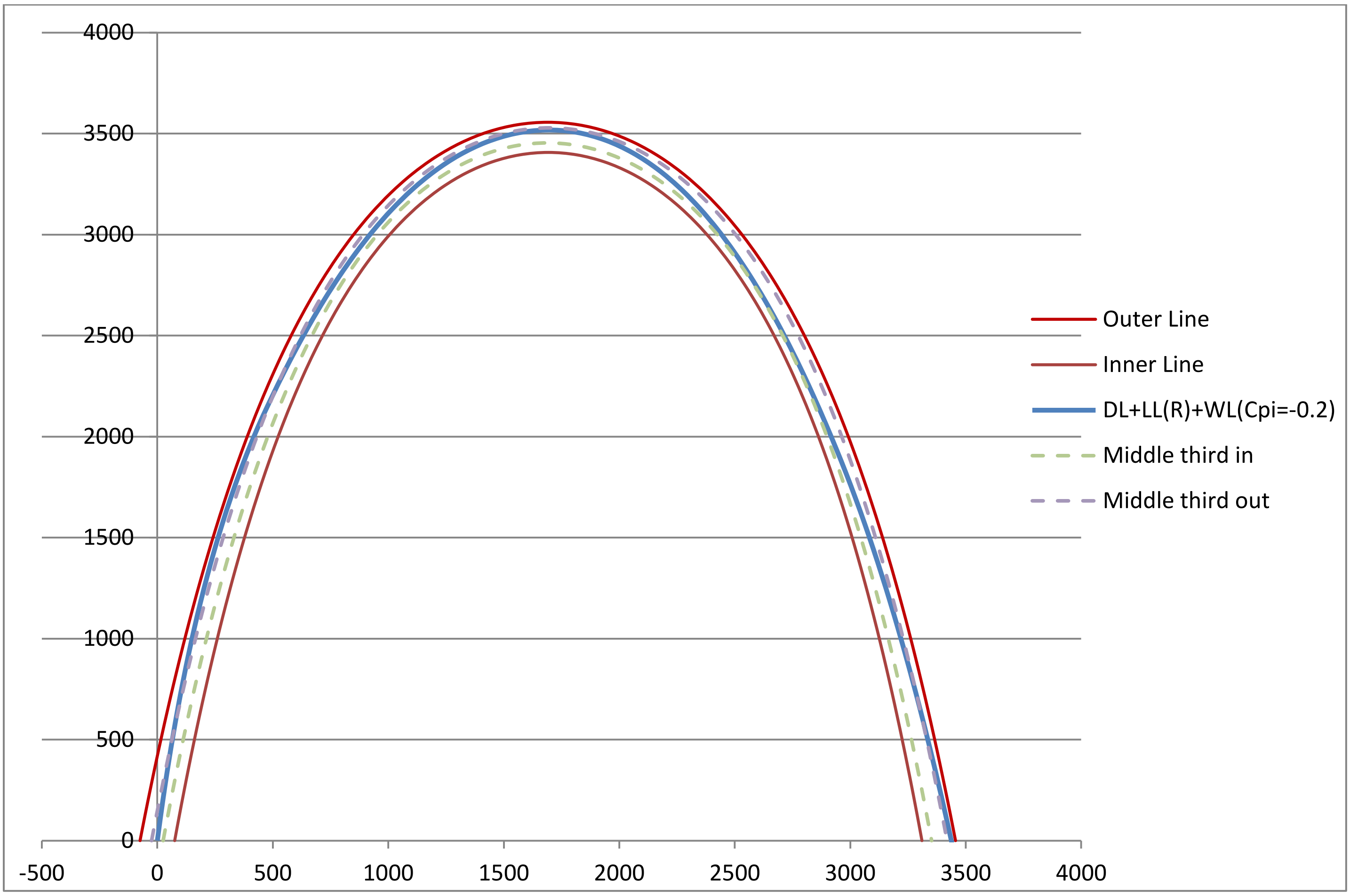

Figure 6-21: The final thrust line obtained for the load case of: ***DL+LL(R)+WL(Cpi=-0.2)***

6.6. Finite Element Analysis

Finite Element Analysis is an important aspect in the design phase. Finite Element was used to verify the accuracy of the equilibrium method and to analyse temperature loading on the structure. LISA version 7.7.1, a finite element analysis programme, was used in the analysis of this project.

6.6.1. Verification Phase

The first step of analysis was done to compare the results obtained from the FEA programme to the segmental equilibrium method. This was done by comparing the reactions and the thrust lines obtained in the two methods. Furthermore, all of the load cases were modelled in the programme and a selected set of critical cases evaluated.

A summary of the reactions obtained are compared and presented in Table 6-8 below. The errors obtained in Table 6-8 are minor and verify that the equilibrium method is correct and is a viable method for the design of catenary curves. The errors obtained for the vertical reactions range between 2.8 and 6.1 percent. The vertical reactions are significantly larger than the horizontal reactions. The horizontal reactions are smaller in magnitude with greater percentage errors, as they are more sensitive to smaller variations in value. The horizontal reaction errors are in the range of 0 and 8.9 percent.

Table 6-8: Load reactions comparison of the results obtained from Finite element Analysis and the Segmental Equilibrium Method

Load Case	*Excel ∑H (kN)*	*LISA ∑H (kN)*	*Error*	*Excel ∑V (kN)*	*LISA ∑V (kN)*	*Error*
Dead Load, Live Load (Full)	0	0	0%	29.588	30.413	2.8%
Dead Load, Live Load (Left half)	0	0	0%	28.529	29.684	4.7%
Dead Load, Wind Load Cpi=-0.2	-1.012	-1.093	8%	19.936	20.924	5%
Dead Load, Live Load (full), Wind Load Cpi=-0.2	-1.016	-1.093	7.6%	27.322	28.462	4.2%
Dead Load, Live Load (Left half), Wind Load Cpi=0	-1.000	-0.911	8.9%	26.814	28.463	6.1%
Dead Load, Live Load (Right half), Wind Load Cpi=-0.2	-1.012	-1.093	8%	27.113	28.238	4.2%

The second phase of verification consists of comparing the thrust lines obtained from the two methods. Figures 6-22 to 6-25 compares the thrust lines obtained from finite element and the segmental equilibrium method. The thrust lines are similar and verify the viability of the segmental equilibrium method. Lateral loads create a greater discrepancy in the thrust lines, than vertical loading. Discrepancies in the thrust lines are due to the approximate nature of the finite element method as a means of designing catenary curves. The discrepancies can also be attributed to the fact that the number of segments and sizes differ, and therefore the plots will vary with accuracy.

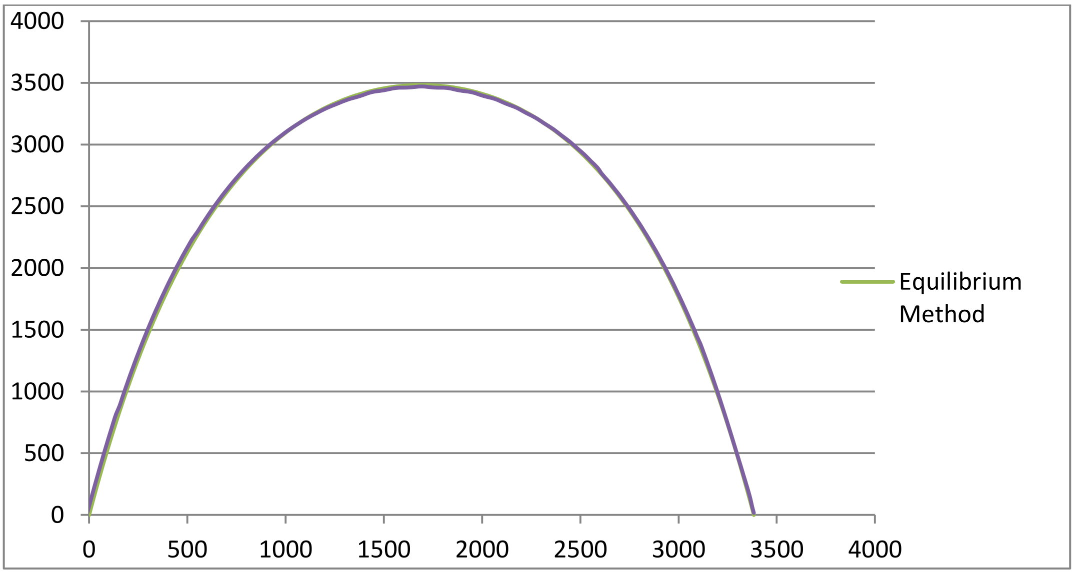

Figure 6-22: A comparison of the Segmental Equilibrium Method and Finite element method when subject to dead loads

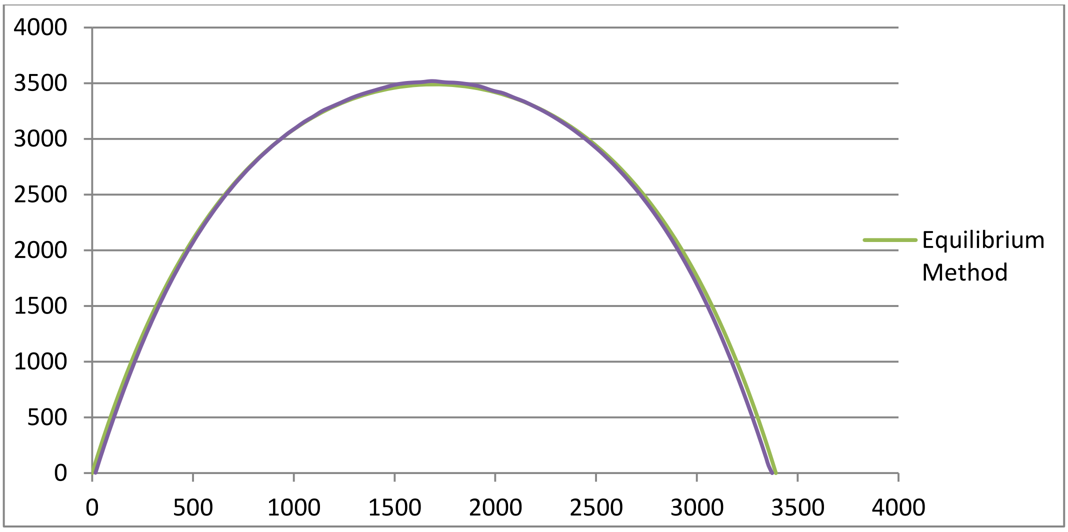

Figure 6-23: A comparison of the Segmental Equilibrium Method and Finite element method when subject to dead and live loads

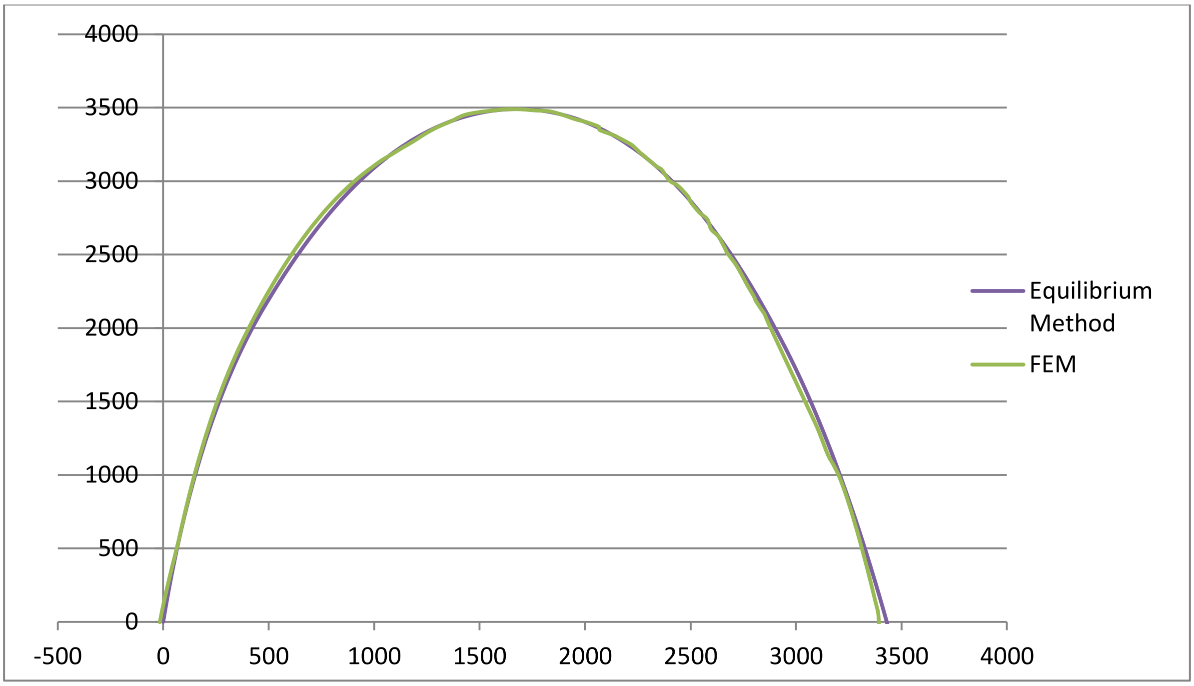

Figure 6-24: A comparison of the Segmental Equilibrium Method and Finite element method when subject to dead, full live and wind loads (Cpi=-0.2)

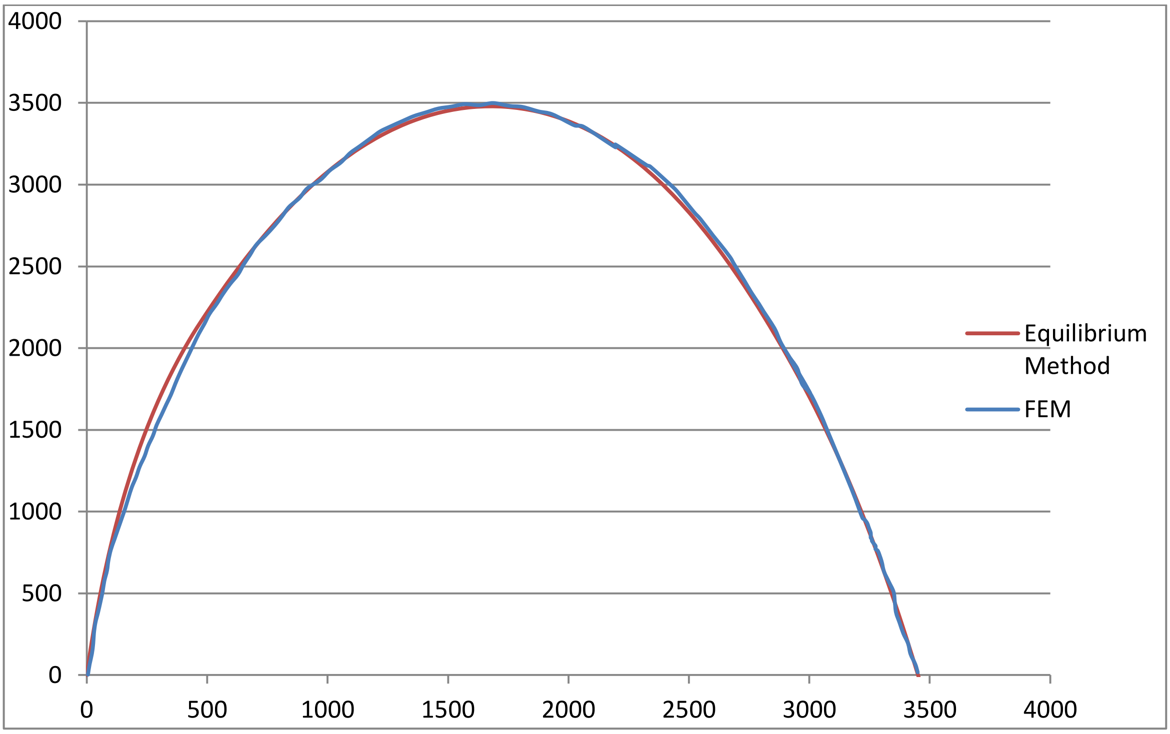

Figure 6-25: A comparison of the Segmental Equilibrium Method and Finite element method when subject to dead and wind loads (Cpi=-0.2)

6.6.2. Analysis of Temperature Loading

Finite Element was used to analyse temperature loading on the structure. A temperature difference of 20°, in expansion and contraction, was analysed when applied to the full and half surface of the structure.

All loading combinations and patterns were investigated in combination with temperature loading. All the finite element results from the loading cases can be found in Appendix B. Here, we will discuss the worst loading case which created the highest stresses within the vault.

The analysis showed that the structure was subject to the highest tensile stresses during temperature changes (±20°) combined with wind action, i.e. Dead Load + Wind Load (C_{pi} = 0) + Temperature Load (±20°). These tensile stresses are predominantly found at the base of the structure and sometimes in small clusters close to the apex. Figures 6-26 to 6-29 demonstrate the distribution of tensile and compressive forces throughout the structure under the worst loading case. Note that the edges of the vault in this project are not restrained in any way, and are therefore allowed to expand and contract naturally.

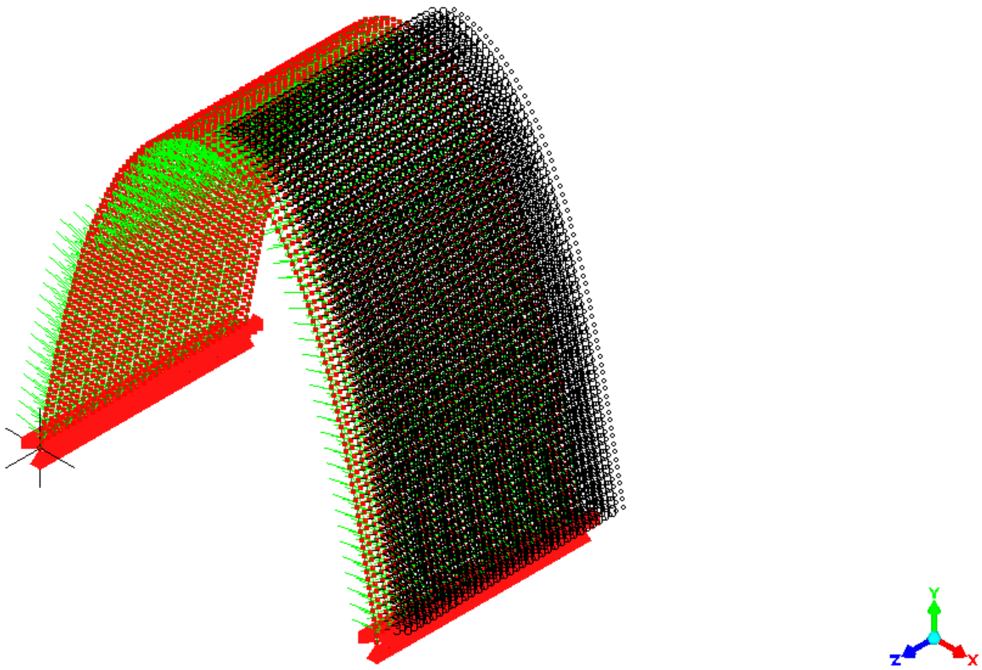

Figure 6-26: A model of the worst load case inputted to LISA 7.7.1: *DL+WL+TL*

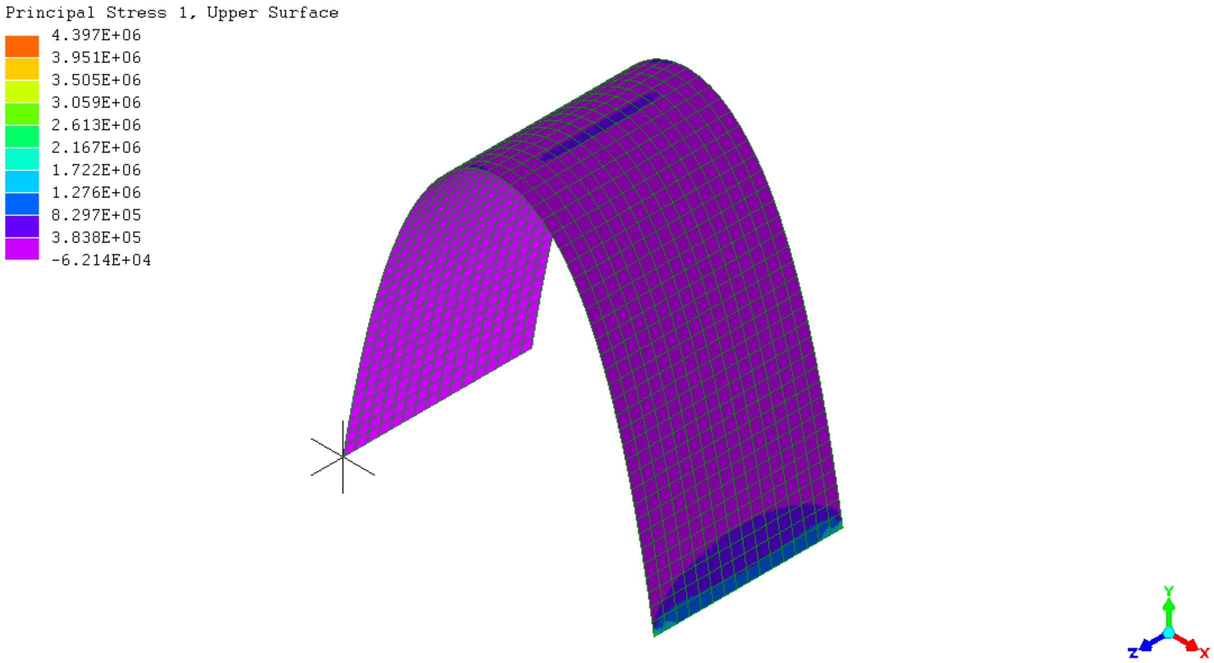

Figure 6-27: The dominant principal stress distribution on the upper surface of the vault under the most severe loading case

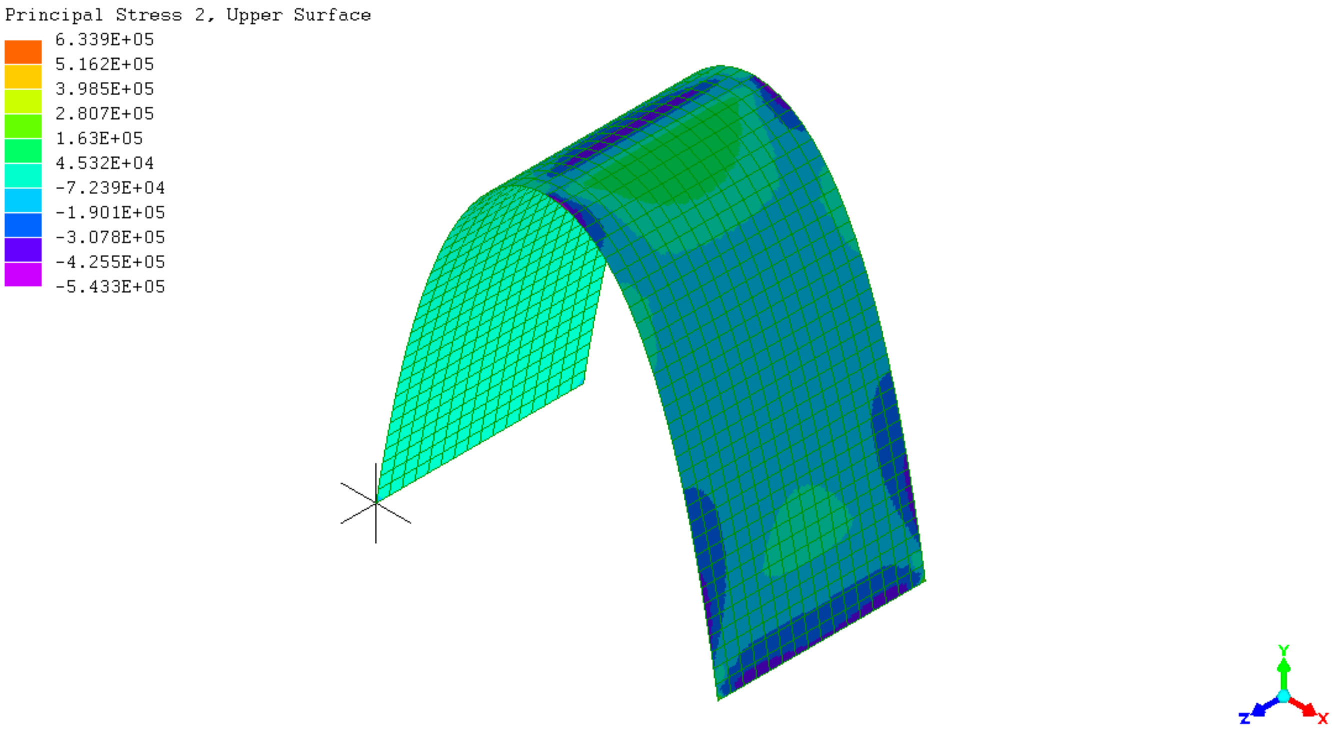

Figure 6-28: The minor principal stress distributions on the upper surface of the vault under the most severe loading case

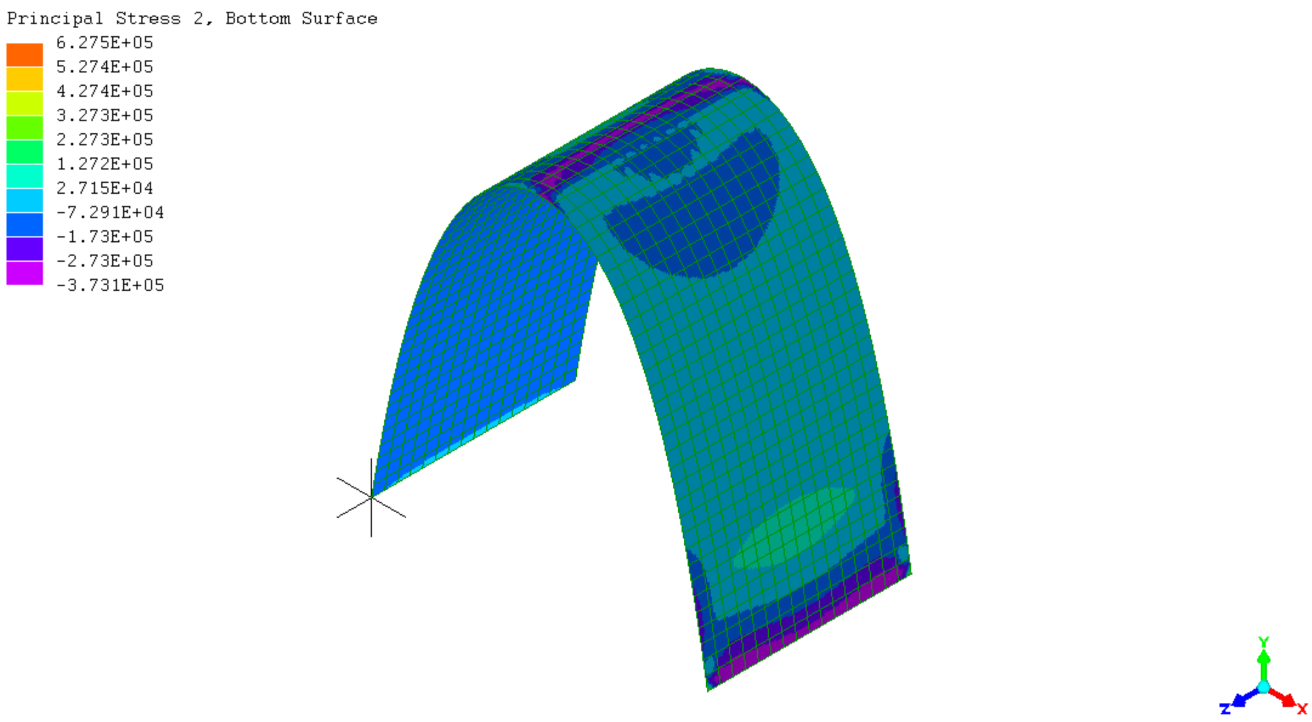

Figure 6-29: The dominant principal stress distribution on the bottom surface of the vault under the most severe loading case

Note: All negative values represent compressive stresses and positive values represent tensile stresses. The analysis displays what occurs on the upper and bottom surfaces of the material with major and minor stresses. From the above figures, it is clear the tensile stress are very concentrated to specific areas, i.e. Figure 6-27 – dark blue, Figure 6-28 – bright green, Figure 6-29 – light green.

6.7. Discussion of Results

6.7.1. Thrust Line Analysis

All loading combinations and patterns were investigated and plotted to identify areas of weakness and further investigation. Figures 6-30 to 6-36 display the thrust lines obtained from all the investigated loading combinations. Figure 6-30 shows the loading patterns which are only loaded with wind loads, Figures 6-31 to 6-33 represent only UDL live loads and Figures 6-34 to 6-36 are loaded with a point live load. Areas which require further investigation are ones where the thrust line falls outside of the middle third.

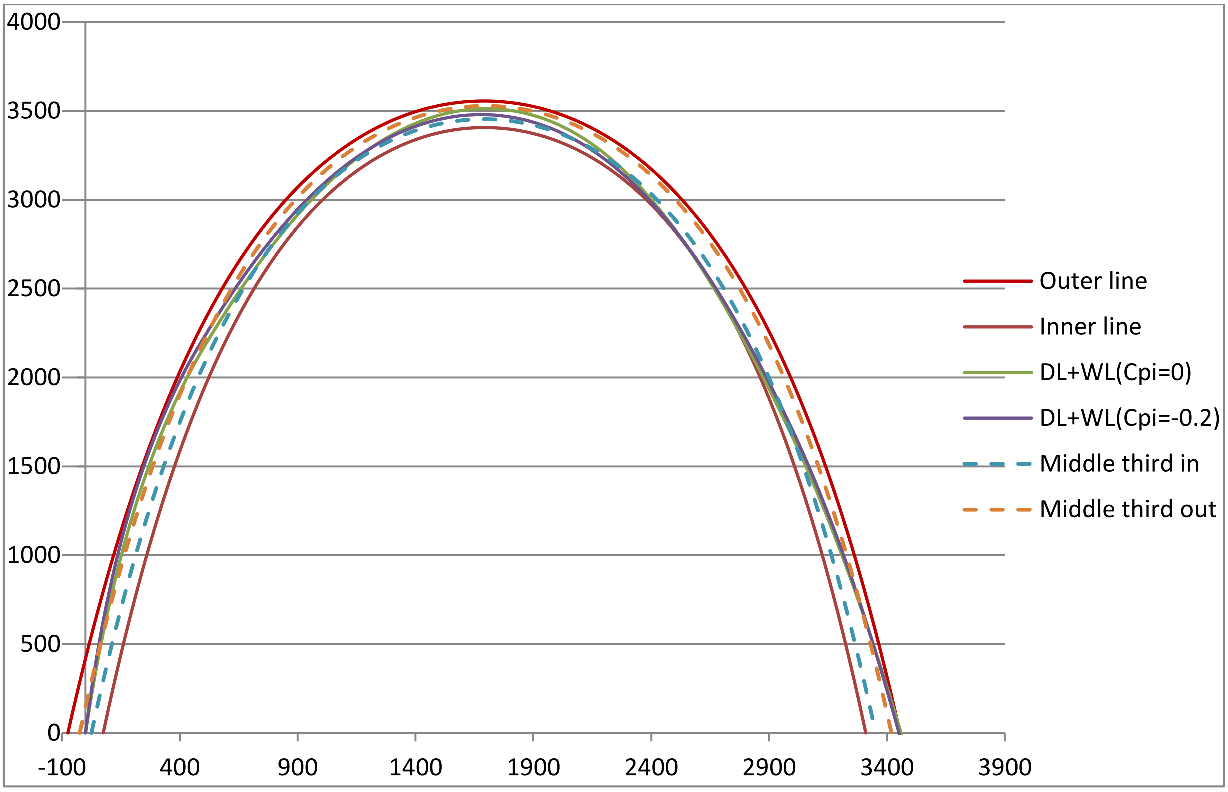

Figure 6-30: A graph representing the thrust lines obtained from only wind and dead load combinations

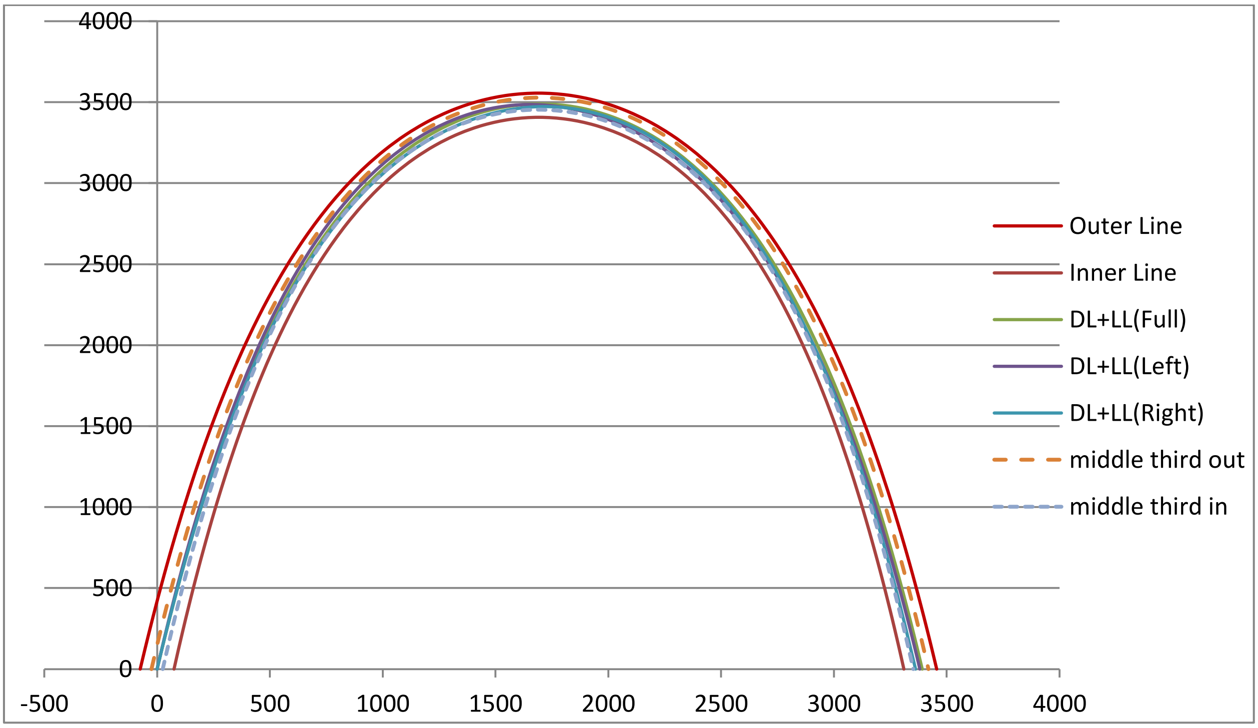

Figure 6-31: A graph representing the thrust lines obtained from only live (udl) and dead load combinations

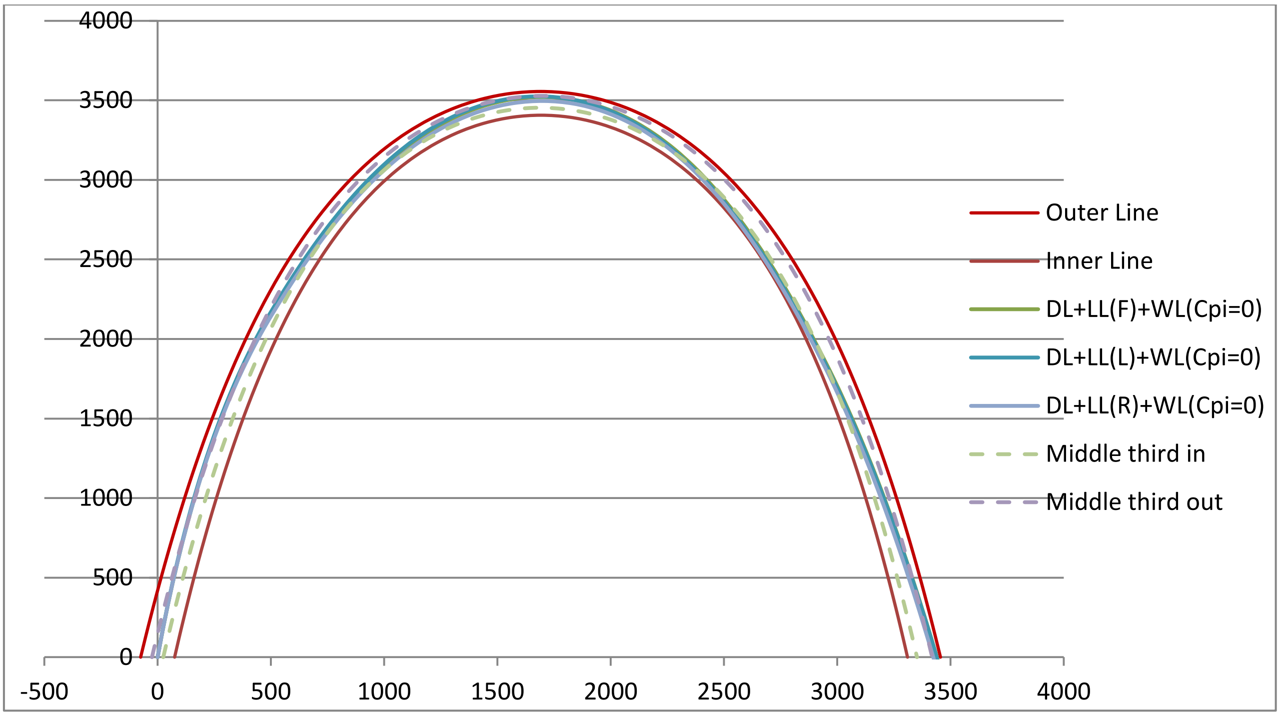

Figure 6-32: A graph representing the thrust lines obtained from wind (cpi=0), live (udl) and dead load combinations

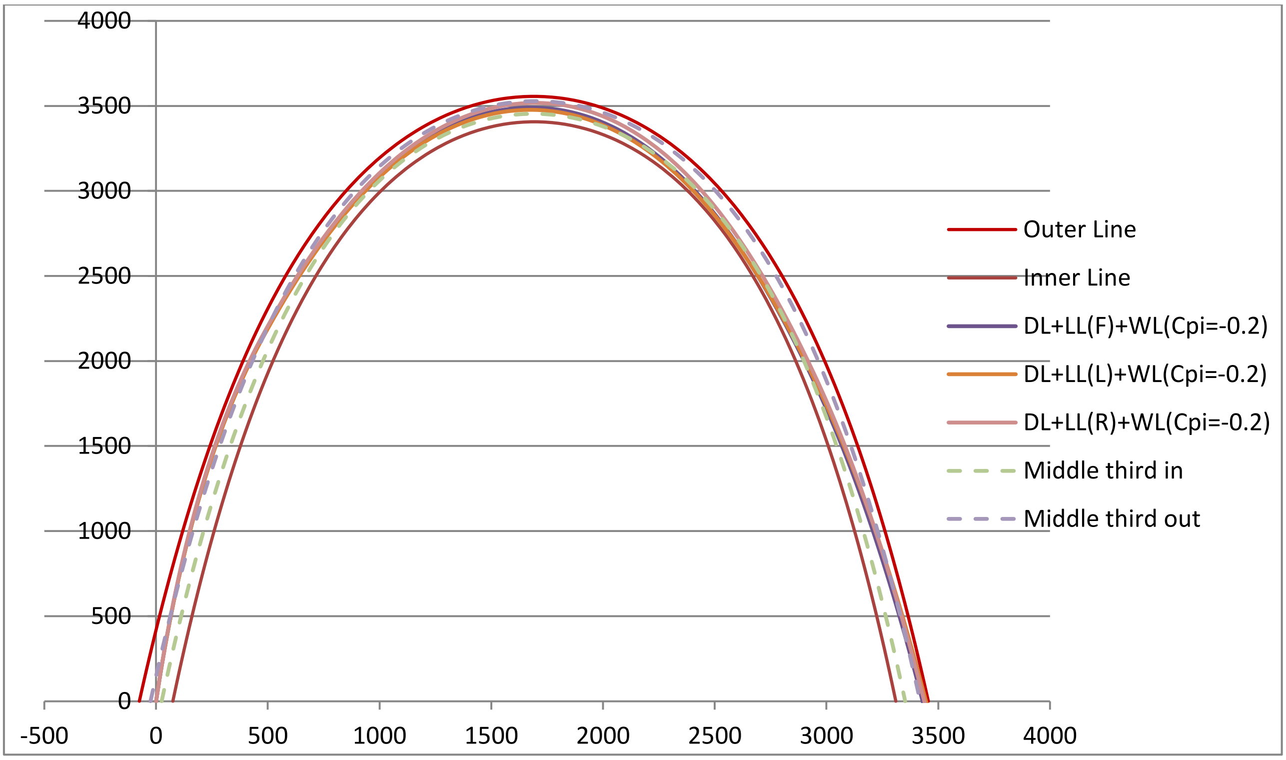

Figure 6-33: A graph representing the thrust lines obtained from wind (cpi=-0.2), live (udl) and dead load combinations

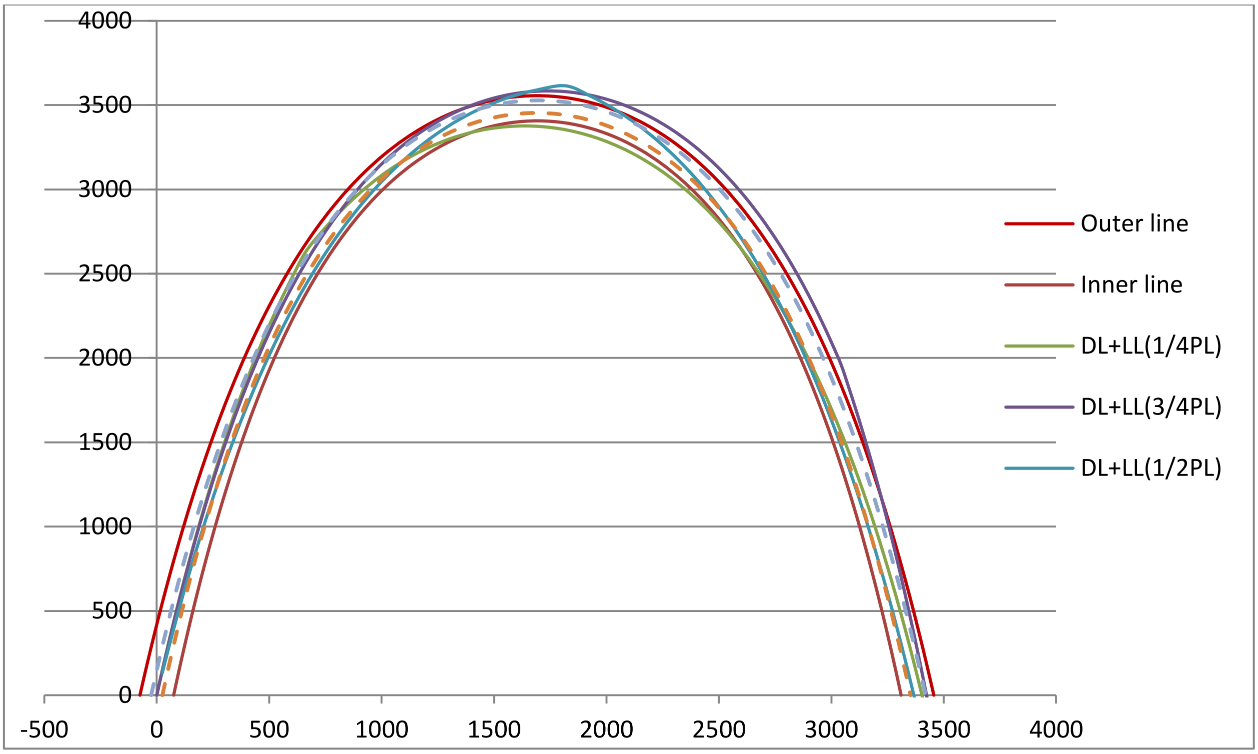

Figure 6-34: A graph representing the thrust lines obtained from only live (point) and dead load combinations

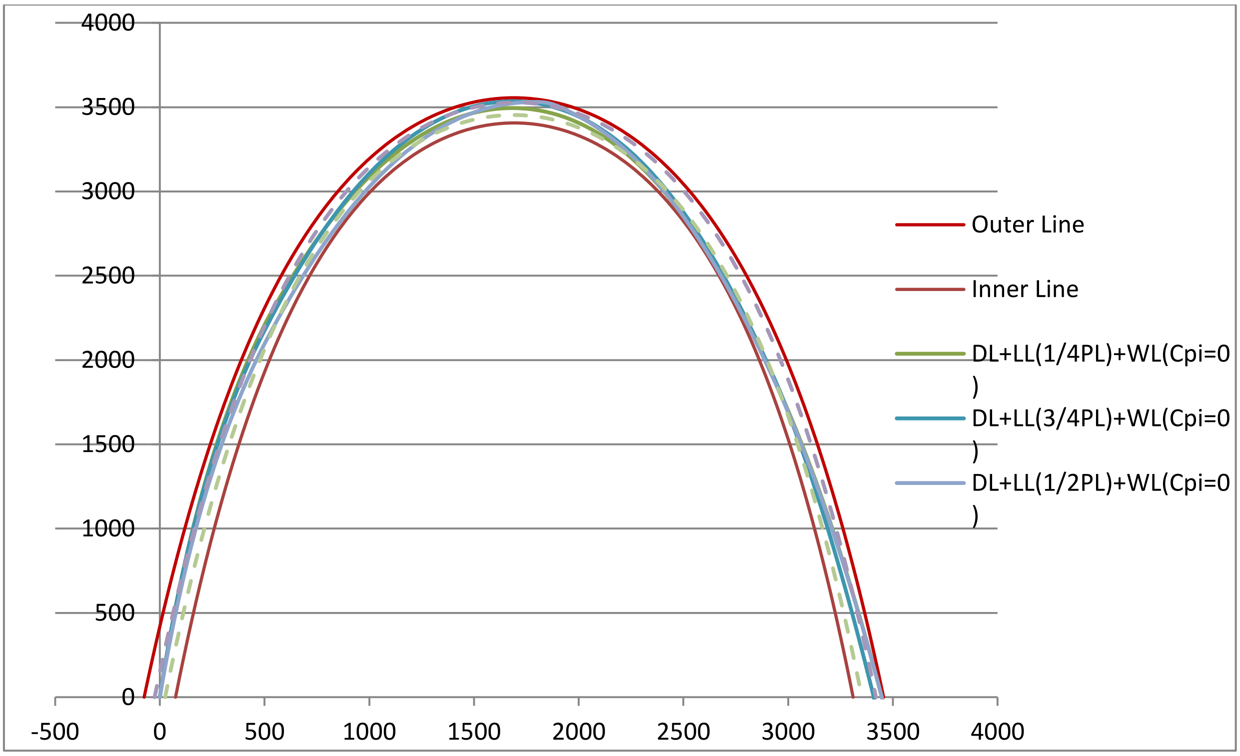

Figure 6-35: A graph representing the thrust lines obtained from wind (cpi=0), live (point) and dead load combinations

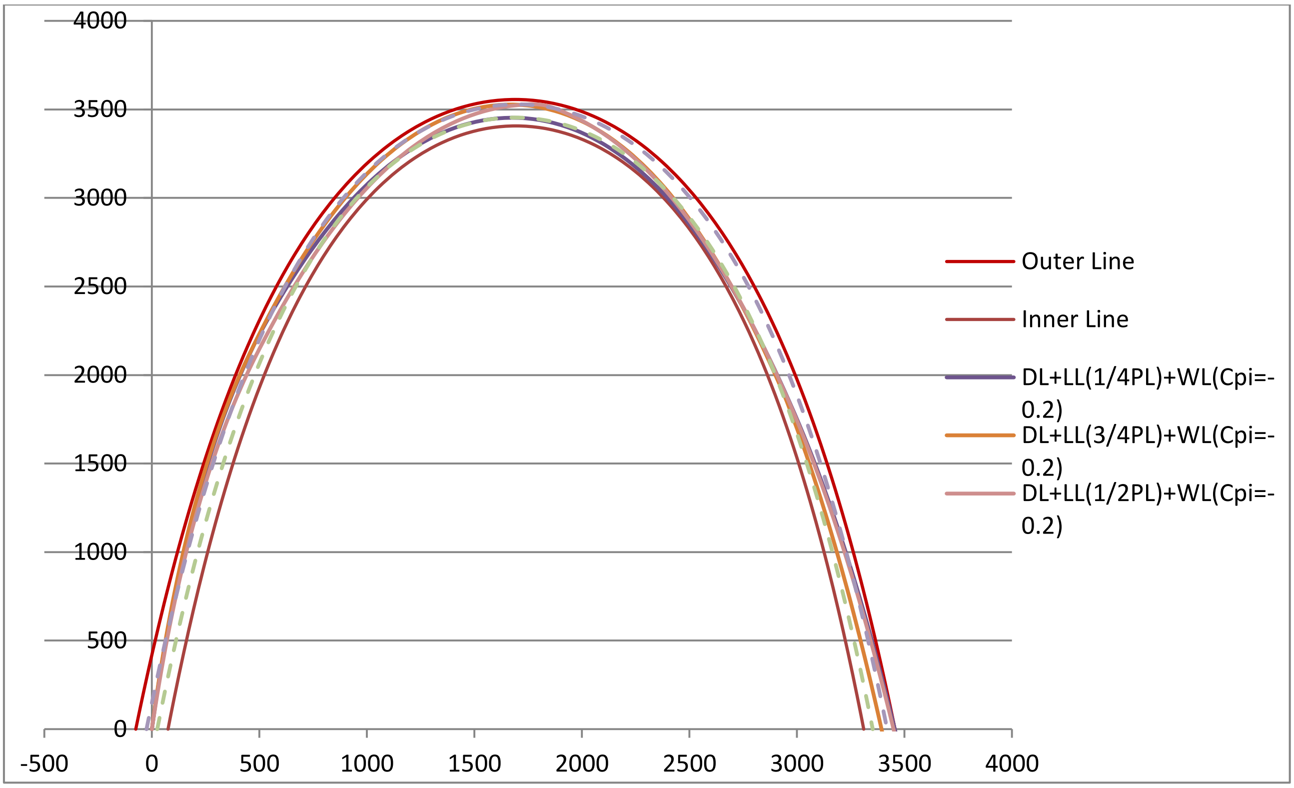

Figure 6-36: A graph representing the thrust lines obtained from wind (cpi=-0.2), live (point) and dead load combinations

Point loading on the vault structure is the most likely concern in causing structural instability and failure. Figure 6-34 to 6-36 show the results obtained when the structure is subject to a point load at various points, i.e. at a ¼ length, ¾ lengths and at the centre of the structure. When this load is applied in combination with a wind load, all thrust lines fall within the thickness of the vault. However, when the structure is subjected to point loads, the thrust lines far exceed the thickness of the vault. This is a clear warning sign and reiterates the fact that catenary's are not robust in supporting point loads; however, this is the case with all shell structures (Wilson, 2005). Thus, it is very important that the structure is not subjected to point loads so as to avoid any complications or structurally instability in the roof. If the roof is to be accessed for maintenance or other such needs, it is strongly advised that supports, scaffolding or other such alternatives are used for safety purposes.

It can be seen that load cases which include wind loads can cause areas of weakness. Figures 6-30 and 6-32 show that two dominant areas fall outside of the middle third. However, they do remain within the thickness of the material. The tensile forces in these areas are obtained from the finite element analysis and compared to the tensile strength of the material. The maximum tensile forces are minor and fall within the tensile limit of 1.1N/mm² (refer to Chapter 4). All tensile stresses obtained are within a range of 0.11-0.95N/mm².

6.7.2. Finite Element Analysis

Finite Element was carried out to assess the effects of temperature loading on the structure. Temperature loading was found to be the most severe loading case, creating the largest tensile and compressive stresses. As discussed previously, there is a change in stresses on the centre line of the curve. However, in this case the change is gradual and not abrupt as is the case for Bapong. Therefore this does not create concern in terms of cracking. All compressive stresses are below the compressive strength of the material. It is advised that the stresses do not exceed a third of the strength (rule of thumb). The maximum compressive stress obtained is 1.02N/mm², where the strength of the masonry is 3.75N/mm². The maximum tensile stresses are of magnitude 0.99N/mm². This value is quite close to the tensile strength of the material and it is advised that additional precautionary measures should be taken once construction is complete.

6.8. Conclusion

It is concluded that all load cases are within the required limits. Thus, the above curve is the finalised design of the roof structure. However, it was decided that a layer of a very lightly coloured form of waterproofing, paint or fabric would be placed over the roof to minimise the temperature loading on the structure. This in turn would minimise the chance of cracking within the roof structure.

7. Structural Member Design

The design of all the members in this chapter were carried out in accordance with the reinforced and pre-stressed concrete codes SABS 0100-1 (2000) and BS8100-1 (1997), as well as the masonry codes BS 5628-1(1992) and ENV1996-1-1 (1996). A number of elements were selected prior to design and the capacity was checked to ensure that the elements were sufficient to support the exerted loading. In this chapter, the design process and detail of all members are discussed. All the members are designed to capacity, finalising the design of the prototype structure before construction can commence.

7.1. Slab

7.1.1. Introduction

The design of the slab was conducted by Spancon, a local distributor of slab systems. A rib and block slab was decided on to minimise the quantity of concrete used, which is approximately 30% less than normal slabs. It is also the most cost effective solution for slab flooring. This is highlighted particularly in the installation process. The slab is very easy to install, and thus less labour is needed in shorter periods. The slab merely utilises lintels as the ribs and hollow precast blocks (void formers) which are placed between the lintels, thus eliminating the need for formwork or scaffolding. A ready mix of concrete is used and minimal steel reinforcing is required. A rib and block slab has also proved to have excellent insulation properties (Spancon, 2013). This is particularly important when designing for a low-cost house.

7.1.2. Design

All slab specifications and designs are supplied by Spancon (Table 7-1, Figure 7-1).

Table 7-1: Properties of materials used in the slab

Loading	1.5kN/m^2
Reinforcing steel	Y10
Ready mix concrete quantity	3m^3
Ready mix concrete strength	25MPa
Floor area	28m^2
Thickness of slab	170mm
Thickness of concrete above rib and block system	50mm

NOTE:
NO SITE MIX CONCRETES ARE PERMITTED - VIBRATION OF CONCRETE IS MANDATORY
NO CONCRETE MAY BE POURED WITHOUT INSPECTION AND APPROVAL BY SUPERVISING
ENGINEER - NO INSPECTION NO CERTIFICATE

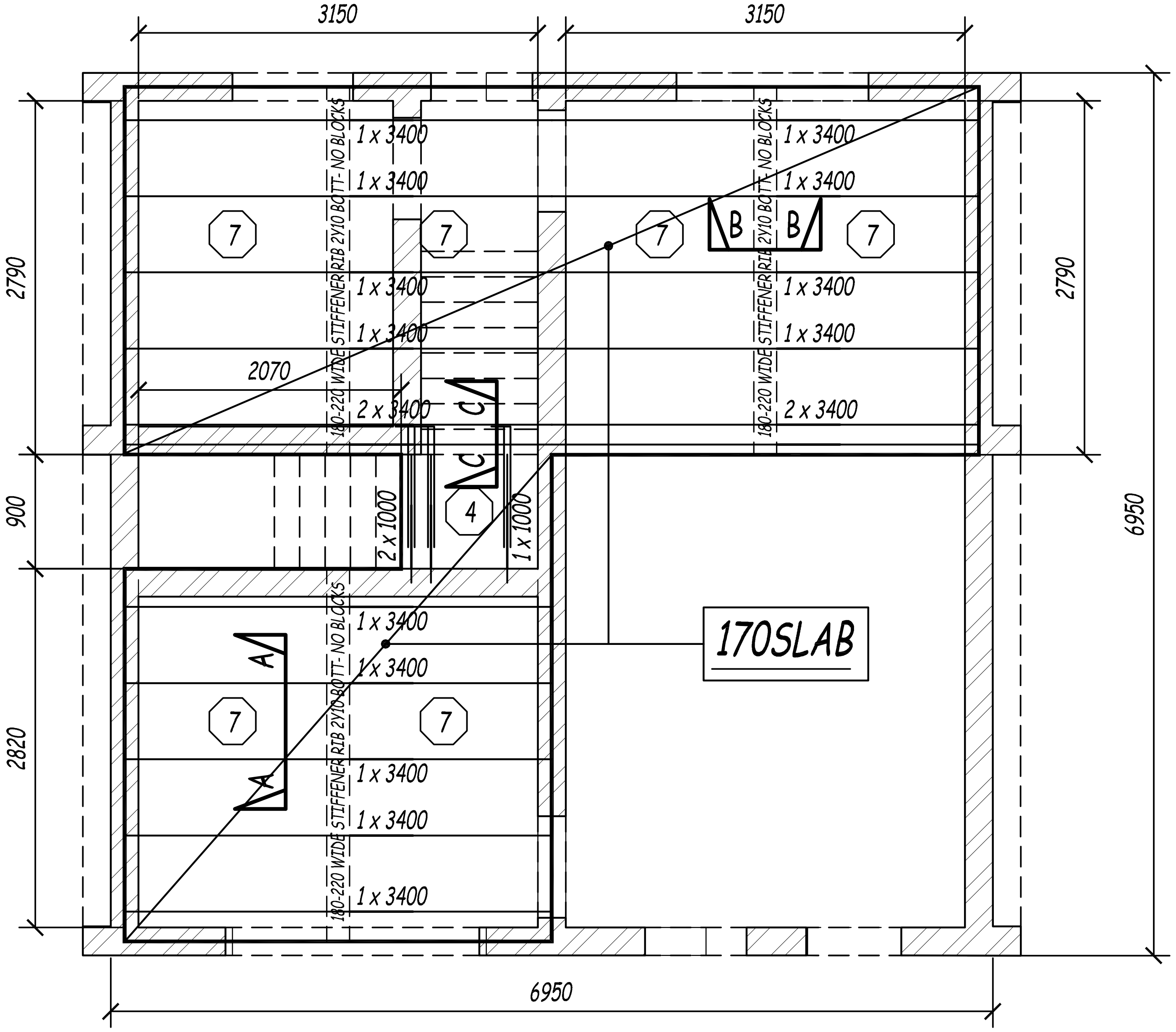

PLAN ON 170 DEEP FIRSTFLOOR SLAB
(UNLESS OTHERWISE SHOWN)
SCALE 1 : 50

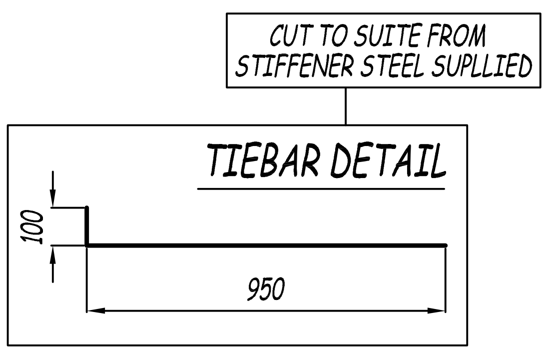

TIEBAR DETAIL

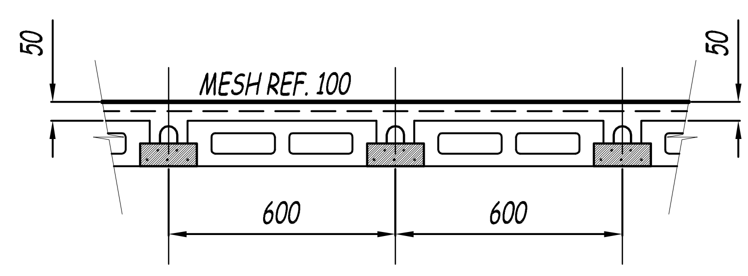

SECTION A – A

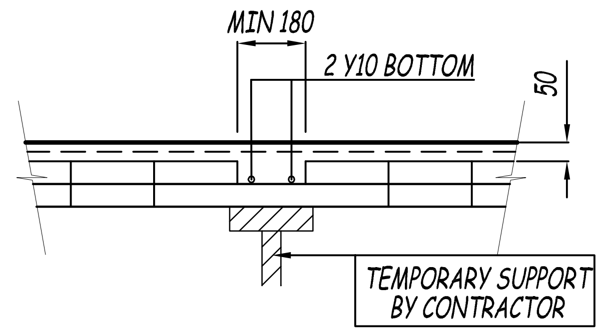

SECTION B – B

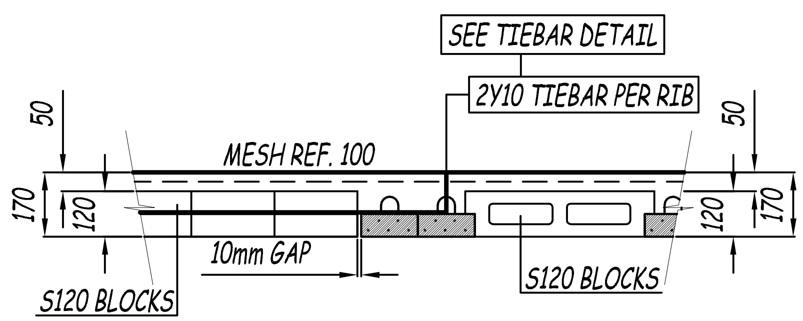

SECTION C – C

LEGEND

SYMBOL	BLOCK TYPE	DIMENSIONS (WxLxH)
○	S120 BLOCK	440x220x120
□	S150 BLOCK	440x220x150
◇	S205 BLOCK	440x220x205
⬡	S290 BLOCK	440x220x290
	LOADBEARING BRICKWORK	
	BEAM STRIPS	
	BEAMS	
	STEPPED BLOCK	
	S TRAY (PIPE SERVICES)	
	SOLID SECTION	
1,5kPa	DESIGN LIVE LOAD	

NOTES

GENERAL
1. THIS DRAWING IS TO BE READ IN CONJUNCTION WITH ALL OTHER RELEVANT DRAWINGS & SPECIFICATIONS.
2. ALL DIMENSIONS TO VERIFIED ON SITE & ANY DISCREPANCIES TO BE REPORTED TO THE ENGINEER.
3. REFER TO ARCHITECTS DETAIL FOR ALL SETTING OUT DIMENSIONS.

CONCRETE
1. ALL CONCRETE WORK TO BE EXECUTED IN ACCORDANCE WITH SABS 1200 G.
2. CONCRETE STRENGTHS AS FOLLOWS :
   FOUNDATIONS - 20 MPa
   COLUMNS - 25 MPa
   SLABS - 25 MPa
3. 6 CUBE TESTS TO BE TAKEN WITH EACH CONCRETE POUR AND TO BE TESTED AS FOLLOWS : - 3 CUBE TESTS @ 7 DAYS
   - 3 CUBE TESTS @ 28 DAYS.
4. ALL STRUCTURAL CONCRETE TO BE CURED FOR 7 DAYS UNLESS OTHERWISE INSTRUCTED.
5. SLIP JOINTS TO BE PROVIDED ON ALL LOAD BEARING WALLS AS PER THE DETAIL.
6. SLAB LEVELS TO ARCHITECTS DETAIL.
7. NO BRICKWORK IS TO BE BUILT ONTO A PROPPED SLAB UNLESS DIRECTLY ABOVE A LOAD BEARING WALL.
8. IT REMAINS THE ERECTION CONTRACTORS RESPONSIBILITY TO ENSURE THAT THE TEMPORARY SUPPORTWORK TO SLABS IS ADEQUATE.

REINFORCEMENT
1. ALL REINFORCEMENT FIXING TO BE INSPECTED & APPROVED BY THE ENGINEER PRIOR TO CONCRETING.
2. ENGINEER TO BE GIVEN AT LEAST 24 HOURS NOTICE OF REQUIRED INSPECTION.
   ALL PREPARATORY WORK TO BE COMPLETED PRIOR TO INSPECTION.
3. COVER TO REINFORCING :
   SLAB SOFFIT - 20 mm
   TOP OF SLAB - 20 mm
   COLUMNS - 30 mm
   BEAMS - 30 mm
   FOUNDATIONS - 50 mm
4. ALL REINFORCEMENT TO COMPLY WITH THE REQUIREMENTS OF SABS 1200 G.

BRICKWORK
1. ALL BRICKWORK TO BE EXECUTED IN ACCORDANCE WITH SABS 0164.
2. LINTELS TO BE PROVIDED OVER ALL OPENINGS IN WALLS.
   INSITU LINTELS FOR LARGER SPANS AS PER THE DETAIL.
3. MORTAR CLASS II - 5 MPa
4. BRICK COMPRESSIVE STRENGTH - 14 MPa.

FOUNDATIONS
1. ALL FOUNDATION EXCAVATIONS TO BE MECHANICALLY COMPACTED TO 95 % MOD AASHTO.
2. ALL FOUNDATION EXCAVATIONS TO BE INSPECTED & APPROVED BY THE ENGINEER PRIOR TO CONCRETING.
3. FOUNDATIONS TO LOAD BEARING WALLS 700 x 250 U.O.N.

ROOF DRAINAGE
1. ROOF DRAINAGE, SCREEDING & WATERPROOFING TO ARCHITECTS DETAIL.

REV	DATE	REVISION DESCRIPTION	BY

TITLE
FIRST FLOOR SLAB LAYOUT

PROJECT
UNIVERSITY OF WITWATERS RAND
LOW-COST HOUSING PROTOTYPE

DATE	DESIGNED BY	
17/09/13	DRAWN BY	BeCKEr
	CHECKED BY	
APPROVED BY CLIENT	DRAWING No.	Q13466

7.2. Masonry wall design

7.2.1. Introduction

The design of the wall is done in accordance with BS 5628-1 (1992) and ENV 1996-1-1 (1996). The method adopted is that of a simple masonry design where the total loads is compared to the resistance of the material and its capacity to support it. The buckling of the wall is also checked during design. The walls that require analysis are the load carrying walls. All of the walls in the prototype are of the same height, and thus only the wall with the highest applied load need be checked.

7.2.2. Loading

The load carried by the walls is simply vertical. This is due to the fact that the lintels and ties (as explained in more detail in section 7.3) resist the horizontal loading. Therefore the walls only need to be checked for buckling and its compressive strength capacity.

Figure 7-2 illustrates which of the walls are load bearing as well as the wall with the highest load. The central wall is the highest load carrier and is therefore selected for design. A metre length section of the wall is designed.

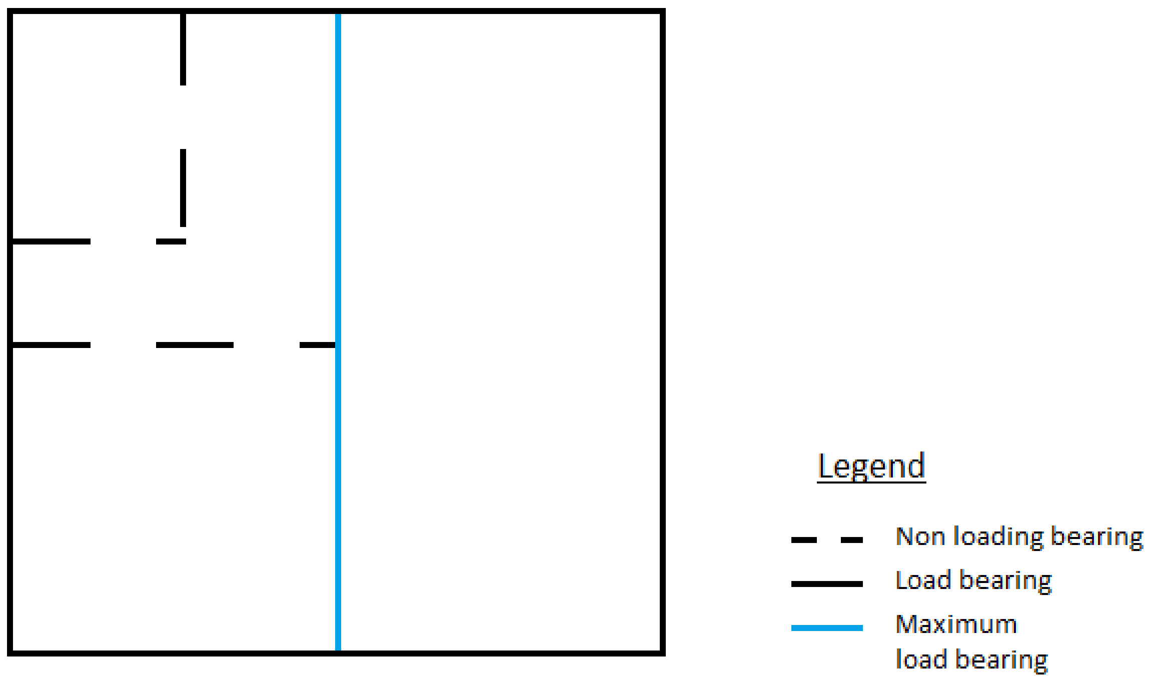

Figure 7-2: Layout of the wall system highlighting the function of each wall as well as the wall with the greatest applied load

The loading exerted on the central wall is summarised as follows:

- *Dead Load*
  - Self-weight of wall = 11.15kN/m
  - Vaults = 12.08kN/m per vault. However, there are two vaults being exerted on the central wall, thus a total load of 24.16kN/m is used
  - Slab = 13.75kN/m
- *Live Load*
  - For dwellings =1.5kN/m^2 x 1.5 = 2.25kN/m

The total load exerted on the wall is 51.31kN/m.

7.2.3. Design

There are two methods that can be employed in the design of a masonry wall. The first method is to calculate the characteristic compressive strength needed to resist the applied load and compare it to the compressive strength of the materials. The second method calculates the stresses exerted by the loading and compares it to the ultimate stress allowed. Both methods were applied and found the design to be satisfactory.

However, the first method also checks for buckling. Thus, method one will be applied and the results are presented below.

When designing a wall, the β value is critical. This value is the capacity reduction factors and is dependent on the slenderness of the wall. It also highlights and combats the likelihood of the wall buckling. In order to obtain the β value, the eccentricity of the loading needs to be calculated. The layout of the loading is described in Figure 7-3 and the eccentricity can calculated as described below.

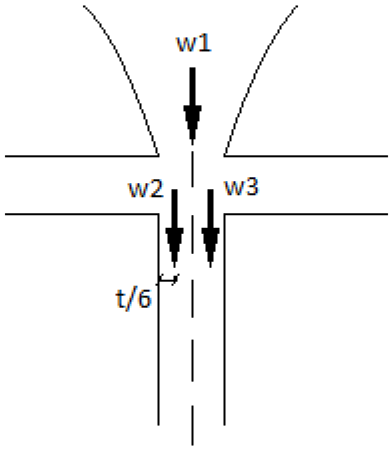

Figure 7-3: The loading and eccentricity as applied to the wall

Where $w1$ = Vault loads and self-weight of wall

$w2$ = Load from the full slab

$w3$ = Load from sectioned slab

t = thickness of the wall (220mm)

In this case, a β value of 1 was obtained. This indicates that the wall is not susceptible to buckling. The design compressive strength is now calculated.

The design strength is calculated using the following equation:

$$Design\ Strength = \frac{\beta t f_k}{\gamma_m} \tag{7-1}$$

Where β is the capacity reduction factor

t is the thickness of the section

f_k is the characteristic compressive strength

γ_m is the material safety factor (3.5)

The compressive strength required, under the stipulated loading, was found to be 1.24MPa. The compressive strength of the material is 10MPa. This value has not been reduced, as it usually would be in combination with mortar, as the wall is dry stack. The wall is clearly suitable in supporting the above loads.

7.3. Thrust Force Structural Components Design

7.3.1. Introduction

The design of the lintels in this project varies slightly to the standard use of lintels. Lintels are generally used to support sections of walls above windows and doors. They act as composite beams, which comprise of concrete lintels and masonry. However, in this project, there is a need for a structural member to counteract the outward thrust of the vaults. Since the masonry walls cannot support these horizontal thrusts, particularly when dry stacked, a new innovative approach is required. A simple, but effective method was established. The solution is a simple combination of lintels, steel tubes and reinforcing bars. As demonstrated in Figure 7-4, the lintels are simply placed within the steel tubes which are then welded to the ties (reinforcing bars). The ties contain the outward thrust force exerted by the vaults.

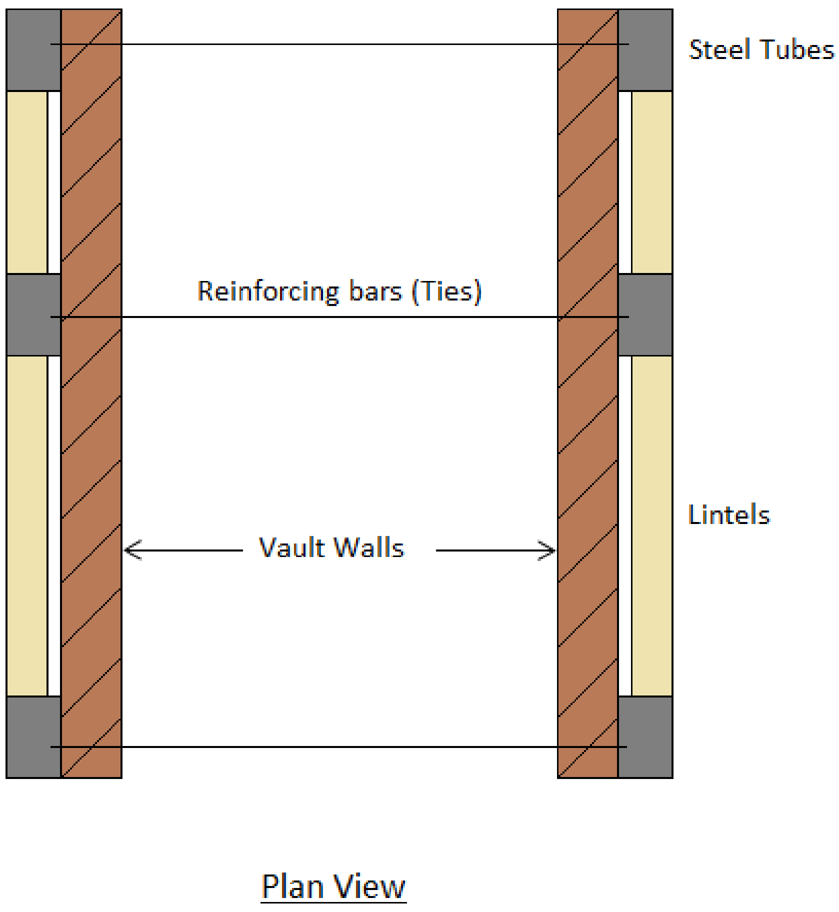

Figure 7-4: A layout describing the manner in which the system is set out to contain the thrust force

7.3.2. Lintel Design

7.3.2.1. Introduction

This design is done in accordance with SABS 0100-1 (2000) and BS 8110-1 (1997). It is designed as a pre-stressed concrete section, satisfying all the relevant checks. The lintel is designed as a 1 metre length section. All material properties are obtained from *Lintel Supplier,* a local supplier of lintels in South Africa. The lintels were precast and pre-tensioned in a plant and shipped to site. It is important to note that lintels are able to resist horizontal forces. The same method of design is used with the sections rotated 90°, as described in Figure 7-5.

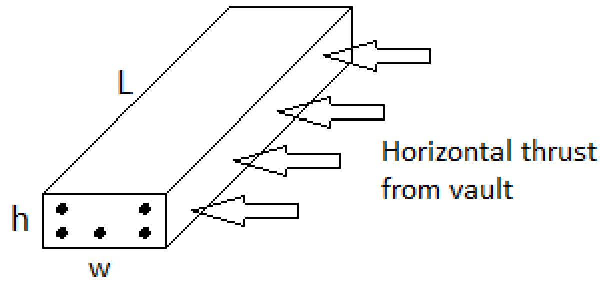

Figure 7-5: The manner in which the lintels are loaded by the horizontal thrust exerted by the vault

It is important to note that the ties attached to the lintels need to be cast within the concrete slab to limit corrosion. To reach the necessary height whereby the ties are covered, two lintels are placed on top of one another and mortared together to act as a single beam. The configuration is illustrated in Figure 7-6.

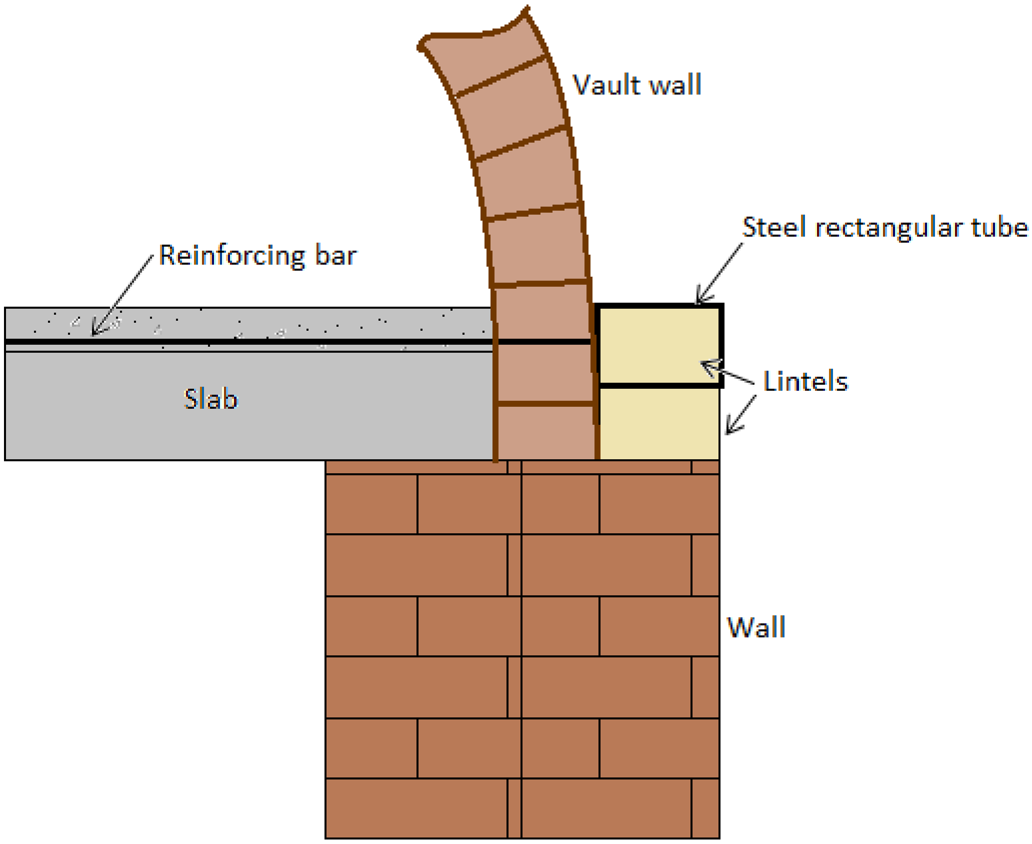

Figure 7-6: Two lintels are placed on top of one another to ensure the ties fall within the concrete section and are therefore covered

7.3.2.2. Loading

The loading exerted on the lintels is the horizontal thrust force exerted by the vaulted roof. This value is obtained from either the segmental equilibrium method or the finite element analysis. All load cases are analysed and the greatest reaction forces are used in the design of the lintels.

The greatest horizontal reaction, exerted by the vaults, is 2kN per metre length. This value is obtained when only a dead load and temperature load (20°C change) are exerted on the vault. This value is applied to the lintels, as demonstrated in Figure 7-5.

7.3.2.3. Design

In the design phase, a pre-stressed concrete analysis was carried out to ensure that the lintels can resist the loading. The properties and dimensions of the lintels are fixed and summarised in Table 7-2. It was decided that the lintels would be orientated in such a way to ensure that the load is carried in the stiff, rigid direction, as can be seen in Figure 7-5.

Table 7-2: A table summarising the material and section properties of the lintels

Concrete Properties	Value	Unit	Notes
Strength at 28days	35	MPa	
Strength at release	12	MPa	
Young's Modulus at 28 days	30000	MPa	
Young's Modulus at release	18171	MPa	
Section Properties			
Height per lintel	70	mm	Two lintels are used, thus a height of 140mm
Width	135	mm	
Strand Properties			
No of wires	4		
Wire Diameter	2.64	mm	
Characteristic strength, P_u	9.31	kN	Per lintel
Initial Jacking Force	70	%	

(Lintel Suppliers, 2009)

The design process is followed in accordance with SABS 0100-1 (2000), pre-stressed concrete. The lintels were analysed and the results are given below:

- Service stresses at Transfer
    - Stress at Top = 5.22 MPa < 6MPa ok
    - Stress at Bottom = 1.79MPa < 6MPa ok
- Long term service Stresses
    - Stresses at Top = 8.19MPa < 11.55MPa ok
    - Stresses at Bottom = 1.35MPa < 11.55MPa ok
- Ultimate Moment of resistance = 11.05kNm > Moment under ultimate load = 2.08kNm ok

- Shear under ultimate load = 4.16 kNmm < 4.75 ok
- Shear under ultimate load = 4.16 kNmm < Shear capacity (uncracked section) = 17.25 kNmm ok
- Shear under ultimate load = 4.16 kNmm < Shear capacity (cracked section) = 9.22 kNmm ok
- Deflection at Camber transfer satisfied
- Long term deflection satisfied (l/300)

The analysis process ensured that all code checks are satisfied and thus the lintels are sufficient to carry the required load.

7.3.3. Steel Ties and Welds

7.3.3.1. Introduction

As previously discussed, one of the most important design aspects of this project is that of the ties required to support the horizontal forces exerted by the vaulted roof. Figure 7-4 and 7-6 illustrates the layout of the steel ties required in the prototype. These ties work in a way such that when the roof kicks outward, the ties (that are attached to the lintels) go into tension and restrain the structure from collapsing. Thus, it is necessary that the welds and ties are strong enough to resist the outward thrust force of 2kN per metre length of the vault.

The ties are to be welded to the steel tubes and therefore a R10 reinforcing bar is chosen to ensure a good quality weld is created and sufficient strength is provided in the section.

7.3.3.2. Design

A weld design is required to ensure that sufficient support is provided to the structure (Figure 7-7).

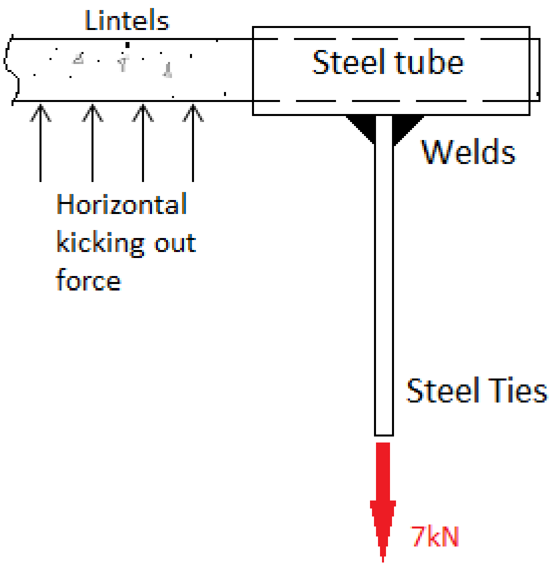

Figure 7-7: The tube-weld-tie connection with an applied force in the tie

A R10 bar, with yield strength (f_y) of 250MPa, is selected to act as the tie. An R8 bar is a round mild steel reinforcing bar, 10mm in diameter. An 'R' bar is selected because it is weldable on site. The weld size is designed as follows:

$$Area\ of\ bar = \pi r^2 = \pi(\frac{10}{2})^2 = 78.54mm^2 \quad (7\text{-}2)$$

The vault, according to Figure 3-4, illustrates how the ties will each support a length of 3.5m thus the total force is:

$$Total\ load = 2\ x\ 3.5 = 7kN$$

Therefore, the stress in the bar can be calculated as follows:

$$Stress\ in\ bar = \frac{Load}{Area} = \frac{7}{78.54} = \ 89.13kN/mm^2 < \frac{250}{1.15} = 217.5MPa \quad (7\text{-}3)$$

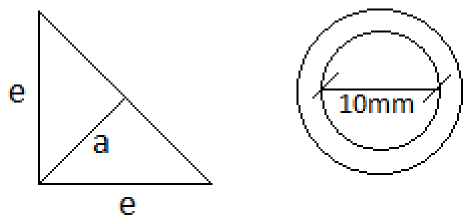

Figure 7-8: Calculation of the weld size

Where *'e'* is the leg length of the weld and '*a'* the throat thickness (Figure 7-8).

If we assume a minimum weld size of 4mm, we can thus calculate '*a',* and effectively determine whether the weld is suitable to carry the load.

$$a = 4 \times \cos(45) = 2.83mm$$

Thus, the unity throat welded area

$$2\pi(6) = 37.70mm$$

$$37.70 \times 2.83 = 106.69mm^2$$

The shear resistance of the steel and weld are compared. The shear resistance of the steel is calculated as follows:

$$V_r = 0.67\emptyset_w A_m f_u \tag{7-4}$$

$$V_r = 0.67 \times 0.67 \times 78.54 \times 250 = 8.8kN$$

The shear resistance of the weld is calculated as follows:

$$V_r = 0.67\emptyset_w A_w x_u (1 + 0.5sin^{1.5}\theta) \tag{7-5}$$

$$V_r = 0.67 \times 0.67 \times 106.69 \times 480 \times (1 + 0.5sin^{1.5}90) = 34kN > 8.8kN \qquad \textit{ok}$$

The minimum weld size of 5mm is used for the prototype. An electrode of 480MPa is used; thus, the weld yield strength exceeds the yield strength of the steel, of 250MPa.

7.4. Foundation design

7.4.1. Introduction

The design of the foundations was done according to the South African concrete design code SABS 0100-1 (2000). The standard method of design takes into consideration sliding, overturning and bearing pressures. Due to the nature of the loading, i.e. vertical loading only, only bearing pressures and shears were calculated and compared, sliding and overturning forces were ignored.

The foundations were placed under the respective load bearing walls. This can be seen in Figure 7-9. The central internal wall is a load bearing wall and carries the load of the vaults and slab. However, the other internal walls are not load bearing and therefore do not require foundations, just slab thickening.

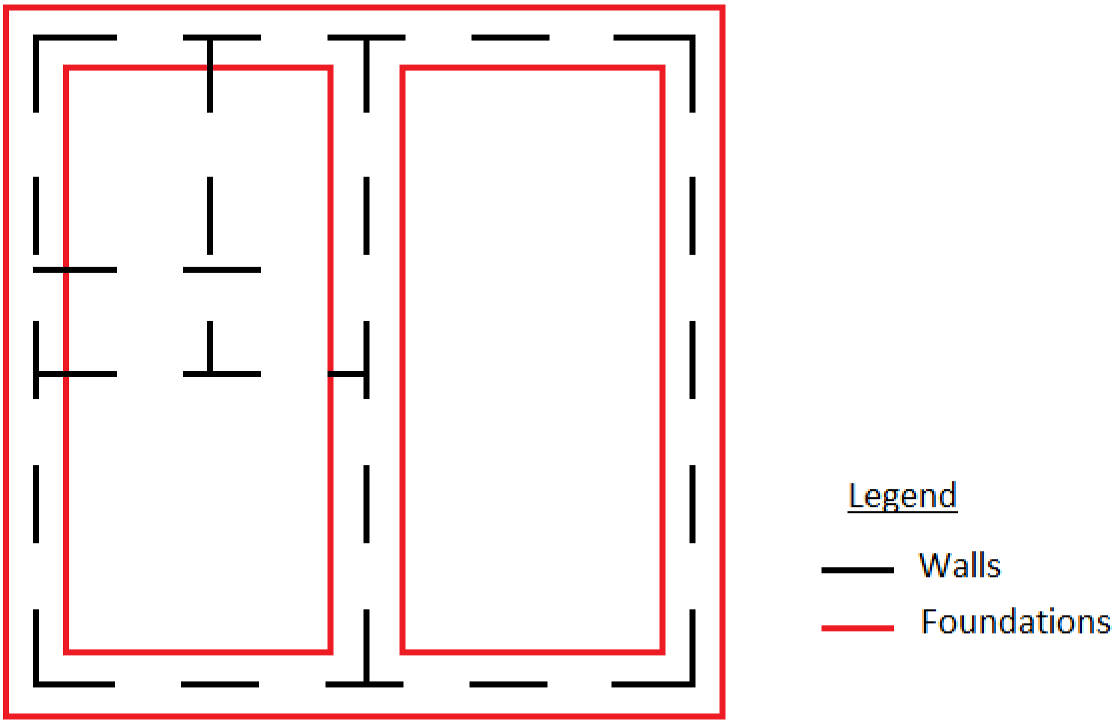

Figure 7-9: A layout showing where the foundations are positioned

The foundations were designed to optimise on materials. However, the foundation has been designed to be extremely stiff, to avoid any cracking that may be caused by differential settlement in the soil. The foundation acts as a stiff beam in the vertical direction with a horizontal footing at the base to ensure that the bearing pressure is never exceeded.

7.4.2. Design

The dimensions of the foundation were selected and optimised in the design process. The final design dimensions and details are shown in Figure 7-10.

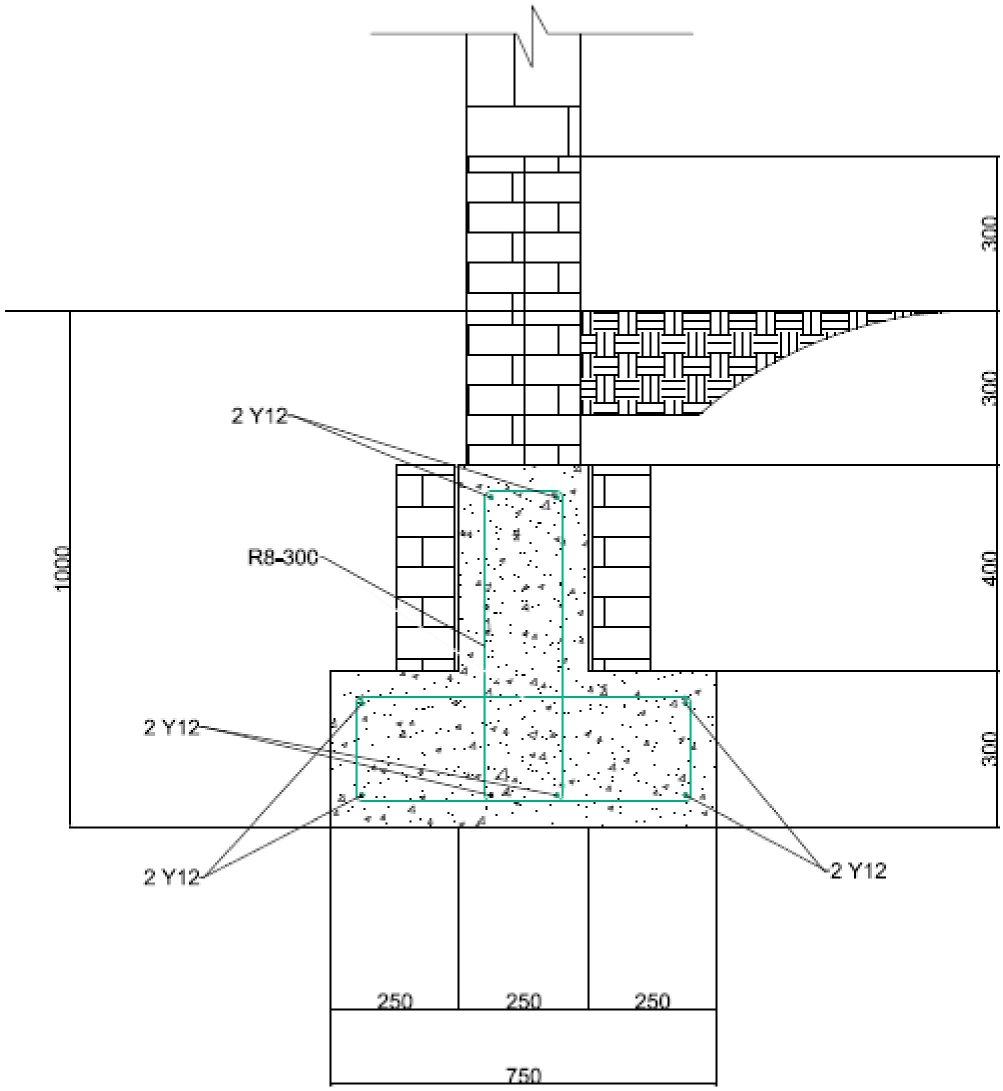

Figure 7-10: Dimensions and detailing of the foundation

7.4.3. Loading

A bearing pressure of 100kPa was selected to design a standard shape, since soil bearing capacities are rarely lower that this value within South Africa. The bearing pressure was compared to the loading to ensure that the foundation is sufficient in supporting the building. The stress from the loading is calculated using the following equation:

$$\sigma = \frac{P_s}{ab} \tag{7-4}$$

Where P_s is the total service load on the structure, and *ab* is the cross sectional area of the foundation. The equation is for vertical loads only.

The loading exerted on the foundation is a combination of dead loads and live loads. The bearing pressure was checked for dead load only, as well as a combination of dead and live loads. The dead load consists of the vault, slab, wall, brick shuttering, soil, surface bed, and self-weight of the foundation, totalling 68.86kN. The live load, as per SABS0100-1 (2000) is taken as 1.5kN/m^2. Once all these values have been calculated and added using the service safety factors, of 1.0DL+1.1LL, a total load of 71.11kN is exerted on the foundation. The bearing pressure was calculated and the results are as follows:

$$\sigma_{DL} = \frac{68.86(10^3)}{0.75(1)} = 91kN/m^2 < 100kPa \qquad Ok$$

$$\sigma_{DL+LL} = \frac{71.11(10^3)}{0.75(1)} = 95kN/m^2 < 100kPa \qquad Ok$$

Note: The soil bearing capacity at the site of the prototype is much greater then 100kPa, but the foundation was designed to be used at almost any location in South Africa.

7.4.4. Flexural steel

As discussed, it is important that the foundations do not move when differential settlement occurs. This, being the worst case scenario, was the basis of design. As a precaution, one metre section of soil was assumed to have settled, which is depicted in Figure 7-11.

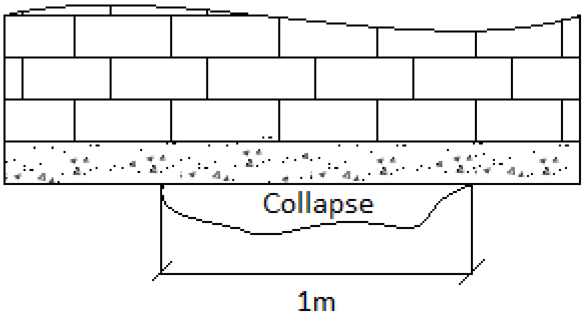

Figure 7-11: An analysis of the foundation of a 1m section of soil collapses

Table 7-3 summarises the steel requirements in the construction of this foundation. The detail of the foundation can be seen in Figure 7-10.

Table 7-3: A table detailing the steel required in the foundation

	Top T section	***Base of inverted T***
Top steel	2Y12	2Y12
Bottom steel	2Y12	2Y12
Shear steel	R8	R8
Shear steel spacing	300mm	300mm

Notes: 2Y12 – Two high yield reinforcing bars, 12mm in diameter

R8 – Mild steel reinforcing bars, 8mm in diameter

8. Construction

8.1. Introduction

The construction process is vital in ensuring that thin shells are favoured over the standard form of rectangular housing. Thin shells are very difficult and complex to construct and a variety of methods have been explored over the years. Some of these methods include using visual guides, balloon formworks (Gohnert, 2011, Wilson, 2005), compacted soil forms (Wilson, 2005) and the like. The aim of this project is to explore innovative methods to simplify and speed up the process of construction. It is just as important that the method of construction is cheap, while maintaining a high level of accuracy. The vault will adopt an original method, which utilises a shifting formwork.

8.2. Site preparation

The site that we were provided with is situated on West Campus at the University of the Witwatersrand, South Africa. The site was previously used as a housing site and building material was strewn over the surface; thus, there is no vegetation that needed to be removed. Builders line was used to measure and layout the foundation before digging began.

8.3. Foundations

Construction commenced by digging the foundations to the required depth. Digging proved to be relatively quick and easy. However, since this is a previously built up site, there were sections that contained concrete members that needed to be demolished. This proved quite difficult and time consuming. Furthermore, approximately 400mm below ground level, a raft foundation was found. This raft foundation served as the foundation for the previous properties. The raft foundation takes up approximately two-thirds of the foundation area. The raft foundation is in excellent condition and it would be very expensive and time consuming to breakdown. It was decided that the raft would be utilised and incorporated into the structure. The section not containing the raft was dug to the required depth and the new foundation was built with ties into the existing raft foundations (Figure 8-1).

Figure 8-1: The foundation is measured and set up using builder's line before it is dug to the required depth

The foundation steel cages were assembled in the inverted "T" shape and dropped into the excavations (Figure 8-2). Holes were drilled into the existing raft foundation and rebar was used to connect the cage to the existing section (Figure 8-3).

Figure 8-2: The steel sections are assembled into the inverted T shape and dropped into the foundations

Figure 8-3: Holes are drilled into the raft foundation so that the edges of the steel cages can be connected into the raft

The concrete was then poured (Figure 8-4). Afrisam, a local concrete supplier in South Africa, sponsored the Readymix concrete, at a strength of 25MPa.

Figure 8-4: Readymix Concrete is poured into the foundation

Figure 8-5: A 10mm layer is positioned over the entire foundation to bind the old and new concrete properly

Once the foundations were complete (Figure 8-5); the next step was the construction of the walls.

8.4. Exterior Walls

It is essential that the exterior walls start at foundation level. Therefore this section forms an important part in the foundation construction process.

A double layer of single cement bricks were used to construct the wall from foundation level to 300mm above ground level (Figure 8-6). The sections around the brickwork were then backfilled with soil (Figure 8-7).

Figure 8-6: Cement bricks are used to construct the base of the wall to 300mm above ground level

Figure 8-7: The cement bricks are built to 300mm before the dry-stack layers begin

At this level, there is a change in the construction material used. Hydraform interlocking dry-stack blocks are to be used to construct the remainder of the external walls.

Durability is an important design consideration which is addressed in considerable detail in this project, particularly when working with earth materials. Therefore it is important to note the use of cement bricks for the first 300mm above ground level and then the change to earth bricks. There have been many durability problems in many projects, in both South Africa and Algeria, where earth blocks are used at ground level. This is due to the collection of rainwater at the base and in turn, the rapid deterioration of these bricks. Soil blocks have been known to loose as much as 70% strength if submerged for long periods of time (Ipinge, 2012).

To ensure that no durability problems arise, to minimise maintenance needs, cement bricks are used to the required height, followed by a damp proof course (DPC) (Figure 8-8). The DPC layer (plastic sheeting) is placed before the first layer of dry stack blocks are placed. This ensures that no water passes through the DPC layer and absorbed by the CSEB. The first layer of blocks has to be mortared to the DPC layer. All succeeding layers are simply dry-stacked and interlocked, with no mortar required in the joints. Builder's line is used to ensure that the first layer of blocks is perfectly level. This is extremely important to ensure that the remainder of the blocks interlock properly. Uneven surfaces will cause openings in joints and interlocking will be difficult.

Figure 8-8: A layer of DPC is placed between the cement bricks and earth blocks

Dry stack interlocking blocks have many benefits, particularly ease and speed of construction. The blocks are designed in such a way to slide into one another without requiring mortar. As demonstrated in Figure 8-9, the succeeding courses lock perfectly, with one another to create a strong and durable wall. The figure also demonstrates how each course is laid and locked in the opposite direction to the previous, i.e. one layer will be laid with the 'front' of the block facing the right and the following layer will face the opposite way, to the left (Hydraform, 2012).

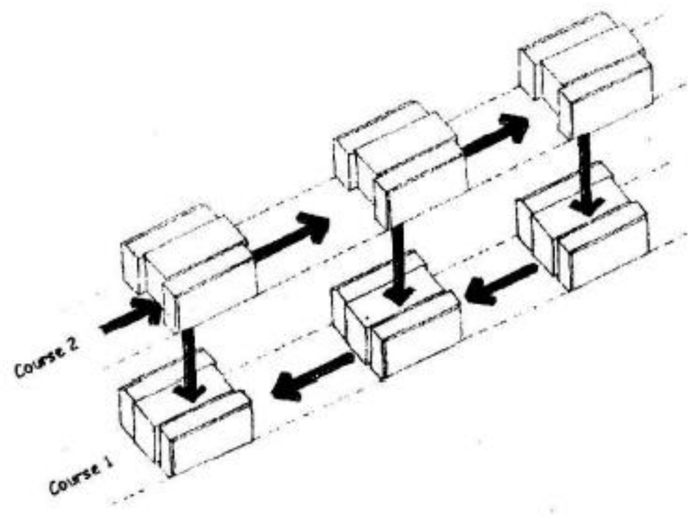

Figure 8-9: The method of constructing two courses of dry stack interlocking blocks (Hydraform, 2012, p 55)

When constructing with interlocking blocks, it is important to understand the exact method of construction to ensure that the blocks interlock properly. The corners are first built up and then constructed inwards towards the wall centre (Figure 8-10). The last block is cut to size to ensure it fits snuggly. The last block acts as a key, locking that specific layer of bricks. This is repeated until the wall is completed (Figure 8-11).

Figure 8-10: Construction of the walls is done from the corners-inwards

Figure 8-11: A completed dry-stack wall

Parts of the walls that contain openings are built in a similar manner. When openings for doors or windows need to be considered, the process is the same, except that blocks will need to be cut at the openings to ensure that the correct sized openings are created. Door frames are built directly into the wall, while openings are left for windows to be fitted at a later stage (Figure 8-12). Lintels are positioned above the doors and windows and mortared in before the standard method of dry-stacking continues (Figure 8-13 and 8-14). It is also important that internal walls are accounted for and thus ties are placed to connect the internal and external walls at a later stage (Figure 8-15). The final layer of blocks is laid with mortar to seal the wall (Figure 8-16).

Figure 8-12: The construction of the wall when openings for windows and doors are required

Figure 8-13: Lintels are positioned above the windows and doors to support the bricks above them

Figure 8-14: Lintels are positioned above all openings to support the bricks above it; the last layer of bricks is mortared in to *lock* the walls

Figure 8-15: Ties are placed in the wall to connect the exterior and interior walls at a later stage

Figure 8-16: The completed walls with the last layer of dry-stack mortared in to *lock* the walls

The final two layers of the first floor walls are completed using cement bricks (Figure 8-17). This is done to 'lock' the wall before the slab is set up, as well as to minimise cracking caused during expansion. Cracking between the slab and the wall can occur if there is a large discrepancy in the material properties. Once the slab is set up, it will expand and shrink with varying temperature variations. By adding two layers of cement bricks, the expansion difference in the expansion of the wall and slab will be considerably less than if the slab is connected to the CSEB directly.

Figure 8-17: The completed first level, where the last two layers of bricks are cement bricks

8.5. Rib and Block Slab

A rib and block slab is a slab systematically made up of lintels as ribs, cement blocks (Figure 8-18), minimal steel meshing and a concrete covering. It is a very economical and quick method of constructing a slab.

Figure 8-18: Cement Blocks used in the rib-and-block slab

The ribs are positioned first at specified distances followed by the placing of the blocks perfectly between the ribs (Figure 8-19). This is done over the entire slab. The blocks are void former, to reduce the weight of the slab. The end product is a series of "T" beams, spanning opposite walls.

Figure 8-19: Placing the blocks between the ribs

Props are positioned underneath the slab for support until the concrete is poured and the slab is sealed (Figure 8-20). Reinforcing and meshing is placed on top of the rib and block system (Figure 8-21).

Figure 8-20: Props are set up under the slab to support it until concrete is poured

Figure 8-21: Steel mesh and reinforcing is positioned on top of the slab

Before the concrete pour can be done, the slab must be shuttered, but just around edges. Wood shuttering is placed around all openings, which is removed once the slab has cured (Figure 8-22). Brick shuttering is used around the edges of the slab so as to allow for an easy continuation of the wall construction.

Figure 8-22: Wood shuttering is used around the openings

Prior to the concrete pour, the lintels and steel ties need to be positioned. This is discussed in detail in section 8.6. Once the ties are set in place, the concrete is poured and the slab is left to cure for 7-14 days (Figure 8-23) before the props are removed.

Figure 8-23: The final concrete pour; the slab is no complete and left to cure

8.6. Lintels and Steel Ties

The steel ties had to be positioned prior to the concrete pour of the slab. The ties, as discussed in Section 7.3, are essential in the construction of the vaulted roof as they prevent the structure from kicking out. The layout is simple. Lintels are placed at the required distance at the ends of the structure. Steel tubes, slightly bigger in size then the lintels, are placed over the lintels at the corresponding tie positions (Figure 8-25). The tubes were filled with grout and all the lintels mortared to one another. Three ties are required on either side of the structure and therefore six ties are welded to the six tubes (Figure 8-24). The corresponding ties are welded together in the middle of the structure to form a continuous tie from one end to the other. Once these ties are connected, the slab is poured and the ties are covered by the concrete. This is important to ensure that no ties are exposed and therefore no rusting occurs. The ties are effective in preventing the vault from kicking out and in turn, collapsing.

Figure 8-24: The steel ties are welded to the tubes at the ends of the structure

Figure 8-25: The tubes are placed over the lintels and then filled with grout

8.7. Vaulted roof

The vaulted roof proved to be the most difficult and time consuming section of the structure. The construction of the vault is a new experience and thus required a considerable amount of brain storming and decision making along the way. The vaults were constructed using the Hydraform Splitter-brick block.

It was decided that a formwork would need to be provided to ensure that the accuracy of the shape is achieved. A number of materials were considered and finally, a steel formwork was chosen. The main motivation for choosing this formwork was accuracy and price. A stencil of the formwork was created and flat bars were bent to the correct shape (Figure 8-26). Steel allowed us to achieve the best possible shape with minimal work involved in creating it.

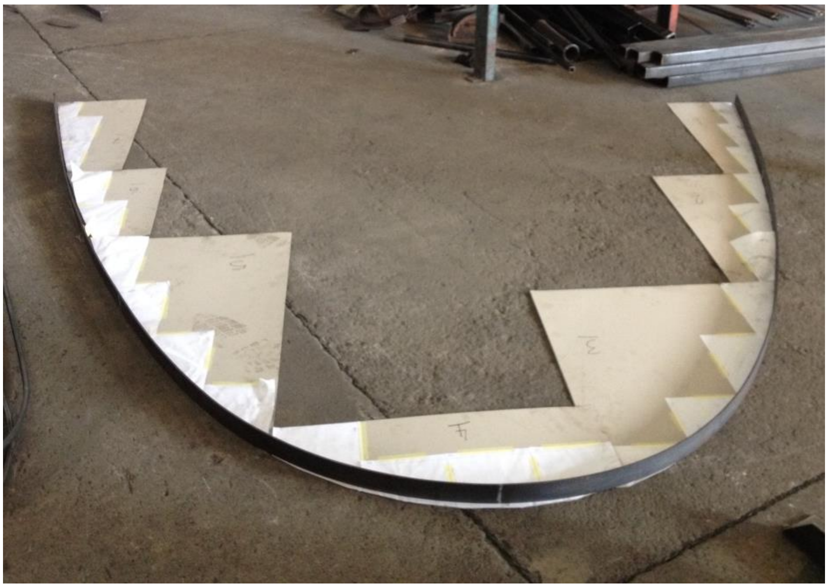

Figure 8-26: A stencil is used to determine the shape and guide the bending of the flat bars

The frames were then assembled and braced into a solid one metre length formwork section (Figure 8-27). Steel sheeting was then riveted onto the outside of the frame, completing the formwork. The formwork was designed and built to be one metre shorter in height than the actual vault to allow for easy dropping and shifting of the formwork. Two identical forms were created so that both vaults could be constructed simultaneously (Figure 8-28).

Figure 8-27: The steel formworks used to construct the vaults

Figure 8-28: The two formworks at site, ready to be lifted and for construction to commence

The form work was lifted onto the slab and propped up on bricks to reach the desired height, before construction commenced (Figure 8-29).

Figure 8-29: The formwork is propped up onto bricks which can easily be pulled out

The first layer of bricks was constructed prior to the pouring of the slab. This was essential for two key reasons:

1. The ties had to be attached to the first few layers of blocks to ensure that they worked effectively in case of any outward thrusts created by the structure at the base
2. The ties had to be covered within the slab to avoid any rusting

Thus, the start of the roof occurs at the slab surface and the remainder is built with the use of the constructed formwork (Figure 8-30).

Figure 8-30: The first layer of bricks as at the same level as the slab

The process of building the vaults is relatively difficult as the scaffolding needs to be set up adequately to allow for safe and accurate construction (Figure 8-31). Once the scaffolding is up, the construction went relatively quickly and accurately due to the effective formwork. A vault was constructed in metre length sections. Once each section is completed and allowed to dry, the formwork dropped and repositioned for the construction of subsequent sections.

Figure 8-31: The start of the construction of the vaults

The construction proved to be relatively difficult and slow. The manner in which the scaffolding was to be positioned, to ensure that the bricks could be laid efficiently, took considerable brain storming. A flexible and easily adjustable system needed to be set up as too much time was spent readjusting the formwork as the construction progressed. The first layer of construction was slow as the scaffolding proved to be a problem. A system was set up that incorporates scaffolding and steel lip channels. The lip channels span the entire length of the structure allowing the builders access between the two vaults.

The first layer of construction was a testing period for the formwork. At the base of the vault, where the forces are predominantly vertical, the formwork was found to work very effectively. Further up, where the angle changes to predominantly horizontal, the formwork began to warp. Certain areas contained insufficient bracing and the bricks sagged slightly. This was easily solved by propping either the bricks or the formwork at the warped point until the mortar had hardened. Additional bracing was added to the formwork once the first layer was completed to avoid continued warping within the vault. Throughout the construction process, a number of mistakes occurred (Figure 8-32). At times, layers of blocks had to be removed and rebuilt to rectify the mistakes.

Figure 8-32: Inaccuracies in following the form during construction

The construction, although slow, was extremely accurate (Figure 8-33). The first layer of construction was the learning curve and the next few layers were completed quickly.

Figure 8-33: Accurate and efficient construction

The two vaults are built simultaneously so that the thrust force is controlled by both structures. The vaults are built from either side to prevent distortions in the formwork and cause inaccuracies in the form (Figure 8-34).

Figure 8-34: Constructing on each side to prevent swaying of the formwork under the weight of the vault

Initially, the first length of the vault was constructed and the formwork was left in position allowing the mortar to set. However, after a day, a crack had formed at the apex of the vault (Figure 8-35). This crack is caused by the shrinking of the vault as the mortar dries. The formwork prevents the vault from contracting naturally, creating a crack along the apex of the vault. Therefore, the manner of drying had to be adjusted. The final layer of blocks was laid, as before, but the mortar was allowed an initial set before the formwork was dropped and the vault was allowed to dry unrestrained. This eliminated cracking at the apex and the remainder of the vaults were completed with precision and efficiency.

Figure 8-35: Cracking occurred along the apex as the vault is restrained from contracting naturally

Once the first layer was complete, the formwork was shifted, repositioned and construction could continue (Figure 8-36 to 8-37). This was repeated until the entire structure was completed (Figure).

Figure 8-36: Completing the last few layers in the construction of the first section

Figure 8-37: The first length is complete: the most difficult section

Figure 8-38: The formwork is shifted and repositioned to continue construction of the vault

Figure 8-39: Construction of the second section is completed, the formwork is dropped and shifted and construction continues

Figure 8-40: The construction of the vaults continues

Figure 8-41: Construction of the first vault is almost complete

Figure 8-42: The second vault nearing completion

Figure 8-43: The completed vaulted roof

Figure 8-44: The completed catenary roof

8.8. Top Floor Walls

The final step of the construction of the superstructure is the top floor walls (Figure 8-45 and 8-46). These walls close up the vaults, making it a habitable living space. The blocks used in the construction of these walls are the Hydraform dry-stack interlocking blocks. The method of construction followed a similar process as described in Section 8.4, where window openings had to be accounted for.

Figure 8-45: The construction of the top floor walls

Figure 8-46: Completion of the top floor walls and thus the superstructure

8.9. Interior Construction and Final Finishes

The final steps in the construction process comprised of the interior construction and finishes. The floor slabs were poured (Figure 8-47), followed by the construction of the internal walls and staircase. The internal walls were constructed using dry stack interlocking blocks (Figure 8-48) and followed the same process as discussed in Section 8.4. The stairs were constructed using lintels and blocks, followed by a layer of mortar mix to stabilise and neaten up the stairs (Figure 8-49). Plaster work was done on the inside and outside walls to cover lintels, protect the steel tubes, cover the insides of the vaults and ceiling, and increase aesthetics (Figure 8-50). Lastly, windows and doors were installed and plastered and the structure was completed with the painting of all the plaster (Figure 8-51 and 8-52). The completed structure is demonstrated in Figures 8-53 to 8-55.

Figure 8-47: The pouring of the floor slabs

Figure 8-48: The construction of the internal walls

Figure 8-49: Construction of the staircase using lintels, blocks and mortar

Figure 8-50: Plastering of the structure

Figure 8-51: The installation of the windows

Figure 8-52: The door is installed and painting of the plaster commences

Figure 8-53: The completion of the painting concludes the construction of the structure

Figure 8-54: The front view of the completed prototype

Figure 8-55: The back view of the completed prototype

9. Cost Analysis

9.1. Introduction

The cost of constructing this project is vital in establishing whether it is a viable option for low-cost housing in South Africa. Considerable research has been done in comparing the costs of various housing solutions, e.g. Talocchino (2005).

When comparing the costs of different housing solutions, various aspects need to be considered. Some of these aspects include ease of construction, floor size, formwork required, labour availability, etc. It is essential that people are satisfied with the final product to ensure it is a success.

In this chapter, a cost breakdown is carried out. This cost is compared to various other projects, in the Section 10.5, to assess its viability.

This project was funded by a number of generous and interested parties. These include Hydraform, Spancon, Afrisam, Lintel Suppliers, WISPECO Aluminium, Macsteel and Robor. Majority of the materials were donated by these companies and the costing below is that of the actual costing has the materials not been donated (Table 9-1).

9.2. Breakdown

Table 9-1: A cost breakdown of the materials required for the construction of the low-cost housing prototype

Cost Breakdown of Prototype				
Component	*Quantity*	*Approximate (Rands)*	*Approximate (US Dollars)*	*Share of cost (%)*
Foundations		**R20889.32**	**$2089**	21.48%
Reinforcing Steel	420kg (Y and R)	R3902.22	$390	
Ready-mix Concrete	10.7m³	R9497	$950	
Brickforce	5 rolls	R213.75	$21	

Bricks	4000	R5000	$500	
Cement	10 bags	R774.50	$78	
Builders sand	3m³	R1466.25	$147	
DPC	2 rolls	R35.60	$4	
Walls		**R15121.10**	**$1512**	16.55%
Hydraform Blocks	2760	R12420	$1242	
Lintels	16	R480	$48	
Cement	3 bags	R232.35	$23	
Builders sand	1m³	R488.75	$49	
Bricks	1200	R1500	$150	
Slab		**R11062.71**	**$1106**	11.38%
Ribs	28m² of slab area	R8400	$840	
Blocks				
Reinforcing steel				
Ready-mix Concrete	3m³	R2662.71	$266	
Structural Ties		**R1600**	**$160**	1.65%
Lintels	12	R990	$99	
Steel tubes	33.164kg	R200	$20	
Steel Ties	6	R288	$29	
Cement	1 bag	R77.45	$8	
Builders sand	0.5m³	R244.38	$24	
Vaulted Roof		**R20167.55**	**$2017**	20.74%
Formwork		*R6362.05*	*$636*	
Steel frames	4	R1181.04	$118	
Bracing	Varies	R2000	$200	
Steel sheeting	6	R1844.81	$185	
Masonite boards	8	R720	$72	
Builders wood	2	R376.20	$38	
Gum poles	4	R240	$24	
Materials		*R13805.50*	*$1381*	

Hydraform Blocks	3400	R10200	$1020	
Builders sand	5	R2443.75	$244	
Cement	15	R1161.75	$116	
Internal Walls		**R2655**	**$266**	2.73%
Bricks	590	R2655	$266	
Staircase		**R420**	**$42**	0.43%
Lintels	14	R420	$42	
Surface Bed		**R5850**	**$585**	6.02%
Cement	6.5m³	R5850	$585	
Finishes		**R17142**	**$1714**	19.03%
Door frames	5	R4000	$400	
Interior Doors	2	R540	$54	
Exterior Doors	2	R1400	$140	
Aluminium Windows	7	R11202	$1120	
TOTAL		***R94 907.50***	***$9 500***	***100%***

Note:

- The costing of the foundation is to the design, i.e. what would be required had the raft foundation not been found.
- The costs above do not include services in terms of electricity, plumbing, etc.
- The costs do not include labour costs, they are merely material costs

Majority of the costs went into the foundations and the roof structure. It is vital that there is no differential settlement in the foundation so that no cracking occurs in the vault. Because of this, the foundations were over-designed and costs could be reduced in this aspect.

In the breakdown, it can also be seen that approximately 30% of the vault cost is attributed to the formwork. However, the formwork is reusable and therefore this cost will diminish significantly. To reduce these costs, other methods of construction need to be investigated. The prices stipulated are for a single building. These prices will change if a larger scale project is implemented. Specific areas where these costs will change include: formwork costs, brick making machines, foundations, finishes, etc. A more expensive, but economical formwork can be applied at a larger scale, i.e. an inflatable formwork (Gohnert, 2011, Wilson, 2005). This method may not be an affordable solution on a small scale, but other construction methods should be explored for larger scale developments.

In terms of brick costs, it is more affordable to purchase a block machine when constructing at a larger scale. This will minimise the costs and time of construction considerably, when materials are mass produced locally.

There are a number of ways in which the costs can be reduced more or kept at a minimum. One aspect, which is not covered in this report, is that of labour. The aim of this project is to involve the community and people who will be living in low-cost houses. Thus, it is expected that labour costs will be at a minimum due to the involvement of the residents in all aspects of the project.

10. Conclusions and Recommendations

10.1. The superior structural form and layout

A superior structure is not simply defined by its image or cost, but by a number of different criteria, such as energy efficiency, durability, social acceptance, etc. The prototype in this project considers a number of various criteria to ensure that the most efficient and comfortable home is produced, utilising a small budget. The orientation of the structure, in relation to the sun, to maximise solar power is vital in ensuring the residents have minimal electricity expenses. In addition, the internal layout of the home is essential. The internal layout of the house is selected to maximise on privacy and space, whilst simultaneously creating comfort and natural light.

A square form is selected for the bottom floor as the most optimal shape for maximising on space. Since most informal settlements are extremely dense and each resident has minimal floor area, the house is designed to be a double story house to maximise on space. Two catenary vaults are designed as the roof structure as well as the upper floor section. The very high vaults are designed to: 1.) utilise the upstairs area as a second bedroom and 2.) create a double volume area to provide natural light and reduce the feeling of confinement. The vaults are also incorporated to minimise on costs, while simultaneously maximising on thermal efficiency. The roof is designed as a natural, sustainable form which will require marginal maintenance due to its superior structural strength.

The most architecturally and structurally efficient structure, the catenary vault, is designed to maximise on space whilst minimising on costs in all areas (i.e. maintenance, costs, electricity, etc.) and providing a safe, durable and environmentally friendly solution for all.

10.2. Essential design considerations for catenary vaults

A method of design, The Segmental Equilibrium Method, was developed in this report to design catenary vaults. This method permits the accurate design of catenary vaults under both vertical and lateral loading. However, at present the

Segmental Equilibrium Method cannot analyse temperature loading, which is carried by using finite elements. The Segmental Equilibrium Method is particularly effective in allowing the user to design the most natural form under the stipulated loading, with an efficient and accurate method.

It would be substantially more time consuming and labour intensive to define the same curve in finite element, or using another form of design. The Segmental Equilibrium Method utilises simple equilibrium equations to define a natural and efficient curve to support the various loading criteria. The thrust lines under each loading combination or pattern can be plotted, and the various areas of weakness identified.

It was found that the loading case which generates the greatest tensile and compressive forces is that of dead load, wind load (C_{pi}=0) and a temperature drop of 20° over the right half of the structure. The form of loading is exaggerated as the temperature will vary along the structure. To simplify analysis and ensure that the structure is sufficiently designed a worst case temperature loading was investigated where the entire side was subject to the temperature change. However, this load does not exceed the strength capacity of the material and the design is therefore adequate.

The structure exhibits a considerable weakness, and possibly failure, under point loads. It is clear that two dimensional shells, such as vaults and arches, are not effective in supporting point loads. Thus, it is recommended that all maintenance is done from an adjacent support system which provides access to the roof. The design of the form also takes into consideration this weakness; therefore, a very steep form is selected where access without additional support is extremely difficult. However, point loads and shell systems do not mix and is a problem with all shell structures.

10.3. Material selection

The materials used in the construction of the prototype proved to be very effective in a number of ways. These blocks have excellent thermal properties, are easy to produce, require minimal energy input in the production phase and are cost effective. The dry stack interlocking blocks eased the construction process considerably and saved costs in the form of mortar and speed of construction. The splitter-brick blocks were very effective in the construction of the vaults, as they provided the required thickness that ordinary bricks would not have. They also ensured that a strong joint was created in the grove, creating a *key* between each block.

The blocks exhibit excellent compressive and tensile strengths and are able to compete with ordinary cement bricks. During the analysis process, the forces exerted by the wall and vault do not exceed the capacity of the building materials. The blocks are satisfactory in the construction of double storey buildings as well as curved forms. However, due to the tensile forces created from the temperature loading, it is recommended that a waterproof layer or paint is applied onto the surface of the vaults to minimise the temperature differences in the material.

10.4. Methods of construction

A number of methods of construction were discussed in this report; however, the method of a sliding formwork was selected and utilised. This method proved to be very effective in ensuring the form was precise. However, it slowed the construction process down considerably. Due to the size of the vaults, it was difficult to determine the amount of bracing required to adequately support the bricks without overloading the formwork. These forms are heavy and therefore difficult to move, but if they are not sufficiently braced, warping occurs causing inaccuracies and thus delays in construction. The formwork must also be dropped after an initial set in the mortar to allow the vault to contract naturally as the mortar dries. This prevents the structure from being restrained so no cracks will form.

Even though the construction was accurate, different methods of formwork should be investigated. More costly methods of construction can also be considered if this project is applied at mass scale, as recycling the formwork could make it more efficient and cost effective

10.5. Costing analysis

The prototype form is an innovative and effective solution to low-cost housing. The cost of current RDP infrastructure programme in South Africa has been found to be ineffective (Blumenfeld, 1996). For smaller floor areas, the cost is only marginally less i.e. costs approximately R1500/m² ($150/m²) (Mica, 2013). However, some literature suggests that costs can reach R2400/m² ($240/m²) for a RDP house (Mabeba, n.d.). This thesis presents a new solution to lost-cost housing which is approximately double in floor size to an RDP house and costs only in the range of 11% to 30% more. However, labour costs still need to be incorporated in the calculations and this could cause the costs to vary considerably depending on the community involvement. The costs provided above will also vary considerably if the project is applied at a larger scale as production and costs of bricks will be considerably less. Catenary vaults as a solution to low-cost housing is a viable and cost effective solution in South Africa.

References

Allen, E., & Zalewski, W. (2010). *From and Forces: Designing efficient, expressive structures.* New Jersey: John Wiley & Sons, Inc.

Argyris, J. (1954). Energy Theorems and Structural Analysis: A Generalized Discourse with Applications on Energy Principles of Structural Analysis Including the Effects of Temperature and Non-Linear Stress-Strain Relations. *Aircraft Engineering and Aerospace Technology*, Vol 26, p 347 - 356.

Atamturktur, H. (2006). *Structural Assesment of Guastavino Domes.* Pennsylvania: The Pennsylvania State University.

Auroville Earth Institute. (2012). *Auroville Earth Institute: UNESCO Chair Earthern Architecture*. Retrieved January 14, 2013, from Auroville Earth Institute Web Site: http://www.earth-auroville.com/index.php

Bahar, R., Benazzoug, M., & Kenai, S. (2004). Performance of compacted cement-stabilised soil. *Elsevier*, Vol 26, p 811-820.

Bartali, H. (1991). La terre arme de paille pour les constructions. *Proceedings of the French-Maghreb Symposium on Construction with Local Materials*, p 551.

Bathe, K., & Chapelle, D. (2011). *The Finite Element Analysis of Shells – Fundamentals (Second Edition).* Berlin: Springer.

Birkinshaw, M. (2008). *A Devil in the Shacks.* Retrieved January 24, 2014, from Pambazuka News: http://www.pambazuka.org/en/category/features/50572

Blackmore, P., & Tsokri, E. (2006). Wind Loads on Curved Roofs. *Journal of Wind Engineering and Industrial Aerodynamics*, Vol 94, p 833–844.

Blumenfeld, J. (1996). *RDP RIP? Reflections on economic growth and development policy in South Africa.* Retrieved January 31, 2013, from Africa Portal Library: http://www.africaportal.org/dspace/articles/rdp-rip-reflections-economic-growth-and-development-policy-south-africa

Braxton, K. (2013). *The Cost Breakdown of a Typical House*. Retrieved September 30, 2013, from RMB Building & Design Llc: http://www.rmbbuildinganddesign.com/blog.php?filter=post&blog_id=85

British Standards Institute. (1996). *EN 1996-1-1: Eurocode 6: Design of Masonry Structures.* London: British Standards Institute.

British Standards Institution. (1992). *BS 5628:Part1- 1992: Structural Use of Unreinforced Masonry.* London: British Standards Institute Group.

British Standards Institution. (1997). *BS 8110-1: Structural use of concrete. Code of practice for design and construction.* London: British Standards Institute Group.

Calderwood, D. (1953). *Native Housing in South Africa.* Johannesburg: University of the Witwatersrand.

Carlson, S. (2013). *Catenary: Encyclopædia Britannica Online Academic Edition.* Retrieved October 14, 2013, from Encyclopædia Britannica: http://www.britannica.com/EBchecked/topic/99414/catenary

Chilton, J. (2000). *The Engineer's Contribution to Contemporary Architecture: Heinz Isler.* London: Thomas Telford Publishing.

Chryso. (2008). *Concrete Admixtures: Chryso Pareflo 10.* Retrieved October 10, 2013, from Chryso: Chemical Solutions for the Construction Material Industry: http://www.chryso.com/upload/t_documents/Fichier_L2/48811/FP_Pareflo10_GB_Issy_L10022-HD.pdf

Chryso SA. (2012). *Foxing Efflorescence.* Retrieved October 10, 2013, from CHRYSO Southern Africa (Pty) Ltd.: http://za.chryso.com/upload/t_documents/Fichier_L1/48885/monier_article.pdf

City of Johannesburg. (2008). *Housing Week starts in a frenzy*. Retrieved September 30, 2013, from Official Website Of The City Of Johannesburg: http://www.joburg.org.za/index.php?option=com_content&task=view&id=2544&Itemid=204

CNERIB. (1991). MATLOC 91; Ministry of Housing. *Proceedings of Maghrebin Symposium on Development of Construction with Local Materials*, p 209.

Conant, K. (1944). Observations on the Vaulting Problems of the Period 1088-1211. *Gazette des Beaux-Arts*, 127-34, ser.6, vol xxvi.

Cowan, H. (1977). A History of Masonry and Concrete Domes in Building Construction. *Building and Construction*, vol. 12, pp.1-24.

Fernandez, R. (2003). *Fibre Reinforced Soil Crete Blocks for the Construction of Low-Cost Housing.* Johannesburg: MSc Dissertation, University of the Witwatersrand.

FinScope. (2007). *My home is my castle/cluster/townhouse/shack – housing in South Africa.* South Africa: FinScope.

Fitchen, J. (1961). *The Construction of Gothic cathedrals.* Oxford: The Clarendon Press.

Fitchett, A. (2009b). *Timbrel Vaults From Stabilized Earth Tile.* Bath: NOCMAT Conference.

Gohnert, M. (2011). *Thin Shell Earth Structures: A Low Cost Housing Solution.* Inaugural speech: University of the Witwatersrand.

Grigonis, R. (2011). *The Gateway Arch — Its History and Architecture.* Retrieved January 15, 2014, from Interesting America: http://www.interestingamerica.com/2011-04-09_Gateway_Arch_Architecture_by_R_Grigonis_41.html

Houben, H., & Boubekeur, S. (1998). *Compressed Earth Blocks: standards.* Brussels: CRATerre-EAG.

Huerta, S. (2003). The Mechanics of Timbrel vaults: A Historical Outline. *Becchi, A, F. Foce and O Pedemonte eds. Essays on the History of Mechanics*. Birkhauser.

Huerta, S. (2006). Structural Design in the Work of Gaudi. *Architectural Science Review*, Vol 49.2, p 324-339.

Hydraform. (2012). *Hydraform Training Manual.* Johnnesburg: Hydraform.

Hymers, P. (2005). Planning and Building a Conservatory. *New Holland*, p 36.

Ipinge, I. (2012). *Durability of compressed stabilised earth blocks.* Johannesburg: MSc Dissertation, University of the Witwatersrand.

Joffroy, T. (1994). *The Basics of Building with Arches, Vaults and Cupolas.* St. Gallen: SKAT.

Lintel Suppliers. (2009). *Services: Lintel Suppliers*. Retrieved November 11, 2013, from Lintel Suppliers: http://www.lintelsuppliers.co.za/services.html

Mabeba, P. (n.d.). *Lynedoch Pilot RDP House.* Cape Town: Sustainability Institute.

Magaia, S. (2003). *Domes in Low-Cost Housing.* Johannesburg: MSc Dissertation, University of the Witwatersrand.

Mica. (2013). *Mica FAQ's*. Retrieved January 23, 2014, from Mica Web site: http://www.mica.co.za/index.php/faqs/item/46-how-much-does-it-cost-to-build-per-square-metre

Minke, G. (2000). *Earth Construction Handbook: The building material earth in a modern architecture.* Boston: WIT Press.

Ochsendorf, J. (2010). *Guastavino Vaulting The Art Of Structural Tiling.* New York: Princeton Architectural Press.

Ramage, M. (2004). *Building A Catalan Vault.* Retrieved from Massachusetts Institute of Technology: http://www.guastavino.net/

Rhyner, K., Melendez, M., Ruiz, P., & Castro, M. (1998). *Un techno como un arcoiris: bovedas de ladrillos en la construccion popular.* ECOSUR, group sofonias/CIDEM.

SABS. (2000). SABS 0100-1: South African Standard Code of Practice; The structural use of concrete. Pretoria: The South African Bureau of Standards.

SAPA. (2011). *RDP houses to 'bona fide' citizens*. Retrieved September 30, 2013, from News24: http://www.news24.com/SouthAfrica/News/RDP-houses-to-bona-fide-citizens-20111019

Sennott, S. (2004). Encyclopedia of Twentieth Century Architecture. *Taylor & Francis*, p 224.

South African Bureau of Standards. (1980). *SABS 0164-1: 1980: Unreinforced Masonry.* Pretoria: SABS.

South African Bureau of Standards. (2000). *SABS 0100-1: South African Standard Code of Practice; The structural use of concrete.* Pretoria: The South African Bureau of Standards.

South African Bureau of Standards. (2009). *SABS 0160-2: South African Standard Code of Practice; Self-weight and Imposed Load.* Pretoria: The South African Bureau of Standards.

South African Bureau of Standards. (2009). *SABS 0160-3: South African Standard Code of Practice; Wind Actions.* Pretoria: The South African Bureau of Standards.

Spancon. (2013). *Rib and Block Slabs*. Retrieved November 10, 2013, from SPANCON: http://www.spancon.co.za/rib-and-block-slabs/

Talocchino, G. (2005). *Design & Construction Criteria for Domes in Low-Cost housing.* Johannesburg: MSc Dissertation, University of the Witwatersrand.

Tarragó, S. (2002). *Guastavino Company (1885-1962), Catalogue of Works in Catalonia and.* Barcelona: Collegi d'Arquitectes de Catalunya.

Taylor, H. (2011). *New Construction Cost Breakdown*. Retrieved September 30, 2013, from National Assocation of Home Builders: http://www.nahb.org/generic.aspx?genericContentID=169974

The Weather Channel. (2009). *Youtube*. Retrieved February 17, 2012, from Man Survives Hurricane Ivan inHUrricane-Proof House: http://www.youtube.com/watch?v=St4umWJttYk&feature=related

Uzoegbo, H., & Hobona, D. (1999). *The Structural Behaviour of dry-stacked walls.* Johannesburg: Research project. University of the Witwatersrand.

Weisstein, E. (n.d.). *Catenary.* From MathWorld--A Wolfram Web Resource: http://mathworld.wolfram.com/Catenary.html.

Wilson, A. (2005). *Practical Design of Concrete Shells.* Monolithic Dome Institute.

Appendix A

Segment no.	Height of Segment	Weight	Left Angle	Left Thrust x	Left Thrust y	***Left Thrust***	Right Thrust x	Right Thrust y	***Right Thrust***	Right angle	Co-ordinates	
											X	Y
1	128.20	0.55	80.50	2.91	17.38	17.62	-2.91	-16.83	17.08	80.19	0	0
2	128.20	0.55	80.19	2.91	16.83	17.08	-2.91	-16.28	16.54	79.87	21.16	126.44
3	128.20	0.55	79.87	2.91	16.28	16.54	-2.91	-15.73	15.99	79.52	42.99	252.76
4	128.20	0.55	79.52	2.91	15.73	15.99	-2.91	-15.17	15.45	79.15	65.54	378.96
5	128.20	0.55	79.15	2.91	15.17	15.45	-2.91	-14.62	14.91	78.75	88.86	505.02
6	128.20	0.55	78.75	2.91	14.62	14.91	-2.91	-14.07	14.37	78.32	112.99	630.93
7	128.20	0.55	78.32	2.91	14.07	14.37	-2.91	-13.52	13.83	77.86	138.00	756.66
8	128.20	0.55	77.86	2.91	13.52	13.83	-2.91	-12.97	13.29	77.36	163.95	882.20
9	128.20	0.55	77.36	2.91	12.97	13.29	-2.91	-12.42	12.75	76.81	190.92	1007.53
10	128.20	0.55	76.81	2.91	12.42	12.75	-2.91	-11.86	12.21	76.22	218.98	1132.62
11	128.20	0.55	76.22	2.91	11.86	12.21	-2.91	-11.31	11.68	75.58	248.22	1257.44
12	128.20	0.55	75.58	2.91	11.31	11.68	-2.91	-10.76	11.15	74.87	278.75	1381.95
13	128.20	0.55	74.87	2.91	10.76	11.15	-2.91	-10.21	10.61	74.10	310.67	1506.11
14	128.20	0.55	74.10	2.91	10.21	10.61	-2.91	-9.66	10.08	73.24	344.13	1629.86
15	128.20	0.55	73.24	2.91	9.66	10.08	-2.91	-9.10	9.56	72.28	379.26	1753.15
16	128.20	0.55	72.28	2.91	9.10	9.56	-2.91	-8.55	9.03	71.22	416.23	1875.90
17	128.20	0.55	71.22	2.91	8.55	9.03	-2.91	-8.00	8.51	70.02	455.24	1998.02
18	128.20	0.55	70.02	2.91	8.00	8.51	-2.91	-7.45	8.00	68.67	496.52	2119.39
19	128.20	0.55	68.67	2.91	7.45	8.00	-2.91	-6.90	7.49	67.13	540.32	2239.87
20	128.20	0.55	67.13	2.91	6.90	7.49	-2.91	-6.35	6.98	65.37	586.95	2359.29
21	128.20	0.55	65.37	2.91	6.35	6.98	-2.91	-5.79	6.48	63.34	636.76	2477.41
22	128.20	0.55	63.34	2.91	5.79	6.48	-2.91	-5.24	5.99	60.98	690.18	2593.95
23	128.20	0.55	60.98	2.91	5.24	5.99	-2.91	-4.69	5.52	58.19	747.70	2708.52
24	128.20	0.55	58.19	2.91	4.69	5.52	-2.91	-4.14	5.06	54.90	809.90	2820.62
25	128.20	0.55	54.90	2.91	4.14	5.06	-2.91	-3.59	4.62	50.96	877.46	2929.57
26	128.20	0.55	50.96	2.91	3.59	4.62	-2.91	-3.03	4.20	46.22	951.18	3034.45
27	128.20	0.55	46.22	2.91	3.03	4.20	-2.91	-2.48	3.82	40.49	1031.92	3134.02
28	128.20	0.55	40.49	2.91	2.48	3.82	-2.91	-1.93	3.49	33.58	1120.63	3226.57
29	128.20	0.55	33.58	2.91	1.93	3.49	-2.91	-1.38	3.22	25.37	1218.13	3309.81
30	128.20	0.55	25.37	2.91	1.38	3.22	-2.91	-0.83	3.02	15.88	1324.93	3380.72
31	128.20	0.55	15.88	2.91	0.83	3.02	-2.91	-0.28	2.92	5.42	1440.76	3435.65
32	128.20	0.55	5.42	2.91	0.28	2.92	-2.91	0.28	2.92	-5.42	1564.06	3470.74

33	128.20	0.55	-5.42	2.91	-0.28	2.92	-2.91	0.83	3.02	-15.88	1691.69	3482.85
34	128.20	0.55	-15.88	2.91	-0.83	3.02	-2.91	1.38	3.22	-25.37	1819.31	3470.74
35	128.20	0.55	-25.37	2.91	-1.38	3.22	-2.91	1.93	3.49	-33.58	1942.61	3435.65
36	128.20	0.55	-33.58	2.91	-1.93	3.49	-2.91	2.48	3.82	-40.49	2058.44	3380.72
37	128.20	0.55	-40.49	2.91	-2.48	3.82	-2.91	3.03	4.20	-46.22	2165.24	3309.81
38	128.20	0.55	-46.22	2.91	-3.03	4.20	-2.91	3.59	4.62	-50.96	2262.74	3226.57
39	128.20	0.55	-50.96	2.91	-3.59	4.62	-2.91	4.14	5.06	-54.90	2351.45	3134.02
40	128.20	0.55	-54.90	2.91	-4.14	5.06	-2.91	4.69	5.52	-58.19	2432.20	3034.45
41	128.20	0.55	-58.19	2.91	-4.69	5.52	-2.91	5.24	5.99	-60.98	2505.91	2929.57
42	128.20	0.55	-60.98	2.91	-5.24	5.99	-2.91	5.79	6.48	-63.34	2573.48	2820.62
43	128.20	0.55	-63.34	2.91	-5.79	6.48	-2.91	6.35	6.98	-65.37	2635.68	2708.52
44	128.20	0.55	-65.37	2.91	-6.35	6.98	-2.91	6.90	7.49	-67.13	2693.19	2593.95
45	128.20	0.55	-67.13	2.91	-6.90	7.49	-2.91	7.45	8.00	-68.67	2746.61	2477.41
46	128.20	0.55	-68.67	2.91	-7.45	8.00	-2.91	8.00	8.51	-70.02	2796.42	2359.29
47	128.20	0.55	-70.02	2.91	-8.00	8.51	-2.91	8.55	9.03	-71.22	2843.05	2239.87
48	128.20	0.55	-71.22	2.91	-8.55	9.03	-2.91	9.10	9.56	-72.28	2886.85	2119.39
49	128.20	0.55	-72.28	2.91	-9.10	9.56	-2.91	9.66	10.08	-73.24	2928.13	1998.02
50	128.20	0.55	-73.24	2.91	-9.66	10.08	-2.91	10.21	10.61	-74.10	2967.14	1875.90
51	128.20	0.55	-74.10	2.91	-10.21	10.61	-2.91	10.76	11.15	-74.87	3004.12	1753.15
52	128.20	0.55	-74.87	2.91	-10.76	11.15	-2.91	11.31	11.68	-75.58	3039.25	1629.86
53	128.20	0.55	-75.58	2.91	-11.31	11.68	-2.91	11.86	12.21	-76.22	3072.70	1506.11
54	128.20	0.55	-76.22	2.91	-11.86	12.21	-2.91	12.42	12.75	-76.81	3104.63	1381.95
55	128.20	0.55	-76.81	2.91	-12.42	12.75	-2.91	12.97	13.29	-77.36	3135.15	1257.44
56	128.20	0.55	-77.36	2.91	-12.97	13.29	-2.91	13.52	13.83	-77.86	3164.39	1132.62
57	128.20	0.55	-77.86	2.91	-13.52	13.83	-2.91	14.07	14.37	-78.32	3192.45	1007.53
58	128.20	0.55	-78.32	2.91	-14.07	14.37	-2.91	14.62	14.91	-78.75	3219.42	882.20
59	128.20	0.55	-78.75	2.91	-14.62	14.91	-2.91	15.17	15.45	-79.15	3245.37	756.66
60	128.20	0.55	-79.15	2.91	-15.17	15.45	-2.91	15.73	15.99	-79.52	3270.38	630.93
61	128.20	0.55	-79.52	2.91	-15.73	15.99	-2.91	16.28	16.54	-79.87	3294.51	505.02
62	128.20	0.55	-79.87	2.91	-16.28	16.54	-2.91	16.83	17.08	-80.19	3317.83	378.96
63	128.20	0.55	-80.19	2.91	-16.83	17.08	-2.91	17.38	17.62	-80.50	3340.38	252.76
											3362.21	126.44
											3383.37	0

Segment no.	Height of Segment	DL+LL(F)	Left Angle	Left Thrust x	Left Thrust y	***Left Thrust***	Right Thrust x	Right Thrust y	***Right Thrust***	Right angle	Co-ordinates	
											X	Y
1	130	0.456	80.200	2.519	14.582	14.797	-2.519	-14.125	14.348	79.890	0	0
2	130	0.457	79.890	2.519	14.125	14.348	-2.519	-13.668	13.899	79.559	22.127	128.103
3	130	0.457	79.559	2.519	13.668	13.899	-2.519	-13.212	13.449	79.207	44.948	256.084
4	130	0.457	79.207	2.519	13.212	13.449	-2.519	-12.754	13.001	78.829	68.506	383.932
5	130	0.458	78.829	2.519	12.754	13.001	-2.519	-12.297	12.552	78.424	92.851	511.632
6	130	0.458	78.424	2.519	12.297	12.552	-2.519	-11.839	12.104	77.989	118.036	639.169
7	130	0.458	77.989	2.519	11.839	12.104	-2.519	-11.380	11.656	77.520	144.122	766.525
8	130	0.459	77.520	2.519	11.380	11.656	-2.519	-10.921	11.208	77.014	171.174	893.679
9	130	0.459	77.014	2.519	10.921	11.208	-2.519	-10.462	10.761	76.464	199.266	1020.608
10	130	0.460	76.464	2.519	10.462	10.761	-2.519	-10.002	10.314	75.866	228.480	1147.283
11	130	0.460	75.866	2.519	10.002	10.314	-2.519	-9.542	9.869	75.213	258.907	1273.672
12	130	0.461	75.213	2.519	9.542	9.869	-2.519	-9.081	9.424	74.498	290.652	1399.736
13	130	0.462	74.498	2.519	9.081	9.424	-2.519	-8.619	8.980	73.711	323.830	1525.431
14	130	0.462	73.711	2.519	8.619	8.980	-2.519	-8.157	8.537	72.840	358.576	1650.702
15	130	0.463	72.840	2.519	8.157	8.537	-2.519	-7.693	8.095	71.873	395.039	1775.483
16	130	0.464	71.873	2.519	7.693	8.095	-2.519	-7.229	7.655	70.792	433.395	1899.696
17	130	0.465	70.792	2.519	7.229	7.655	-2.519	-6.764	7.218	69.577	473.841	2023.244
18	130	0.466	69.577	2.519	6.764	7.218	-2.519	-6.298	6.783	68.202	516.612	2146.007
19	130	0.468	68.202	2.519	6.298	6.783	-2.519	-5.830	6.351	66.636	561.975	2267.835
20	130	0.469	66.636	2.519	5.830	6.351	-2.519	-5.361	5.923	64.836	610.248	2388.540
21	130	0.471	64.836	2.519	5.361	5.923	-2.519	-4.891	5.501	62.752	661.803	2507.881
22	130	0.473	62.752	2.519	4.891	5.501	-2.519	-4.418	5.086	60.314	717.079	2625.543
23	130	0.475	60.314	2.519	4.418	5.086	-2.519	-3.943	4.679	57.434	776.599	2741.117
24	130	0.477	57.434	2.519	3.943	4.679	-2.519	-3.466	4.285	53.998	840.982	2854.055
25	130	0.480	53.998	2.519	3.466	4.285	-2.519	-2.986	3.907	49.857	910.957	2963.615
26	130	0.483	49.857	2.519	2.986	3.907	-2.519	-2.503	3.551	44.825	987.373	3068.785
27	130	0.487	44.825	2.519	2.503	3.551	-2.519	-2.017	3.227	38.684	1071.184	3168.161
28	130	0.490	38.684	2.519	2.017	3.227	-2.519	-1.526	2.945	31.216	1163.388	3259.804
29	130	0.494	31.216	2.519	1.526	2.945	-2.519	-1.032	2.722	22.288	1264.866	3341.058
30	130	0.497	22.288	2.519	1.032	2.722	-2.519	-0.535	2.575	12.002	1376.044	3408.433
31	130	0.499	12.002	2.519	0.535	2.575	-2.519	-0.037	2.519	0.836	1496.332	3457.738
32	130	0.499	0.836	2.519	0.037	2.519	-2.519	0.462	2.561	-10.398	1623.490	3484.770

33	130	0.499	-10.398	2.519	-0.462	2.561	-2.519	0.961	2.696	-20.881	1753.476	3486.667
34	130	0.497	-20.881	2.519	-0.961	2.696	-2.519	1.458	2.910	-30.062	1881.342	3463.205
35	130	0.494	-30.062	2.519	-1.458	2.910	-2.519	1.952	3.186	-37.773	2002.803	3416.868
36	130	0.490	-37.773	2.519	-1.952	3.186	-2.519	2.442	3.508	-44.116	2115.316	3351.747
37	130	0.487	-44.116	2.519	-2.442	3.508	-2.519	2.929	3.863	-49.305	2218.074	3272.118
38	130	0.483	-49.305	2.519	-2.929	3.863	-2.519	3.412	4.241	-53.565	2311.406	3181.623
39	130	0.480	-53.565	2.519	-3.412	4.241	-2.519	3.892	4.636	-57.090	2396.170	3083.058
40	130	0.477	-57.090	2.519	-3.892	4.636	-2.519	4.369	5.043	-60.037	2473.379	2978.470
41	130	0.475	-60.037	2.519	-4.369	5.043	-2.519	4.844	5.459	-62.525	2544.010	2869.331
42	130	0.473	-62.525	2.519	-4.844	5.459	-2.519	5.316	5.883	-64.649	2608.938	2756.707
43	130	0.471	-64.649	2.519	-5.316	5.883	-2.519	5.787	6.311	-66.479	2668.915	2641.369
44	130	0.469	-66.479	2.519	-5.787	6.311	-2.519	6.256	6.744	-68.069	2724.575	2523.887
45	130	0.468	-68.069	2.519	-6.256	6.744	-2.519	6.723	7.180	-69.463	2776.457	2404.688
46	130	0.466	-69.463	2.519	-6.723	7.180	-2.519	7.190	7.618	-70.693	2825.010	2284.096
47	130	0.465	-70.693	2.519	-7.190	7.618	-2.519	7.655	8.058	-71.787	2870.615	2162.358
48	130	0.464	-71.787	2.519	-7.655	8.058	-2.519	8.119	8.501	-72.765	2913.596	2039.669
49	130	0.463	-72.765	2.519	-8.119	8.501	-2.519	8.582	8.944	-73.644	2954.228	1916.181
50	130	0.462	-73.644	2.519	-8.582	8.944	-2.519	9.044	9.389	-74.439	2992.746	1792.019
51	130	0.462	-74.439	2.519	-9.044	9.389	-2.519	9.506	9.834	-75.160	3029.355	1667.280
52	130	0.461	-75.160	2.519	-9.506	9.834	-2.519	9.967	10.280	-75.818	3064.229	1542.045
53	130	0.460	-75.818	2.519	-9.967	10.280	-2.519	10.428	10.727	-76.421	3097.524	1416.381
54	130	0.460	-76.421	2.519	-10.428	10.727	-2.519	10.887	11.175	-76.974	3129.374	1290.343
55	130	0.459	-76.974	2.519	-10.887	11.175	-2.519	11.347	11.623	-77.485	3159.896	1163.977
56	130	0.459	-77.485	2.519	-11.347	11.623	-2.519	11.806	12.071	-77.957	3189.196	1037.322
57	130	0.458	-77.957	2.519	-11.806	12.071	-2.519	12.264	12.520	-78.395	3217.367	910.411
58	130	0.458	-78.395	2.519	-12.264	12.520	-2.519	12.722	12.969	-78.802	3244.491	783.272
59	130	0.458	-78.802	2.519	-12.722	12.969	-2.519	13.180	13.418	-79.181	3270.643	655.930
60	130	0.457	-79.181	2.519	-13.180	13.418	-2.519	13.637	13.868	-79.536	3295.890	528.405
61	130	0.457	-79.536	2.519	-13.637	13.868	-2.519	14.094	14.317	-79.868	3320.292	400.715
62	130	0.457	-79.868	2.519	-14.094	14.317	-2.519	14.551	14.767	-80.180	3343.903	272.878
63	130	0.456	-80.180	2.519	-14.551	14.767	-2.519	15.007	15.217	-80.473	3366.772	144.905
											3388.945	16.810
											3391.849	0

Segment no.	Height of Segment	DL+LL(L)	Left Angle	Left Thrust x	Left Thrust y	***Left Thrust***	Right Thrust x	Right Thrust y	***Right Thrust***	Right angle	Co-ordinates	
											X	Y
1	129	0.450	80.500	2.412	14.412	14.613	-2.412	-13.962	14.169	80.200	0	0
2	129	0.450	80.200	2.412	13.962	14.169	-2.412	-13.512	13.725	79.879	21.291	127.231
3	129	0.451	79.879	2.412	13.512	13.725	-2.412	-13.061	13.282	79.538	43.249	254.348
4	129	0.451	79.538	2.412	13.061	13.282	-2.412	-12.610	12.838	79.172	65.917	381.341
5	129	0.451	79.172	2.412	12.610	12.838	-2.412	-12.158	12.395	78.780	89.342	508.196
6	129	0.452	78.780	2.412	12.158	12.395	-2.412	-11.707	11.953	78.359	113.575	634.900
7	129	0.452	78.359	2.412	11.707	11.953	-2.412	-11.254	11.510	77.905	138.675	761.434
8	129	0.453	77.905	2.412	11.254	11.510	-2.412	-10.802	11.068	77.414	164.705	887.781
9	129	0.453	77.414	2.412	10.802	11.068	-2.412	-10.349	10.626	76.881	191.735	1013.917
10	129	0.454	76.881	2.412	10.349	10.626	-2.412	-9.895	10.185	76.302	219.846	1139.817
11	129	0.454	76.302	2.412	9.895	10.185	-2.412	-9.441	9.744	75.670	249.125	1265.450
12	129	0.455	75.670	2.412	9.441	9.744	-2.412	-8.986	9.304	74.976	279.673	1390.781
13	129	0.455	74.976	2.412	8.986	9.304	-2.412	-8.531	8.865	74.213	311.602	1515.767
14	129	0.456	74.213	2.412	8.531	8.865	-2.412	-8.074	8.427	73.369	345.042	1640.358
15	129	0.457	73.369	2.412	8.074	8.427	-2.412	-7.617	7.990	72.431	380.137	1764.492
16	129	0.458	72.431	2.412	7.617	7.990	-2.412	-7.159	7.555	71.383	417.057	1888.096
17	129	0.459	71.383	2.412	7.159	7.555	-2.412	-6.700	7.121	70.204	455.996	2011.079
18	129	0.460	70.204	2.412	6.700	7.121	-2.412	-6.240	6.690	68.869	497.178	2133.329
19	129	0.461	68.869	2.412	6.240	6.690	-2.412	-5.779	6.262	67.348	540.867	2254.705
20	129	0.463	67.348	2.412	5.779	6.262	-2.412	-5.316	5.838	65.598	587.371	2375.031
21	129	0.464	65.598	2.412	5.316	5.838	-2.412	-4.852	5.418	63.568	637.054	2494.080
22	129	0.466	63.568	2.412	4.852	5.418	-2.412	-4.386	5.005	61.192	690.349	2611.556
23	129	0.468	61.192	2.412	4.386	5.005	-2.412	-3.917	4.600	58.379	747.770	2727.072
24	129	0.471	58.379	2.412	3.917	4.600	-2.412	-3.446	4.206	55.014	809.933	2840.106
25	129	0.474	55.014	2.412	3.446	4.206	-2.412	-2.972	3.828	50.945	877.568	2949.954
26	129	0.477	50.945	2.412	2.972	3.828	-2.412	-2.496	3.471	45.978	951.534	3055.642
27	129	0.480	45.978	2.412	2.496	3.471	-2.412	-2.015	3.143	39.880	1032.813	3155.816
28	129	0.484	39.880	2.412	2.015	3.143	-2.412	-1.531	2.857	32.407	1122.460	3248.576
29	129	0.488	32.407	2.412	1.531	2.857	-2.412	-1.043	2.628	23.391	1221.453	3331.288
30	129	0.491	23.391	2.412	1.043	2.628	-2.412	-0.552	2.474	12.902	1330.363	3400.422
31	129	0.492	12.902	2.412	0.552	2.474	-2.412	-0.060	2.413	1.425	1448.762	3451.636
32	129	0.492	1.425	2.412	0.060	2.413	-2.412	0.432	2.450	-10.166	1574.505	3480.440

33	129	0.441	-10.166	2.412	-0.432	2.450	-2.412	0.874	2.565	-19.917	1703.465	3483.649
34	129	0.441	-19.917	2.412	-0.874	2.565	-2.412	1.315	2.747	-28.607	1830.440	3460.880
35	129	0.441	-28.607	2.412	-1.315	2.747	-2.412	1.757	2.984	-36.069	1951.724	3416.934
36	129	0.441	-36.069	2.412	-1.757	2.984	-2.412	2.198	3.263	-42.347	2064.976	3355.170
37	129	0.441	-42.347	2.412	-2.198	3.263	-2.412	2.640	3.575	-47.582	2169.248	3279.220
38	129	0.441	-47.582	2.412	-2.640	3.575	-2.412	3.081	3.913	-51.946	2264.589	3192.323
39	129	0.441	-51.946	2.412	-3.081	3.913	-2.412	3.522	4.269	-55.601	2351.604	3097.090
40	129	0.441	-55.601	2.412	-3.522	4.269	-2.412	3.964	4.640	-58.682	2431.120	2995.511
41	129	0.441	-58.682	2.412	-3.964	4.640	-2.412	4.405	5.022	-61.300	2504.000	2889.071
42	129	0.441	-61.300	2.412	-4.405	5.022	-2.412	4.847	5.414	-63.544	2571.053	2778.867
43	129	0.441	-63.544	2.412	-4.847	5.414	-2.412	5.288	5.812	-65.483	2633.001	2665.715
44	129	0.441	-65.483	2.412	-5.288	5.812	-2.412	5.730	6.216	-67.172	2690.471	2550.224
45	129	0.441	-67.172	2.412	-5.730	6.216	-2.412	6.171	6.626	-68.653	2744.001	2432.855
46	129	0.441	-68.653	2.412	-6.171	6.626	-2.412	6.612	7.038	-69.961	2794.049	2313.959
47	129	0.441	-69.961	2.412	-6.612	7.038	-2.412	7.054	7.455	-71.124	2841.007	2193.809
48	129	0.441	-71.124	2.412	-7.054	7.455	-2.412	7.495	7.874	-72.163	2885.210	2072.619
49	129	0.441	-72.163	2.412	-7.495	7.874	-2.412	7.937	8.295	-73.097	2926.945	1950.557
50	129	0.441	-73.097	2.412	-7.937	8.295	-2.412	8.378	8.718	-73.940	2966.459	1827.757
51	129	0.441	-73.940	2.412	-8.378	8.718	-2.412	8.820	9.143	-74.706	3003.966	1704.330
52	129	0.441	-74.706	2.412	-8.820	9.143	-2.412	9.261	9.570	-75.403	3039.652	1580.365
53	129	0.441	-75.403	2.412	-9.261	9.570	-2.412	9.702	9.998	-76.040	3073.679	1455.933
54	129	0.441	-76.040	2.412	-9.702	9.998	-2.412	10.144	10.427	-76.626	3106.190	1331.097
55	129	0.441	-76.626	2.412	-10.144	10.427	-2.412	10.585	10.856	-77.164	3137.309	1205.907
56	129	0.441	-77.164	2.412	-10.585	10.856	-2.412	11.027	11.287	-77.662	3167.149	1080.406
57	129	0.441	-77.662	2.412	-11.027	11.287	-2.412	11.468	11.719	-78.123	3195.807	954.629
58	129	0.441	-78.123	2.412	-11.468	11.719	-2.412	11.909	12.151	-78.552	3223.370	828.608
59	129	0.441	-78.552	2.412	-11.909	12.151	-2.412	12.351	12.584	-78.951	3249.919	702.370
60	129	0.441	-78.951	2.412	-12.351	12.584	-2.412	12.792	13.018	-79.323	3275.523	575.936
61	129	0.441	-79.323	2.412	-12.792	13.018	-2.412	13.234	13.452	-79.671	3300.247	449.328
62	129	0.441	-79.671	2.412	-13.234	13.452	-2.412	13.675	13.886	-79.998	3324.147	322.561
63	129	0.441	-79.998	2.412	-13.675	13.886	-2.412	14.117	14.321	-80.305	3347.275	195.651
											3369.680	68.612
											3381.162	0

Segment no.	Height of Segment	DL+LL(R)	Left Angle	Left Thrust x	Left Thrust y	***Left Thrust***	Right Thrust x	Right Thrust y	***Right Thrust***	Right angle	Co-ordinates	
											X	Y
1	127	0.441	80.200	2.431	14.074	14.282	-2.431	-13.633	13.848	79.889	0	0
2	127	0.441	79.889	2.431	13.633	13.848	-2.431	-13.191	13.413	79.558	21.617	125.147
3	127	0.441	79.558	2.431	13.191	13.413	-2.431	-12.750	12.979	79.205	43.912	250.174
4	127	0.441	79.205	2.431	12.750	12.979	-2.431	-12.308	12.546	78.827	66.929	375.071
5	127	0.441	78.827	2.431	12.308	12.546	-2.431	-11.867	12.113	78.423	90.716	499.824
6	127	0.441	78.423	2.431	11.867	12.113	-2.431	-11.425	11.681	77.988	115.324	624.417
7	127	0.441	77.988	2.431	11.425	11.681	-2.431	-10.984	11.250	77.520	140.812	748.833
8	127	0.441	77.520	2.431	10.984	11.250	-2.431	-10.543	10.819	77.015	167.242	873.052
9	127	0.441	77.015	2.431	10.543	10.819	-2.431	-10.101	10.390	76.468	194.685	997.052
10	127	0.441	76.468	2.431	10.101	10.390	-2.431	-9.660	9.961	75.874	223.221	1120.804
11	127	0.441	75.874	2.431	9.660	9.961	-2.431	-9.218	9.533	75.227	252.937	1244.279
12	127	0.441	75.227	2.431	9.218	9.533	-2.431	-8.777	9.107	74.519	283.932	1367.439
13	127	0.441	74.519	2.431	8.777	9.107	-2.431	-8.335	8.683	73.741	316.316	1490.240
14	127	0.441	73.741	2.431	8.335	8.683	-2.431	-7.894	8.260	72.884	350.216	1612.632
15	127	0.441	72.884	2.431	7.894	8.260	-2.431	-7.453	7.839	71.934	385.774	1734.553
16	127	0.441	71.934	2.431	7.453	7.839	-2.431	-7.011	7.421	70.877	423.151	1855.928
17	127	0.441	70.877	2.431	7.011	7.421	-2.431	-6.570	7.005	69.694	462.536	1976.667
18	127	0.441	69.694	2.431	6.570	7.005	-2.431	-6.128	6.593	68.363	504.140	2096.659
19	127	0.441	68.363	2.431	6.128	6.593	-2.431	-5.687	6.185	66.855	548.213	2215.766
20	127	0.441	66.855	2.431	5.687	6.185	-2.431	-5.246	5.781	65.135	595.042	2333.818
21	127	0.441	65.135	2.431	5.246	5.781	-2.431	-4.804	5.384	63.159	644.961	2450.596
22	127	0.441	63.159	2.431	4.804	5.384	-2.431	-4.363	4.994	60.872	698.362	2565.823
23	127	0.441	60.872	2.431	4.363	4.994	-2.431	-3.921	4.614	58.203	755.704	2679.141
24	127	0.441	58.203	2.431	3.921	4.614	-2.431	-3.480	4.245	55.062	817.522	2790.080
25	127	0.441	55.062	2.431	3.480	4.245	-2.431	-3.038	3.891	51.337	884.440	2898.020
26	127	0.441	51.337	2.431	3.038	3.891	-2.431	-2.597	3.557	46.891	957.171	3002.131
27	127	0.441	46.891	2.431	2.597	3.557	-2.431	-2.156	3.249	41.563	1036.513	3101.297
28	127	0.441	41.563	2.431	2.156	3.249	-2.431	-1.714	2.975	35.188	1123.303	3194.014
29	127	0.441	35.188	2.431	1.714	2.975	-2.431	-1.273	2.744	27.634	1218.327	3278.272
30	127	0.441	27.634	2.431	1.273	2.744	-2.431	-0.831	2.569	18.879	1322.119	3351.458
31	127	0.441	18.879	2.431	0.831	2.569	-2.431	-0.390	2.462	9.111	1434.632	3410.363
32	127	0.492	9.111	2.431	0.390	2.462	-2.431	0.103	2.433	-2.417	1554.801	3451.455

33	127	0.492	-2.417	2.431	-0.103	2.433	-2.431	0.595	2.503	-13.755	1680.198	3471.567
34	127	0.491	-13.755	2.431	-0.595	2.503	-2.431	1.086	2.662	-24.068	1807.085	3466.212
35	127	0.488	-24.068	2.431	-1.086	2.662	-2.431	1.574	2.896	-32.915	1930.443	3436.016
36	127	0.484	-32.915	2.431	-1.574	2.896	-2.431	2.058	3.185	-40.246	2046.402	3384.223
37	127	0.480	-40.246	2.431	-2.058	3.185	-2.431	2.538	3.515	-46.235	2153.016	3315.212
38	127	0.477	-46.235	2.431	-2.538	3.515	-2.431	3.015	3.873	-51.121	2249.953	3233.161
39	127	0.474	-51.121	2.431	-3.015	3.873	-2.431	3.489	4.252	-55.131	2337.799	3141.444
40	127	0.471	-55.131	2.431	-3.489	4.252	-2.431	3.960	4.646	-58.453	2417.514	3042.578
41	127	0.468	-58.453	2.431	-3.960	4.646	-2.431	4.428	5.052	-61.234	2490.120	2938.379
42	127	0.466	-61.234	2.431	-4.428	5.052	-2.431	4.894	5.465	-63.587	2556.567	2830.149
43	127	0.464	-63.587	2.431	-4.894	5.465	-2.431	5.359	5.884	-65.599	2617.685	2718.822
44	127	0.463	-65.599	2.431	-5.359	5.884	-2.431	5.822	6.309	-67.336	2674.179	2605.080
45	127	0.461	-67.336	2.431	-5.822	6.309	-2.431	6.283	6.737	-68.848	2726.646	2489.424
46	127	0.460	-68.848	2.431	-6.283	6.737	-2.431	6.743	7.168	-70.175	2775.583	2372.231
47	127	0.459	-70.175	2.431	-6.743	7.168	-2.431	7.202	7.601	-71.348	2821.411	2253.788
48	127	0.458	-71.348	2.431	-7.202	7.601	-2.431	7.660	8.036	-72.392	2864.483	2134.315
49	127	0.457	-72.392	2.431	-7.660	8.036	-2.431	8.117	8.473	-73.327	2905.100	2013.985
50	127	0.456	-73.327	2.431	-8.117	8.473	-2.431	8.573	8.911	-74.169	2943.517	1892.935
51	127	0.455	-74.169	2.431	-8.573	8.911	-2.431	9.029	9.350	-74.930	2979.954	1771.274
52	127	0.455	-74.930	2.431	-9.029	9.350	-2.431	9.483	9.790	-75.622	3014.600	1649.091
53	127	0.454	-75.622	2.431	-9.483	9.790	-2.431	9.938	10.231	-76.254	3047.619	1526.459
54	127	0.454	-76.254	2.431	-9.938	10.231	-2.431	10.391	10.672	-76.833	3079.155	1403.436
55	127	0.453	-76.833	2.431	-10.391	10.672	-2.431	10.844	11.114	-77.365	3109.332	1280.074
56	127	0.453	-77.365	2.431	-10.844	11.114	-2.431	11.297	11.556	-77.856	3138.262	1156.413
57	127	0.452	-77.856	2.431	-11.297	11.556	-2.431	11.749	11.998	-78.310	3166.043	1032.489
58	127	0.452	-78.310	2.431	-11.749	11.998	-2.431	12.201	12.441	-78.732	3192.760	908.331
59	127	0.451	-78.732	2.431	-12.201	12.441	-2.431	12.652	12.884	-79.124	3218.492	783.965
60	127	0.451	-79.124	2.431	-12.652	12.884	-2.431	13.104	13.327	-79.490	3243.309	659.413
61	127	0.451	-79.490	2.431	-13.104	13.327	-2.431	13.554	13.771	-79.832	3267.272	534.694
62	127	0.450	-79.832	2.431	-13.554	13.771	-2.431	14.005	14.214	-80.152	3290.438	409.825
63	127	0.450	-80.152	2.431	-14.005	14.214	-2.431	14.455	14.658	-80.453	3312.858	284.820
											3334.578	159.691
											3362.161	0

Segment no.	Height of Segment	DL + LL(F)	Wind Load (Cpi=0)	WL H	WL V	Left Angle	Left Thrust x	Left Thrust y	***Left Thrust***	Right Thrust x	Right Thrust y	***Right Thrust***	Right angle	Co-ordinates	
														X	Y
1	134	0.444	0.046	0.045	0.008	82.500	1.736	13.183	13.296	-1.780	-12.731	12.855	82.038	0	0
2	134	0.444	0.046	0.045	0.008	82.038	1.780	12.731	12.855	-1.825	-12.279	12.414	81.544	17.491	132.854
3	134	0.444	0.046	0.045	0.008	81.544	1.825	12.279	12.414	-1.870	-11.827	11.974	81.013	36.051	265.562
4	134	0.444	0.046	0.045	0.008	81.013	1.870	11.827	11.974	-1.915	-11.374	11.534	80.442	55.755	398.105
5	134	0.445	0.046	0.045	0.009	80.442	1.915	11.374	11.534	-1.960	-10.921	11.095	79.825	76.686	530.461
6	134	0.445	0.046	0.045	0.009	79.825	1.960	10.921	11.095	-2.005	-10.467	10.657	79.158	98.936	662.600
7	134	0.445	0.046	0.045	0.009	79.158	2.005	10.467	10.657	-2.049	-10.013	10.221	78.433	122.607	794.493
8	134	0.445	0.046	0.045	0.010	78.433	2.049	10.013	10.221	-2.094	-9.559	9.785	77.644	147.812	926.101
9	134	0.445	0.046	0.044	0.010	77.644	2.094	9.559	9.785	-2.138	-9.103	9.351	76.781	174.680	1057.380
10	134	0.445	0.046	0.044	0.010	76.781	2.138	9.103	9.351	-2.183	-8.648	8.919	75.834	203.354	1188.276
11	134	0.445	0.046	0.044	0.011	75.834	2.183	8.648	8.919	-2.227	-8.192	8.489	74.791	233.996	1318.726
12	134	0.446	0.046	0.044	0.011	74.791	2.227	8.192	8.489	-2.271	-7.735	8.061	73.636	266.790	1448.651
13	134	0.446	0.046	0.044	0.012	73.636	2.271	7.735	8.061	-2.315	-7.277	7.636	72.351	301.945	1577.957
14	134	0.446	0.046	0.044	0.012	72.351	2.315	7.277	7.636	-2.359	-6.818	7.215	70.915	339.699	1706.529
15	134	0.446	0.046	0.044	0.013	70.915	2.359	6.818	7.215	-2.403	-6.359	6.798	69.301	380.325	1834.222
16	134	0.447	0.046	0.043	0.014	69.301	2.403	6.359	6.798	-2.446	-5.898	6.386	67.476	424.140	1960.856
17	134	0.447	-0.068	-0.065	-0.022	67.476	2.446	5.898	6.386	-2.381	-5.474	5.969	66.487	471.504	2086.206
18	134	0.447	-0.068	-0.064	-0.023	66.487	2.381	5.474	5.969	-2.317	-5.050	5.556	65.351	522.836	2209.984
19	134	0.448	-0.068	-0.064	-0.025	65.351	2.317	5.050	5.556	-2.253	-4.627	5.146	64.033	576.296	2332.859
20	134	0.448	-0.068	-0.063	-0.027	64.033	2.253	4.627	5.146	-2.190	-4.205	4.742	62.487	632.181	2454.649
21	134	0.449	-0.068	-0.062	-0.028	62.487	2.190	4.205	4.742	-2.128	-3.785	4.343	60.654	690.854	2575.121
22	134	0.449	-0.068	-0.061	-0.031	60.654	2.128	3.785	4.343	-2.067	-3.367	3.951	58.451	752.755	2693.966
23	134	0.450	-0.068	-0.060	-0.033	58.451	2.067	3.367	3.951	-2.007	-2.950	3.568	55.768	818.427	2810.770
24	134	0.451	-0.068	-0.058	-0.036	55.768	2.007	2.950	3.568	-1.949	-2.536	3.198	52.449	888.539	2924.964
25	134	0.452	-0.068	-0.056	-0.039	52.449	1.949	2.536	3.198	-1.893	-2.123	2.845	48.279	963.920	3035.751
26	134	0.453	-0.068	-0.053	-0.043	48.279	1.893	2.123	2.845	-1.840	-1.714	2.515	42.966	1045.590	3141.987
27	134	0.454	-0.068	-0.049	-0.047	42.966	1.840	1.714	2.515	-1.791	-1.308	2.217	36.137	1134.768	3242.003
28	134	0.455	-0.068	-0.044	-0.052	36.137	1.791	1.308	2.217	-1.746	-0.905	1.967	27.391	1232.823	3333.333
29	134	0.456	-0.068	-0.038	-0.057	27.391	1.746	0.905	1.967	-1.708	-0.506	1.782	16.495	1341.042	3412.356
30	134	0.457	-0.068	-0.029	-0.062	16.495	1.708	0.506	1.782	-1.679	-0.111	1.683	3.778	1460.019	3474.004
31	134	0.457	-0.068	-0.019	-0.066	3.778	1.679	0.111	1.683	-1.660	0.281	1.684	-9.595	1588.504	3512.051
32	134	0.457	-0.068	-0.006	-0.068	-9.595	1.660	-0.281	1.684	-1.654	0.670	1.785	-22.054	1722.213	3520.881

33	134	0.457	-0.068	0.006	-0.068	-22.054	1.654	-0.670	1.785	-1.660	1.059	1.970	-32.538	1854.338	3498.544
34	134	0.457	-0.068	0.019	-0.066	-32.538	1.660	-1.059	1.970	-1.679	1.450	2.219	-40.819	1978.534	3448.230
35	134	0.456	-0.068	0.029	-0.062	-40.819	1.679	-1.450	2.219	-1.708	1.845	2.514	-47.193	2091.501	3376.158
36	134	0.455	-0.068	0.038	-0.057	-47.193	1.708	-1.845	2.514	-1.746	2.242	2.842	-52.088	2192.909	3288.566
37	134	0.454	-0.068	0.044	-0.052	-52.088	1.746	-2.242	2.842	-1.791	2.644	3.193	-55.890	2283.967	3190.258
38	134	0.453	-0.068	0.049	-0.047	-55.890	1.791	-2.644	3.193	-1.840	3.049	3.561	-58.889	2366.302	3084.537
39	134	0.452	-0.068	0.053	-0.043	-58.889	1.840	-3.049	3.561	-1.893	3.458	3.942	-61.296	2441.447	2973.590
40	134	0.451	-0.068	0.056	-0.039	-61.296	1.893	-3.458	3.942	-1.949	3.869	4.332	-63.260	2510.684	2858.863
41	134	0.450	-0.068	0.058	-0.036	-63.260	1.949	-3.869	4.332	-2.007	4.283	4.730	-64.887	2575.041	2741.329
42	134	0.449	-0.068	0.060	-0.033	-64.887	2.007	-4.283	4.730	-2.067	4.699	5.133	-66.254	2635.333	2621.659
43	134	0.449	-0.068	0.061	-0.031	-66.254	2.067	-4.699	5.133	-2.128	5.117	5.542	-67.415	2692.203	2500.326
44	134	0.448	-0.068	0.062	-0.028	-67.415	2.128	-5.117	5.542	-2.190	5.536	5.954	-68.414	2746.163	2377.671
45	134	0.448	-0.068	0.063	-0.027	-68.414	2.190	-5.536	5.954	-2.253	5.957	6.369	-69.280	2797.626	2253.947
46	134	0.447	-0.068	0.064	-0.025	-69.280	2.253	-5.957	6.369	-2.317	6.380	6.787	-70.039	2846.925	2129.345
47	134	0.447	-0.068	0.064	-0.023	-70.039	2.317	-6.380	6.787	-2.381	6.803	7.208	-70.708	2894.334	2004.012
48	134	0.447	-0.023	0.022	-0.007	-70.708	2.381	-6.803	7.208	-2.403	7.242	7.631	-71.644	2940.080	1878.062
49	134	0.446	-0.023	0.022	-0.007	-71.644	2.403	-7.242	7.631	-2.425	7.682	8.055	-72.482	2984.352	1751.587
50	134	0.446	-0.023	0.022	-0.007	-72.482	2.425	-7.682	8.055	-2.447	8.121	8.482	-73.235	3026.551	1624.405
51	134	0.446	-0.023	0.022	-0.006	-73.235	2.447	-8.121	8.482	-2.468	8.561	8.910	-73.915	3066.886	1496.620
52	134	0.446	-0.023	0.022	-0.006	-73.915	2.468	-8.561	8.910	-2.490	9.000	9.339	-74.533	3105.538	1368.315
53	134	0.445	-0.023	0.022	-0.006	-74.533	2.490	-9.000	9.339	-2.513	9.440	9.769	-75.096	3142.664	1239.561
54	134	0.445	-0.023	0.022	-0.005	-75.096	2.513	-9.440	9.769	-2.535	9.880	10.200	-75.611	3178.400	1110.414
55	134	0.445	-0.023	0.022	-0.005	-75.611	2.535	-9.880	10.200	-2.557	10.320	10.632	-76.084	3212.865	980.922
56	134	0.445	-0.023	0.022	-0.005	-76.084	2.557	-10.320	10.632	-2.579	10.760	11.065	-76.520	3246.164	851.126
57	134	0.445	-0.023	0.022	-0.005	-76.520	2.579	-10.760	11.065	-2.601	11.200	11.498	-76.923	3278.390	721.058
58	134	0.445	-0.023	0.022	-0.005	-76.923	2.601	-11.200	11.498	-2.624	11.640	11.932	-77.297	3309.625	590.750
59	134	0.445	-0.023	0.022	-0.004	-77.297	2.624	-11.640	11.932	-2.646	12.080	12.366	-77.644	3339.943	460.224
60	134	0.444	-0.023	0.022	-0.004	-77.644	2.646	-12.080	12.366	-2.669	12.520	12.801	-77.968	3369.409	329.504
61	134	0.444	-0.023	0.022	-0.004	-77.968	2.669	-12.520	12.801	-2.691	12.960	13.237	-78.270	3398.082	198.608
62	134	0.444	-0.023	0.022	-0.004	-78.270	2.691	-12.960	13.237	-2.713	13.401	13.672	-78.553	3426.015	67.552
63	134	0.444	-0.023	0.022	-0.004	-78.553	2.713	-13.401	13.672	-2.736	13.841	14.109	-78.819	3453.256	-63.650
														3479.849	-194.985

Segment no.	Height of Segment	DL + LL(F)	Wind Load (Cpi=-0.2)	WL H	WL V	Left Angle	Left Thrust x	Left Thrust y	***Left Thrust***	Right Thrust x	Right Thrust y	***Right Thrust***	Right angle	Co-ordinates	
														X	Y
1	132.3	0.444	0.057	0.056	0.009	83.200	1.598	13.401	13.496	-1.654	-12.947	13.052	82.719	0	0
2	132.3	0.444	0.057	0.056	0.010	82.719	1.654	12.947	13.052	-1.710	-12.493	12.610	82.205	15.665	131.369
3	132.3	0.444	0.057	0.056	0.010	82.205	1.710	12.493	12.610	-1.766	-12.039	12.168	81.653	32.431	262.603
4	132.3	0.444	0.057	0.056	0.010	81.653	1.766	12.039	12.168	-1.822	-11.584	11.726	81.059	50.376	393.680
5	132.3	0.445	0.057	0.056	0.011	81.059	1.822	11.584	11.726	-1.878	-11.129	11.286	80.419	69.582	524.578
6	132.3	0.445	0.057	0.056	0.011	80.419	1.878	11.129	11.286	-1.934	-10.673	10.847	79.727	90.144	655.271
7	132.3	0.445	0.057	0.056	0.012	79.727	1.934	10.673	10.847	-1.990	-10.217	10.409	78.977	112.163	785.726
8	132.3	0.445	0.057	0.056	0.012	78.977	1.990	10.217	10.409	-2.046	-9.760	9.972	78.161	135.757	915.905
9	132.3	0.445	0.057	0.056	0.012	78.161	2.046	9.760	9.972	-2.101	-9.302	9.537	77.270	161.053	1045.764
10	132.3	0.445	0.057	0.055	0.013	77.270	2.101	9.302	9.537	-2.157	-8.844	9.103	76.293	188.197	1175.250
11	132.3	0.445	0.057	0.055	0.014	76.293	2.157	8.844	9.103	-2.212	-8.385	8.672	75.219	217.351	1304.297
12	132.3	0.446	0.057	0.055	0.014	75.219	2.212	8.385	8.672	-2.268	-7.925	8.243	74.033	248.699	1432.830
13	132.3	0.446	0.057	0.055	0.015	74.033	2.268	7.925	8.243	-2.323	-7.464	7.817	72.716	282.452	1560.752
14	132.3	0.446	0.057	0.055	0.016	72.716	2.323	7.464	7.817	-2.377	-7.003	7.395	71.248	318.845	1687.948
15	132.3	0.446	0.057	0.055	0.016	71.248	2.377	7.003	7.395	-2.432	-6.540	6.978	69.602	358.152	1814.274
16	132.3	0.447	0.057	0.054	0.017	69.602	2.432	6.540	6.978	-2.486	-6.076	6.565	67.746	400.683	1939.551
17	132.3	0.447	-0.057	-0.054	-0.018	67.746	2.486	6.076	6.565	-2.432	-5.648	6.149	66.699	446.795	2063.555
18	132.3	0.447	-0.057	-0.054	-0.019	66.699	2.432	5.648	6.149	-2.379	-5.220	5.736	65.500	496.898	2186.001
19	132.3	0.448	-0.057	-0.053	-0.021	65.500	2.379	5.220	5.736	-2.326	-4.793	5.327	64.116	549.231	2307.510
20	132.3	0.448	-0.057	-0.053	-0.022	64.116	2.326	4.793	5.327	-2.273	-4.367	4.923	62.501	604.094	2427.899
21	132.3	0.449	-0.057	-0.052	-0.024	62.501	2.273	4.367	4.923	-2.221	-3.942	4.525	60.599	661.850	2546.926
22	132.3	0.449	-0.057	-0.051	-0.026	60.599	2.221	3.942	4.525	-2.170	-3.518	4.134	58.331	722.937	2664.279
23	132.3	0.450	-0.057	-0.050	-0.028	58.331	2.170	3.518	4.134	-2.121	-3.096	3.753	55.593	787.885	2779.539
24	132.3	0.451	-0.057	-0.048	-0.030	55.593	2.121	3.096	3.753	-2.072	-2.676	3.384	52.244	857.344	2892.139
25	132.3	0.452	-0.057	-0.047	-0.033	52.244	2.072	2.676	3.384	-2.025	-2.257	3.032	48.092	932.103	3001.293
26	132.3	0.453	-0.057	-0.044	-0.036	48.092	2.025	2.257	3.032	-1.981	-1.840	2.704	42.887	1013.110	3105.892
27	132.3	0.454	-0.057	-0.041	-0.039	42.887	1.981	1.840	2.704	-1.940	-1.426	2.408	36.318	1101.477	3204.353
28	132.3	0.455	-0.057	-0.037	-0.043	36.318	1.940	1.426	2.408	-1.903	-1.015	2.157	28.064	1198.413	3294.391
29	132.3	0.456	-0.057	-0.032	-0.047	28.064	1.903	1.015	2.157	-1.872	-0.606	1.967	17.947	1305.013	3372.747
30	132.3	0.457	-0.057	-0.024	-0.051	17.947	1.872	0.606	1.967	-1.847	-0.201	1.858	6.206	1421.757	3434.989
31	132.3	0.457	-0.057	-0.016	-0.055	6.206	1.847	0.201	1.858	-1.831	0.202	1.843	-6.285	1547.620	3475.756
32	132.3	0.457	-0.057	-0.005	-0.057	-6.285	1.831	-0.202	1.843	-1.826	0.602	1.923	-18.257	1679.144	3490.057

33	132.3	0.457	-0.057	0.005	-0.057	-18.257	1.826	-0.602	1.923	-1.831	1.003	2.088	-28.708	1810.649	3475.574
34	132.3	0.457	-0.057	0.016	-0.055	-28.708	1.831	-1.003	2.088	-1.847	1.405	2.321	-37.260	1936.289	3434.126
35	132.3	0.456	-0.057	0.024	-0.051	-37.260	1.847	-1.405	2.321	-1.872	1.809	2.603	-44.035	2052.326	3370.575
36	132.3	0.455	-0.057	0.032	-0.047	-44.035	1.872	-1.809	2.603	-1.903	2.217	2.922	-49.355	2157.623	3290.476
37	132.3	0.454	-0.057	0.037	-0.043	-49.355	1.903	-2.217	2.922	-1.940	2.627	3.266	-53.554	2252.736	3198.515
38	132.3	0.453	-0.057	0.041	-0.039	-53.554	1.940	-2.627	3.266	-1.981	3.040	3.629	-56.908	2338.913	3098.131
39	132.3	0.452	-0.057	0.044	-0.036	-56.908	1.981	-3.040	3.629	-2.025	3.456	4.006	-59.625	2417.506	2991.706
40	132.3	0.451	-0.057	0.047	-0.033	-59.625	2.025	-3.456	4.006	-2.072	3.874	4.393	-61.856	2489.740	2880.866
41	132.3	0.450	-0.057	0.048	-0.030	-61.856	2.072	-3.874	4.393	-2.121	4.293	4.789	-63.715	2556.639	2766.726
42	132.3	0.449	-0.057	0.050	-0.028	-63.715	2.121	-4.293	4.789	-2.170	4.715	5.190	-65.283	2619.042	2650.068
43	132.3	0.449	-0.057	0.051	-0.026	-65.283	2.170	-4.715	5.190	-2.221	5.138	5.598	-66.620	2677.629	2531.448
44	132.3	0.448	-0.057	0.052	-0.024	-66.620	2.221	-5.138	5.598	-2.273	5.562	6.009	-67.772	2732.949	2411.269
45	132.3	0.448	-0.057	0.053	-0.022	-67.772	2.273	-5.562	6.009	-2.326	5.988	6.424	-68.774	2785.450	2289.831
46	132.3	0.447	-0.057	0.053	-0.021	-68.774	2.326	-5.988	6.424	-2.379	6.414	6.841	-69.653	2835.498	2167.363
47	132.3	0.447	-0.057	0.054	-0.019	-69.653	2.379	-6.414	6.841	-2.432	6.842	7.261	-70.429	2883.396	2044.038
48	132.3	0.447	-0.011	0.011	-0.004	-70.429	2.432	-6.842	7.261	-2.443	7.285	7.683	-71.460	2929.397	1919.993
49	132.3	0.446	-0.011	0.011	-0.003	-71.460	2.443	-7.285	7.683	-2.454	7.728	8.108	-72.382	2973.713	1795.336
50	132.3	0.446	-0.011	0.011	-0.003	-72.382	2.454	-7.728	8.108	-2.465	8.170	8.534	-73.212	3015.780	1669.902
51	132.3	0.446	-0.011	0.011	-0.003	-73.212	2.465	-8.170	8.534	-2.476	8.613	8.962	-73.963	3055.823	1543.807
52	132.3	0.446	-0.011	0.011	-0.003	-73.963	2.476	-8.613	8.962	-2.487	9.056	9.391	-74.644	3094.035	1417.146
53	132.3	0.445	-0.011	0.011	-0.003	-74.644	2.487	-9.056	9.391	-2.498	9.498	9.821	-75.266	3130.584	1289.995
54	132.3	0.445	-0.011	0.011	-0.003	-75.266	2.498	-9.498	9.821	-2.509	9.941	10.252	-75.835	3165.619	1162.418
55	132.3	0.445	-0.011	0.011	-0.003	-75.835	2.509	-9.941	10.252	-2.520	10.383	10.685	-76.358	3199.268	1034.468
56	132.3	0.445	-0.011	0.011	-0.002	-76.358	2.520	-10.383	10.685	-2.531	10.826	11.118	-76.840	3231.644	906.191
57	132.3	0.445	-0.011	0.011	-0.002	-76.840	2.531	-10.826	11.118	-2.542	11.268	11.551	-77.286	3262.847	777.623
58	132.3	0.445	-0.011	0.011	-0.002	-77.286	2.542	-11.268	11.551	-2.553	11.710	11.986	-77.699	3292.968	648.798
59	132.3	0.445	-0.011	0.011	-0.002	-77.699	2.553	-11.710	11.986	-2.565	12.153	12.420	-78.083	3322.086	519.742
60	132.3	0.444	-0.011	0.011	-0.002	-78.083	2.565	-12.153	12.420	-2.576	12.595	12.856	-78.442	3350.272	390.479
61	132.3	0.444	-0.011	0.011	-0.002	-78.442	2.576	-12.595	12.856	-2.587	13.037	13.291	-78.776	3377.590	261.030
62	132.3	0.444	-0.011	0.011	-0.002	-78.776	2.587	-13.037	13.291	-2.598	13.480	13.728	-79.090	3404.098	131.413
63	132.3	0.444	-0.011	0.011	-0.002	-79.090	2.598	-13.480	13.728	-2.610	13.922	14.164	-79.384	3429.849	1.644
														3454.890	-128.265

Segment no.	Height of Segment	DL + LL(L)	Wind Load (Cpi=0)	WL H	WL V	Left Angle	Left Thrust x	Left Thrust y	***Left Thrust***	Right Thrust x	Right Thrust y	***Right Thrust***	Right angle	Co-ordinates	
														X	Y
1	134.5	0.444	0.046	0.045	0.008	82.600	1.705	13.130	13.240	-1.750	-12.678	12.798	82.140	0	0
2	134.5	0.444	0.046	0.045	0.008	82.140	1.750	12.678	12.798	-1.795	-12.226	12.357	81.647	17.323	133.380
3	134.5	0.444	0.046	0.045	0.008	81.647	1.795	12.226	12.357	-1.840	-11.774	11.917	81.117	35.717	266.616
4	134.5	0.444	0.046	0.045	0.008	81.117	1.840	11.774	11.917	-1.885	-11.321	11.477	80.547	55.256	399.689
5	134.5	0.445	0.046	0.045	0.009	80.547	1.885	11.321	11.477	-1.930	-10.868	11.038	79.932	76.024	532.576
6	134.5	0.445	0.046	0.045	0.009	79.932	1.930	10.868	11.038	-1.974	-10.414	10.600	79.265	98.113	665.250
7	134.5	0.445	0.046	0.045	0.009	79.265	1.974	10.414	10.600	-2.019	-9.960	10.163	78.541	121.627	797.679
8	134.5	0.445	0.046	0.045	0.010	78.541	2.019	9.960	10.163	-2.064	-9.506	9.727	77.752	146.680	929.825
9	134.5	0.445	0.046	0.044	0.010	77.752	2.064	9.506	9.727	-2.108	-9.051	9.293	76.888	173.401	1061.644
10	134.5	0.445	0.046	0.044	0.010	76.888	2.108	9.051	9.293	-2.152	-8.595	8.860	75.940	201.935	1193.082
11	134.5	0.445	0.046	0.044	0.011	75.940	2.152	8.595	8.860	-2.197	-8.139	8.430	74.895	232.447	1324.076
12	134.5	0.446	0.046	0.044	0.011	74.895	2.197	8.139	8.430	-2.241	-7.682	8.002	73.737	265.121	1454.546
13	134.5	0.446	0.046	0.044	0.012	73.737	2.241	7.682	8.002	-2.285	-7.224	7.577	72.448	300.171	1584.399
14	134.5	0.446	0.046	0.044	0.012	72.448	2.285	7.224	7.577	-2.329	-6.766	7.155	71.006	337.838	1713.517
15	134.5	0.446	0.046	0.044	0.013	71.006	2.329	6.766	7.155	-2.372	-6.306	6.738	69.383	378.399	1841.755
16	134.5	0.447	0.046	0.043	0.014	69.383	2.372	6.306	6.738	-2.416	-5.846	6.325	67.545	422.176	1968.932
17	134.5	0.447	-0.068	-0.065	-0.022	67.545	2.416	5.846	6.325	-2.351	-5.421	5.909	66.552	469.537	2094.818
18	134.5	0.447	-0.068	-0.064	-0.023	66.552	2.351	5.421	5.909	-2.287	-4.997	5.495	65.408	520.909	2219.120
19	134.5	0.448	-0.068	-0.064	-0.025	65.408	2.287	4.997	5.495	-2.223	-4.574	5.086	64.079	574.429	2342.513
20	134.5	0.448	-0.068	-0.063	-0.027	64.079	2.223	4.574	5.086	-2.160	-4.153	4.681	62.517	630.402	2464.813
21	134.5	0.449	-0.068	-0.062	-0.028	62.517	2.160	4.153	4.681	-2.098	-3.732	4.282	60.660	689.197	2585.782
22	134.5	0.449	-0.068	-0.061	-0.031	60.660	2.098	3.732	4.282	-2.037	-3.314	3.890	58.424	751.267	2705.103
23	134.5	0.450	-0.068	-0.060	-0.033	58.424	2.037	3.314	3.890	-1.977	-2.897	3.508	55.691	817.171	2822.350
24	134.5	0.451	-0.068	-0.058	-0.036	55.691	1.977	2.897	3.508	-1.919	-2.483	3.138	52.298	887.600	2936.937
25	134.5	0.452	-0.068	-0.056	-0.039	52.298	1.919	2.483	3.138	-1.863	-2.070	2.785	48.020	963.412	3048.035
26	134.5	0.453	-0.068	-0.053	-0.043	48.020	1.863	2.070	2.785	-1.810	-1.661	2.457	42.545	1045.665	3154.452
27	134.5	0.454	-0.068	-0.049	-0.047	42.545	1.810	1.661	2.457	-1.760	-1.255	2.162	35.479	1135.629	3254.436
28	134.5	0.455	-0.068	-0.044	-0.052	35.479	1.760	1.255	2.162	-1.716	-0.852	1.916	26.403	1234.721	3345.381
29	134.5	0.456	-0.068	-0.038	-0.057	26.403	1.716	0.852	1.916	-1.678	-0.453	1.738	15.108	1344.248	3423.445
30	134.5	0.457	-0.068	-0.029	-0.062	15.108	1.678	0.453	1.738	-1.649	-0.058	1.650	2.015	1464.718	3483.256
31	134.5	0.457	-0.068	-0.019	-0.066	2.015	1.649	0.058	1.650	-1.630	0.334	1.664	-11.564	1594.569	3518.311
32	134.5	0.457	-0.068	-0.006	-0.068	-11.564	1.630	-0.334	1.664	-1.624	0.723	1.777	-23.998	1728.986	3523.041

33	134.5	0.441	-0.068	0.006	-0.068	-23.998	1.624	-0.723	1.777	-1.630	1.096	1.964	-33.918	1860.756	3496.077
34	134.5	0.441	-0.068	0.019	-0.066	-33.918	1.630	-1.096	1.964	-1.649	1.472	2.210	-41.753	1983.630	3441.376
35	134.5	0.441	-0.068	0.029	-0.062	-41.753	1.649	-1.472	2.210	-1.678	1.851	2.499	-47.810	2095.242	3366.323
36	134.5	0.441	-0.068	0.038	-0.057	-47.810	1.678	-1.851	2.499	-1.716	2.236	2.819	-52.494	2195.583	3276.758
37	134.5	0.441	-0.068	0.044	-0.052	-52.494	1.716	-2.236	2.819	-1.760	2.625	3.161	-56.155	2285.912	3177.104
38	134.5	0.441	-0.068	0.049	-0.047	-56.155	1.760	-2.625	3.161	-1.810	3.019	3.520	-59.062	2367.802	3070.406
39	134.5	0.441	-0.068	0.053	-0.043	-59.062	1.810	-3.019	3.520	-1.863	3.418	3.892	-61.406	2442.710	2958.697
40	134.5	0.441	-0.068	0.056	-0.039	-61.406	1.863	-3.418	3.892	-1.919	3.820	4.275	-63.327	2511.859	2843.334
41	134.5	0.441	-0.068	0.058	-0.036	-63.327	1.919	-3.820	4.275	-1.977	4.225	4.665	-64.924	2576.231	2725.238
42	134.5	0.441	-0.068	0.060	-0.033	-64.924	1.977	-4.225	4.665	-2.037	4.633	5.061	-66.270	2636.607	2605.051
43	134.5	0.441	-0.068	0.061	-0.031	-66.270	2.037	-4.633	5.061	-2.098	5.044	5.463	-67.417	2693.610	2483.228
44	134.5	0.441	-0.068	0.062	-0.028	-67.417	2.098	-5.044	5.463	-2.160	5.457	5.869	-68.404	2747.736	2360.100
45	134.5	0.441	-0.068	0.063	-0.027	-68.404	2.160	-5.457	5.869	-2.223	5.872	6.279	-69.263	2799.388	2235.913
46	134.5	0.441	-0.068	0.064	-0.025	-69.263	2.223	-5.872	6.279	-2.287	6.289	6.691	-70.016	2848.891	2110.854
47	134.5	0.441	-0.068	0.064	-0.023	-70.016	2.287	-6.289	6.691	-2.351	6.707	7.107	-70.681	2896.515	1985.068
48	134.5	0.441	-0.023	0.022	-0.007	-70.681	2.351	-6.707	7.107	-2.373	7.141	7.525	-71.619	2942.482	1858.666
49	134.5	0.441	-0.023	0.022	-0.007	-71.619	2.373	-7.141	7.525	-2.394	7.575	7.945	-72.459	2986.979	1731.740
50	134.5	0.441	-0.023	0.022	-0.007	-72.459	2.394	-7.575	7.945	-2.416	8.010	8.366	-73.214	3029.391	1604.102
51	134.5	0.441	-0.023	0.022	-0.006	-73.214	2.416	-8.010	8.366	-2.438	8.445	8.790	-73.896	3069.929	1475.857
52	134.5	0.441	-0.023	0.022	-0.006	-73.896	2.438	-8.445	8.790	-2.460	8.881	9.215	-74.516	3108.773	1347.088
53	134.5	0.441	-0.023	0.022	-0.006	-74.516	2.460	-8.881	9.215	-2.482	9.316	9.641	-75.080	3146.081	1217.866
54	134.5	0.441	-0.023	0.022	-0.005	-75.080	2.482	-9.316	9.641	-2.504	9.752	10.069	-75.597	3181.989	1088.248
55	134.5	0.441	-0.023	0.022	-0.005	-75.597	2.504	-9.752	10.069	-2.527	10.189	10.497	-76.072	3216.618	958.282
56	134.5	0.441	-0.023	0.022	-0.005	-76.072	2.527	-10.189	10.497	-2.549	10.625	10.926	-76.510	3250.073	828.009
57	134.5	0.441	-0.023	0.022	-0.005	-76.510	2.549	-10.625	10.926	-2.571	11.062	11.357	-76.915	3282.446	697.463
58	134.5	0.441	-0.023	0.022	-0.005	-76.915	2.571	-11.062	11.357	-2.594	11.498	11.787	-77.290	3313.822	566.674
59	134.5	0.441	-0.023	0.022	-0.004	-77.290	2.594	-11.498	11.787	-2.616	11.935	12.219	-77.638	3344.273	435.667
60	134.5	0.441	-0.023	0.022	-0.004	-77.638	2.616	-11.935	12.219	-2.638	12.373	12.651	-77.963	3373.867	304.463
61	134.5	0.441	-0.023	0.022	-0.004	-77.963	2.638	-12.373	12.651	-2.661	12.810	13.083	-78.266	3402.661	173.081
62	134.5	0.441	-0.023	0.022	-0.004	-78.266	2.661	-12.810	13.083	-2.683	13.247	13.516	-78.550	3430.711	41.538
63	134.5	0.441	-0.023	0.022	-0.004	-78.550	2.683	-13.247	13.516	-2.706	13.685	13.950	-78.816	3458.063	-90.151
														3484.763	-221.974

Segment no.	Height of Segment	DL + LL(L)	Wind Load (Cpi=-0.2)	WL H	WL V	Left Angle	Left Thrust x	Left Thrust y	***Left Thrust***	Right Thrust x	Right Thrust y	***Right Thrust***	Right angle	Co-ordinates	
														X	Y
1	132.4	0.444	0.057	0.056	0.009	83.200	1.592	13.348	13.442	-1.648	-12.894	12.999	82.717	0	0
2	132.4	0.444	0.057	0.056	0.010	82.717	1.648	12.894	12.999	-1.704	-12.440	12.556	82.200	15.677	131.469
3	132.4	0.444	0.057	0.056	0.010	82.200	1.704	12.440	12.556	-1.760	-11.986	12.114	81.646	32.460	262.801
4	132.4	0.444	0.057	0.056	0.010	81.646	1.760	11.986	12.114	-1.816	-11.531	11.673	81.049	50.428	393.976
5	132.4	0.445	0.057	0.056	0.011	81.049	1.816	11.531	11.673	-1.872	-11.076	11.233	80.406	69.665	524.971
6	132.4	0.445	0.057	0.056	0.011	80.406	1.872	11.076	11.233	-1.928	-10.620	10.794	79.710	90.264	655.759
7	132.4	0.445	0.057	0.056	0.012	79.710	1.928	10.620	10.794	-1.984	-10.164	10.356	78.955	112.330	786.307
8	132.4	0.445	0.057	0.056	0.012	78.955	1.984	10.164	10.356	-2.040	-9.707	9.919	78.134	135.981	916.577
9	132.4	0.445	0.057	0.056	0.012	78.134	2.040	9.707	9.919	-2.095	-9.249	9.484	77.236	161.345	1046.525
10	132.4	0.445	0.057	0.055	0.013	77.236	2.095	9.249	9.484	-2.151	-8.791	9.050	76.253	188.570	1176.096
11	132.4	0.445	0.057	0.055	0.014	76.253	2.151	8.791	9.050	-2.206	-8.332	8.619	75.170	217.821	1305.224
12	132.4	0.446	0.057	0.055	0.014	75.170	2.206	8.332	8.619	-2.261	-7.872	8.191	73.974	249.284	1433.831
13	132.4	0.446	0.057	0.055	0.015	73.974	2.261	7.872	8.191	-2.316	-7.412	7.765	72.645	283.172	1561.821
14	132.4	0.446	0.057	0.055	0.016	72.645	2.316	7.412	7.765	-2.371	-6.950	7.343	71.162	319.725	1689.075
15	132.4	0.446	0.057	0.055	0.016	71.162	2.371	6.950	7.343	-2.426	-6.487	6.926	69.498	359.219	1815.448
16	132.4	0.447	0.057	0.054	0.017	69.498	2.426	6.487	6.926	-2.480	-6.023	6.514	67.621	401.970	1940.756
17	132.4	0.447	-0.057	-0.054	-0.018	67.621	2.480	6.023	6.514	-2.426	-5.595	6.098	66.557	448.342	2064.770
18	132.4	0.447	-0.057	-0.054	-0.019	66.557	2.426	5.595	6.098	-2.372	-5.167	5.685	65.337	498.750	2187.198
19	132.4	0.448	-0.057	-0.053	-0.021	65.337	2.372	5.167	5.685	-2.319	-4.740	5.277	63.927	551.423	2308.670
20	132.4	0.448	-0.057	-0.053	-0.022	63.927	2.319	4.740	5.277	-2.267	-4.314	4.873	62.280	606.670	2428.992
21	132.4	0.449	-0.057	-0.052	-0.024	62.280	2.267	4.314	4.873	-2.215	-3.889	4.476	60.337	664.862	2547.918
22	132.4	0.449	-0.057	-0.051	-0.026	60.337	2.215	3.889	4.476	-2.164	-3.465	4.086	58.017	726.448	2665.123
23	132.4	0.450	-0.057	-0.050	-0.028	58.017	2.164	3.465	4.086	-2.114	-3.043	3.706	55.212	791.973	2780.172
24	132.4	0.451	-0.057	-0.048	-0.030	55.212	2.114	3.043	3.706	-2.066	-2.623	3.339	51.774	862.101	2892.474
25	132.4	0.452	-0.057	-0.047	-0.033	51.774	2.066	2.623	3.339	-2.019	-2.204	2.989	47.506	937.641	3001.210
26	132.4	0.453	-0.057	-0.044	-0.036	47.506	2.019	2.204	2.989	-1.975	-1.787	2.664	42.146	1019.566	3105.220
27	132.4	0.454	-0.057	-0.041	-0.039	42.146	1.975	1.787	2.664	-1.934	-1.373	2.372	35.379	1109.005	3202.844
28	132.4	0.455	-0.057	-0.037	-0.043	35.379	1.934	1.373	2.372	-1.897	-0.962	2.127	26.887	1207.171	3291.688
29	132.4	0.456	-0.057	-0.032	-0.047	26.887	1.897	0.962	2.127	-1.865	-0.553	1.946	16.523	1315.122	3368.345
30	132.4	0.457	-0.057	-0.024	-0.051	16.523	1.865	0.553	1.946	-1.841	-0.148	1.847	4.596	1433.209	3428.221
31	132.4	0.457	-0.057	-0.016	-0.055	4.596	1.841	0.148	1.847	-1.825	0.255	1.843	-7.941	1560.142	3465.876
32	132.4	0.457	-0.057	-0.005	-0.057	-7.941	1.825	-0.255	1.843	-1.820	0.655	1.934	-19.801	1692.116	3476.485

33	132.4	0.441	-0.057	0.005	-0.057	-19.801	1.820	-0.655	1.934	-1.825	1.040	2.101	-29.672	1823.247	3458.195
34	132.4	0.441	-0.057	0.016	-0.055	-29.672	1.825	-1.040	2.101	-1.841	1.426	2.329	-37.774	1947.818	3413.343
35	132.4	0.441	-0.057	0.024	-0.051	-37.774	1.841	-1.426	2.329	-1.865	1.816	2.604	-44.241	2062.857	3347.799
36	132.4	0.441	-0.057	0.032	-0.047	-44.241	1.865	-1.816	2.604	-1.897	2.210	2.913	-49.367	2167.510	3266.698
37	132.4	0.441	-0.057	0.037	-0.043	-49.367	1.897	-2.210	2.913	-1.934	2.608	3.247	-53.449	2262.363	3174.326
38	132.4	0.441	-0.057	0.041	-0.039	-53.449	1.934	-2.608	3.247	-1.975	3.010	3.600	-56.735	2348.584	3073.848
39	132.4	0.441	-0.057	0.044	-0.036	-56.735	1.975	-3.010	3.600	-2.019	3.416	3.968	-59.413	2427.433	2967.487
40	132.4	0.441	-0.057	0.047	-0.033	-59.413	2.019	-3.416	3.968	-2.066	3.825	4.347	-61.625	2500.057	2856.783
41	132.4	0.441	-0.057	0.048	-0.030	-61.625	2.066	-3.825	4.347	-2.114	4.236	4.734	-63.476	2567.428	2742.805
42	132.4	0.441	-0.057	0.050	-0.028	-63.476	2.114	-4.236	4.734	-2.164	4.650	5.129	-65.042	2630.350	2626.312
43	132.4	0.441	-0.057	0.051	-0.026	-65.042	2.164	-4.650	5.129	-2.215	5.066	5.529	-66.382	2689.476	2507.848
44	132.4	0.441	-0.057	0.052	-0.024	-66.382	2.215	-5.066	5.529	-2.267	5.483	5.933	-67.540	2745.343	2387.812
45	132.4	0.441	-0.057	0.053	-0.022	-67.540	2.267	-5.483	5.933	-2.319	5.903	6.342	-68.548	2798.387	2266.502
46	132.4	0.441	-0.057	0.053	-0.021	-68.548	2.319	-5.903	6.342	-2.372	6.323	6.754	-69.434	2848.970	2144.145
47	132.4	0.441	-0.057	0.054	-0.019	-69.434	2.372	-6.323	6.754	-2.426	6.745	7.168	-70.218	2897.390	2020.917
48	132.4	0.441	-0.011	0.011	-0.004	-70.218	2.426	-6.745	7.168	-2.437	7.183	7.585	-71.261	2943.900	1896.955
49	132.4	0.441	-0.011	0.011	-0.003	-71.261	2.437	-7.183	7.585	-2.448	7.621	8.004	-72.194	2988.709	1772.368
50	132.4	0.441	-0.011	0.011	-0.003	-72.194	2.448	-7.621	8.004	-2.459	8.059	8.426	-73.035	3031.244	1646.986
51	132.4	0.441	-0.011	0.011	-0.003	-73.035	2.459	-8.059	8.426	-2.470	8.497	8.849	-73.795	3071.731	1520.928
52	132.4	0.441	-0.011	0.011	-0.003	-73.795	2.470	-8.497	8.849	-2.481	8.936	9.274	-74.486	3110.364	1394.290
53	132.4	0.441	-0.011	0.011	-0.003	-74.486	2.481	-8.936	9.274	-2.492	9.374	9.700	-75.116	3147.313	1267.151
54	132.4	0.441	-0.011	0.011	-0.003	-75.116	2.492	-9.374	9.700	-2.503	9.813	10.127	-75.693	3182.728	1139.575
55	132.4	0.441	-0.011	0.011	-0.003	-75.693	2.503	-9.813	10.127	-2.514	10.252	10.556	-76.223	3216.737	1011.617
56	132.4	0.441	-0.011	0.011	-0.002	-76.223	2.514	-10.252	10.556	-2.525	10.691	10.985	-76.712	3249.455	883.324
57	132.4	0.441	-0.011	0.011	-0.002	-76.712	2.525	-10.691	10.985	-2.536	11.130	11.415	-77.164	3280.985	754.733
58	132.4	0.441	-0.011	0.011	-0.002	-77.164	2.536	-11.130	11.415	-2.547	11.569	11.846	-77.583	3311.417	625.878
59	132.4	0.441	-0.011	0.011	-0.002	-77.583	2.547	-11.569	11.846	-2.558	12.008	12.278	-77.973	3340.831	496.786
60	132.4	0.441	-0.011	0.011	-0.002	-77.973	2.558	-12.008	12.278	-2.570	12.447	12.710	-78.336	3369.300	367.483
61	132.4	0.441	-0.011	0.011	-0.002	-78.336	2.570	-12.447	12.710	-2.581	12.887	13.143	-78.676	3396.889	237.989
62	132.4	0.441	-0.011	0.011	-0.002	-78.676	2.581	-12.887	13.143	-2.592	13.326	13.576	-78.993	3423.656	108.323
63	132.4	0.441	-0.011	0.011	-0.002	-78.993	2.592	-13.326	13.576	-2.603	13.766	14.010	-79.291	3449.654	-21.499
														3474.933	-151.463

Segment no.	Height of Segment	DL + LL(R)	Wind Load (Cpi=0)	WL H	WL V	Left Angle	Left Thrust x	Left Thrust y	***Left Thrust***	Right Thrust x	Right Thrust y	***Right Thrust***	Right angle	Co-ordinates	
														X	Y
1	132.7	0.441	0.046	0.045	0.008	82.500	1.717	13.043	13.156	-1.762	-12.594	12.717	82.035	0	0
2	132.7	0.441	0.046	0.045	0.008	82.035	1.762	12.594	12.717	-1.807	-12.145	12.279	81.537	17.321	131.565
3	132.7	0.441	0.046	0.045	0.008	81.537	1.807	12.145	12.279	-1.852	-11.696	11.841	81.002	35.709	262.985
4	132.7	0.441	0.046	0.045	0.008	81.002	1.852	11.696	11.841	-1.897	-11.246	11.405	80.426	55.238	394.240
5	132.7	0.441	0.046	0.045	0.009	80.426	1.897	11.246	11.405	-1.942	-10.796	10.969	79.805	75.992	525.307
6	132.7	0.441	0.046	0.045	0.009	79.805	1.942	10.796	10.969	-1.986	-10.346	10.535	79.132	98.062	656.158
7	132.7	0.441	0.046	0.045	0.009	79.132	1.986	10.346	10.535	-2.031	-9.895	10.101	78.401	121.551	786.763
8	132.7	0.441	0.046	0.045	0.010	78.401	2.031	9.895	10.101	-2.076	-9.444	9.669	77.605	146.571	917.083
9	132.7	0.441	0.046	0.044	0.010	77.605	2.076	9.444	9.669	-2.120	-8.993	9.239	76.735	173.252	1047.073
10	132.7	0.441	0.046	0.044	0.010	76.735	2.120	8.993	9.239	-2.164	-8.541	8.811	75.779	201.736	1176.680
11	132.7	0.441	0.046	0.044	0.011	75.779	2.164	8.541	8.811	-2.209	-8.089	8.385	74.727	232.185	1305.839
12	132.7	0.441	0.046	0.044	0.011	74.727	2.209	8.089	8.385	-2.253	-7.636	7.961	73.562	264.784	1434.473
13	132.7	0.441	0.046	0.044	0.012	73.562	2.253	7.636	7.961	-2.297	-7.182	7.541	72.266	299.740	1562.486
14	132.7	0.441	0.046	0.044	0.012	72.266	2.297	7.182	7.541	-2.341	-6.729	7.124	70.818	337.292	1689.762
15	132.7	0.441	0.046	0.044	0.013	70.818	2.341	6.729	7.124	-2.384	-6.274	6.712	69.191	377.712	1816.156
16	132.7	0.441	0.046	0.043	0.014	69.191	2.384	6.274	6.712	-2.428	-5.819	6.305	67.352	421.313	1941.489
17	132.7	0.441	-0.068	-0.065	-0.022	67.352	2.428	5.819	6.305	-2.363	-5.399	5.894	66.362	468.456	2065.532
18	132.7	0.441	-0.068	-0.064	-0.023	66.362	2.363	5.399	5.894	-2.299	-4.981	5.486	65.227	519.556	2187.999
19	132.7	0.441	-0.068	-0.064	-0.025	65.227	2.299	4.981	5.486	-2.235	-4.565	5.082	63.911	572.762	2309.566
20	132.7	0.441	-0.068	-0.063	-0.027	63.911	2.235	4.565	5.082	-2.172	-4.150	4.684	62.372	628.367	2430.054
21	132.7	0.441	-0.068	-0.062	-0.028	62.372	2.172	4.150	4.684	-2.110	-3.737	4.291	60.550	686.723	2549.233
22	132.7	0.441	-0.068	-0.061	-0.031	60.550	2.110	3.737	4.291	-2.049	-3.326	3.907	58.369	748.261	2666.802
23	132.7	0.441	-0.068	-0.060	-0.033	58.369	2.049	3.326	3.907	-1.989	-2.918	3.531	55.720	813.504	2782.356
24	132.7	0.441	-0.068	-0.058	-0.036	55.720	1.989	2.918	3.531	-1.931	-2.513	3.169	52.458	883.099	2895.342
25	132.7	0.441	-0.068	-0.056	-0.039	52.458	1.931	2.513	3.169	-1.875	-2.110	2.823	48.383	957.841	3004.991
26	132.7	0.441	-0.068	-0.053	-0.043	48.383	1.875	2.110	2.823	-1.822	-1.712	2.500	43.222	1038.700	3110.210
27	132.7	0.441	-0.068	-0.049	-0.047	43.222	1.822	1.712	2.500	-1.772	-1.318	2.209	36.636	1126.833	3209.416
28	132.7	0.441	-0.068	-0.044	-0.052	36.636	1.772	1.318	2.209	-1.728	-0.929	1.962	28.253	1223.532	3300.293
29	132.7	0.441	-0.068	-0.038	-0.057	28.253	1.728	0.929	1.962	-1.690	-0.544	1.776	17.846	1330.016	3379.479
30	132.7	0.441	-0.068	-0.029	-0.062	17.846	1.690	0.544	1.776	-1.661	-0.165	1.669	5.657	1446.907	3442.295
31	132.7	0.441	-0.068	-0.019	-0.066	5.657	1.661	0.165	1.669	-1.642	0.211	1.656	-7.326	1573.222	3482.962
32	132.7	0.457	-0.068	-0.006	-0.068	-7.326	1.642	-0.211	1.656	-1.636	0.600	1.742	-20.157	1705.276	3496.044

33	132.7	0.457	-0.068	0.006	-0.068	-20.157	1.636	-0.600	1.742	-1.642	0.990	1.917	-31.077	1836.892	3479.123
34	132.7	0.457	-0.068	0.019	-0.066	-31.077	1.642	-0.990	1.917	-1.661	1.381	2.160	-39.738	1961.465	3433.397
35	132.7	0.456	-0.068	0.029	-0.062	-39.738	1.661	-1.381	2.160	-1.690	1.775	2.451	-46.400	2075.120	3364.899
36	132.7	0.455	-0.068	0.038	-0.057	-46.400	1.690	-1.775	2.451	-1.728	2.173	2.776	-51.503	2177.162	3280.066
37	132.7	0.454	-0.068	0.044	-0.052	-51.503	1.728	-2.173	2.776	-1.772	2.574	3.125	-55.452	2268.674	3183.968
38	132.7	0.453	-0.068	0.049	-0.047	-55.452	1.772	-2.574	3.125	-1.822	2.979	3.492	-58.556	2351.276	3080.111
39	132.7	0.452	-0.068	0.053	-0.043	-58.556	1.822	-2.979	3.492	-1.875	3.388	3.872	-61.039	2426.529	2970.812
40	132.7	0.451	-0.068	0.056	-0.039	-61.039	1.875	-3.388	3.872	-1.931	3.799	4.262	-63.059	2495.754	2857.599
41	132.7	0.450	-0.068	0.058	-0.036	-63.059	1.931	-3.799	4.262	-1.989	4.213	4.659	-64.728	2560.009	2741.493
42	132.7	0.449	-0.068	0.060	-0.033	-64.728	1.989	-4.213	4.659	-2.049	4.629	5.062	-66.126	2620.132	2623.195
43	132.7	0.449	-0.068	0.061	-0.031	-66.126	2.049	-4.629	5.062	-2.110	5.047	5.470	-67.312	2676.784	2503.196
44	132.7	0.448	-0.068	0.062	-0.028	-67.312	2.110	-5.047	5.470	-2.172	5.467	5.882	-68.330	2730.491	2381.850
45	132.7	0.448	-0.068	0.063	-0.027	-68.330	2.172	-5.467	5.882	-2.235	5.888	6.298	-69.212	2781.675	2259.418
46	132.7	0.447	-0.068	0.064	-0.025	-69.212	2.235	-5.888	6.298	-2.299	6.310	6.716	-69.983	2830.676	2136.096
47	132.7	0.447	-0.068	0.064	-0.023	-69.983	2.299	-6.310	6.716	-2.363	6.733	7.136	-70.662	2877.773	2012.035
48	132.7	0.447	-0.023	0.022	-0.007	-70.662	2.363	-6.733	7.136	-2.385	7.173	7.559	-71.610	2923.197	1887.352
49	132.7	0.446	-0.023	0.022	-0.007	-71.610	2.385	-7.173	7.559	-2.406	7.612	7.983	-72.457	2967.140	1762.139
50	132.7	0.446	-0.023	0.022	-0.007	-72.457	2.406	-7.612	7.983	-2.428	8.052	8.410	-73.218	3009.005	1636.216
51	132.7	0.446	-0.023	0.022	-0.006	-73.218	2.428	-8.052	8.410	-2.450	8.491	8.838	-73.904	3049.004	1509.688
52	132.7	0.446	-0.023	0.022	-0.006	-73.904	2.450	-8.491	8.838	-2.472	8.931	9.267	-74.527	3087.320	1382.640
53	132.7	0.445	-0.023	0.022	-0.006	-74.527	2.472	-8.931	9.267	-2.494	9.371	9.697	-75.095	3124.110	1255.141
54	132.7	0.445	-0.023	0.022	-0.005	-75.095	2.494	-9.371	9.697	-2.516	9.810	10.128	-75.614	3159.511	1127.251
55	132.7	0.445	-0.023	0.022	-0.005	-75.614	2.516	-9.810	10.128	-2.539	10.250	10.560	-76.090	3193.645	999.016
56	132.7	0.445	-0.023	0.022	-0.005	-76.090	2.539	-10.250	10.560	-2.561	10.690	10.993	-76.529	3226.616	870.477
57	132.7	0.445	-0.023	0.022	-0.005	-76.529	2.561	-10.690	10.993	-2.583	11.130	11.426	-76.934	3258.516	741.669
58	132.7	0.445	-0.023	0.022	-0.005	-76.934	2.583	-11.130	11.426	-2.605	11.570	11.860	-77.310	3289.430	612.620
59	132.7	0.445	-0.023	0.022	-0.004	-77.310	2.605	-11.570	11.860	-2.628	12.010	12.294	-77.658	3319.430	483.355
60	132.7	0.444	-0.023	0.022	-0.004	-77.658	2.628	-12.010	12.294	-2.650	12.450	12.729	-77.983	3348.582	353.897
61	132.7	0.444	-0.023	0.022	-0.004	-77.983	2.650	-12.450	12.729	-2.673	12.891	13.165	-78.287	3376.945	224.264
62	132.7	0.444	-0.023	0.022	-0.004	-78.287	2.673	-12.891	13.165	-2.695	13.331	13.601	-78.571	3404.573	94.471
63	132.7	0.444	-0.023	0.022	-0.004	-78.571	2.695	-13.331	13.601	-2.718	13.771	14.037	-78.837	3431.512	-35.465
														3457.808	-165.534

Segment no.	Height of Segment	DL + LL(R)	Wind Load (Cpi=-0.2)	WL H	WL V	Left Angle	Left Thrust x	Left Thrust y	***Left Thrust***	Right Thrust x	Right Thrust y	***Right Thrust***	Right angle	Co-ordinates	
														X	Y
1	133	0.441	0.057	0.056	0.009	83.300	1.556	13.242	13.333	-1.612	-12.791	12.892	82.818	0	0
2	133	0.441	0.057	0.056	0.010	82.818	1.612	12.791	12.892	-1.668	-12.340	12.452	82.302	15.517	132.092
3	133	0.441	0.057	0.056	0.010	82.302	1.668	12.340	12.452	-1.724	-11.889	12.013	81.749	32.145	264.048
4	133	0.441	0.057	0.056	0.010	81.749	1.724	11.889	12.013	-1.780	-11.437	11.575	81.153	49.960	395.850
5	133	0.441	0.057	0.056	0.011	81.153	1.780	11.437	11.575	-1.836	-10.985	11.137	80.511	69.048	527.473
6	133	0.441	0.057	0.056	0.011	80.511	1.836	10.985	11.137	-1.892	-10.532	10.701	79.816	89.502	658.890
7	133	0.441	0.057	0.056	0.012	79.816	1.892	10.532	10.701	-1.948	-10.079	10.266	79.062	111.429	790.071
8	133	0.441	0.057	0.056	0.012	79.062	1.948	10.079	10.266	-2.004	-9.626	9.832	78.242	134.945	920.975
9	133	0.441	0.057	0.056	0.012	78.242	2.004	9.626	9.832	-2.059	-9.172	9.400	77.347	160.180	1051.559
10	133	0.441	0.057	0.055	0.013	77.347	2.059	9.172	9.400	-2.115	-8.717	8.970	76.365	187.282	1181.768
11	133	0.441	0.057	0.055	0.014	76.365	2.115	8.717	8.970	-2.170	-8.262	8.543	75.285	216.417	1311.538
12	133	0.441	0.057	0.055	0.014	75.285	2.170	8.262	8.543	-2.225	-7.807	8.118	74.091	247.770	1440.790
13	133	0.441	0.057	0.055	0.015	74.091	2.225	7.807	8.118	-2.280	-7.351	7.696	72.766	281.554	1569.427
14	133	0.441	0.057	0.055	0.016	72.766	2.280	7.351	7.696	-2.335	-6.894	7.278	71.287	318.012	1697.333
15	133	0.441	0.057	0.055	0.016	71.287	2.335	6.894	7.278	-2.390	-6.436	6.865	69.630	357.417	1824.361
16	133	0.441	0.057	0.054	0.017	69.630	2.390	6.436	6.865	-2.444	-5.977	6.457	67.761	400.087	1950.331
17	133	0.441	-0.057	-0.054	-0.018	67.761	2.444	5.977	6.457	-2.390	-5.554	6.046	66.717	446.382	2075.013
18	133	0.441	-0.057	-0.054	-0.019	66.717	2.390	5.554	6.046	-2.336	-5.132	5.639	65.522	496.720	2198.120
19	133	0.441	-0.057	-0.053	-0.021	65.522	2.336	5.132	5.639	-2.283	-4.711	5.235	64.143	549.292	2320.288
20	133	0.441	-0.057	-0.053	-0.022	64.143	2.283	4.711	5.235	-2.231	-4.292	4.837	62.536	604.400	2441.334
21	133	0.441	-0.057	-0.052	-0.024	62.536	2.231	4.292	4.837	-2.179	-3.874	4.445	60.646	662.406	2561.018
22	133	0.441	-0.057	-0.051	-0.026	60.646	2.179	3.874	4.445	-2.128	-3.458	4.061	58.395	723.744	2679.030
23	133	0.441	-0.057	-0.050	-0.028	58.395	2.128	3.458	4.061	-2.078	-3.045	3.686	55.683	788.942	2794.953
24	133	0.441	-0.057	-0.048	-0.030	55.683	2.078	3.045	3.686	-2.030	-2.633	3.325	52.374	858.642	2908.226
25	133	0.441	-0.057	-0.047	-0.033	52.374	2.030	2.633	3.325	-1.983	-2.225	2.980	48.284	933.623	3018.076
26	133	0.441	-0.057	-0.044	-0.036	48.284	1.983	2.225	2.980	-1.939	-1.819	2.659	43.174	1014.820	3123.414
27	133	0.441	-0.057	-0.041	-0.039	43.174	1.939	1.819	2.659	-1.898	-1.417	2.368	36.750	1103.323	3222.692
28	133	0.441	-0.057	-0.037	-0.043	36.750	1.898	1.417	2.368	-1.861	-1.019	2.121	28.707	1200.317	3313.693
29	133	0.441	-0.057	-0.032	-0.047	28.707	1.861	1.019	2.121	-1.829	-0.625	1.933	18.866	1306.884	3393.269
30	133	0.441	-0.057	-0.024	-0.051	18.866	1.829	0.625	1.933	-1.805	-0.235	1.820	7.422	1423.537	3457.153
31	133	0.441	-0.057	-0.016	-0.055	7.422	1.805	0.235	1.820	-1.789	0.151	1.796	-4.840	1549.392	3500.158
32	133	0.457	-0.057	-0.005	-0.057	-4.840	1.789	-0.151	1.796	-1.784	0.552	1.867	-17.199	1681.278	3517.339

33	133	0.457	-0.057	0.005	-0.057	-17.199	1.784	-0.552	1.867	-1.789	0.953	2.027	-28.037	1813.804	3506.118
34	133	0.457	-0.057	0.016	-0.055	-28.037	1.789	-0.953	2.027	-1.805	1.355	2.257	-36.895	1940.856	3466.791
35	133	0.456	-0.057	0.024	-0.051	-36.895	1.805	-1.355	2.257	-1.829	1.759	2.538	-43.883	2058.249	3404.276
36	133	0.455	-0.057	0.032	-0.047	-43.883	1.829	-1.759	2.538	-1.861	2.166	2.856	-49.342	2164.614	3324.430
37	133	0.454	-0.057	0.037	-0.043	-49.342	1.861	-2.166	2.856	-1.898	2.577	3.200	-53.629	2260.475	3232.236
38	133	0.453	-0.057	0.041	-0.039	-53.629	1.898	-2.577	3.200	-1.939	2.990	3.563	-57.037	2347.129	3131.340
39	133	0.452	-0.057	0.044	-0.036	-57.037	1.939	-2.990	3.563	-1.983	3.405	3.941	-59.786	2425.999	3024.249
40	133	0.451	-0.057	0.047	-0.033	-59.786	1.983	-3.405	3.941	-2.030	3.823	4.329	-62.037	2498.363	2912.658
41	133	0.450	-0.057	0.048	-0.030	-62.037	2.030	-3.823	4.329	-2.078	4.243	4.725	-63.906	2565.293	2797.726
42	133	0.449	-0.057	0.050	-0.028	-63.906	2.078	-4.243	4.725	-2.128	4.665	5.127	-65.478	2627.657	2680.254
43	133	0.449	-0.057	0.051	-0.026	-65.478	2.128	-4.665	5.127	-2.179	5.088	5.535	-66.816	2686.158	2560.811
44	133	0.448	-0.057	0.052	-0.024	-66.816	2.179	-5.088	5.535	-2.231	5.512	5.946	-67.966	2741.359	2439.807
45	133	0.448	-0.057	0.053	-0.022	-67.966	2.231	-5.512	5.946	-2.283	5.938	6.361	-68.966	2793.720	2317.548
46	133	0.447	-0.057	0.053	-0.021	-68.966	2.283	-5.938	6.361	-2.336	6.364	6.779	-69.841	2843.615	2194.262
47	133	0.447	-0.057	0.054	-0.019	-69.841	2.336	-6.364	6.779	-2.390	6.791	7.200	-70.613	2891.352	2070.124
48	133	0.447	-0.011	0.011	-0.004	-70.613	2.390	-6.791	7.200	-2.401	7.234	7.622	-71.642	2937.188	1945.272
49	133	0.446	-0.011	0.011	-0.003	-71.642	2.401	-7.234	7.622	-2.412	7.677	8.047	-72.561	2981.337	1819.813
50	133	0.446	-0.011	0.011	-0.003	-72.561	2.412	-7.677	8.047	-2.423	8.120	8.474	-73.388	3023.226	1693.582
51	133	0.446	-0.011	0.011	-0.003	-73.388	2.423	-8.120	8.474	-2.433	8.563	8.902	-74.135	3063.084	1566.695
52	133	0.446	-0.011	0.011	-0.003	-74.135	2.433	-8.563	8.902	-2.444	9.005	9.331	-74.813	3101.107	1439.246
53	133	0.445	-0.011	0.011	-0.003	-74.813	2.444	-9.005	9.331	-2.456	9.448	9.762	-75.431	3137.465	1311.312
54	133	0.445	-0.011	0.011	-0.003	-75.431	2.456	-9.448	9.762	-2.467	9.890	10.193	-75.997	3172.307	1182.957
55	133	0.445	-0.011	0.011	-0.003	-75.997	2.467	-9.890	10.193	-2.478	10.333	10.626	-76.516	3205.762	1054.233
56	133	0.445	-0.011	0.011	-0.002	-76.516	2.478	-10.333	10.626	-2.489	10.775	11.059	-76.994	3237.946	925.186
57	133	0.445	-0.011	0.011	-0.002	-76.994	2.489	-10.775	11.059	-2.500	11.218	11.493	-77.437	3268.958	795.852
58	133	0.445	-0.011	0.011	-0.002	-77.437	2.500	-11.218	11.493	-2.511	11.660	11.927	-77.846	3298.890	666.264
59	133	0.445	-0.011	0.011	-0.002	-77.846	2.511	-11.660	11.927	-2.522	12.102	12.362	-78.227	3327.820	536.449
60	133	0.444	-0.011	0.011	-0.002	-78.227	2.522	-12.102	12.362	-2.533	12.545	12.798	-78.582	3355.821	406.430
61	133	0.444	-0.011	0.011	-0.002	-78.582	2.533	-12.545	12.798	-2.545	12.987	13.234	-78.914	3382.956	276.227
62	133	0.444	-0.011	0.011	-0.002	-78.914	2.545	-12.987	13.234	-2.556	13.429	13.670	-79.224	3409.285	145.859
63	133	0.444	-0.011	0.011	-0.002	-79.224	2.556	-13.429	13.670	-2.567	13.871	14.107	-79.515	3434.859	15.341
														3459.726	-115.313

Segment no.	Height of Segment	DL per block	Wind Load (Cpi=0)	WL H	WL V	Left Angle	Left Thrust x	Left Thrust y	***Left Thrust***	Right Thrust x	Right Thrust y	***Right Thrust***	Right angle	Co-ordinates	
														X	Y
1	136.3	0.331	0.046	0.045	0.008	83.300	1.115	9.495	9.560	-1.160	-9.156	9.230	82.777	0	0
2	136.3	0.331	0.046	0.045	0.008	82.777	1.160	9.156	9.230	-1.205	-8.817	8.899	82.216	15.902	135.369
3	136.3	0.331	0.046	0.045	0.008	82.216	1.205	8.817	8.899	-1.250	-8.478	8.570	81.612	33.038	270.588
4	136.3	0.331	0.046	0.045	0.008	81.612	1.250	8.478	8.570	-1.295	-8.139	8.241	80.959	51.498	405.632
5	136.3	0.331	0.046	0.045	0.009	80.959	1.295	8.139	8.241	-1.340	-7.799	7.914	80.253	71.381	540.474
6	136.3	0.331	0.046	0.045	0.009	80.253	1.340	7.799	7.914	-1.385	-7.459	7.587	79.485	92.799	675.081
7	136.3	0.331	0.046	0.045	0.009	79.485	1.385	7.459	7.587	-1.429	-7.119	7.261	78.649	115.875	809.413
8	136.3	0.331	0.046	0.045	0.010	78.649	1.429	7.119	7.261	-1.474	-6.778	6.937	77.734	140.748	943.424
9	136.3	0.331	0.046	0.044	0.010	77.734	1.474	6.778	6.937	-1.518	-6.437	6.614	76.729	167.576	1077.058
10	136.3	0.331	0.046	0.044	0.010	76.729	1.518	6.437	6.614	-1.563	-6.096	6.293	75.622	196.533	1210.246
11	136.3	0.331	0.046	0.044	0.011	75.622	1.563	6.096	6.293	-1.607	-5.754	5.974	74.397	227.821	1342.907
12	136.3	0.331	0.046	0.044	0.011	74.397	1.607	5.754	5.974	-1.651	-5.412	5.658	73.033	261.666	1474.938
13	136.3	0.331	0.046	0.044	0.012	73.033	1.651	5.412	5.658	-1.695	-5.069	5.345	71.508	298.327	1606.215
14	136.3	0.331	0.046	0.044	0.012	71.508	1.695	5.069	5.345	-1.739	-4.725	5.035	69.795	338.103	1736.582
15	136.3	0.331	0.046	0.044	0.013	69.795	1.739	4.725	5.035	-1.783	-4.381	4.730	67.858	381.332	1865.845
16	136.3	0.331	0.046	0.043	0.014	67.858	1.783	4.381	4.730	-1.826	-4.036	4.430	65.656	428.408	1993.757
17	136.3	0.331	-0.068	-0.065	-0.022	65.656	1.826	4.036	4.430	-1.761	-3.727	4.122	64.705	479.779	2120.005
18	136.3	0.331	-0.068	-0.064	-0.023	64.705	1.761	3.727	4.122	-1.697	-3.419	3.817	63.604	535.965	2244.186
19	136.3	0.331	-0.068	-0.064	-0.025	63.604	1.697	3.419	3.817	-1.633	-3.113	3.515	62.315	594.204	2367.418
20	136.3	0.331	-0.068	-0.063	-0.027	62.315	1.633	3.113	3.515	-1.570	-2.808	3.218	60.789	654.800	2489.507
21	136.3	0.331	-0.068	-0.062	-0.028	60.789	1.570	2.808	3.218	-1.508	-2.506	2.925	58.960	718.126	2610.203
22	136.3	0.331	-0.068	-0.061	-0.031	58.960	1.508	2.506	2.925	-1.447	-2.206	2.638	56.732	784.643	2729.170
23	136.3	0.331	-0.068	-0.060	-0.033	56.732	1.447	2.206	2.638	-1.387	-1.908	2.359	53.977	854.925	2845.952
24	136.3	0.331	-0.068	-0.058	-0.036	53.977	1.387	1.908	2.359	-1.329	-1.613	2.090	50.506	929.693	2959.915
25	136.3	0.331	-0.068	-0.056	-0.039	50.506	1.329	1.613	2.090	-1.273	-1.321	1.835	46.056	1009.853	3070.151
26	136.3	0.331	-0.068	-0.053	-0.043	46.056	1.273	1.321	1.835	-1.220	-1.033	1.599	40.253	1096.539	3175.333
27	136.3	0.331	-0.068	-0.049	-0.047	40.253	1.220	1.033	1.599	-1.171	-0.749	1.390	32.619	1191.126	3273.470
28	136.3	0.331	-0.068	-0.044	-0.052	32.619	1.171	0.749	1.390	-1.126	-0.470	1.220	22.657	1295.150	3361.543
29	136.3	0.331	-0.068	-0.038	-0.057	22.657	1.126	0.470	1.220	-1.088	-0.196	1.106	10.210	1409.952	3435.015
30	136.3	0.331	-0.068	-0.029	-0.062	10.210	1.088	0.196	1.106	-1.059	0.073	1.062	-3.956	1535.733	3487.520
31	136.3	0.331	-0.068	-0.019	-0.066	-3.956	1.059	-0.073	1.062	-1.040	0.339	1.094	-18.025	1669.875	3511.680
32	136.3	0.331	-0.068	-0.006	-0.068	-18.025	1.040	-0.339	1.094	-1.034	0.602	1.196	-30.191	1805.850	3502.276

33	136.3	0.331	-0.068	0.006	-0.068	-30.191	1.034	-0.602	1.196	-1.040	0.864	1.353	-39.726	1935.460	3460.099
34	136.3	0.331	-0.068	0.019	-0.066	-39.726	1.040	-0.864	1.353	-1.059	1.130	1.549	-46.851	2053.272	3391.556
35	136.3	0.331	-0.068	0.029	-0.062	-46.851	1.059	-1.130	1.549	-1.088	1.399	1.773	-52.120	2158.102	3304.445
36	136.3	0.331	-0.068	0.038	-0.057	-52.120	1.088	-1.399	1.773	-1.126	1.673	2.017	-56.055	2251.318	3205.004
37	136.3	0.331	-0.068	0.044	-0.052	-56.055	1.126	-1.673	2.017	-1.171	1.952	2.276	-59.052	2335.008	3097.423
38	136.3	0.331	-0.068	0.049	-0.047	-59.052	1.171	-1.952	2.276	-1.220	2.236	2.547	-61.382	2411.117	2984.352
39	136.3	0.331	-0.068	0.053	-0.043	-61.382	1.220	-2.236	2.547	-1.273	2.524	2.827	-63.233	2481.211	2867.457
40	136.3	0.331	-0.068	0.056	-0.039	-63.233	1.273	-2.524	2.827	-1.329	2.816	3.114	-64.732	2546.494	2747.808
41	136.3	0.331	-0.068	0.058	-0.036	-64.732	1.329	-2.816	3.114	-1.387	3.111	3.406	-65.966	2607.879	2626.113
42	136.3	0.331	-0.068	0.060	-0.033	-65.966	1.387	-3.111	3.406	-1.447	3.409	3.703	-66.998	2666.060	2502.855
43	136.3	0.331	-0.068	0.061	-0.031	-66.998	1.447	-3.409	3.703	-1.508	3.709	4.004	-67.873	2721.572	2378.372
44	136.3	0.331	-0.068	0.062	-0.028	-67.873	1.508	-3.709	4.004	-1.570	4.011	4.308	-68.622	2774.833	2252.909
45	136.3	0.331	-0.068	0.063	-0.027	-68.622	1.570	-4.011	4.308	-1.633	4.316	4.615	-69.272	2826.173	2126.648
46	136.3	0.331	-0.068	0.064	-0.025	-69.272	1.633	-4.316	4.615	-1.697	4.622	4.924	-69.839	2875.857	1999.725
47	136.3	0.331	-0.068	0.064	-0.023	-69.839	1.697	-4.622	4.924	-1.761	4.930	5.235	-70.340	2924.098	1872.248
48	136.3	0.331	-0.023	0.022	-0.007	-70.340	1.761	-4.930	5.235	-1.783	5.254	5.548	-71.255	2971.074	1744.299
49	136.3	0.331	-0.023	0.022	-0.007	-71.255	1.783	-5.254	5.548	-1.805	5.578	5.862	-72.072	3016.931	1615.945
50	136.3	0.331	-0.023	0.022	-0.007	-72.072	1.805	-5.578	5.862	-1.826	5.902	6.178	-72.805	3060.733	1486.875
51	136.3	0.331	-0.023	0.022	-0.006	-72.805	1.826	-5.902	6.178	-1.848	6.227	6.496	-73.468	3102.690	1357.193
52	136.3	0.331	-0.023	0.022	-0.006	-73.468	1.848	-6.227	6.496	-1.870	6.552	6.814	-74.068	3142.982	1226.985
53	136.3	0.331	-0.023	0.022	-0.006	-74.068	1.870	-6.552	6.814	-1.892	6.878	7.133	-74.615	3181.767	1096.319
54	136.3	0.331	-0.023	0.022	-0.005	-74.615	1.892	-6.878	7.133	-1.915	7.203	7.453	-75.115	3219.181	965.255
55	136.3	0.331	-0.023	0.022	-0.005	-75.115	1.915	-7.203	7.453	-1.937	7.529	7.774	-75.574	3255.341	833.839
56	136.3	0.331	-0.023	0.022	-0.005	-75.574	1.937	-7.529	7.774	-1.959	7.855	8.096	-75.996	3290.354	702.113
57	136.3	0.331	-0.023	0.022	-0.005	-75.996	1.959	-7.855	8.096	-1.981	8.181	8.418	-76.387	3324.310	570.110
58	136.3	0.331	-0.023	0.022	-0.005	-76.387	1.981	-8.181	8.418	-2.004	8.508	8.741	-76.748	3357.293	437.861
59	136.3	0.331	-0.023	0.022	-0.004	-76.748	2.004	-8.508	8.741	-2.026	8.834	9.064	-77.084	3389.374	305.390
60	136.3	0.331	-0.023	0.022	-0.004	-77.084	2.026	-8.834	9.064	-2.048	9.161	9.387	-77.396	3420.618	172.720
61	136.3	0.331	-0.023	0.022	-0.004	-77.396	2.048	-9.161	9.387	-2.071	9.488	9.712	-77.688	3451.085	39.869
62	136.3	0.331	-0.023	0.022	-0.004	-77.688	2.071	-9.488	9.712	-2.093	9.815	10.036	-77.961	3480.826	-93.147
63	136.3	0.331	-0.023	0.022	-0.004	-77.961	2.093	-9.815	10.036	-2.116	10.142	10.361	-78.217	3509.890	-226.312
														3538.319	-359.615

Segment no.	Height of Segment	DL per block	Wind Load (Cpi=-0.2)	WL H	WL V	Left Angle	Left Thrust x	Left Thrust y	***Left Thrust***	Right Thrust x	Right Thrust y	***Right Thrust***	Right angle	Co-ordinates	
														X	Y
1	134	0.331	0.057	0.056	0.009	84.300	0.969	9.713	9.761	-1.026	-9.372	9.428	83.755	0	0
2	134	0.331	0.057	0.056	0.010	83.755	1.026	9.372	9.428	-1.082	-9.032	9.096	83.169	13.309	133.337
3	134	0.331	0.057	0.056	0.010	83.169	1.082	9.032	9.096	-1.138	-8.691	8.765	82.540	27.886	266.542
4	134	0.331	0.057	0.056	0.010	82.540	1.138	8.691	8.765	-1.194	-8.349	8.434	81.861	43.824	399.591
5	134	0.331	0.057	0.056	0.011	81.861	1.194	8.349	8.434	-1.250	-8.007	8.104	81.127	61.221	532.457
6	134	0.331	0.057	0.056	0.011	81.127	1.250	8.007	8.104	-1.306	-7.665	7.776	80.332	80.192	665.107
7	134	0.331	0.057	0.056	0.012	80.332	1.306	7.665	7.776	-1.362	-7.323	7.448	79.466	100.859	797.504
8	134	0.331	0.057	0.056	0.012	79.466	1.362	7.323	7.448	-1.417	-6.980	7.122	78.520	123.364	929.600
9	134	0.331	0.057	0.056	0.012	78.520	1.417	6.980	7.122	-1.473	-6.636	6.798	77.485	147.863	1061.342
10	134	0.331	0.057	0.055	0.013	77.485	1.473	6.636	6.798	-1.529	-6.292	6.475	76.345	174.532	1192.661
11	134	0.331	0.057	0.055	0.014	76.345	1.529	6.292	6.475	-1.584	-5.947	6.155	75.087	203.570	1323.477
12	134	0.331	0.057	0.055	0.014	75.087	1.584	5.947	6.155	-1.639	-5.602	5.837	73.691	235.203	1453.690
13	134	0.331	0.057	0.055	0.015	73.691	1.639	5.602	5.837	-1.694	-5.256	5.522	72.135	269.688	1583.176
14	134	0.331	0.057	0.055	0.016	72.135	1.694	5.256	5.522	-1.749	-4.909	5.212	70.392	307.318	1711.784
15	134	0.331	0.057	0.055	0.016	70.392	1.749	4.909	5.212	-1.804	-4.562	4.905	68.429	348.426	1839.323
16	134	0.331	0.057	0.054	0.017	68.429	1.804	4.562	4.905	-1.858	-4.213	4.605	66.206	393.394	1965.553
17	134	0.331	-0.057	-0.054	-0.018	66.206	1.858	4.213	4.605	-1.804	-3.901	4.298	65.183	442.659	2090.168
18	134	0.331	-0.057	-0.054	-0.019	65.183	1.804	3.901	4.298	-1.750	-3.589	3.993	64.004	496.720	2212.778
19	134	0.331	-0.057	-0.053	-0.021	64.004	1.750	3.589	3.993	-1.697	-3.279	3.692	62.633	552.964	2334.404
20	134	0.331	-0.057	-0.053	-0.022	62.633	1.697	3.279	3.692	-1.645	-2.970	3.395	61.024	611.698	2454.846
21	134	0.331	-0.057	-0.052	-0.024	61.024	1.645	2.970	3.395	-1.593	-2.663	3.103	59.111	673.295	2573.849
22	134	0.331	-0.057	-0.051	-0.026	59.111	1.593	2.663	3.103	-1.542	-2.357	2.817	56.809	738.212	2691.074
23	134	0.331	-0.057	-0.050	-0.028	56.809	1.542	2.357	2.817	-1.492	-2.054	2.538	54.000	807.005	2806.068
24	134	0.331	-0.057	-0.048	-0.030	54.000	1.492	2.054	2.538	-1.444	-1.753	2.271	50.522	880.360	2918.206
25	134	0.331	-0.057	-0.047	-0.033	50.522	1.444	1.753	2.271	-1.397	-1.454	2.017	46.153	959.123	3026.615
26	134	0.331	-0.057	-0.044	-0.036	46.153	1.397	1.454	2.017	-1.353	-1.159	1.781	40.595	1044.316	3130.046
27	134	0.331	-0.057	-0.041	-0.039	40.595	1.353	1.159	1.781	-1.312	-0.868	1.573	33.484	1137.143	3226.686
28	134	0.331	-0.057	-0.037	-0.043	33.484	1.312	0.868	1.573	-1.275	-0.580	1.400	24.463	1238.894	3313.880
29	134	0.331	-0.057	-0.032	-0.047	24.463	1.275	0.580	1.400	-1.243	-0.296	1.278	13.406	1350.656	3387.807
30	134	0.331	-0.057	-0.024	-0.051	13.406	1.243	0.296	1.278	-1.219	-0.017	1.219	0.786	1472.627	3443.297
31	134	0.331	-0.057	-0.016	-0.055	0.786	1.219	0.017	1.219	-1.203	0.260	1.231	-12.174	1602.975	3474.365
32	134	0.331	-0.057	-0.005	-0.057	-12.174	1.203	-0.260	1.231	-1.198	0.534	1.311	-24.025	1736.963	3476.203

33	134	0.331	-0.057	0.005	-0.057	-24.025	1.198	-0.534	1.311	-1.203	0.808	1.449	-33.893	1867.949	3447.944
34	134	0.331	-0.057	0.016	-0.055	-33.893	1.203	-0.808	1.449	-1.219	1.084	1.631	-41.665	1990.340	3393.387
35	134	0.331	-0.057	0.024	-0.051	-41.665	1.219	-1.084	1.631	-1.243	1.364	1.845	-47.656	2101.571	3318.663
36	134	0.331	-0.057	0.032	-0.047	-47.656	1.243	-1.364	1.845	-1.275	1.648	2.083	-52.274	2201.675	3229.583
37	134	0.331	-0.057	0.037	-0.043	-52.274	1.275	-1.648	2.083	-1.312	1.935	2.338	-55.874	2291.934	3130.541
38	134	0.331	-0.057	0.041	-0.039	-55.874	1.312	-1.935	2.338	-1.353	2.227	2.606	-58.724	2373.926	3024.554
39	134	0.331	-0.057	0.044	-0.036	-58.724	1.353	-2.227	2.606	-1.397	2.522	2.883	-61.018	2449.102	2913.628
40	134	0.331	-0.057	0.047	-0.033	-61.018	1.397	-2.522	2.883	-1.444	2.820	3.168	-62.894	2518.671	2799.102
41	134	0.331	-0.057	0.048	-0.030	-62.894	1.444	-2.820	3.168	-1.492	3.121	3.460	-64.452	2583.599	2681.883
42	134	0.331	-0.057	0.050	-0.028	-64.452	1.492	-3.121	3.460	-1.542	3.425	3.756	-65.762	2644.654	2562.601
43	134	0.331	-0.057	0.051	-0.026	-65.762	1.542	-3.425	3.756	-1.593	3.730	4.056	-66.878	2702.445	2441.703
44	134	0.331	-0.057	0.052	-0.024	-66.878	1.593	-3.730	4.056	-1.645	4.038	4.360	-67.837	2757.455	2319.515
45	134	0.331	-0.057	0.053	-0.022	-67.837	1.645	-4.038	4.360	-1.697	4.347	4.666	-68.671	2810.077	2196.280
46	134	0.331	-0.057	0.053	-0.021	-68.671	1.697	-4.347	4.666	-1.750	4.657	4.975	-69.402	2860.627	2072.180
47	134	0.331	-0.057	0.054	-0.019	-69.402	1.750	-4.657	4.975	-1.804	4.969	5.286	-70.046	2909.365	1947.358
48	134	0.331	-0.011	0.011	-0.004	-70.046	1.804	-4.969	5.286	-1.815	5.296	5.598	-71.086	2956.509	1821.925
49	134	0.331	-0.011	0.011	-0.003	-71.086	1.815	-5.296	5.598	-1.825	5.623	5.912	-72.016	3002.238	1695.969
50	134	0.331	-0.011	0.011	-0.003	-72.016	1.825	-5.623	5.912	-1.836	5.951	6.228	-72.851	3045.673	1569.204
51	134	0.331	-0.011	0.011	-0.003	-72.851	1.836	-5.951	6.228	-1.847	6.279	6.545	-73.606	3087.047	1441.751
52	134	0.331	-0.011	0.011	-0.003	-73.606	1.847	-6.279	6.545	-1.858	6.607	6.864	-74.291	3126.558	1313.709
53	134	0.331	-0.011	0.011	-0.003	-74.291	1.858	-6.607	6.864	-1.869	6.936	7.183	-74.915	3164.378	1185.157
54	134	0.331	-0.011	0.011	-0.003	-74.915	1.869	-6.936	7.183	-1.880	7.264	7.503	-75.486	3200.659	1056.162
55	134	0.331	-0.011	0.011	-0.003	-75.486	1.880	-7.264	7.503	-1.892	7.592	7.824	-76.010	3235.533	926.780
56	134	0.331	-0.011	0.011	-0.002	-76.010	1.892	-7.592	7.824	-1.903	7.921	8.146	-76.493	3269.116	797.056
57	134	0.331	-0.011	0.011	-0.002	-76.493	1.903	-7.921	8.146	-1.914	8.250	8.469	-76.939	3301.511	667.031
58	134	0.331	-0.011	0.011	-0.002	-76.939	1.914	-8.250	8.469	-1.925	8.578	8.792	-77.352	3332.809	536.737
59	134	0.331	-0.011	0.011	-0.002	-77.352	1.925	-8.578	8.792	-1.936	8.907	9.115	-77.736	3363.092	406.204
60	134	0.331	-0.011	0.011	-0.002	-77.736	1.936	-8.907	9.115	-1.947	9.236	9.439	-78.094	3392.432	275.455
61	134	0.331	-0.011	0.011	-0.002	-78.094	1.947	-9.236	9.439	-1.959	9.565	9.764	-78.428	3420.896	144.513
62	134	0.331	-0.011	0.011	-0.002	-78.428	1.959	-9.565	9.764	-1.970	9.894	10.088	-78.740	3448.541	13.396
63	134	0.331	-0.011	0.011	-0.002	-78.740	1.970	-9.894	10.088	-1.981	10.223	10.413	-79.033	3475.422	-117.880
														3501.586	-249.301

Segment no.	Height of Segment	DL+LL(PL-3/4)	Left Angle	Left Thrust x	Left Thrust y	***Left Thrust***	Right Thrust x	Right Thrust y	***Right Thrust***	Right angle	Co-ordinates	
											X	Y
1	134	0.461	80.500	2.394	14.305	14.504	-2.394	-13.843	14.049	80.189	0	0
2	134	0.461	80.189	2.394	13.843	14.049	-2.394	-13.382	13.594	79.858	22.116	132.162
3	134	0.461	79.858	2.394	13.382	13.594	-2.394	-12.921	13.140	79.504	44.949	264.203
4	134	0.461	79.504	2.394	12.921	13.140	-2.394	-12.459	12.687	79.124	68.545	396.109
5	134	0.461	79.124	2.394	12.459	12.687	-2.394	-11.998	12.234	78.716	92.955	527.867
6	134	0.461	78.716	2.394	11.998	12.234	-2.394	-11.536	11.782	78.277	118.239	659.460
7	134	0.461	78.277	2.394	11.536	11.782	-2.394	-11.075	11.331	77.803	144.457	790.870
8	134	0.461	77.803	2.394	11.075	11.331	-2.394	-10.614	10.880	77.290	171.683	922.075
9	134	0.461	77.290	2.394	10.614	10.880	-2.394	-10.152	10.431	76.732	199.992	1053.050
10	134	0.461	76.732	2.394	10.152	10.431	-2.394	-9.691	9.982	76.125	229.474	1183.767
11	134	0.461	76.125	2.394	9.691	9.982	-2.394	-9.229	9.535	75.460	260.227	1314.190
12	134	0.461	75.460	2.394	9.229	9.535	-2.394	-8.768	9.089	74.729	292.362	1444.280
13	134	0.461	74.729	2.394	8.768	9.089	-2.394	-8.307	8.645	73.924	326.004	1573.988
14	134	0.461	73.924	2.394	8.307	8.645	-2.394	-7.845	8.202	73.031	361.296	1703.257
15	134	0.461	73.031	2.394	7.845	8.202	-2.394	-7.384	7.762	72.037	398.403	1832.017
16	134	0.461	72.037	2.394	7.384	7.762	-2.394	-6.922	7.325	70.924	437.510	1960.183
17	134	0.461	70.924	2.394	6.922	7.325	-2.394	-6.461	6.890	69.670	478.835	2087.652
18	134	0.461	69.670	2.394	6.461	6.890	-2.394	-6.000	6.459	68.248	522.629	2214.294
19	134	0.461	68.248	2.394	6.000	6.459	-2.394	-5.538	6.033	66.624	569.184	2339.947
20	134	0.461	66.624	2.394	5.538	6.033	-2.394	-5.077	5.613	64.755	618.842	2464.405
21	134	0.461	64.755	2.394	5.077	5.613	-2.394	-4.615	5.199	62.586	672.008	2587.407
22	134	0.461	62.586	2.394	4.615	5.199	-2.394	-4.154	4.794	60.046	729.158	2708.609
23	134	0.461	60.046	2.394	4.154	4.794	-2.394	-3.693	4.401	57.045	790.854	2827.561
24	134	0.461	57.045	2.394	3.693	4.401	-2.394	-3.231	4.021	53.467	857.760	2943.663
25	134	0.461	53.467	2.394	3.231	4.021	-2.394	-2.770	3.661	49.164	930.653	3056.102
26	134	0.461	49.164	2.394	2.770	3.661	-2.394	-2.308	3.325	43.959	1010.421	3163.773
27	134	0.461	43.959	2.394	2.308	3.325	-2.394	-1.847	3.023	37.652	1098.043	3265.156
28	134	0.461	37.652	2.394	1.847	3.023	-2.394	-1.386	2.766	30.062	1194.502	3358.170
29	134	0.461	30.062	2.394	1.386	2.766	-2.394	-0.924	2.566	21.109	1300.594	3440.026
30	134	0.461	21.109	2.394	0.924	2.566	-2.394	-0.463	2.438	10.940	1416.569	3507.151
31	134	0.461	10.940	2.394	0.463	2.438	-2.394	-0.001	2.394	0.032	1541.577	3555.411
32	134	0.461	0.032	2.394	0.001	2.394	-2.394	0.460	2.438	-10.879	1673.142	3580.842

33	134	0.461	-10.879	2.394	-0.460	2.438	-2.394	0.921	2.565	-21.054	1807.142	3580.916
34	134	0.461	-21.054	2.394	-0.921	2.565	-2.394	1.383	2.765	-30.015	1938.733	3555.624
35	134	0.461	-30.015	2.394	-1.383	2.765	-2.394	1.844	3.022	-37.612	2063.788	3507.485
36	134	0.461	-37.612	2.394	-1.844	3.022	-2.394	2.306	3.324	-43.926	2179.818	3440.455
37	134	0.461	-43.926	2.394	-2.306	3.324	-2.394	2.767	3.659	-49.137	2285.967	3358.672
38	134	0.461	-49.137	2.394	-2.767	3.659	-2.394	3.229	4.019	-53.445	2382.479	3265.713
39	134	0.461	-53.445	2.394	-3.229	4.019	-2.394	3.690	4.398	-57.027	2470.149	3164.372
40	134	0.461	-57.027	2.394	-3.690	4.398	-2.394	4.151	4.792	-60.031	2549.959	3056.732
41	134	0.461	-60.031	2.394	-4.151	4.792	-2.394	4.613	5.197	-62.573	2622.888	2944.316
42	134	0.461	-62.573	2.394	-4.613	5.197	-2.394	5.074	5.610	-64.744	2689.826	2828.233
43	134	0.461	-64.744	2.394	-5.074	5.610	-2.394	5.536	6.031	-66.614	2751.550	2709.295
44	134	0.461	-66.614	2.394	-5.536	6.031	-2.394	5.997	6.457	-68.239	2808.724	2588.105
45	134	0.461	-68.239	2.394	-5.997	6.457	-2.394	6.458	6.888	-69.663	2861.911	2465.112
46	134	0.461	-69.663	2.394	-6.458	6.888	-2.394	6.920	7.322	-70.917	2911.589	2340.661
47	134	0.461	-70.917	2.394	-6.920	7.322	-2.394	7.381	7.760	-72.031	2958.160	2215.014
48	134	2.061	-72.031	2.394	-7.381	7.760	-2.394	9.443	9.741	-75.774	3001.969	2088.378
49	134	0.461	-75.774	2.394	-9.443	9.741	-2.394	9.904	10.189	-76.412	3043.307	1960.914
50	134	0.461	-76.412	2.394	-9.904	10.189	-2.394	10.365	10.638	-76.996	3076.236	1831.023
51	134	0.461	-76.996	2.394	-10.365	10.638	-2.394	10.827	11.088	-77.532	3107.718	1700.773
52	134	0.461	-77.532	2.394	-10.827	11.088	-2.394	11.288	11.539	-78.027	3137.870	1570.210
53	134	0.461	-78.027	2.394	-11.288	11.539	-2.394	11.750	11.991	-78.484	3166.799	1439.370
54	134	0.461	-78.484	2.394	-11.750	11.991	-2.394	12.211	12.443	-78.909	3194.598	1308.285
55	134	0.461	-78.909	2.394	-12.211	12.443	-2.394	12.672	12.896	-79.303	3221.349	1176.982
56	134	0.461	-79.303	2.394	-12.672	12.896	-2.394	13.134	13.350	-79.670	3247.127	1045.485
57	134	0.461	-79.670	2.394	-13.134	13.350	-2.394	13.595	13.804	-80.014	3272.000	913.814
58	134	0.461	-80.014	2.394	-13.595	13.804	-2.394	14.057	14.259	-80.335	3296.027	781.985
59	134	0.461	-80.335	2.394	-14.057	14.259	-2.394	14.518	14.714	-80.637	3319.264	650.016
60	134	0.461	-80.637	2.394	-14.518	14.714	-2.394	14.979	15.169	-80.921	3341.760	517.917
61	134	0.461	-80.921	2.394	-14.979	15.169	-2.394	15.441	15.625	-81.188	3363.561	385.703
62	134	0.461	-81.188	2.394	-15.441	15.625	-2.394	15.902	16.081	-81.439	3384.706	253.382
63	134	0.461	-81.439	2.394	-15.902	16.081	-2.394	16.364	16.538	-81.677	3405.235	120.963
											3425.182	-11.544

Segment no.	Height of Segment	DL+LL(1/2 PL)	Left Angle	Left Thrust x	Left Thrust y	***Left Thrust***	Right Thrust x	Right Thrust y	***Right Thrust***	Right angle	Co-ordinates	
											X	Y
1	133	0.458	79.500	2.725	14.705	14.955	-2.725	-14.247	14.505	79.170	0	0
2	133	0.458	79.170	2.725	14.247	14.505	-2.725	-13.789	14.056	78.820	24.237	130.773
3	133	0.458	78.820	2.725	13.789	14.056	-2.725	-13.331	13.607	78.446	49.227	261.404
4	133	0.458	78.446	2.725	13.331	13.607	-2.725	-12.873	13.158	78.046	75.015	391.880
5	133	0.458	78.046	2.725	12.873	13.158	-2.725	-12.415	12.711	77.619	101.655	522.185
6	133	0.458	77.619	2.725	12.415	12.711	-2.725	-11.957	12.264	77.160	129.202	652.301
7	133	0.458	77.160	2.725	11.957	12.264	-2.725	-11.499	11.818	76.666	157.719	782.207
8	133	0.458	76.666	2.725	11.499	11.818	-2.725	-11.041	11.373	76.134	187.276	911.882
9	133	0.458	76.134	2.725	11.041	11.373	-2.725	-10.583	10.928	75.559	217.948	1041.297
10	133	0.458	75.559	2.725	10.583	10.928	-2.725	-10.125	10.486	74.935	249.821	1170.421
11	133	0.458	74.935	2.725	10.125	10.486	-2.725	-9.667	10.044	74.256	282.989	1299.219
12	133	0.458	74.256	2.725	9.667	10.044	-2.725	-9.209	9.604	73.515	317.558	1427.648
13	133	0.458	73.515	2.725	9.209	9.604	-2.725	-8.751	9.166	72.702	353.647	1555.658
14	133	0.458	72.702	2.725	8.751	9.166	-2.725	-8.293	8.730	71.808	391.388	1683.191
15	133	0.458	71.808	2.725	8.293	8.730	-2.725	-7.835	8.296	70.821	430.934	1810.175
16	133	0.458	70.821	2.725	7.835	8.296	-2.725	-7.377	7.865	69.725	472.456	1936.528
17	133	0.458	69.725	2.725	7.377	7.865	-2.725	-6.920	7.437	68.502	516.150	2062.146
18	133	0.458	68.502	2.725	6.920	7.437	-2.725	-6.462	7.013	67.131	562.238	2186.905
19	133	0.458	67.131	2.725	6.462	7.013	-2.725	-6.004	6.593	65.584	610.979	2310.652
20	133	0.458	65.584	2.725	6.004	6.593	-2.725	-5.546	6.179	63.828	662.666	2433.198
21	133	0.458	63.828	2.725	5.546	6.179	-2.725	-5.088	5.772	61.823	717.643	2554.303
22	133	0.458	61.823	2.725	5.088	5.772	-2.725	-4.630	5.372	59.516	776.304	2673.667
23	133	0.458	59.516	2.725	4.630	5.372	-2.725	-4.172	4.983	56.844	839.107	2790.906
24	133	0.458	56.844	2.725	4.172	4.983	-2.725	-3.714	4.607	53.727	906.578	2905.521
25	133	0.458	53.727	2.725	3.714	4.607	-2.725	-3.256	4.246	50.068	979.319	3016.866
26	133	0.458	50.068	2.725	3.256	4.246	-2.725	-2.798	3.906	45.752	1058.007	3124.091
27	133	0.458	45.752	2.725	2.798	3.906	-2.725	-2.340	3.592	40.648	1143.377	3226.077
28	133	0.458	40.648	2.725	2.340	3.592	-2.725	-1.882	3.312	34.626	1236.180	3321.348
29	133	0.458	34.626	2.725	1.882	3.312	-2.725	-1.424	3.075	27.587	1337.090	3407.985
30	133	0.458	27.587	2.725	1.424	3.075	-2.725	-0.966	2.892	19.517	1446.533	3483.558
31	133	0.458	19.517	2.725	0.966	2.892	-2.725	-0.508	2.772	10.560	1564.412	3545.149
32	133	2.058	10.560	2.725	0.508	2.772	-2.725	1.550	3.135	-29.627	1689.771	3589.583

33	133	0.458	-29.627	2.725	-1.550	3.135	-2.725	2.008	3.385	-36.380	1820.518	3613.957
34	133	0.458	-36.380	2.725	-2.008	3.385	-2.725	2.466	3.675	-42.138	1936.130	3548.209
35	133	0.458	-42.138	2.725	-2.466	3.675	-2.725	2.924	3.997	-47.011	2043.209	3469.321
36	133	0.458	-47.011	2.725	-2.924	3.997	-2.725	3.382	4.343	-51.134	2141.833	3380.090
37	133	0.458	-51.134	2.725	-3.382	4.343	-2.725	3.840	4.709	-54.633	2232.519	3282.802
38	133	0.458	-54.633	2.725	-3.840	4.709	-2.725	4.298	5.089	-57.619	2315.976	3179.245
39	133	0.458	-57.619	2.725	-4.298	5.089	-2.725	4.756	5.481	-60.184	2392.958	3070.789
40	133	0.458	-60.184	2.725	-4.756	5.481	-2.725	5.214	5.883	-62.402	2464.186	2958.469
41	133	0.458	-62.402	2.725	-5.214	5.883	-2.725	5.672	6.292	-64.334	2530.316	2843.075
42	133	0.458	-64.334	2.725	-5.672	6.292	-2.725	6.130	6.708	-66.028	2591.931	2725.208
43	133	0.458	-66.028	2.725	-6.130	6.708	-2.725	6.587	7.129	-67.524	2649.536	2605.331
44	133	0.458	-67.524	2.725	-6.587	7.129	-2.725	7.045	7.554	-68.852	2703.572	2483.802
45	133	0.458	-68.852	2.725	-7.045	7.554	-2.725	7.503	7.983	-70.038	2754.417	2360.905
46	133	0.458	-70.038	2.725	-7.503	7.983	-2.725	7.961	8.415	-71.103	2802.400	2236.862
47	133	0.458	-71.103	2.725	-7.961	8.415	-2.725	8.419	8.849	-72.063	2847.806	2111.853
48	133	0.458	-72.063	2.725	-8.419	8.849	-2.725	8.877	9.286	-72.933	2890.882	1986.022
49	133	0.458	-72.933	2.725	-8.877	9.286	-2.725	9.335	9.725	-73.725	2931.842	1859.486
50	133	0.458	-73.725	2.725	-9.335	9.725	-2.725	9.793	10.165	-74.448	2970.876	1732.343
51	133	0.458	-74.448	2.725	-9.793	10.165	-2.725	10.251	10.607	-75.112	3008.149	1604.673
52	133	0.458	-75.112	2.725	-10.251	10.607	-2.725	10.709	11.050	-75.722	3043.807	1476.542
53	133	0.458	-75.722	2.725	-10.709	11.050	-2.725	11.167	11.495	-76.285	3077.979	1348.007
54	133	0.458	-76.285	2.725	-11.167	11.495	-2.725	11.625	11.940	-76.806	3110.781	1219.115
55	133	0.458	-76.806	2.725	-11.625	11.940	-2.725	12.083	12.387	-77.289	3142.315	1089.908
56	133	0.458	-77.289	2.725	-12.083	12.387	-2.725	12.541	12.834	-77.739	3172.672	960.419
57	133	0.458	-77.739	2.725	-12.541	12.834	-2.725	12.999	13.282	-78.159	3201.936	830.678
58	133	0.458	-78.159	2.725	-12.999	13.282	-2.725	13.457	13.730	-78.551	3230.180	700.712
59	133	0.458	-78.551	2.725	-13.457	13.730	-2.725	13.915	14.179	-78.918	3257.472	570.542
60	133	0.458	-78.918	2.725	-13.915	14.179	-2.725	14.373	14.629	-79.263	3283.872	440.188
61	133	0.458	-79.263	2.725	-14.373	14.629	-2.725	14.831	15.079	-79.587	3309.436	309.668
62	133	0.458	-79.587	2.725	-14.831	15.079	-2.725	15.289	15.530	-79.893	3334.214	178.997
63	133	0.458	-79.893	2.725	-15.289	15.530	-2.725	15.747	15.981	-80.181	3358.252	48.187
											3381.593	-82.749

Segment no.	Height of Segment	DL + LL (1/4PL)	Wind Load (Cpi=0)	WL H	WL V	Left Angle	Left Thrust x	Left Thrust y	***Left Thrust***	Right Thrust x	Right Thrust y	***Right Thrust***	Right angle	Co-ordinates X	Co-ordinates Y
1	135	0.441	0.046	0.045	0.008	82.700	1.710	13.346	13.455	-1.755	-12.897	13.016	82.253	0	0
2	135	0.441	0.046	0.045	0.008	82.253	1.755	12.897	13.016	-1.800	-12.448	12.577	81.774	17.154	133.906
3	135	0.441	0.046	0.045	0.008	81.774	1.800	12.448	12.577	-1.844	-11.999	12.139	81.261	35.353	267.673
4	135	0.441	0.046	0.045	0.008	81.261	1.844	11.999	12.139	-1.889	-11.549	11.702	80.709	54.669	401.284
5	135	0.441	0.046	0.045	0.009	80.709	1.889	11.549	11.702	-1.934	-11.099	11.266	80.115	75.180	534.717
6	135	0.441	0.046	0.045	0.009	80.115	1.934	11.099	11.266	-1.979	-10.648	10.831	79.473	96.976	667.946
7	135	0.441	0.046	0.045	0.009	79.473	1.979	10.648	10.831	-2.023	-10.198	10.397	78.777	120.152	800.942
8	135	0.441	0.046	0.045	0.010	78.777	2.023	10.198	10.397	-2.068	-9.747	9.964	78.021	144.816	933.670
9	135	0.441	0.046	0.044	0.010	78.021	2.068	9.747	9.964	-2.113	-9.295	9.532	77.196	171.091	1066.088
10	135	0.441	0.046	0.044	0.010	77.196	2.113	9.295	9.532	-2.157	-8.844	9.103	76.293	199.111	1198.148
11	135	0.441	0.046	0.044	0.011	76.293	2.157	8.844	9.103	-2.201	-8.391	8.675	75.301	229.029	1329.791
12	135	0.441	0.046	0.044	0.011	75.301	2.201	8.391	8.675	-2.245	-7.939	8.250	74.207	261.017	1460.947
13	135	0.441	0.046	0.044	0.012	74.207	2.245	7.939	8.250	-2.289	-7.485	7.827	72.994	295.271	1591.529
14	135	0.441	0.046	0.044	0.012	72.994	2.289	7.485	7.827	-2.333	-7.031	7.408	71.642	332.014	1721.432
15	135	0.441	0.046	0.044	0.013	71.642	2.333	7.031	7.408	-2.377	-6.577	6.993	70.130	371.499	1850.529
16	135	0.441	0.046	0.043	0.014	70.130	2.377	6.577	6.993	-2.420	-6.121	6.583	68.427	414.017	1978.659
17	135	0.941	-0.068	-0.065	-0.022	68.427	2.420	6.121	6.583	-2.356	-5.202	5.710	65.638	459.902	2105.621
18	135	0.441	-0.068	-0.064	-0.023	65.638	2.356	5.202	5.710	-2.291	-4.784	5.304	64.408	509.541	2231.164
19	135	0.441	-0.068	-0.064	-0.025	64.408	2.291	4.784	5.304	-2.228	-4.367	4.903	62.976	565.228	2354.144
20	135	0.441	-0.068	-0.063	-0.027	62.976	2.228	4.367	4.903	-2.165	-3.953	4.506	61.293	623.543	2475.899
21	135	0.441	-0.068	-0.062	-0.028	61.293	2.165	3.953	4.506	-2.102	-3.540	4.117	59.292	684.882	2596.159
22	135	0.441	-0.068	-0.061	-0.031	59.292	2.102	3.540	4.117	-2.041	-3.129	3.736	56.880	749.726	2714.567
23	135	0.441	-0.068	-0.060	-0.033	56.880	2.041	3.129	3.736	-1.981	-2.721	3.366	53.934	818.666	2830.637
24	135	0.441	-0.068	-0.058	-0.036	53.934	1.981	2.721	3.366	-1.923	-2.315	3.010	50.283	892.429	2943.703
25	135	0.441	-0.068	-0.056	-0.039	50.283	1.923	2.315	3.010	-1.867	-1.913	2.673	45.694	971.906	3052.829
26	135	0.441	-0.068	-0.053	-0.043	45.694	1.867	1.913	2.673	-1.814	-1.515	2.364	39.861	1058.170	3156.673
27	135	0.441	-0.068	-0.049	-0.047	39.861	1.814	1.515	2.364	-1.765	-1.121	2.091	32.417	1152.465	3253.282
28	135	0.441	-0.068	-0.044	-0.052	32.417	1.765	1.121	2.091	-1.720	-0.731	1.869	23.030	1256.091	3339.808
29	135	0.441	-0.068	-0.038	-0.057	23.030	1.720	0.731	1.869	-1.683	-0.347	1.718	11.650	1370.054	3412.178
30	135	0.441	-0.068	-0.029	-0.062	11.650	1.683	0.347	1.718	-1.653	0.033	1.654	-1.134	1494.294	3464.992
31	135	0.441	-0.068	-0.019	-0.066	-1.134	1.653	-0.033	1.654	-1.635	0.408	1.685	-14.026	1626.514	3492.252
32	135	0.441	-0.068	-0.006	-0.068	-14.026	1.635	-0.408	1.685	-1.628	0.782	1.806	-25.646	1761.487	3489.581

33	135	0.441	-0.068	0.006	-0.068	-25.646	1.628	-0.782	1.806	-1.635	1.155	2.001	-35.245	1892.462	3456.861
34	135	0.441	-0.068	0.019	-0.066	-35.245	1.635	-1.155	2.001	-1.653	1.531	2.253	-42.794	2014.162	3398.432
35	135	0.441	-0.068	0.029	-0.062	-42.794	1.653	-1.531	2.253	-1.683	1.910	2.546	-48.625	2124.416	3320.526
36	135	0.441	-0.068	0.038	-0.057	-48.625	1.683	-1.910	2.546	-1.720	2.295	2.868	-53.139	2223.479	3228.813
37	135	0.441	-0.068	0.044	-0.052	-53.139	1.720	-2.295	2.868	-1.765	2.684	3.212	-56.674	2312.711	3127.508
38	135	0.441	-0.068	0.049	-0.047	-56.674	1.765	-2.684	3.212	-1.814	3.078	3.573	-59.486	2393.694	3019.495
39	135	0.441	-0.068	0.053	-0.043	-59.486	1.814	-3.078	3.573	-1.867	3.477	3.946	-61.758	2467.863	2906.694
40	135	0.441	-0.068	0.056	-0.039	-61.758	1.867	-3.477	3.946	-1.923	3.879	4.329	-63.624	2536.410	2790.392
41	135	0.441	-0.068	0.058	-0.036	-63.624	1.923	-3.879	4.329	-1.981	4.284	4.720	-65.178	2600.290	2671.462
42	135	0.441	-0.068	0.060	-0.033	-65.178	1.981	-4.284	4.720	-2.041	4.692	5.117	-66.490	2660.265	2550.516
43	135	0.441	-0.068	0.061	-0.031	-66.490	2.041	-4.692	5.117	-2.102	5.103	5.519	-67.609	2716.937	2427.987
44	135	0.441	-0.068	0.062	-0.028	-67.609	2.102	-5.103	5.519	-2.165	5.516	5.925	-68.574	2770.790	2304.193
45	135	0.441	-0.068	0.063	-0.027	-68.574	2.165	-5.516	5.925	-2.228	5.931	6.335	-69.414	2822.216	2179.372
46	135	0.441	-0.068	0.064	-0.025	-69.414	2.228	-5.931	6.335	-2.291	6.347	6.748	-70.151	2871.531	2053.702
47	135	0.441	-0.068	0.064	-0.023	-70.151	2.291	-6.347	6.748	-2.356	6.765	7.164	-70.803	2918.999	1927.322
48	135	0.441	-0.023	0.022	-0.007	-70.803	2.356	-6.765	7.164	-2.377	7.199	7.582	-71.728	2964.837	1800.342
49	135	0.441	-0.023	0.022	-0.007	-71.728	2.377	-7.199	7.582	-2.399	7.634	8.002	-72.555	3009.227	1672.849
50	135	0.441	-0.023	0.022	-0.007	-72.555	2.399	-7.634	8.002	-2.421	8.069	8.424	-73.300	3051.555	1544.656
51	135	0.441	-0.023	0.022	-0.006	-73.300	2.421	-8.069	8.424	-2.443	8.504	8.848	-73.974	3092.026	1415.866
52	135	0.441	-0.023	0.022	-0.006	-73.974	2.443	-8.504	8.848	-2.465	8.939	9.273	-74.586	3130.819	1286.559
53	135	0.441	-0.023	0.022	-0.006	-74.586	2.465	-8.939	9.273	-2.487	9.375	9.699	-75.145	3168.089	1156.806
54	135	0.441	-0.023	0.022	-0.005	-75.145	2.487	-9.375	9.699	-2.509	9.811	10.127	-75.656	3203.970	1026.661
55	135	0.441	-0.023	0.022	-0.005	-75.656	2.509	-9.811	10.127	-2.531	10.247	10.555	-76.126	3238.581	896.174
56	135	0.441	-0.023	0.022	-0.005	-76.126	2.531	-10.247	10.555	-2.553	10.684	10.985	-76.559	3272.026	765.382
57	135	0.441	-0.023	0.022	-0.005	-76.559	2.553	-10.684	10.985	-2.576	11.120	11.415	-76.960	3304.398	634.321
58	135	0.441	-0.023	0.022	-0.005	-76.960	2.576	-11.120	11.415	-2.598	11.557	11.846	-77.331	3335.778	503.018
59	135	0.441	-0.023	0.022	-0.004	-77.331	2.598	-11.557	11.846	-2.620	11.994	12.277	-77.677	3366.239	371.500
60	135	0.441	-0.023	0.022	-0.004	-77.677	2.620	-11.994	12.277	-2.643	12.431	12.709	-77.999	3395.846	239.787
61	135	0.441	-0.023	0.022	-0.004	-77.999	2.643	-12.431	12.709	-2.665	12.869	13.142	-78.299	3424.659	107.897
62	135	0.441	-0.023	0.022	-0.004	-78.299	2.665	-12.869	13.142	-2.688	13.306	13.575	-78.581	3452.730	-24.152
63	135	0.441	-0.023	0.022	-0.004	-78.581	2.688	-13.306	13.575	-2.710	13.744	14.008	-78.845	3480.107	-156.347
														3506.835	-288.675

Segment no.	Height of Segment	DL + LL (1/4PL)	Wind Load (Cpi=-0.2)	WL H	WL V	Left Angle	Left Thrust x	Left Thrust y	***Left Thrust***	Right Thrust x	Right Thrust y	***Right Thrust***	Right angle	Co-ordinates	
														X	Y
1	133	0.441	0.057	0.056	0.009	83.300	1.593	13.564	13.657	-1.650	-13.113	13.217	82.830	0	0
2	133	0.441	0.057	0.056	0.010	82.830	1.650	13.113	13.217	-1.706	-12.662	12.777	82.328	15.517	132.092
3	133	0.441	0.057	0.056	0.010	82.328	1.706	12.662	12.777	-1.762	-12.211	12.337	81.789	32.118	264.052
4	133	0.441	0.057	0.056	0.010	81.789	1.762	12.211	12.337	-1.818	-11.759	11.899	81.212	49.874	395.861
5	133	0.441	0.057	0.056	0.011	81.212	1.818	11.759	11.899	-1.874	-11.307	11.461	80.590	68.868	527.498
6	133	0.441	0.057	0.056	0.011	80.590	1.874	11.307	11.461	-1.930	-10.854	11.025	79.918	89.189	658.936
7	133	0.441	0.057	0.056	0.012	79.918	1.930	10.854	11.025	-1.986	-10.401	10.589	79.192	110.935	790.146
8	133	0.441	0.057	0.056	0.012	79.192	1.986	10.401	10.589	-2.041	-9.948	10.155	78.404	134.217	921.093
9	133	0.441	0.057	0.056	0.012	78.404	2.041	9.948	10.155	-2.097	-9.494	9.723	77.545	159.157	1051.733
10	133	0.441	0.057	0.055	0.013	77.545	2.097	9.494	9.723	-2.152	-9.040	9.292	76.606	185.892	1182.019
11	133	0.441	0.057	0.055	0.014	76.606	2.152	9.040	9.292	-2.208	-8.585	8.864	75.577	214.577	1311.888
12	133	0.441	0.057	0.055	0.014	75.577	2.208	8.585	8.864	-2.263	-8.129	8.438	74.443	245.385	1441.271
13	133	0.441	0.057	0.055	0.015	74.443	2.263	8.129	8.438	-2.318	-7.673	8.015	73.189	278.513	1570.079
14	133	0.441	0.057	0.055	0.016	73.189	2.318	7.673	8.015	-2.373	-7.216	7.596	71.796	314.182	1698.207
15	133	0.441	0.057	0.055	0.016	71.796	2.373	7.216	7.596	-2.427	-6.758	7.181	70.241	352.647	1825.523
16	133	0.441	0.057	0.054	0.017	70.241	2.427	6.758	7.181	-2.482	-6.299	6.770	68.496	394.196	1951.867
17	133	0.941	-0.057	-0.054	-0.018	68.496	2.482	6.299	6.770	-2.428	-5.376	5.899	65.696	439.158	2077.037
18	133	0.441	-0.057	-0.054	-0.019	65.696	2.428	5.376	5.899	-2.374	-4.954	5.494	64.394	487.911	2200.779
19	133	0.441	-0.057	-0.053	-0.021	64.394	2.374	4.954	5.494	-2.321	-4.533	5.093	62.887	542.651	2321.992
20	133	0.441	-0.057	-0.053	-0.022	62.887	2.321	4.533	5.093	-2.269	-4.114	4.698	61.126	600.131	2441.929
21	133	0.441	-0.057	-0.052	-0.024	61.126	2.269	4.114	4.698	-2.217	-3.696	4.310	59.048	660.746	2560.313
22	133	0.441	-0.057	-0.051	-0.026	59.048	2.217	3.696	4.310	-2.166	-3.280	3.931	56.566	724.969	2676.779
23	133	0.441	-0.057	-0.050	-0.028	56.566	2.166	3.280	3.931	-2.116	-2.867	3.563	53.568	793.374	2790.840
24	133	0.441	-0.057	-0.048	-0.030	53.568	2.116	2.867	3.563	-2.068	-2.455	3.210	49.900	866.653	2901.831
25	133	0.441	-0.057	-0.047	-0.033	49.900	2.068	2.455	3.210	-2.021	-2.047	2.876	45.363	945.638	3008.838
26	133	0.441	-0.057	-0.044	-0.036	45.363	2.021	2.047	2.876	-1.977	-1.641	2.569	39.702	1031.306	3110.573
27	133	0.441	-0.057	-0.041	-0.039	39.702	1.977	1.641	2.569	-1.936	-1.239	2.298	32.629	1124.755	3205.211
28	133	0.441	-0.057	-0.037	-0.043	32.629	1.936	1.239	2.298	-1.899	-0.841	2.077	23.895	1227.082	3290.170
29	133	0.441	-0.057	-0.032	-0.047	23.895	1.899	0.841	2.077	-1.867	-0.447	1.920	13.469	1339.093	3361.883
30	133	0.441	-0.057	-0.024	-0.051	13.469	1.867	0.447	1.920	-1.843	-0.057	1.843	1.779	1460.693	3415.756
31	133	0.441	-0.057	-0.016	-0.055	1.779	1.843	0.057	1.843	-1.827	0.329	1.856	-10.219	1590.035	3446.735
32	133	0.441	-0.057	-0.005	-0.057	-10.219	1.827	-0.329	1.856	-1.822	0.714	1.957	-21.405	1722.971	3450.865

33	133	0.441	-0.057	0.005	-0.057	-21.405	1.822	-0.714	1.957	-1.827	1.099	2.132	-31.022	1853.861	3427.268
34	133	0.441	-0.057	0.016	-0.055	-31.022	1.827	-1.099	2.132	-1.843	1.485	2.367	-38.873	1977.687	3378.730
35	133	0.441	-0.057	0.024	-0.051	-38.873	1.843	-1.485	2.367	-1.867	1.875	2.646	-45.126	2091.664	3310.186
36	133	0.441	-0.057	0.032	-0.047	-45.126	1.867	-1.875	2.646	-1.899	2.269	2.959	-50.082	2195.210	3226.716
37	133	0.441	-0.057	0.037	-0.043	-50.082	1.899	-2.269	2.959	-1.936	2.667	3.296	-54.033	2289.048	3132.463
38	133	0.441	-0.057	0.041	-0.039	-54.033	1.936	-2.667	3.296	-1.977	3.069	3.651	-57.217	2374.392	3030.457
39	133	0.441	-0.057	0.044	-0.036	-57.217	1.977	-3.069	3.651	-2.021	3.475	4.020	-59.817	2452.505	2922.812
40	133	0.441	-0.057	0.047	-0.033	-59.817	2.021	-3.475	4.020	-2.068	3.883	4.400	-61.969	2524.518	2810.995
41	133	0.441	-0.057	0.048	-0.030	-61.969	2.068	-3.883	4.400	-2.116	4.295	4.788	-63.771	2591.385	2696.026
42	133	0.441	-0.057	0.050	-0.028	-63.771	2.116	-4.295	4.788	-2.166	4.709	5.183	-65.298	2653.889	2578.628
43	133	0.441	-0.057	0.051	-0.026	-65.298	2.166	-4.709	5.183	-2.217	5.124	5.583	-66.607	2712.670	2459.323
44	133	0.441	-0.057	0.052	-0.024	-66.607	2.217	-5.124	5.583	-2.269	5.542	5.988	-67.739	2768.249	2338.493
45	133	0.441	-0.057	0.053	-0.022	-67.739	2.269	-5.542	5.988	-2.321	5.961	6.397	-68.726	2821.055	2216.425
46	133	0.441	-0.057	0.053	-0.021	-68.726	2.321	-5.961	6.397	-2.374	6.382	6.809	-69.594	2871.440	2093.338
47	133	0.441	-0.057	0.054	-0.019	-69.594	2.374	-6.382	6.809	-2.428	6.804	7.224	-70.363	2919.696	1969.401
48	133	0.441	-0.011	0.011	-0.004	-70.363	2.428	-6.804	7.224	-2.439	7.242	7.641	-71.390	2966.069	1844.747
49	133	0.441	-0.011	0.011	-0.003	-71.390	2.439	-7.242	7.641	-2.449	7.680	8.061	-72.310	3010.765	1719.483
50	133	0.441	-0.011	0.011	-0.003	-72.310	2.449	-7.680	8.061	-2.460	8.118	8.483	-73.139	3053.209	1593.437
51	133	0.441	-0.011	0.011	-0.003	-73.139	2.460	-8.118	8.483	-2.471	8.556	8.906	-73.889	3093.624	1466.726
52	133	0.441	-0.011	0.011	-0.003	-73.889	2.471	-8.556	8.906	-2.482	8.995	9.331	-74.572	3132.200	1339.443
53	133	0.441	-0.011	0.011	-0.003	-74.572	2.482	-8.995	9.331	-2.493	9.433	9.757	-75.194	3169.107	1211.667
54	133	0.441	-0.011	0.011	-0.003	-75.194	2.493	-9.433	9.757	-2.504	9.872	10.185	-75.765	3204.489	1083.459
55	133	0.441	-0.011	0.011	-0.003	-75.765	2.504	-9.872	10.185	-2.516	10.311	10.613	-76.289	3238.476	954.875
56	133	0.441	-0.011	0.011	-0.002	-76.289	2.516	-10.311	10.613	-2.527	10.750	11.043	-76.773	3271.181	825.959
57	133	0.441	-0.011	0.011	-0.002	-76.773	2.527	-10.750	11.043	-2.538	11.189	11.473	-77.221	3302.705	696.749
58	133	0.441	-0.011	0.011	-0.002	-77.221	2.538	-11.189	11.473	-2.549	11.628	11.904	-77.636	3333.136	567.277
59	133	0.441	-0.011	0.011	-0.002	-77.636	2.549	-11.628	11.904	-2.560	12.067	12.336	-78.022	3362.556	437.572
60	133	0.441	-0.011	0.011	-0.002	-78.022	2.560	-12.067	12.336	-2.571	12.506	12.768	-78.382	3391.035	307.657
61	133	0.441	-0.011	0.011	-0.002	-78.382	2.571	-12.506	12.768	-2.583	12.946	13.201	-78.718	3418.638	177.553
62	133	0.441	-0.011	0.011	-0.002	-78.718	2.583	-12.946	13.201	-2.594	13.385	13.634	-79.033	3445.423	47.278
63	133	0.441	-0.011	0.011	-0.002	-79.033	2.594	-13.385	13.634	-2.605	13.825	14.068	-79.329	3471.443	-83.152
														3496.745	-213.723

Segment no.	Height of Segment	DL + LL(3/4PL)	Wind Load (Cpi=0)	WL H	WL V	Left Angle	Left Thrust x	Left Thrust y	***Left Thrust***	Right Thrust x	Right Thrust y	***Right Thrust***	Right angle	Co-ordinates X	Co-ordinates Y
1	133	0.441	0.046	0.045	0.008	82.700	1.678	13.096	13.203	-1.723	-12.647	12.764	82.244	0	0
2	133	0.441	0.046	0.045	0.008	82.244	1.723	12.647	12.764	-1.768	-12.198	12.325	81.755	16.900	131.922
3	133	0.441	0.046	0.045	0.008	81.755	1.768	12.198	12.325	-1.812	-11.749	11.888	81.230	34.849	263.705
4	133	0.441	0.046	0.045	0.008	81.230	1.812	11.749	11.888	-1.857	-11.299	11.450	80.665	53.923	395.330
5	133	0.441	0.046	0.045	0.009	80.665	1.857	11.299	11.450	-1.902	-10.849	11.014	80.056	74.200	526.775
6	133	0.441	0.046	0.045	0.009	80.056	1.902	10.849	11.014	-1.947	-10.398	10.579	79.396	95.773	658.014
7	133	0.441	0.046	0.045	0.009	79.396	1.947	10.398	10.579	-1.991	-9.948	10.145	78.680	118.741	789.016
8	133	0.441	0.046	0.045	0.010	78.680	1.991	9.948	10.145	-2.036	-9.497	9.713	77.900	143.216	919.745
9	133	0.441	0.046	0.044	0.010	77.900	2.036	9.497	9.713	-2.081	-9.045	9.282	77.047	169.323	1050.157
10	133	0.441	0.046	0.044	0.010	77.047	2.081	9.045	9.282	-2.125	-8.594	8.852	76.111	197.203	1180.202
11	133	0.441	0.046	0.044	0.011	76.111	2.125	8.594	8.852	-2.169	-8.141	8.425	75.081	227.015	1309.818
12	133	0.441	0.046	0.044	0.011	75.081	2.169	8.141	8.425	-2.213	-7.689	8.001	73.940	258.940	1438.930
13	133	0.441	0.046	0.044	0.012	73.940	2.213	7.689	8.001	-2.257	-7.235	7.579	72.672	293.182	1567.446
14	133	0.441	0.046	0.044	0.012	72.672	2.257	7.235	7.579	-2.301	-6.781	7.161	71.256	329.975	1695.255
15	133	0.441	0.046	0.044	0.013	71.256	2.301	6.781	7.161	-2.345	-6.327	6.747	69.664	369.588	1822.219
16	133	0.441	0.046	0.043	0.014	69.664	2.345	6.327	6.747	-2.388	-5.871	6.339	67.865	412.327	1948.165
17	133	0.441	-0.068	-0.065	-0.022	67.865	2.388	5.871	6.339	-2.324	-5.452	5.926	66.917	458.548	2072.875
18	133	0.441	-0.068	-0.064	-0.023	66.917	2.324	5.452	5.926	-2.259	-5.034	5.518	65.829	508.661	2196.073
19	133	0.441	-0.068	-0.064	-0.025	65.829	2.259	5.034	5.518	-2.196	-4.617	5.113	64.569	560.806	2318.425
20	133	0.441	-0.068	-0.063	-0.027	64.569	2.196	4.617	5.113	-2.133	-4.203	4.713	63.095	615.264	2439.765
21	133	0.441	-0.068	-0.062	-0.028	63.095	2.133	4.203	4.713	-2.070	-3.790	4.318	61.351	672.377	2559.878
22	133	0.441	-0.068	-0.061	-0.031	61.351	2.070	3.790	4.318	-2.009	-3.379	3.931	59.263	732.561	2678.481
23	133	0.441	-0.068	-0.060	-0.033	59.263	2.009	3.379	3.931	-1.949	-2.971	3.553	56.726	796.326	2795.199
24	133	0.441	-0.068	-0.058	-0.036	56.726	1.949	2.971	3.553	-1.891	-2.565	3.187	53.600	864.303	2909.515
25	133	0.441	-0.068	-0.056	-0.039	53.600	1.891	2.565	3.187	-1.835	-2.163	2.837	49.687	937.272	3020.710
26	133	0.441	-0.068	-0.053	-0.043	49.687	1.835	2.163	2.837	-1.782	-1.765	2.508	44.719	1016.197	3127.761
27	133	0.441	-0.068	-0.049	-0.047	44.719	1.782	1.765	2.508	-1.733	-1.371	2.209	38.346	1102.243	3229.177
28	133	0.441	-0.068	-0.044	-0.052	38.346	1.733	1.371	2.209	-1.688	-0.981	1.953	30.166	1196.748	3322.761
29	133	0.441	-0.068	-0.038	-0.057	30.166	1.688	0.981	1.953	-1.651	-0.597	1.755	19.882	1301.057	3405.274
30	133	0.441	-0.068	-0.029	-0.062	19.882	1.651	0.597	1.755	-1.621	-0.217	1.636	7.633	1416.045	3472.108
31	133	0.441	-0.068	-0.019	-0.066	7.633	1.621	0.217	1.636	-1.603	0.158	1.610	-5.643	1541.118	3517.338
32	133	0.441	-0.068	-0.006	-0.068	-5.643	1.603	-0.158	1.610	-1.596	0.532	1.682	-18.423	1672.940	3535.005

33	133	0.441	-0.068	0.006	-0.068	-18.423	1.596	-0.532	1.682	-1.603	0.905	1.840	-29.455	1805.295	3521.926
34	133	0.441	-0.068	0.019	-0.066	-29.455	1.603	-0.905	1.840	-1.621	1.281	2.066	-38.305	1931.478	3479.893
35	133	0.441	-0.068	0.029	-0.062	-38.305	1.621	-1.281	2.066	-1.651	1.660	2.341	-45.167	2047.288	3414.493
36	133	0.441	-0.068	0.038	-0.057	-45.167	1.651	-1.660	2.341	-1.688	2.045	2.652	-50.452	2151.656	3332.053
37	133	0.441	-0.068	0.044	-0.052	-50.452	1.688	-2.045	2.652	-1.733	2.434	2.988	-54.553	2245.426	3237.733
38	133	0.441	-0.068	0.049	-0.047	-54.553	1.733	-2.434	2.988	-1.782	2.828	3.343	-57.783	2330.111	3135.179
39	133	0.441	-0.068	0.053	-0.043	-57.783	1.782	-2.828	3.343	-1.835	3.227	3.712	-60.368	2407.244	3026.830
40	133	0.441	-0.068	0.056	-0.039	-60.368	1.835	-3.227	3.712	-1.891	3.629	4.092	-62.471	2478.150	2914.308
41	133	0.441	-0.068	0.058	-0.036	-62.471	1.891	-3.629	4.092	-1.949	4.034	4.480	-64.208	2543.910	2798.702
42	133	0.441	-0.068	0.060	-0.033	-64.208	1.949	-4.034	4.480	-2.009	4.442	4.876	-65.663	2605.382	2680.761
43	133	0.441	-0.068	0.061	-0.031	-65.663	2.009	-4.442	4.876	-2.070	4.853	5.276	-66.896	2663.251	2561.010
44	133	0.441	-0.068	0.062	-0.028	-66.896	2.070	-4.853	5.276	-2.133	5.266	5.681	-67.954	2718.061	2439.829
45	133	0.441	-0.068	0.063	-0.027	-67.954	2.133	-5.266	5.681	-2.196	5.681	6.090	-68.869	2770.250	2317.496
46	133	0.441	-0.068	0.064	-0.025	-68.869	2.196	-5.681	6.090	-2.259	6.097	6.502	-69.669	2820.173	2194.221
47	133	0.441	-0.068	0.064	-0.023	-69.669	2.259	-6.097	6.502	-2.324	6.515	6.917	-70.372	2868.119	2070.164
48	133	0.941	-0.023	0.022	-0.007	-70.372	2.324	-6.515	6.917	-2.345	7.449	7.810	-72.526	2914.330	1945.450
49	133	0.441	-0.023	0.022	-0.007	-72.526	2.345	-7.449	7.810	-2.367	7.884	8.232	-73.290	2959.005	1820.178
50	133	0.441	-0.023	0.022	-0.007	-73.290	2.367	-7.884	8.232	-2.389	8.319	8.655	-73.979	2998.942	1693.316
51	133	0.441	-0.023	0.022	-0.006	-73.979	2.389	-8.319	8.655	-2.411	8.754	9.080	-74.604	3037.184	1565.932
52	133	0.441	-0.023	0.022	-0.006	-74.604	2.411	-8.754	9.080	-2.433	9.189	9.506	-75.173	3073.891	1438.098
53	133	0.441	-0.023	0.022	-0.006	-75.173	2.433	-9.189	9.506	-2.455	9.625	9.933	-75.693	3109.201	1309.871
54	133	0.441	-0.023	0.022	-0.005	-75.693	2.455	-9.625	9.933	-2.477	10.061	10.362	-76.170	3143.237	1181.300
55	133	0.441	-0.023	0.022	-0.005	-76.170	2.477	-10.061	10.362	-2.499	10.497	10.791	-76.609	3176.103	1052.425
56	133	0.441	-0.023	0.022	-0.005	-76.609	2.499	-10.497	10.791	-2.521	10.934	11.221	-77.015	3207.896	923.280
57	133	0.441	-0.023	0.022	-0.005	-77.015	2.521	-10.934	11.221	-2.544	11.370	11.651	-77.391	3238.697	793.896
58	133	0.441	-0.023	0.022	-0.005	-77.391	2.544	-11.370	11.651	-2.566	11.807	12.083	-77.739	3268.582	664.297
59	133	0.441	-0.023	0.022	-0.004	-77.739	2.566	-11.807	12.083	-2.588	12.244	12.515	-78.064	3297.617	534.505
60	133	0.441	-0.023	0.022	-0.004	-78.064	2.588	-12.244	12.515	-2.611	12.681	12.947	-78.367	3325.860	404.538
61	133	0.441	-0.023	0.022	-0.004	-78.367	2.611	-12.681	12.947	-2.633	13.119	13.380	-78.651	3353.367	274.414
62	133	0.441	-0.023	0.022	-0.004	-78.651	2.633	-13.119	13.380	-2.656	13.556	13.814	-78.917	3380.184	144.146
63	133	0.441	-0.023	0.022	-0.004	-78.917	2.656	-13.556	13.814	-2.678	13.994	14.248	-79.166	3406.357	13.746
														3431.925	-116.773

Segment no.	Height of	DL + LL(3/4PL)	Wind Load	WL H	WL V	Left Angle	Left Thrust x	Left Thrust y	***Left Thrust***	Right Thrust x	Right Thrust y	***Right Thrust***	Right angle	Co-ordinates	
														X	Y
1	132	0.441	0.057	0.056	0.009	83.500	1.517	13.314	13.400	-1.573	-12.863	12.959	83.027	0	0
2	132	0.441	0.057	0.056	0.010	83.027	1.573	12.863	12.959	-1.629	-12.412	12.519	82.522	14.943	131.151
3	132	0.441	0.057	0.056	0.010	82.522	1.629	12.412	12.519	-1.685	-11.961	12.079	81.979	30.967	262.175
4	132	0.441	0.057	0.056	0.010	81.979	1.685	11.961	12.079	-1.741	-11.509	11.640	81.396	48.147	393.052
5	132	0.441	0.057	0.056	0.011	81.396	1.741	11.509	11.640	-1.797	-11.057	11.202	80.766	66.566	523.761
6	132	0.441	0.057	0.056	0.011	80.766	1.797	11.057	11.202	-1.853	-10.604	10.765	80.086	86.315	654.275
7	132	0.441	0.057	0.056	0.012	80.086	1.853	10.604	10.765	-1.909	-10.151	10.329	79.349	107.495	784.565
8	132	0.441	0.057	0.056	0.012	79.349	1.909	10.151	10.329	-1.965	-9.698	9.895	78.546	130.221	914.594
9	132	0.441	0.057	0.056	0.012	78.546	1.965	9.698	9.895	-2.021	-9.244	9.462	77.670	154.619	1044.320
10	132	0.441	0.057	0.055	0.013	77.670	2.021	9.244	9.462	-2.076	-8.790	9.031	76.711	180.831	1173.691
11	132	0.441	0.057	0.055	0.014	76.711	2.076	8.790	9.031	-2.131	-8.335	8.603	75.655	209.018	1302.646
12	132	0.441	0.057	0.055	0.014	75.655	2.131	8.335	8.603	-2.187	-7.879	8.177	74.490	239.360	1431.112
13	132	0.441	0.057	0.055	0.015	74.490	2.187	7.879	8.177	-2.242	-7.423	7.754	73.196	272.064	1558.996
14	132	0.441	0.057	0.055	0.016	73.196	2.242	7.423	7.754	-2.296	-6.966	7.334	71.754	307.362	1686.189
15	132	0.441	0.057	0.055	0.016	71.754	2.296	6.966	7.334	-2.351	-6.508	6.919	70.137	345.523	1812.553
16	132	0.441	0.057	0.054	0.017	70.137	2.351	6.508	6.919	-2.405	-6.049	6.510	68.316	386.852	1937.916
17	132	0.441	-0.057	-0.054	-0.018	68.316	2.405	6.049	6.510	-2.351	-5.626	6.098	67.318	431.702	2062.063
18	132	0.441	-0.057	-0.054	-0.019	67.318	2.351	5.626	6.098	-2.298	-5.204	5.689	66.177	480.475	2184.722
19	132	0.441	-0.057	-0.053	-0.021	66.177	2.298	5.204	5.689	-2.245	-4.783	5.284	64.861	531.376	2306.513
20	132	0.441	-0.057	-0.053	-0.022	64.861	2.245	4.783	5.284	-2.192	-4.364	4.884	63.329	584.693	2427.266
21	132	0.441	-0.057	-0.052	-0.024	63.329	2.192	4.364	4.884	-2.140	-3.946	4.489	61.526	640.769	2546.763
22	132	0.441	-0.057	-0.051	-0.026	61.526	2.140	3.946	4.489	-2.089	-3.530	4.102	59.382	700.020	2664.717
23	132	0.441	-0.057	-0.050	-0.028	59.382	2.089	3.530	4.102	-2.040	-3.117	3.725	56.800	762.952	2780.750
24	132	0.441	-0.057	-0.048	-0.030	56.800	2.040	3.117	3.725	-1.991	-2.705	3.359	53.647	830.180	2894.348
25	132	0.441	-0.057	-0.047	-0.033	53.647	1.991	2.705	3.359	-1.944	-2.297	3.009	49.747	902.459	3004.800
26	132	0.441	-0.057	-0.044	-0.036	49.747	1.944	2.297	3.009	-1.900	-1.891	2.681	44.863	980.703	3111.110
27	132	0.441	-0.057	-0.041	-0.039	44.863	1.900	1.891	2.681	-1.859	-1.489	2.382	38.696	1065.996	3211.853
28	132	0.441	-0.057	-0.037	-0.043	38.696	1.859	1.489	2.382	-1.822	-1.091	2.124	30.915	1159.557	3304.968
29	132	0.441	-0.057	-0.032	-0.047	30.915	1.822	1.091	2.124	-1.791	-0.697	1.921	21.274	1262.579	3387.493
30	132	0.441	-0.057	-0.024	-0.051	21.274	1.791	0.697	1.921	-1.766	-0.307	1.793	9.869	1375.826	3455.309
31	132	0.441	-0.057	-0.016	-0.055	9.869	1.766	0.307	1.793	-1.751	0.079	1.752	-2.596	1498.831	3503.203
32	132	0.441	-0.057	-0.005	-0.057	-2.596	1.751	-0.079	1.752	-1.745	0.464	1.806	-14.891	1628.878	3525.827

33	132	0.441	-0.057	0.005	-0.057	-14.891	1.745	-0.464	1.806	-1.751	0.849	1.945	-25.866	1760.742	3519.849
34	132	0.441	-0.057	0.016	-0.055	-25.866	1.751	-0.849	1.945	-1.766	1.235	2.155	-34.971	1888.310	3485.928
35	132	0.441	-0.057	0.024	-0.051	-34.971	1.766	-1.235	2.155	-1.791	1.625	2.418	-42.230	2007.085	3428.340
36	132	0.441	-0.057	0.032	-0.047	-42.230	1.791	-1.625	2.418	-1.822	2.019	2.720	-47.938	2115.251	3352.682
37	132	0.441	-0.057	0.037	-0.043	-47.938	1.822	-2.019	2.720	-1.859	2.417	3.049	-52.437	2212.991	3263.964
38	132	0.441	-0.057	0.041	-0.039	-52.437	1.859	-2.417	3.049	-1.900	2.819	3.400	-56.019	2301.423	3165.965
39	132	0.441	-0.057	0.044	-0.036	-56.019	1.900	-2.819	3.400	-1.944	3.225	3.766	-58.911	2381.895	3061.331
40	132	0.441	-0.057	0.047	-0.033	-58.911	1.944	-3.225	3.766	-1.991	3.633	4.143	-61.277	2455.671	2951.873
41	132	0.441	-0.057	0.048	-0.030	-61.277	1.991	-3.633	4.143	-2.040	4.045	4.530	-63.241	2523.832	2838.833
42	132	0.441	-0.057	0.050	-0.028	-63.241	2.040	-4.045	4.530	-2.089	4.459	4.924	-64.891	2587.268	2723.075
43	132	0.441	-0.057	0.051	-0.026	-64.891	2.089	-4.459	4.924	-2.140	4.874	5.324	-66.294	2646.699	2605.211
44	132	0.441	-0.057	0.052	-0.024	-66.294	2.140	-4.874	5.324	-2.192	5.292	5.728	-67.499	2702.712	2485.685
45	132	0.441	-0.057	0.053	-0.022	-67.499	2.192	-5.292	5.728	-2.245	5.711	6.137	-68.544	2755.782	2364.823
46	132	0.441	-0.057	0.053	-0.021	-68.544	2.245	-5.711	6.137	-2.298	6.132	6.548	-69.458	2806.298	2242.871
47	132	0.441	-0.057	0.054	-0.019	-69.458	2.298	-6.132	6.548	-2.351	6.554	6.963	-70.264	2854.580	2120.019
48	132	0.941	-0.011	0.011	-0.004	-70.264	2.351	-6.554	6.963	-2.362	7.492	7.855	-72.500	2900.897	1996.411
49	132	0.441	-0.011	0.011	-0.003	-72.500	2.362	-7.492	7.855	-2.373	7.930	8.277	-73.340	2945.472	1872.165
50	132	0.441	-0.011	0.011	-0.003	-73.340	2.373	-7.930	8.277	-2.384	8.368	8.701	-74.099	2985.165	1746.274
51	132	0.441	-0.011	0.011	-0.003	-74.099	2.384	-8.368	8.701	-2.395	8.806	9.126	-74.786	3023.007	1619.815
52	132	0.441	-0.011	0.011	-0.003	-74.786	2.395	-8.806	9.126	-2.406	9.245	9.553	-75.413	3059.173	1492.866
53	132	0.441	-0.011	0.011	-0.003	-75.413	2.406	-9.245	9.553	-2.417	9.683	9.980	-75.986	3093.813	1365.493
54	132	0.441	-0.011	0.011	-0.003	-75.986	2.417	-9.683	9.980	-2.428	10.122	10.409	-76.511	3127.058	1237.748
55	132	0.441	-0.011	0.011	-0.003	-76.511	2.428	-10.122	10.409	-2.439	10.561	10.839	-76.995	3159.024	1109.677
56	132	0.441	-0.011	0.011	-0.002	-76.995	2.439	-10.561	10.839	-2.450	11.000	11.269	-77.442	3189.813	981.318
57	132	0.441	-0.011	0.011	-0.002	-77.442	2.450	-11.000	11.269	-2.461	11.439	11.700	-77.856	3219.518	852.703
58	132	0.441	-0.011	0.011	-0.002	-77.856	2.461	-11.439	11.700	-2.472	11.878	12.132	-78.241	3248.217	723.861
59	132	0.441	-0.011	0.011	-0.002	-78.241	2.472	-11.878	12.132	-2.484	12.317	12.565	-78.599	3275.985	594.815
60	132	0.441	-0.011	0.011	-0.002	-78.599	2.484	-12.317	12.565	-2.495	12.756	12.998	-78.934	3302.886	465.585
61	132	0.441	-0.011	0.011	-0.002	-78.934	2.495	-12.756	12.998	-2.506	13.196	13.431	-79.247	3328.978	336.189
62	132	0.441	-0.011	0.011	-0.002	-79.247	2.506	-13.196	13.431	-2.517	13.635	13.865	-79.540	3354.314	206.644
63	132	0.441	-0.011	0.011	-0.002	-79.540	2.517	-13.635	13.865	-2.529	14.075	14.300	-79.815	3378.943	76.962
														3402.908	-52.845

Segment no.	Height of Segment	DL + LL (1/2PL)	Wind Load (Cpi=0)	WL H	WL V	Left Angle	Left Thrust x	Left Thrust y	***Left Thrust***	Right Thrust x	Right Thrust y	***Right Thrust***	Right angle	Co-ordinates	
														X	Y
1	133	0.441	0.046	0.045	0.008	82.050	1.846	13.221	13.349	-1.891	-12.772	12.911	81.577	0.000	0.000
2	133	0.441	0.046	0.045	0.008	81.577	1.891	12.772	12.911	-1.936	-12.323	12.474	81.070	18.395	131.722
3	133	0.441	0.046	0.045	0.008	81.070	1.936	12.323	12.474	-1.981	-11.874	12.038	80.527	37.877	263.287
4	133	0.441	0.046	0.045	0.008	80.527	1.981	11.874	12.038	-2.026	-11.424	11.602	79.943	58.522	394.675
5	133	0.441	0.046	0.045	0.009	79.943	2.026	11.424	11.602	-2.071	-10.974	11.167	79.314	80.411	525.862
6	133	0.441	0.046	0.045	0.009	79.314	2.071	10.974	11.167	-2.115	-10.523	10.734	78.634	103.635	656.818
7	133	0.441	0.046	0.045	0.009	78.634	2.115	10.523	10.734	-2.160	-10.073	10.302	77.896	128.297	787.512
8	133	0.441	0.046	0.045	0.010	77.896	2.160	10.073	10.302	-2.205	-9.622	9.871	77.094	154.509	917.903
9	133	0.441	0.046	0.044	0.010	77.094	2.205	9.622	9.871	-2.249	-9.170	9.442	76.219	182.397	1047.946
10	133	0.441	0.046	0.044	0.010	76.219	2.249	9.170	9.442	-2.294	-8.719	9.015	75.261	212.102	1177.587
11	133	0.441	0.046	0.044	0.011	75.261	2.294	8.719	9.015	-2.338	-8.266	8.591	74.208	243.783	1306.758
12	133	0.441	0.046	0.044	0.011	74.208	2.338	8.266	8.591	-2.382	-7.814	8.169	73.046	277.620	1435.382
13	133	0.441	0.046	0.044	0.012	73.046	2.382	7.814	8.169	-2.426	-7.360	7.750	71.757	313.815	1563.362
14	133	0.441	0.046	0.044	0.012	71.757	2.426	7.360	7.750	-2.470	-6.906	7.335	70.321	352.599	1690.582
15	133	0.441	0.046	0.044	0.013	70.321	2.470	6.906	7.335	-2.514	-6.452	6.924	68.714	394.235	1816.897
16	133	0.441	0.046	0.043	0.014	68.714	2.514	6.452	6.924	-2.557	-5.996	6.519	66.906	439.022	1942.129
17	133	0.441	-0.068	-0.065	-0.022	66.906	2.557	5.996	6.519	-2.492	-5.577	6.109	65.921	487.303	2066.056
18	133	0.441	-0.068	-0.064	-0.023	65.921	2.492	5.577	6.109	-2.428	-5.159	5.702	64.797	539.472	2188.397
19	133	0.441	-0.068	-0.064	-0.025	64.797	2.428	5.159	5.702	-2.364	-4.742	5.299	63.502	593.735	2309.824
20	133	0.441	-0.068	-0.063	-0.027	63.502	2.364	4.742	5.299	-2.301	-4.328	4.901	61.998	650.371	2430.163
21	133	0.441	-0.068	-0.062	-0.028	61.998	2.301	4.328	4.901	-2.239	-3.915	4.510	60.232	709.710	2549.192
22	133	0.441	-0.068	-0.061	-0.031	60.232	2.239	3.915	4.510	-2.178	-3.504	4.126	58.136	772.155	2666.621
23	133	0.441	-0.068	-0.060	-0.033	58.136	2.178	3.504	4.126	-2.118	-3.096	3.751	55.619	838.188	2782.071
24	133	0.441	-0.068	-0.058	-0.036	55.619	2.118	3.096	3.751	-2.060	-2.690	3.388	52.558	908.399	2895.028
25	133	0.441	-0.068	-0.056	-0.039	52.558	2.060	2.690	3.388	-2.004	-2.288	3.042	48.788	983.503	3004.793
26	133	0.441	-0.068	-0.053	-0.043	48.788	2.004	2.288	3.042	-1.951	-1.890	2.716	44.089	1064.361	3110.392
27	133	0.441	-0.068	-0.049	-0.047	44.089	1.951	1.890	2.716	-1.902	-1.496	2.419	38.189	1151.989	3210.444
28	133	0.441	-0.068	-0.044	-0.052	38.189	1.902	1.496	2.419	-1.857	-1.106	2.162	30.784	1247.517	3302.982
29	133	0.441	-0.068	-0.038	-0.057	30.784	1.857	1.106	2.162	-1.819	-0.722	1.957	21.644	1352.052	3385.210
30	133	0.441	-0.068	-0.029	-0.062	21.644	1.819	0.722	1.957	-1.790	-0.342	1.822	10.826	1466.313	3453.279
31	133	0.441	-0.068	-0.019	-0.066	10.826	1.790	0.342	1.822	-1.771	0.033	1.772	-1.079	1589.936	3502.334
32	133	0.941	-0.068	-0.006	-0.068	-1.079	1.771	-0.033	1.772	-1.765	0.907	1.984	-27.192	1720.569	3527.314

33	133	0.441	-0.068	0.006	-0.068	-27.192	1.765	-0.907	1.984	-1.771	1.280	2.185	-35.854	1853.546	3524.810
34	133	0.441	-0.068	0.019	-0.066	-35.854	1.771	-1.280	2.185	-1.790	1.656	2.438	-42.767	1971.846	3464.032
35	133	0.441	-0.068	0.029	-0.062	-42.767	1.790	-1.656	2.438	-1.819	2.035	2.730	-48.207	2079.644	3386.131
36	133	0.441	-0.068	0.038	-0.057	-48.207	1.819	-2.035	2.730	-1.857	2.420	3.050	-52.494	2177.282	3295.821
37	133	0.441	-0.068	0.044	-0.052	-52.494	1.857	-2.420	3.050	-1.902	2.809	3.392	-55.905	2265.918	3196.662
38	133	0.441	-0.068	0.049	-0.047	-55.905	1.902	-2.809	3.392	-1.951	3.203	3.751	-58.657	2346.895	3091.154
39	133	0.441	-0.068	0.053	-0.043	-58.657	1.951	-3.203	3.751	-2.004	3.602	4.122	-60.907	2421.450	2981.015
40	133	0.441	-0.068	0.056	-0.039	-60.907	2.004	-3.602	4.122	-2.060	4.004	4.503	-62.773	2490.632	2867.425
41	133	0.441	-0.068	0.058	-0.036	-62.773	2.060	-4.004	4.503	-2.118	4.409	4.891	-64.340	2555.300	2751.205
42	133	0.441	-0.068	0.060	-0.033	-64.340	2.118	-4.409	4.891	-2.178	4.817	5.287	-65.672	2616.150	2632.942
43	133	0.441	-0.068	0.061	-0.031	-65.672	2.178	-4.817	5.287	-2.239	5.228	5.687	-66.816	2673.743	2513.058
44	133	0.441	-0.068	0.062	-0.028	-66.816	2.239	-5.228	5.687	-2.301	5.641	6.092	-67.807	2728.534	2391.868
45	133	0.441	-0.068	0.063	-0.027	-67.807	2.301	-5.641	6.092	-2.364	6.056	6.501	-68.674	2780.895	2269.609
46	133	0.441	-0.068	0.064	-0.025	-68.674	2.364	-6.056	6.501	-2.428	6.472	6.913	-69.437	2831.133	2146.462
47	133	0.441	-0.068	0.064	-0.023	-69.437	2.428	-6.472	6.913	-2.492	6.890	7.327	-70.115	2879.502	2022.569
48	133	0.441	-0.023	0.022	-0.007	-70.115	2.492	-6.890	7.327	-2.514	7.324	7.744	-71.057	2926.216	1898.043
49	133	0.441	-0.023	0.022	-0.007	-71.057	2.514	-7.324	7.744	-2.536	7.759	8.163	-71.903	2971.454	1772.973
50	133	0.441	-0.023	0.022	-0.007	-71.903	2.536	-7.759	8.163	-2.557	8.194	8.584	-72.666	3014.628	1647.175
51	133	0.441	-0.023	0.022	-0.006	-72.666	2.557	-8.194	8.584	-2.579	8.629	9.006	-73.358	3055.941	1520.755
52	133	0.441	-0.023	0.022	-0.006	-73.358	2.579	-8.629	9.006	-2.601	9.064	9.430	-73.988	3095.567	1393.795
53	133	0.441	-0.023	0.022	-0.006	-73.988	2.601	-9.064	9.430	-2.623	9.500	9.856	-74.563	3133.657	1266.366
54	133	0.441	-0.023	0.022	-0.005	-74.563	2.623	-9.500	9.856	-2.646	9.936	10.282	-75.091	3170.344	1138.526
55	133	0.441	-0.023	0.022	-0.005	-75.091	2.646	-9.936	10.282	-2.668	10.372	10.710	-75.576	3205.746	1010.324
56	133	0.441	-0.023	0.022	-0.005	-75.576	2.668	-10.372	10.710	-2.690	10.809	11.139	-76.025	3239.965	881.801
57	133	0.441	-0.023	0.022	-0.005	-76.025	2.690	-10.809	11.139	-2.712	11.245	11.568	-76.440	3273.094	752.994
58	133	0.441	-0.023	0.022	-0.005	-76.440	2.712	-11.245	11.568	-2.735	11.682	11.998	-76.825	3305.214	623.930
59	133	0.441	-0.023	0.022	-0.004	-76.825	2.735	-11.682	11.998	-2.757	12.119	12.429	-77.184	3336.398	494.638
60	133	0.441	-0.023	0.022	-0.004	-77.184	2.757	-12.119	12.429	-2.779	12.556	12.860	-77.519	3366.711	365.138
61	133	0.441	-0.023	0.022	-0.004	-77.519	2.779	-12.556	12.860	-2.802	12.994	13.292	-77.832	3396.213	235.452
62	133	0.441	-0.023	0.022	-0.004	-77.832	2.802	-12.994	13.292	-2.824	13.431	13.725	-78.125	3424.956	105.595
63	133	0.441	-0.023	0.022	-0.004	-78.125	2.824	-13.431	13.725	-2.847	13.869	14.158	-78.401	3452.990	-24.417
														3480.358	-154.571

Segment no.	Height of segment	DL + LL(1/2PL)	Wind Load (Cpi=-0.2)	WL H	WL V	Left Angle	Left Thrust x	Left Thrust y	***Left Thrust***	Right Thrust x	Right Thrust y	***Right Thrust***	Right angle	Co-ordinates	
														X	Y
1	132.3	0.441	0.057	0.056	0.009	82.800	1.698	13.439	13.546	-1.754	-12.988	13.106	82.309	0	0
2	132.3	0.441	0.057	0.056	0.010	82.309	1.754	12.988	13.106	-1.810	-12.537	12.667	81.784	16.582	131.257
3	132.3	0.441	0.057	0.056	0.010	81.784	1.810	12.537	12.667	-1.866	-12.086	12.229	81.222	34.287	262.367
4	132.3	0.441	0.057	0.056	0.010	81.222	1.866	12.086	12.229	-1.922	-11.634	11.792	80.618	53.193	393.309
5	132.3	0.441	0.057	0.056	0.011	80.618	1.922	11.634	11.792	-1.978	-11.182	11.355	79.967	73.383	524.059
6	132.3	0.441	0.057	0.056	0.011	79.967	1.978	11.182	11.355	-2.034	-10.729	10.920	79.265	94.950	654.589
7	132.3	0.441	0.057	0.056	0.012	79.265	2.034	10.729	10.920	-2.090	-10.276	10.487	78.504	117.999	784.866
8	132.3	0.441	0.057	0.056	0.012	78.504	2.090	10.276	10.487	-2.146	-9.823	10.055	77.678	142.643	914.851
9	132.3	0.441	0.057	0.056	0.012	77.678	2.146	9.823	10.055	-2.201	-9.369	9.624	76.778	169.010	1044.497
10	132.3	0.441	0.057	0.055	0.013	76.778	2.201	9.369	9.624	-2.257	-8.915	9.196	75.793	197.244	1173.749
11	132.3	0.441	0.057	0.055	0.014	75.793	2.257	8.915	9.196	-2.312	-8.460	8.770	74.713	227.505	1302.542
12	132.3	0.441	0.057	0.055	0.014	74.713	2.312	8.460	8.770	-2.367	-8.004	8.347	73.523	259.973	1430.796
13	132.3	0.441	0.057	0.055	0.015	73.523	2.367	8.004	8.347	-2.422	-7.548	7.927	72.206	294.854	1558.415
14	132.3	0.441	0.057	0.055	0.016	72.206	2.422	7.548	7.927	-2.477	-7.091	7.511	70.742	332.378	1685.282
15	132.3	0.441	0.057	0.055	0.016	70.742	2.477	7.091	7.511	-2.532	-6.633	7.100	69.108	372.808	1811.253
16	132.3	0.441	0.057	0.054	0.017	69.108	2.532	6.633	7.100	-2.586	-6.174	6.694	67.273	416.443	1936.150
17	132.3	0.441	-0.057	-0.054	-0.018	67.273	2.586	6.174	6.694	-2.532	-5.751	6.284	66.236	463.623	2059.751
18	132.3	0.441	-0.057	-0.054	-0.019	66.236	2.532	5.751	6.284	-2.479	-5.329	5.877	65.056	514.736	2181.779
19	132.3	0.441	-0.057	-0.053	-0.021	65.056	2.479	5.329	5.877	-2.425	-4.908	5.475	63.703	568.048	2302.862
20	132.3	0.441	-0.057	-0.053	-0.022	63.703	2.425	4.908	5.475	-2.373	-4.489	5.078	62.139	623.843	2422.821
21	132.3	0.441	-0.057	-0.052	-0.024	62.139	2.373	4.489	5.078	-2.321	-4.071	4.687	60.312	682.454	2541.430
22	132.3	0.441	-0.057	-0.051	-0.026	60.312	2.321	4.071	4.687	-2.270	-3.655	4.303	58.158	744.282	2658.394
23	132.3	0.441	-0.057	-0.050	-0.028	58.158	2.270	3.655	4.303	-2.220	-3.242	3.929	55.592	809.808	2773.328
24	132.3	0.441	-0.057	-0.048	-0.030	55.592	2.220	3.242	3.929	-2.172	-2.830	3.568	52.498	879.606	2885.718
25	132.3	0.441	-0.057	-0.047	-0.033	52.498	2.172	2.830	3.568	-2.125	-2.422	3.222	48.730	954.367	2994.869
26	132.3	0.441	-0.057	-0.044	-0.036	48.730	2.125	2.422	3.222	-2.081	-2.016	2.898	44.093	1034.909	3099.828
27	132.3	0.441	-0.057	-0.041	-0.039	44.093	2.081	2.016	2.898	-2.040	-1.614	2.601	38.355	1122.176	3199.265
28	132.3	0.441	-0.057	-0.037	-0.043	38.355	2.040	1.614	2.601	-2.003	-1.216	2.343	31.266	1217.195	3291.323
29	132.3	0.441	-0.057	-0.032	-0.047	31.266	2.003	1.216	2.343	-1.971	-0.822	2.136	22.639	1320.941	3373.420
30	132.3	0.441	-0.057	-0.024	-0.051	22.639	1.971	0.822	2.136	-1.947	-0.432	1.994	12.518	1434.028	3442.084
31	132.3	0.441	-0.057	-0.016	-0.055	12.518	1.947	0.432	1.994	-1.931	-0.046	1.932	1.354	1556.134	3493.010
32	132.3	0.941	-0.057	-0.005	-0.057	1.354	1.931	0.046	1.932	-1.926	0.839	2.101	-23.541	1685.289	3521.684

33	132.3	0.441	-0.057	0.005	-0.057	-23.541	1.926	-0.839	2.101	-1.931	1.224	2.286	-32.359	1817.552	3524.810
34	132.3	0.441	-0.057	0.016	-0.055	-32.359	1.931	-1.224	2.286	-1.947	1.610	2.527	-39.595	1938.842	3471.970
35	132.3	0.441	-0.057	0.024	-0.051	-39.595	1.947	-1.610	2.527	-1.971	2.000	2.808	-45.417	2050.597	3401.159
36	132.3	0.441	-0.057	0.032	-0.047	-45.417	1.971	-2.000	2.808	-2.003	2.394	3.121	-50.086	2152.543	3316.837
37	132.3	0.441	-0.057	0.037	-0.043	-50.086	2.003	-2.394	3.121	-2.040	2.792	3.458	-53.850	2245.410	3222.608
38	132.3	0.441	-0.057	0.041	-0.039	-53.850	2.040	-2.792	3.458	-2.081	3.194	3.812	-56.916	2330.299	3121.133
39	132.3	0.441	-0.057	0.044	-0.036	-56.916	2.081	-3.194	3.812	-2.125	3.600	4.180	-59.443	2408.342	3014.304
40	132.3	0.441	-0.057	0.047	-0.033	-59.443	2.125	-3.600	4.180	-2.172	4.008	4.559	-61.549	2480.560	2903.453
41	132.3	0.441	-0.057	0.048	-0.030	-61.549	2.172	-4.008	4.559	-2.220	4.420	4.946	-63.327	2547.822	2789.527
42	132.3	0.441	-0.057	0.050	-0.028	-63.327	2.220	-4.420	4.946	-2.270	4.834	5.340	-64.842	2610.849	2673.205
43	132.3	0.441	-0.057	0.051	-0.026	-64.842	2.270	-4.834	5.340	-2.321	5.249	5.740	-66.146	2670.239	2554.985
44	132.3	0.441	-0.057	0.052	-0.024	-66.146	2.321	-5.249	5.740	-2.373	5.667	6.144	-67.280	2726.482	2435.235
45	132.3	0.441	-0.057	0.053	-0.022	-67.280	2.373	-5.667	6.144	-2.425	6.086	6.552	-68.272	2779.984	2314.236
46	132.3	0.441	-0.057	0.053	-0.021	-68.272	2.425	-6.086	6.552	-2.479	6.507	6.963	-69.148	2831.083	2192.202
47	132.3	0.441	-0.057	0.054	-0.019	-69.148	2.479	-6.507	6.963	-2.532	6.929	7.377	-69.926	2880.059	2069.301
48	132.3	0.441	-0.011	0.011	-0.004	-69.926	2.532	-6.929	7.377	-2.543	7.367	7.793	-70.956	2927.152	1945.666
49	132.3	0.441	-0.011	0.011	-0.003	-70.956	2.543	-7.367	7.793	-2.554	7.805	8.212	-71.881	2972.562	1821.404
50	132.3	0.441	-0.011	0.011	-0.003	-71.881	2.554	-7.805	8.212	-2.565	8.243	8.633	-72.717	3015.731	1696.345
51	132.3	0.441	-0.011	0.011	-0.003	-72.717	2.565	-8.243	8.633	-2.576	8.681	9.055	-73.475	3056.874	1570.605
52	132.3	0.441	-0.011	0.011	-0.003	-73.475	2.576	-8.681	9.055	-2.587	9.120	9.479	-74.165	3096.180	1444.278
53	132.3	0.441	-0.011	0.011	-0.003	-74.165	2.587	-9.120	9.479	-2.598	9.558	9.905	-74.796	3133.811	1317.443
54	132.3	0.441	-0.011	0.011	-0.003	-74.796	2.598	-9.558	9.905	-2.609	9.997	10.332	-75.374	3169.912	1190.164
55	132.3	0.441	-0.011	0.011	-0.003	-75.374	2.609	-9.997	10.332	-2.620	10.436	10.760	-75.907	3204.609	1062.495
56	132.3	0.441	-0.011	0.011	-0.002	-75.907	2.620	-10.436	10.760	-2.631	10.875	11.188	-76.399	3238.015	934.482
57	132.3	0.441	-0.011	0.011	-0.002	-76.399	2.631	-10.875	11.188	-2.642	11.314	11.618	-76.855	3270.229	806.164
58	132.3	0.441	-0.011	0.011	-0.002	-76.855	2.642	-11.314	11.618	-2.653	11.753	12.049	-77.278	3301.340	677.574
59	132.3	0.441	-0.011	0.011	-0.002	-77.278	2.653	-11.753	12.049	-2.664	12.192	12.480	-77.672	3331.427	548.740
60	132.3	0.441	-0.011	0.011	-0.002	-77.672	2.664	-12.192	12.480	-2.676	12.631	12.912	-78.040	3360.562	419.688
61	132.3	0.441	-0.011	0.011	-0.002	-78.040	2.676	-12.631	12.912	-2.687	13.071	13.344	-78.384	3388.808	290.438
62	132.3	0.441	-0.011	0.011	-0.002	-78.384	2.687	-13.071	13.344	-2.698	13.510	13.777	-78.706	3416.225	161.010
63	132.3	0.441	-0.011	0.011	-0.002	-78.706	2.698	-13.510	13.777	-2.709	13.950	14.210	-79.009	3442.864	31.420
														3468.775	-98.318

Appendix B

I. *Dead Load, T=20° full*

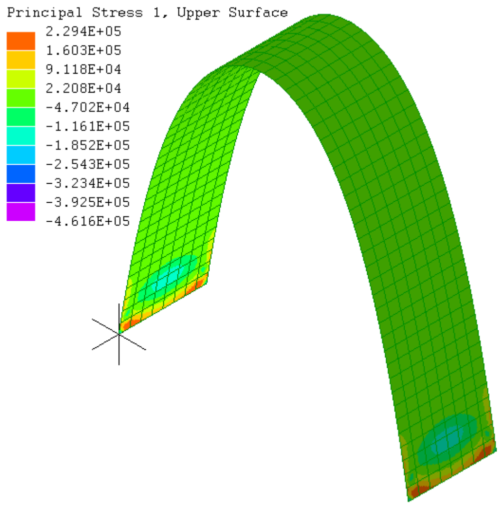

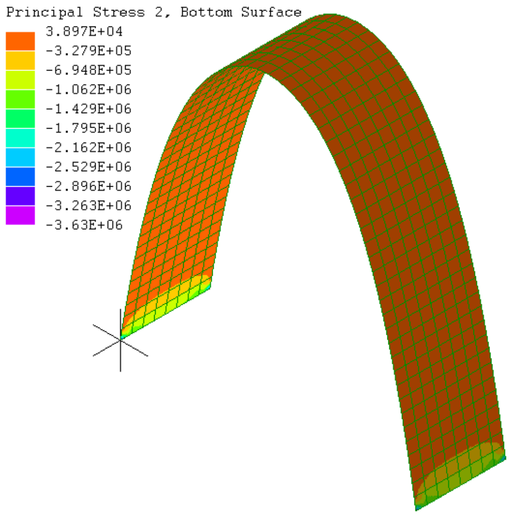

II. *Dead Load, T=20° left half*

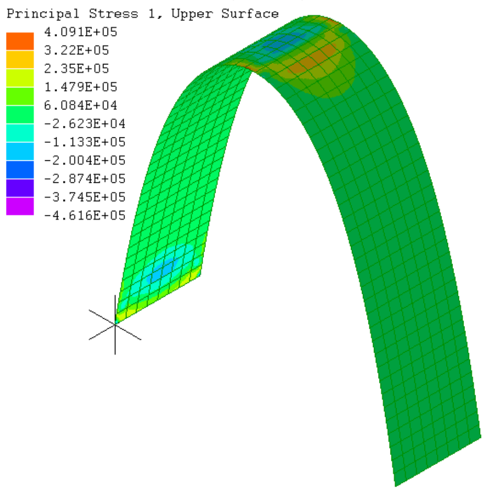

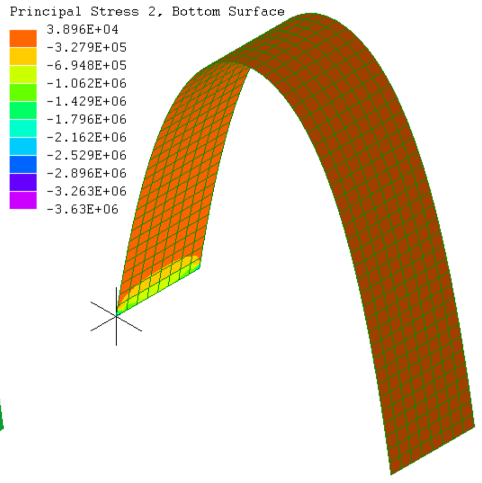

III. Dead Load, T=20° right half

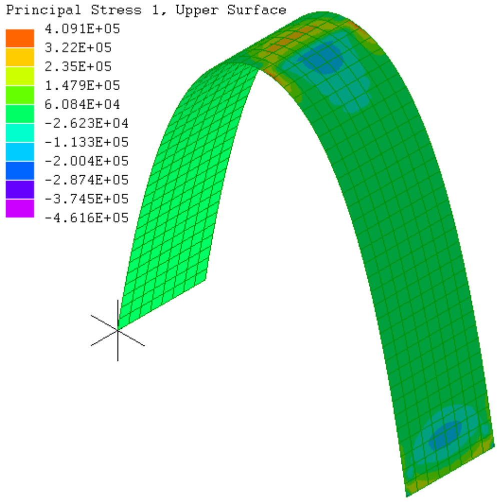

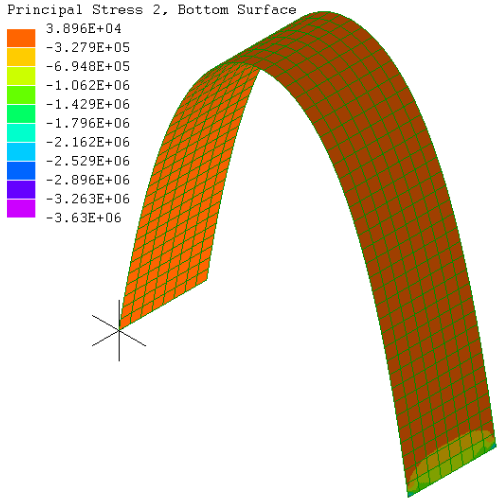

IV. Dead Load, T=-20° full

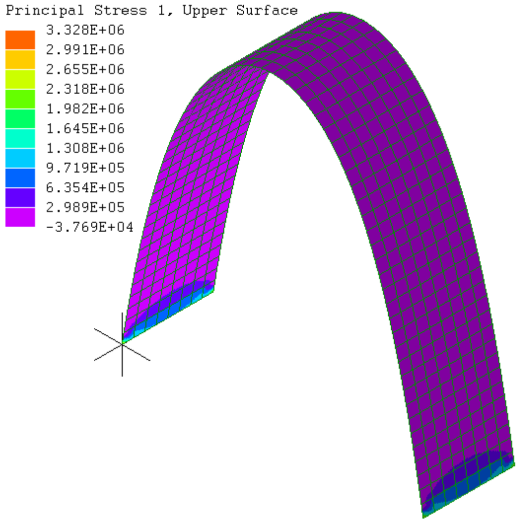

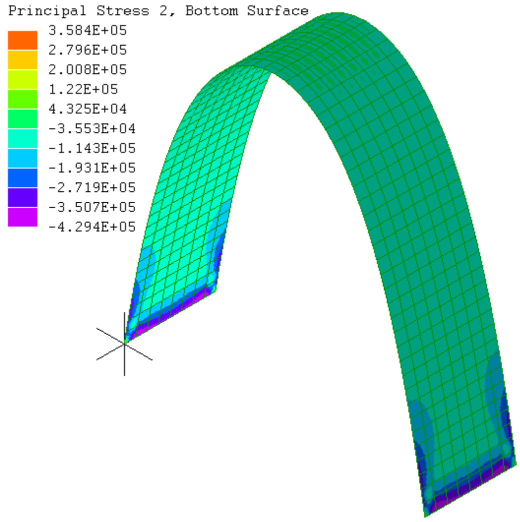

V. Dead Load, T=-20° left half

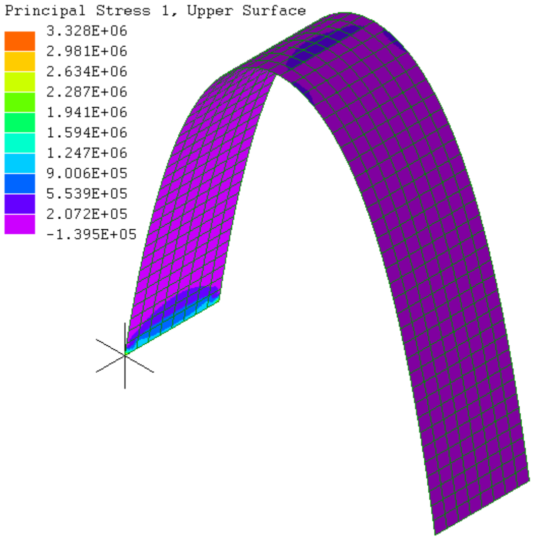

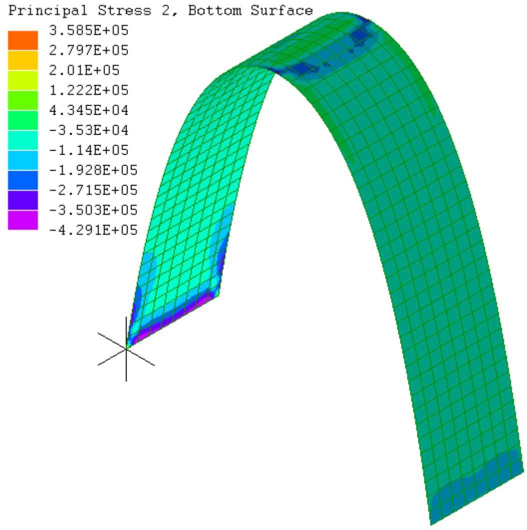

VI. Dead Load, T=-20° right half

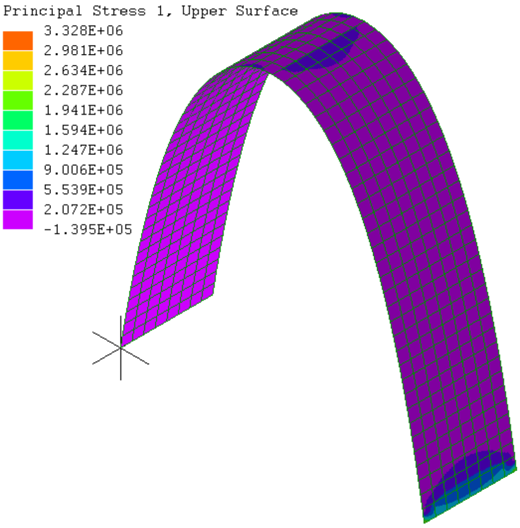

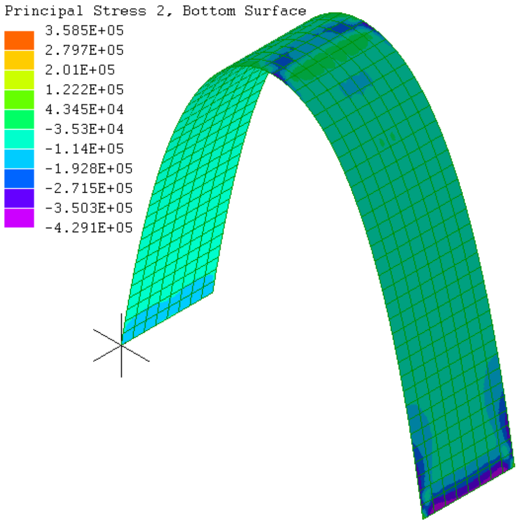

VII. Dead Load, Live Load full, T=20° left half

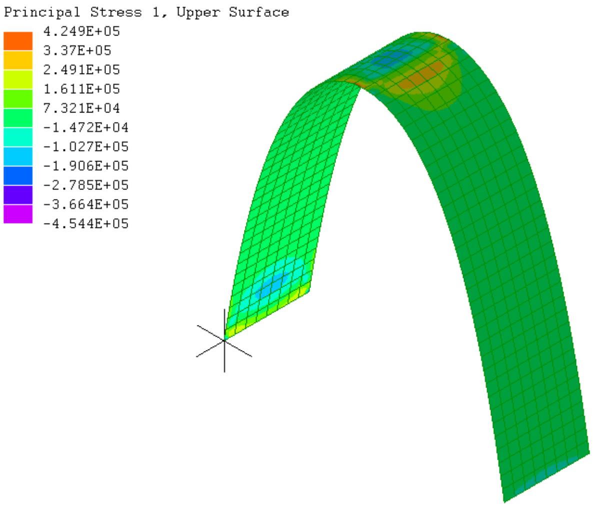

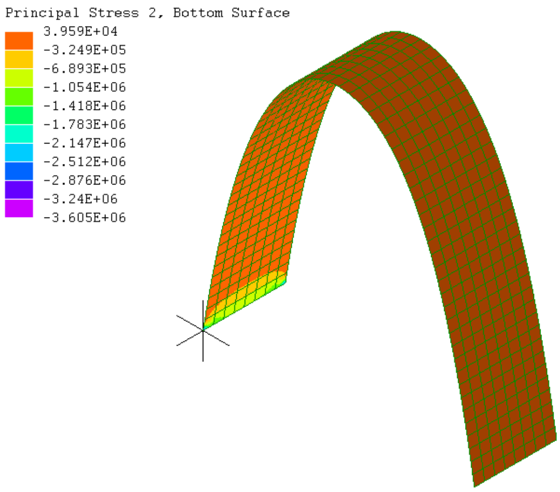

VIII. Dead Load, Live Load full, T=-20° left half

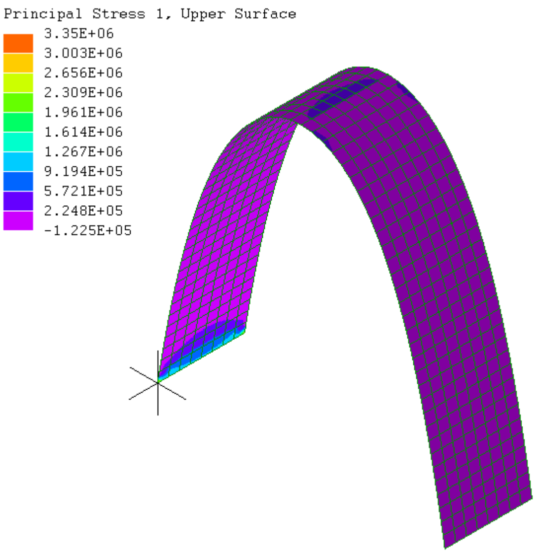

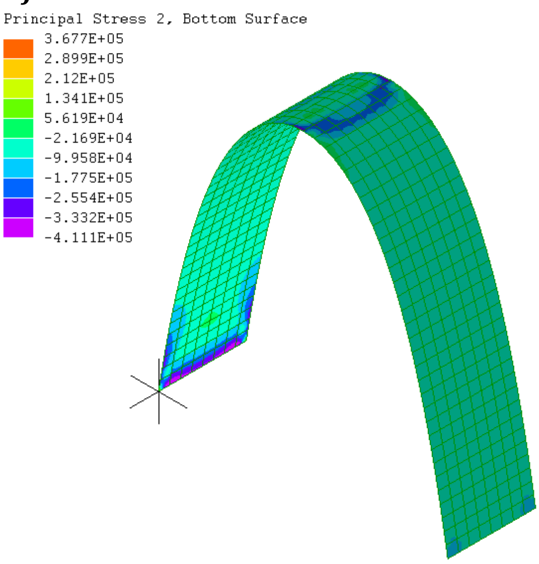

IX. Dead Load, Live Load full, Wind Load (Cpi=0), T=20° left half

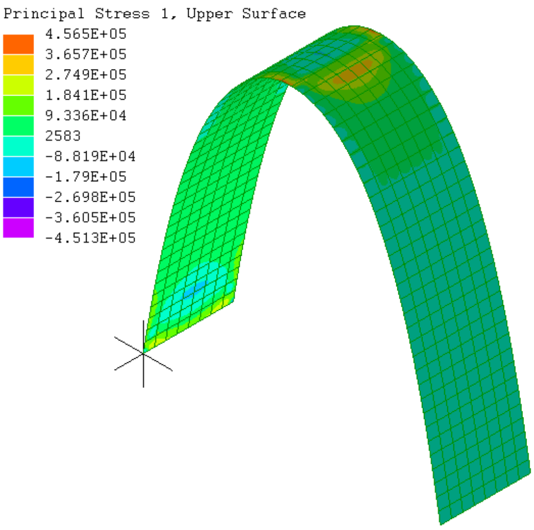

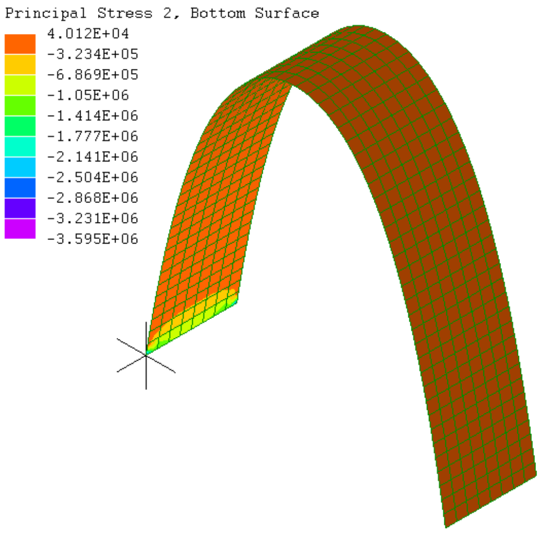

X. Dead Load, Live Load full, Wind Load (Cpi=0), T=-20° right half

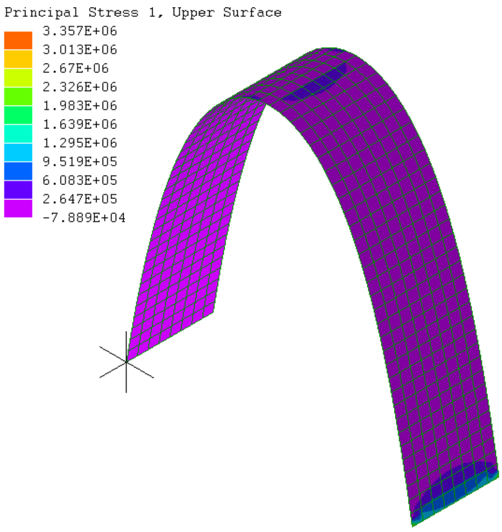

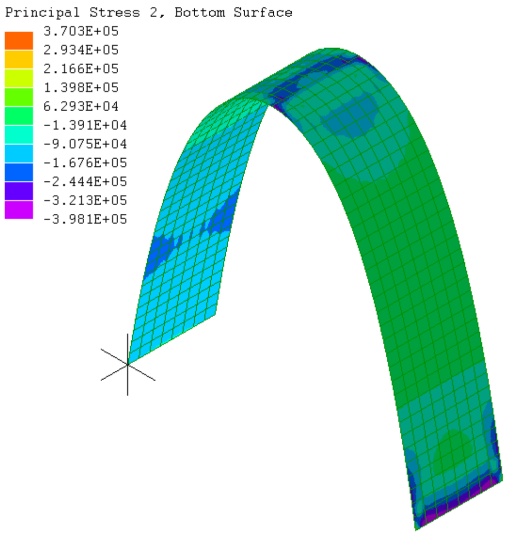

XI. Dead Load, Live Load full, Wind Load (Cpi=-0.2), T=20° left half

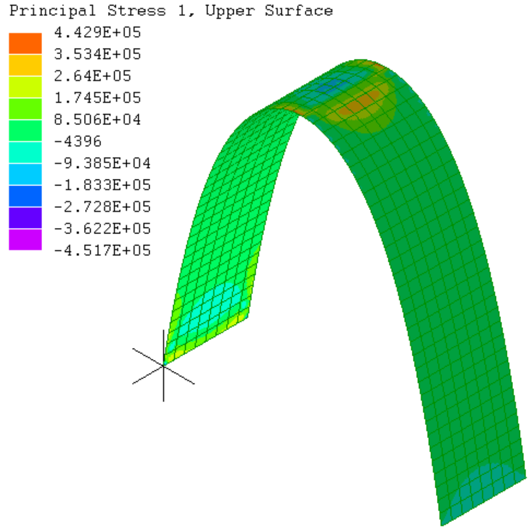

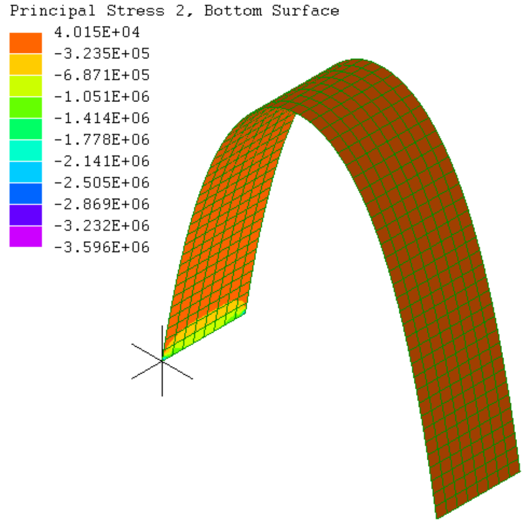

XII. Dead Load, Live Load full, Wind Load (Cpi=-0.2), T=-20° right half

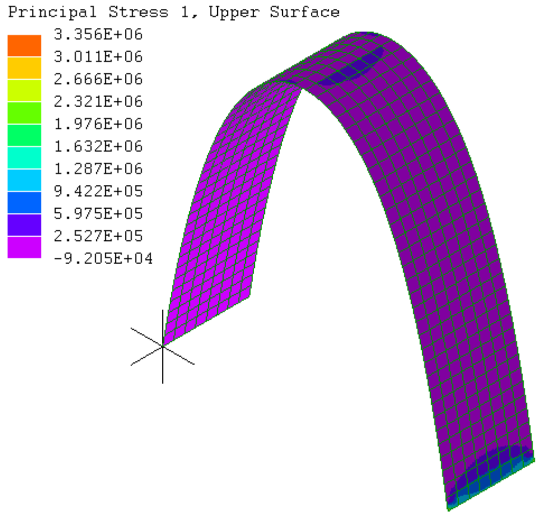

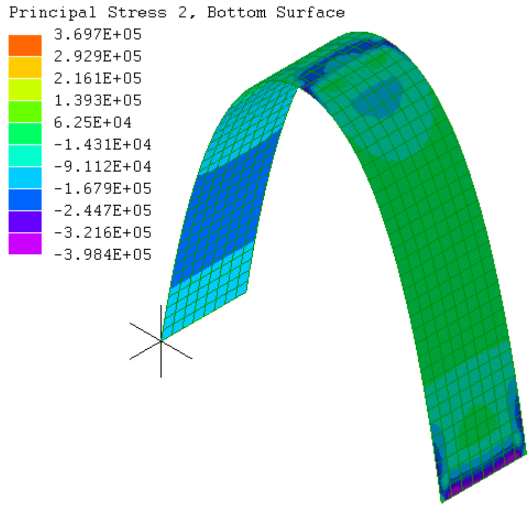

XIII. Dead Load, Live Load left half, T=20° left half

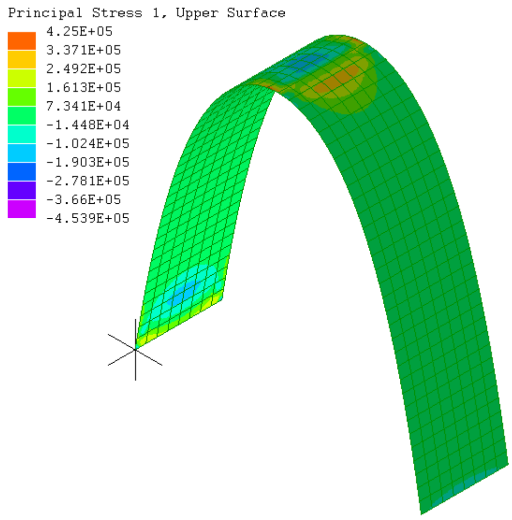

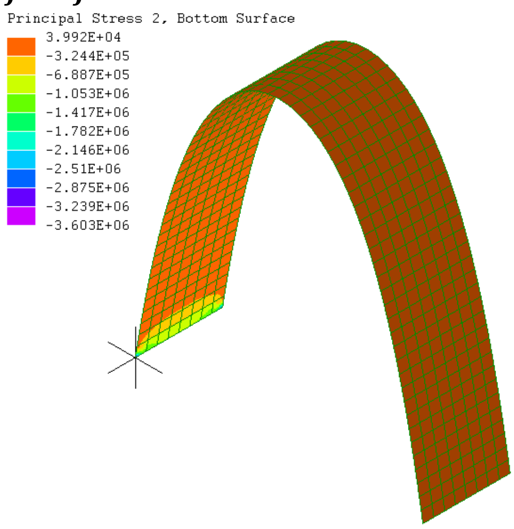

XIV. *Dead Load, Live Load left half, T=-20° right half*

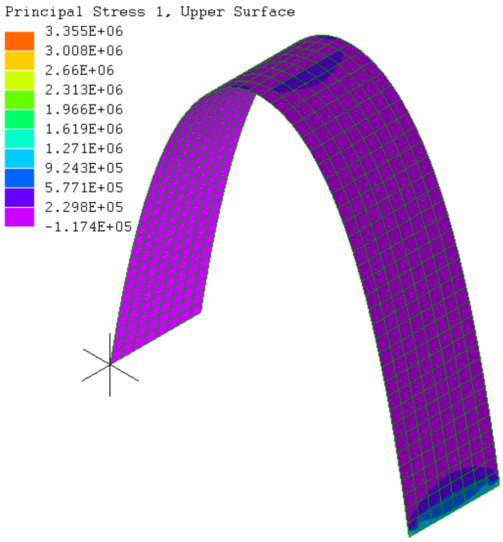

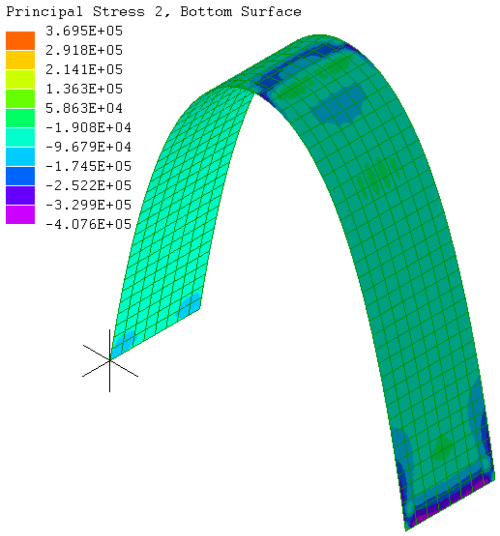

XV. *Dead Load, Live Load left half, Wind Load (Cpi=0), T=20° left half*

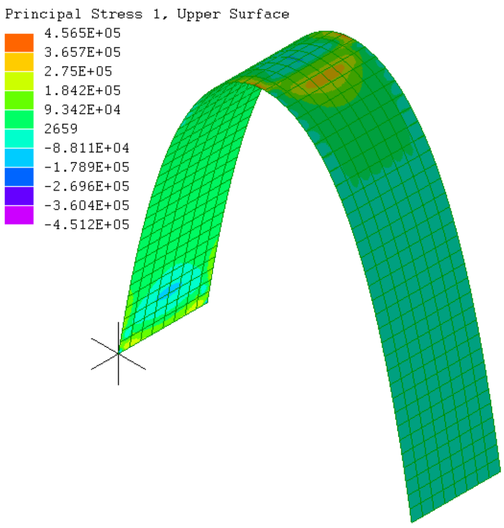

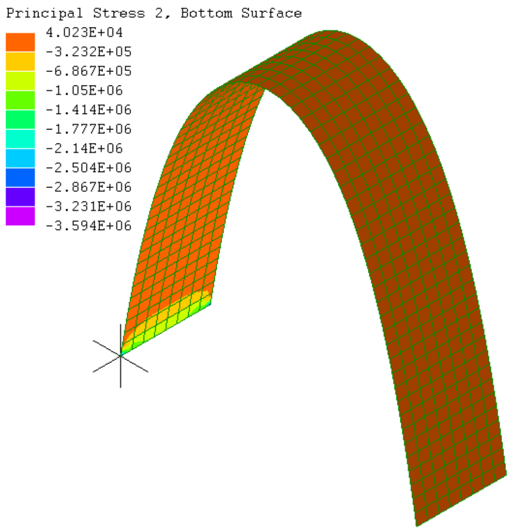

XVI. *Dead Load, Live Load left half, Wind Load (Cpi=0), T=-20° right half*

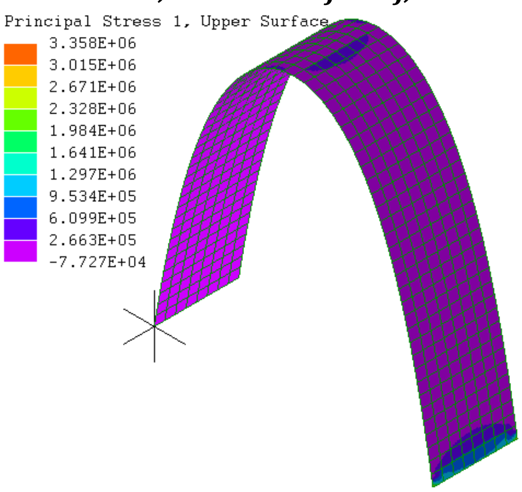

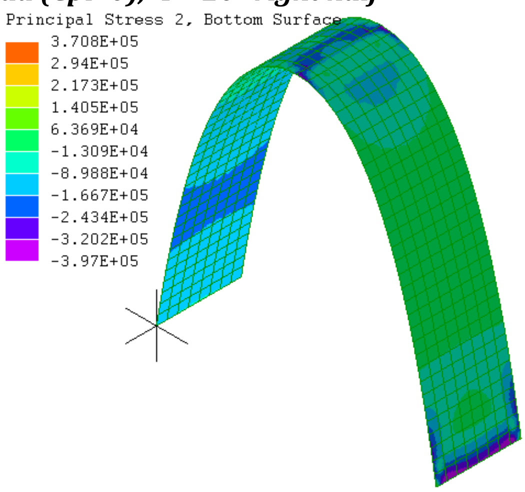

XVII. Dead Load, Live Load left half, Wind Load (Cpi=-0.2), T=20° left half

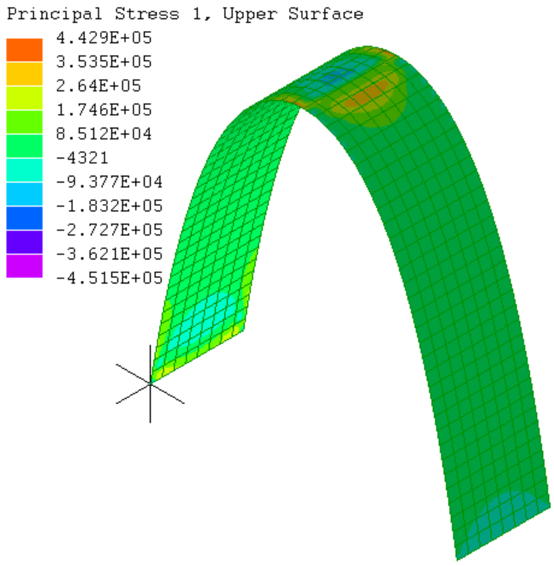

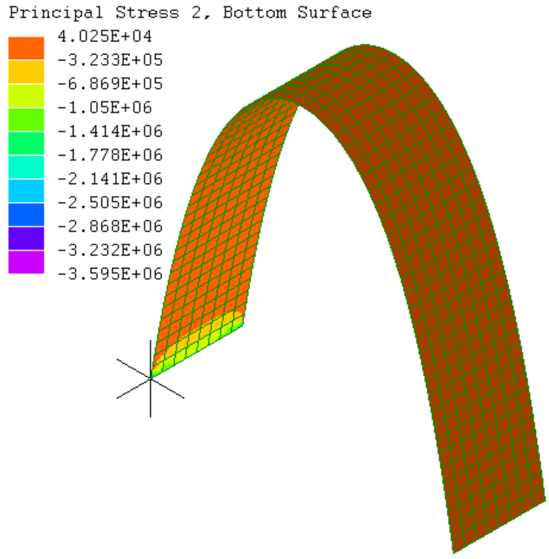

XVIII. Dead Load, Live Load left half, Wind Load (Cpi=-0.2), T=-20° right half

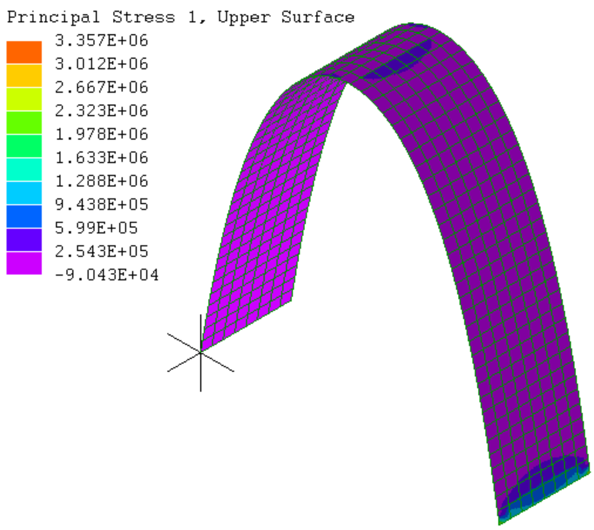

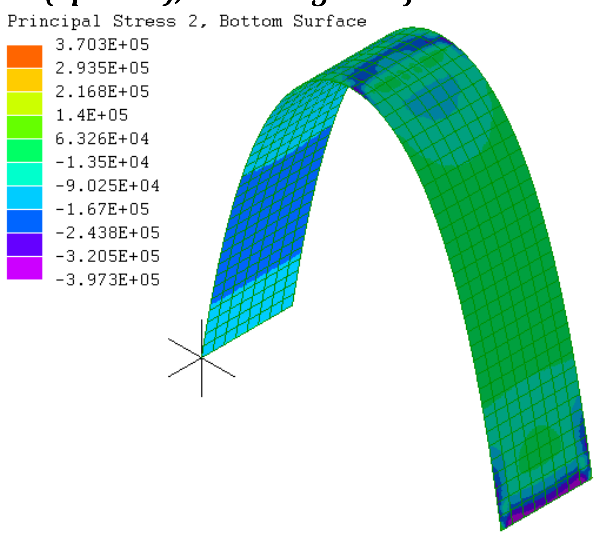

XIX. *Dead Load, Live Load right half, T=20° right half*

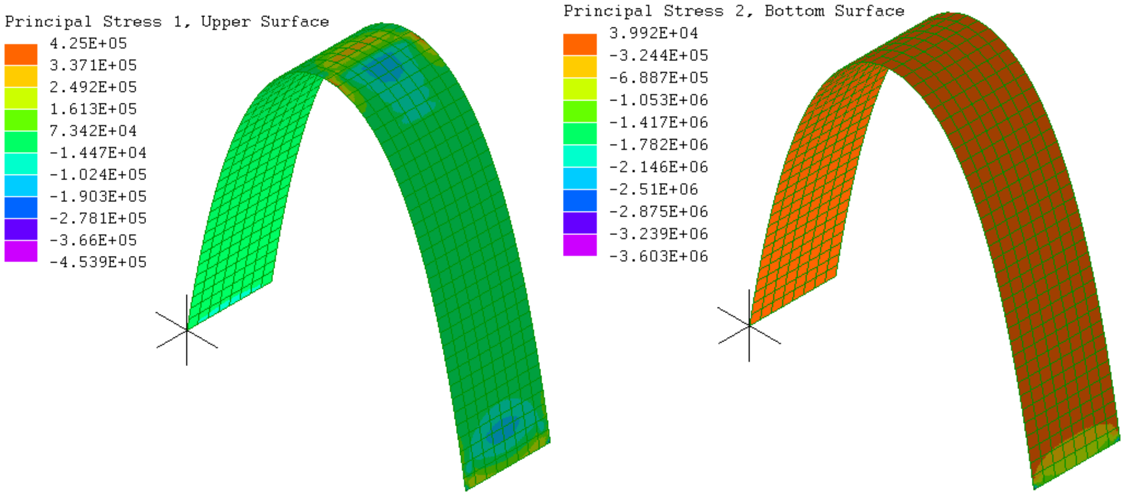

XX. *Dead Load, Live Load right half, T=-20° left half*

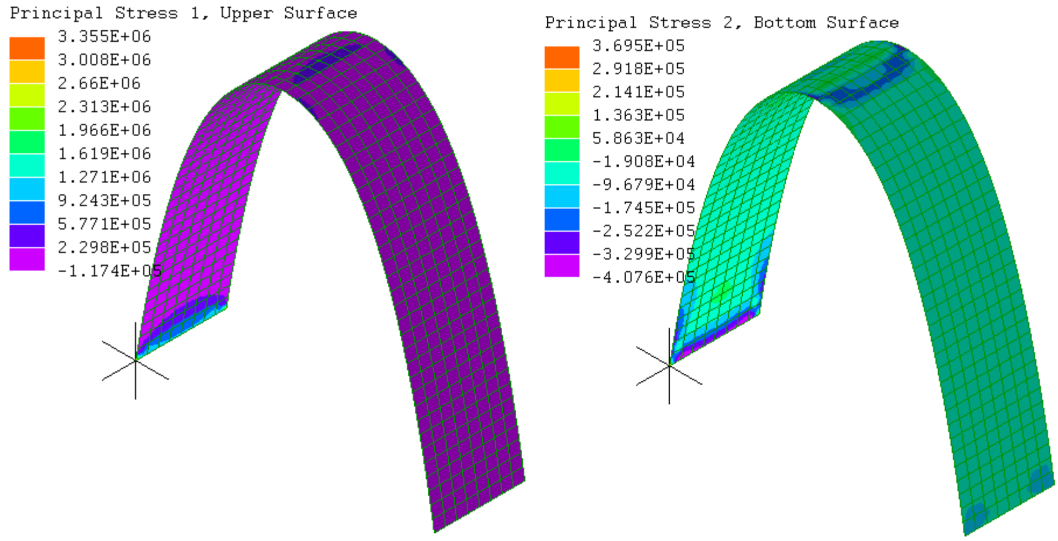

XXI. *Dead Load, Live Load right half, Wind Load (Cpi=0), T=20° left half*

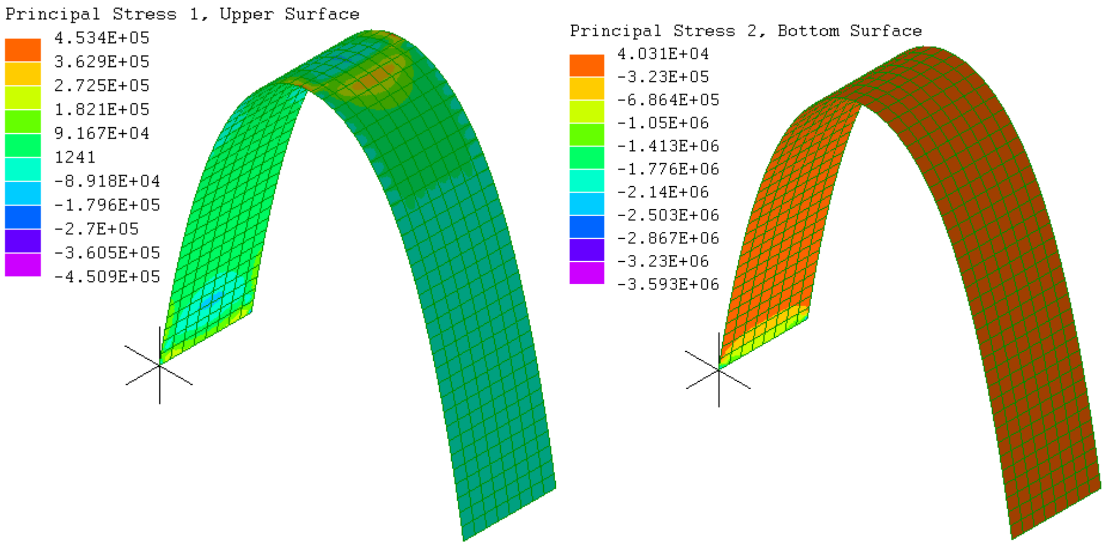

XXII. Dead Load, Live Load right half, Wind Load (Cpi=0), T=-20° right half

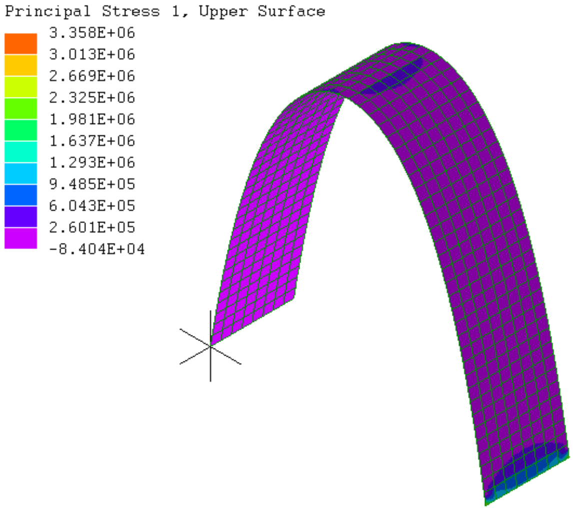

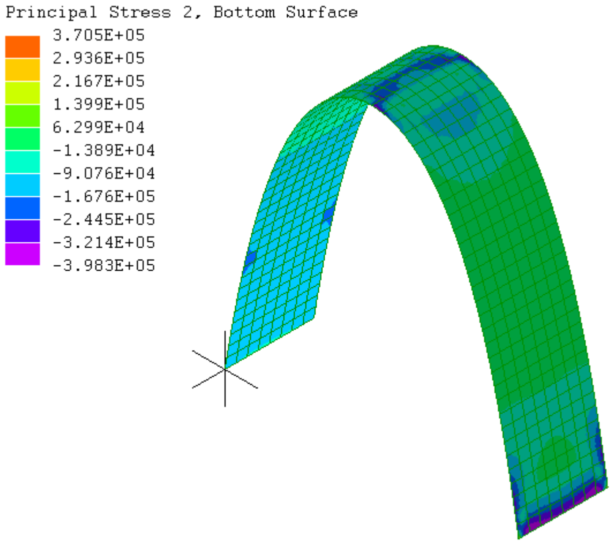

XXIII. Dead Load, Live Load right half, Wind Load (Cpi=-0.2), T=20° left half

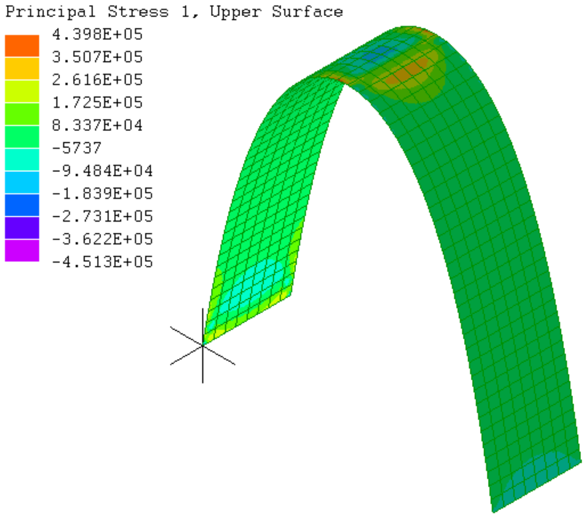

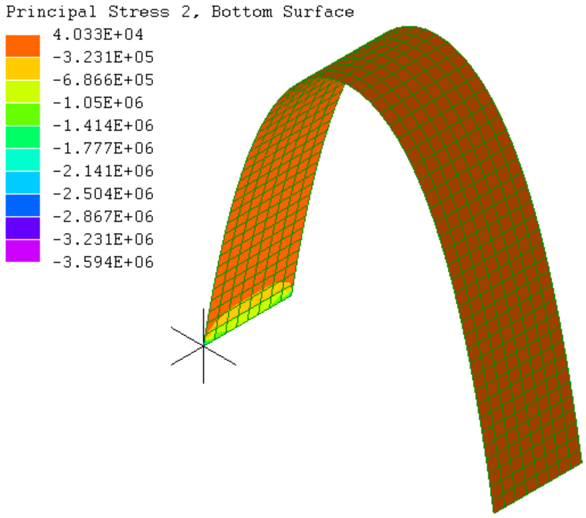

XXIV. Dead Load, Live Load right half, Wind Load (Cpi=-0.2), T=-20° right half

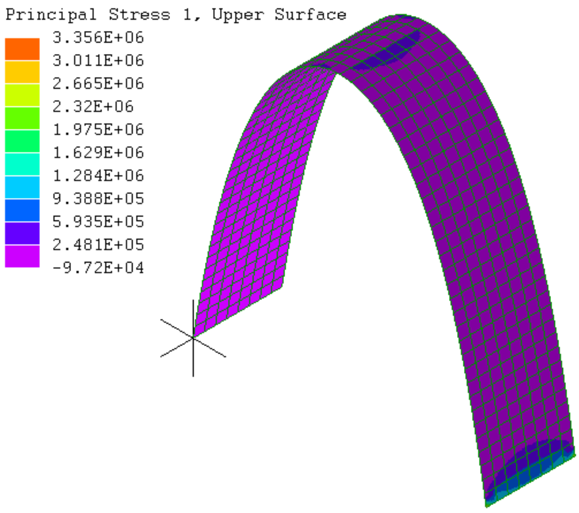

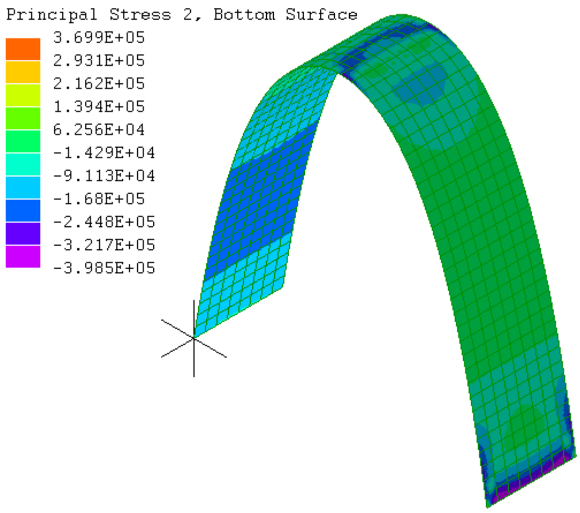

XXV. Dead Load, Wind Load (Cpi=0), T=20° left half

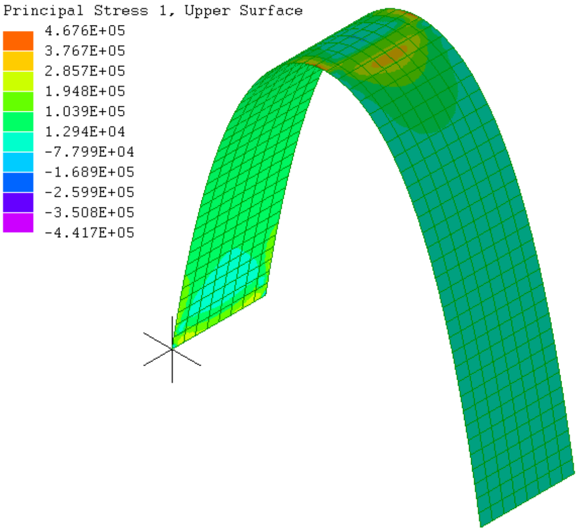

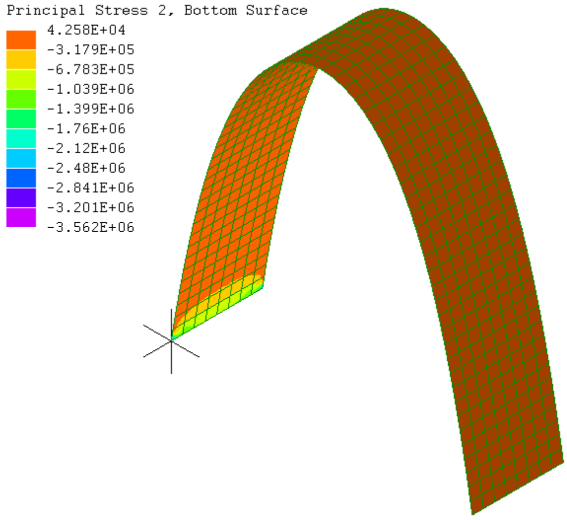

XXVI. Dead Load, Wind Load (Cpi=-0.2), T=20° left half

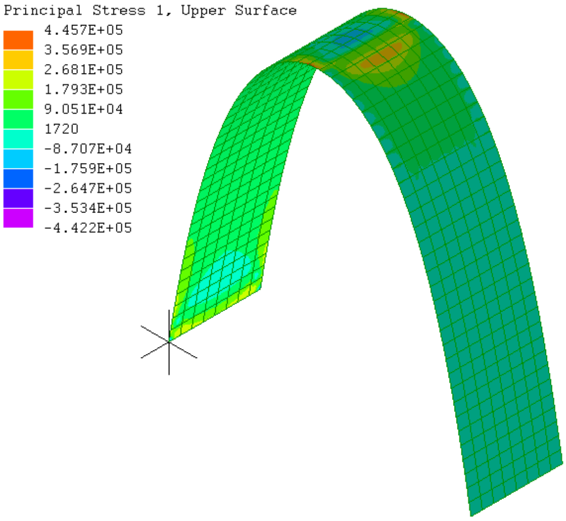

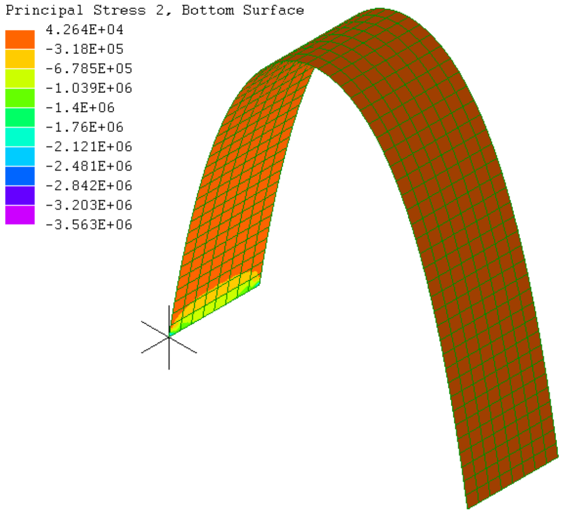

XXVII. Dead Load, Wind Load (Cpi=0), T=-20° right half

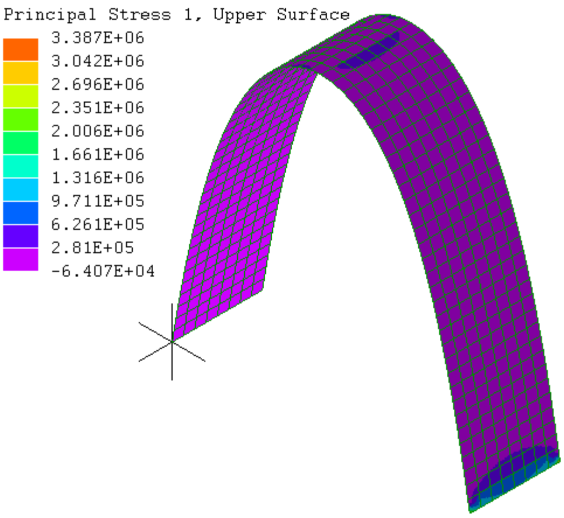

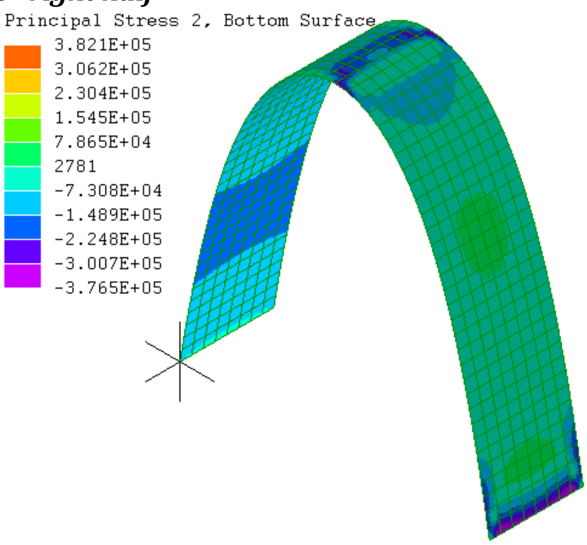

XXVIII. Dead Load, Wind Load (Cpi=0), T=-20° right half